For Reference

NOT TO BE TAKEN FROM THIS ROOM

For Reference

NOT TO BE TAKEN FROM THIS ROOM

Ex libris
universitatis
albertaensis

University of Alberta
Printing Department

Digitized by the Internet Archive
in 2018 with funding from
University of Alberta Libraries

https://archive.org/details/Weaver1962

Thesis
1963
#73

THE UNIVERSITY OF ALBERTA

SEISMOLOGICAL DETERMINATION OF CRUSTAL THICKNESS IN SOUTHERN ALBERTA

by

David F. Weaver

A THESIS
SUBMITTED TO THE FACULTY OF GRADUATE STUDIES
IN PARTIAL FULFILMENT OF THE REQUIREMENTS FOR THE DEGREE
OF MASTER OF SCIENCE

DEPARTMENT OF PHYSICS

Edmonton, Alberta

December, 1962

SEISMOLOGICAL DETERMINATION OF CRUSTAL THICKNESS IN SOUTHERN ALBERTA

ABSTRACT

A reverse seismic profile was shot in Southern Alberta in an east-west direction between Suffield and High River, a distance of some 150 miles. Eighteen useful records were obtained from an eastern shot point on the Suffield range, and eight useful records were obtained from a western shot point 12 miles north of Vulcan. The spread lengths varied from 0. 91 km. to 2. 50 km., and the shot sizes ranged from 240 pounds to 1000 pounds buried, and from 5 tons to 20 tons surface. Much useful information has been obtained from an analysis of these records.

Wave groups from deep seismic boundaries in the earth's crust were isolated on the seismograms. The results indicate a limestone layer with a velocity of 5. 88 kms. /sec. at an average depth of 1. 4 kms. Refractions from the basement indicate a boundary velocity of 6. 40 kms. /sec., and an average depth of 2. 7 kms., with a 6 minute dip to the east. Good refractions were also observed from an intermediate layer with a boundary velocity of 7. 32 kms. /sec. at an average depth of 34. 2 kms. This layer has a dip of 34 minutes to the east. Reflection data also supports this discontinuity. It "may or may not" be the so-called Conrad discontinuity. Good refractions and a clear broad reflection curve were isolated on the records, and attributed to the Mohorovicic discontinuity. The velocity just below this discontinuity is 8. 25 kms. /sec., and the boundary has a dip of 29 minutes east over the region sampled by the seismic waves. The average depth to the Moho is 47. 5 kms.

A low velocity layer was introduced between the basement and the intermediate layer, with a velocity of 6.10 kms./sec. This was necessary in order to make critical points from the intermediate layer and the Mohorovicic discontinuity agree with strong energy bursts. Support for this layer is given in the body of the thesis.

All of these results are compared with those of Richards and Walker (1959), and those of Steinhart et al. in Montana. Very good agreement is seen in some phases of the work. Basement and Mississippian arrivals are also compared with the theoretically predicted arrivals, based on a geological cross section of the area.

Many ambiguities are still present in the results of this year. More work will be carried out next year by the University of Alberta in the same general area. This should clear up any ambiguities which are present.

ACKNOWLEDGEMENTS

The successful completion of this seismic investigation was made possible by the interest and co-operation of the Suffield Experimental Station, the members of the field parties, and the staff members of the Physics Department of the University of Alberta. Dr. G. D. Garland of the University of Alberta suggested the problem and I am particularly indebted to him and to Dr. G. L. Cumming for many helpful discussions. The Suffield Experimental Station was very co-operative in setting off the shots whenever we were ready for them. Many thanks to Messrs. Erik Hjartenberg, Doug McClure, Dave Robertson, and Gordon Sande for their assistance on the field trips to Southern Alberta, and to M. D. Burke for his technical assistance in getting the project under way in June. The project was financed by a USAF grant.

Many of the observations from the west shot point were made by groups from the United States Geological Survey and the United States Coast and Geodetic Survey, and for this, we are indebted to them.

TABLE OF CONTENTS

Page

CHAPTER 1: INTRODUCTION 1

CHAPTER 2: BACKGROUND INFORMATION 4

General 4

Carnegie Institution 5

Japan 7

U. S. S. R. 8

Others 10

University of Wisconsin 13

Richards and Walker 18

CHAPTER 3: GENERAL SEISMIC THEORY 23

A. Seismic Refraction 24

B. Seismic Reflection 33

C. Time Term Method 48

D. Plus-Minus Method 55

E. Least Square Fitting 56

F. Correlation of Seismic Waves 57

G. Distance Calculation 61

H. Air-coupled waves 62

I. Theory used for U. of A. work 65

Page

CHAPTER 4: FIELD EQUIPMENT 68

Power Supply and Amplifier 70

Recording Oscillograph 73

S-36 Seismometer 76

Oscillations 77

Radio Equipment 79

CHAPTER 5: LABORATORY TESTING OF EQUIPMENT 83

CHAPTER 6: GEOLOGY OF THE AREA AND THEORETICALLY PREDICTED SEISMIC ARRIVALS 93

CHAPTER 7: ORGANIZATION OF THE FIELD WORK 99

Table of Shots 103

CHAPTER 8: INTERPRETATION OF THE SEISMIC RECORDS 104

Distances 104

Times 104

Picking of Arrivals and Plotting of them 105

Summary of the More Important Models and Reasons for Rejection of them 107

Validity of Assumption of a Low Velocity Layer 108

Preferred Crustal Model 113

Final Calculations on Preferred Crustal Model 117

Reflection Data 120

Page

Portions of Field Records 121

Air-Coupled Waves 123

CHAPTER 9: CONCLUSIONS AND SUGGESTIONS FOR FUTURE WORK 125

BIBLIOGRAPHY 130

APPENDIX I: The Nature of the Mohorovicic Discontinuity

APPENDIX II: Tables of Arrival Times

APPENDIX III: Shot and Recording Location Diagrams

LIST OF FIGURES

Page

Figure 1. Montana Crustal Models 17a

Figure 2. Richards' and Walker's Original Curves 19a

Figure 3. University of Alberta Reinterpretation of Richards' and Walker's Data For South Shot Point 20a

Figure 4. Amplifier (VLF) 72a

Figure 5. VLF System Frequency Response 72b

Figure 6. VLF System Phase Response 72c

Figure 7. VLF System Gain versus Frequency 72d

Figure 8. Camera (VLF) 72a

Figure 9. Response of the S-36 Seismometer 76a

Figure 10. System Oscillations 78a

Figure 11. Large Voltage "KICK" 78b

Figure 12. Tone Test 80a

Figure 13. Chronometer and WWV Timing 82a

Figure 14. Seismometer Photograph 83a

Figure 15. Amplitude and Phase Check in the Lab. 83b

Figure 16. Testing of the 6 db. Attenuation Steps 85a

Figure 17. Reduction of High Frequency by Filter Settings 86a

Figure 18. Amplifier Distortion 86b

Figure 19. Amplifier Crossfeed 88a

Figure 20. Testing Phase of Seismometers 89a

Page

Figure 21. Dynamic Test of Geophones 89b

Figure 22. Southern Alberta Cross-Section From Well Data 94a

Figure 23. Plot of 1/V in Mississippian 97a

Figure 24. Location Map 100a

Figure 25. Example of Large Scale Plot for Apparent Velocity 106a

Figure 26. East Travel Time Graph 106b

Figure 27. West Travel Time Graph 106c

Figure 28. Bouguer Anomaly Across Southern Alberta 108a

Figure 29. Amplitude Ratio Plot 113a

Figure 30. Southern Alberta Preferred Model 119a

Figure 31. Juliet 2, Field Record 121a

Figure 32. Shot 10, truck 2, Field Record 121b

Figure 33. Shot 11, truck 2, Field Record 121c

Figure 34. Shot 15, truck 1, Field Record 122a

Figure 35. Shot 10, truck 2, Field Record 123a

Figure 36. Air-Coupled Waves 123b

Figure 37. Phase Diagrams For Mohorovicic Discontinuity 16a, App.I.

CHAPTER I

INTRODUCTION

In the summer of 1962, the University of Alberta undertook a study of the crust of the earth in Southern Alberta, using the large scale seismic method. The program was sponsored by the USAF and ARPA of the United States, and was under the supervision of Dr. G. D. Garland of the University of Alberta. Dr. G. L. Cumming was in charge of many of the field trips. The University purchased two sets of VLF Seismic equipment from Texas Instruments, with 12 geophones per set. One unit was installed in each of our two panel trucks, which were used throughout the summer for transportation. Each truck was manned by a graduate student and an undergraduate assistant. The shots from the east were all set off by the Suffield Experimental Station, who co-operated with us fully on this project. Very high frequency radio communication was established from Suffield out to High River by the use of two repeater stations, one at Rainier, and the other north of Vulcan on Buffalo Hill. Two-way General Electric TPL mobile radio sets were installed in each of our trucks. Thus, the trucks were always in direct communication with the shot point for shots from the east. Timing on the records was provided by a one-second tone from -1 sec. to zero transmitted by Suffield to the truck. The shot always went off within 3 millisecs. after the end of the tone.

The shots from the West were set off by the Century Geophysical Company. Timing was provided by a chronometer and a WWV receiver at both the shot point and the recording trucks. Two American groups, the United States Geological Survey and the United States Coast and

Geodetic Survey, assisted us by recording some of the shots from the west.

Each of the University trucks had 12 geophones, with an average spacing of 410 ft. The original idea was to have one spread every 8 to 12 miles from Suffield out to High River, but, due to unforeseen problems, this idea was not carried out. The coverage from the east, however, is quite good, with records spaced from 1 mile to 15 miles, although a few of the records are of extremely poor quality.

The main purpose of the project was to determine the depth and dip, if any, of the Mohorovicic discontinuity in Southern Alberta. This was accomplished, and many other interesting things were discovered as well. It was possible, for example, to determine the relative merits of a buried and surface shot. Several microseismic experiments were carried out by Erik Hjortenberg, and they will form part of his Ph. D. thesis. Much valuable information was also obtained about the VLF seismic equipment. This will enable future seismic expeditions of the University of Alberta to be even more successful, and to yield more information. The seismic records also yield important information about other seismic discontinuities in the crust of the earth, and even indicate possible discontinuities below the Moho. However, many ambiguities are still present, and additional work will be necessary in Southern Alberta before a complete picture of the earth's crust in that area can be determined. This additional work will be done next summer by the University.

The region of Southern Alberta was chosen for this work for several reasons: (1) it is open, flat country very suitable for seismic

work; (2) an independent determination of depth to M was carried out by Richards + Walker in 1958 using a very short NW-SE profile in the area near Calgary; (3) the Suffield experimental station agreed to co-operate with us by setting off the explosions for us; (4) the area is relatively close to Edmonton.

This thesis is mainly concerned with the interpretation of all the seismic work done in Southern Alberta this summer (1962) by the University. Several earth models are tried, and one is finally decided upon as best fitting the data. The probable nature of the Moho itself, however, is also discussed, and other crustal thickness determinations in this general area near the Rocky Mountains are summarized. A collection of seismic theory is also given.

I feel that the summer's work added a great deal to our knowledge of the crust of the earth in this area.

CHAPTER 2

BACKGROUND INFORMATION

The study of the crust of the earth has certainly been carried on for a long time, especially through the use of near-earthquake observations. The analysis of near-earthquake records has provided us with most of our data on the structure of the earth. Two very important contributions were made by Mohorovicic (1910) and Conrad (1925). Mohorovicic discovered the discontinuity which has been named after him and which seems to be present over the whole earth at a depth of 30-60 kms. under the continents and 4 - 8 kms. under the ocean floors. Conrad discovered a discontinuity above the Moho, which does not seem to be as universal as the Moho. Explosion studies have proven to be more accurate in the determination of the crustal properties of the earth than have earthquake studies. The reasons for this are clear. In explosion work, we can always be prepared well in advance, and we can very often choose the actual explosion site, and designate the time of detonation. But, even if we cannot do this, we always know exactly the location of the blast, and the time that it was detonated. None of this holds true in earthquake work as one never knows when a quake will occur or where it will occur. The focus and time of a quake can never be known exactly. In explosion work, we can lay out our geophones in a profile which makes interpretation easier, and, since we know roughly the arrival times of the waves for the distance we are working, we can run the seismic cameras at a faster speed for much better resolution and correlation of the seismic energy.

Then, we can often shoot reverse profiles in explosion work to get reciprocal times and to calculate dip.

Explosion work began in Europe with Weichert who made use of portable seismic equipment to record quarry blasts from 1926 on. By 1929, recordings were being made at ranges greater than 50 kms.

Explosion work began in North America in the early 1930's with the studies of quarry blasts mostly in Southern California (Wood and Richter, 1931, 1933; Byerly and Dyk, 1932; and Byerly and Wilson, 1935). None of this explosion work as yet had found the depth to the Moho. The first determination of crustal thickness from blast studies was that of Leet in 1936. He used quarry blast recordings in New England, and found a depth to M of 23 kms. This figure he modified in 1941 to 35 kms. due to additional information from earthquake data. Slichter (1938, 1939) recorded more quarry blasts in New England, and he gave the depth to M as 23.5 kms. for a 350 kms. profile in the Connecticut valley. Explosion studies of the earth's crust were largely discontinued during World War II. After the war, the modern era of controlled explosion studies began. Three main groups of workers have been the Carnegie Institution of Washington, the Research Group for Explosion Seismology in Japan, and work in the U. S. S. R. The main conclusions of each group will be discussed in the following few pages. Then, a more detailed analysis of the work in Montana will be given, followed by a reinterpretation of the work by Richards and Walker in Southern Alberta.

(1) Carnegie Institution of Washington: Tuve and his fellow workers in the years 1946-49, developed instruments capable of detecting ground motion of the order of 10^{-8}cm. at 4-10 c. p. s. The

detectors used had a resonant frequency of 2 c. p. s. They used charge sizes of 600 to 4000 lb. and observed the blasts at distances of up to 350 km. The results from about 140 records were published in 1948. The results gave 0-10 km., 6. 0-6. 17 km/ sec.; 10-24 km ., 6. 7 km. /sec.; 24-42 kms., 7. 0 km. /sec.; and 8. 15 km. /sec. below M. The crossover distance method of calculation from the refraction results was used. They did not report any reflections. In 1949, experiments were carried out in California, and the model obtained for the upper crust of the earth was: a velocity of 5. 7 km. /sec. from 0 to 10 km., and a velocity of 6. 8 km. /sec. below 10 km. This was quite different from other regions. In the next few years, the Carnegie Institution carried out experiments to try to interpret the very complex pattern of ground motion shown by the seismic records. They concluded that the reverberation and quasi-coherence (phases coherent over small areas, but disappearing when source or detector were moved a small amount) were caused by conversion of body waves to surface waves near the detectors. Some of this complex motion may be due to the nature of the motion at the source as well as to the response characteristics of the ground-detector system. Model experiments were conducted, which proved that obstacles on the free surface of a layered model converted P waves to Rayleigh waves.

A significant contribution of the Carnegie group was their identification of critical reflections. For identification of the Moho, they imposed the double criterion that the refraction data and critical reflection data both had to be satisfied. An important point is that the Carnegie group have never identified a vertical reflection from the Moho. They have seen arrivals at the correct times, but there were

always other arrivals just as strong very close to the ones at the correct times. The reverberation level was always higher than the amplitude of the expected vertical reflections anyway.

Another important point is that the Carnegie group have reported again and again that no definite intermediate layers were found. They imposed the criterion that critical reflections and/or a very good number of refraction arrivals must be found before a layer could be definitely identified. According to Steinhart and Meyer, the preceding points, which I have summarized, are the chief contributions of the Carnegie Institution of Washington to date.

(2) The Research Group for Explosion Seismology, Japan: The first work in Japan was done in northeastern Japan in the years 1951-55 with the observations of commercial blasts. The velocity below the crust was not very well defined, and the velocities varied with different directions of observation. The trouble was attributed to lack of enough recordings and dip of the layers. The seismometers were generally of a 3 c.p.s. resonant frequency. Overall magnification of the system was between 10^6 and 10^7. Overall timing accuracy was 0.1 sec. or better (they employed direct recording of JJY, the Japanese radio time standards). Distance was measured from large scale maps, the accuracy being about ± 30 meters. The method they used in choosing models was given by Matuzawa (1959). They used only the seismic data for interpretation, and geological and gravity data were only considered after the model was chosen. Models were to be as simple as possible and still satisfy the data. Models were considered adequate when the remaining residuals were less than ± 0.03 sec. The method of

interpreting the data consisted of solving for dips which would explain apparent velocities in different directions, and then introducing some relief into the discontinuities to explain the "early" or "late" groups of arrivals. But, often several models will fit one group of data. Thus, the group realized that reverse profiles were necessary to determine the velocities accurately. Some attempt was made to determine crustal structure by using shear waves, but this was not successful.

Vertical reflections from deep within the crust were reported twice by this group. But, there are always other arrivals very near the ones chosen which may just as well have been used. Also, on one record, an arrival at 11. 35 secs. is attributed to the Moho, while a second arrival of the same strength at 12. 85 secs. is just ignored.

A notable feature of the Japanese work is the lower P_n velocity (Moho) of 7. 7 km. /sec. This also agrees with the near-earthquake results in Japan.

The above are the chief contributions of the Japanese work, summarized from the more complete detail of Steinhart and Meyer.

(3) Work in the U. S. S. R. : Explosion work in Russia began just before World War II with Koridalin and Tvaltvedze. Then, Gamburtsev and his co-workers carried out experiments to improve refraction prospecting methods. They especially suggested the close-spacing of geophones and very careful control of the gain (for amplitude studies). Gamburtsev also stated that it may be necessary sometimes to use second refraction arrivals for crustal study, and further

pointed out that under certain conditions, a refracted arrival may never be a first arrival. Riznichenko in 1946 made a detailed investigation of the application of ray theory to refraction paths, and also compiled a bibliography of over 200 references concerning work in the U. S. S. R. to that time. In 1952, Gamburtsev published a handbook called the "Correlation Method of Refracted Waves." This was a compilation of principles, instruments, field technique, theoretical considerations, and interpretation of the method.

The method of determination of crustal structure that finally developed from all this was the method of deep seismic sounding (DSS). Field techniques used for this method were as follows: geophone arrays were used to increase S/n ratio; shots were usually fired in water at depths of 10-20 metres; 10 c.p.s. was found as the most suitable frequency; spreads of 24-48 locations were used, with 100-300 m. between stations, profiles were constructed whereby sections of 10-20 kms. of continuous coverage alternated with gaps of 10-30 kms.; several shots were usually used; quiet sites, etc., were always used. They always attempted to get a three-dimensional picture of the subsurface layers. Standard cameras were used with 12 to 60 channels and a paper speed of 8-12 cm./sec. (3-5 in./sec.). Shot instants were found by use of an oscillator triggered by a thyratron, in the firing circuit, and this tone was recorded by radio at the observing sites.

An important paper by Veitsman came out in 1957, on the correlation of waves and wave groups in seismic interpretation. This paper will be discussed later (in the next chapter), and so I will not comment on it here.

It is important to note that no reflections at less than the critical angle have been reported in the U. S. S. R. with the exception of the work by Koridalin (1939). In this latter work again, other phases could just as well be used.

Very often the Russian work shows rather low basement (P_1) velocities. But, this is probably not due to error, but due to the fact that most of their work has been concentrated in areas of recent mountain building. Note that low P_1 velocities are also reported in California.

Steinhart and Meyer state that the relatively simple crustal models presented by the U. S. S. R. are due partly to preconceived assumptions about crustal structure which has come from Jeffreys. The trend more recently in Russia seems to be toward more complex crustal structure.

Steinhart and Meyer have made a careful compilation of all the previous work done by the Carnegie workers, the Japanese workers, and the workers in the U. S. S. R. All I have done is very briefly summarize their work.

Work on crustal studies has been carried on by other people as well. An important contribution to the work was made by Gutenberg when he suggested that low velocity layers may possibly exist within the crust. If such a zone exists, it should produce a shadow zone where first arrivals of P_1 would not be seen, followed by a reappearance of these arrivals in a displaced position on the travel time graph. Evidence for such a reversal of velocity has had some support from near-earthquake data (Shor, 1954; and Tocher, 1956, in California),

but no evidence has ever been found from explosion studies. A paper in 1957 by Markus Bath discusses theoretical computations, using ray theory, and considering an asthenosphere low velocity layer. However, that will not be discussed here.

In 1949 L. Mintrop published a paper combining the results from the Heligoland explosion and the Messina earthquake. His earth model consists of 8 very well defined interfaces between Heligoland and Messina. They are at depths of 4, 13, 28, 57, 110, 118, 170, and 183 km., with velocities of the P waves in each layer being 3. 5, 5. 2, 6. 5, 8. 1, 9. 2, 7. 0, 11. 0, and 16. 3 kms. /sec. First arrivals seem to have been observed for all the layers except the 7. 0 kms. /sec. layer (which is an assumed velocity, considering that it may represent the melting point of the 9. 2 kms. /sec. layer), and 183 km. layer, and reflections seem to have been observed from the layers at 57 km., 110 kms., 118 kms., and 170 kms. depth. The Moho is considered as the layer with the velocity of 8. 1 kms. /sec. at a depth of 28 kms. The evidence for some of the layers is not very convincing. In the paper, Mintrop shows generally only those arrivals which fall on the time-distance curves for the various layers, but many more unaccounted-for arrivals were no doubt present. It is very difficult to determine from the paper which layers are most probable and which are least probable.

Hoffman, Berg, and Cook published a paper in 1961 on results from quarry blasts in Utah. They found that reflected events (or possible reflected events) were present which would indicate discontinuities at depths of 190, 520, and 910 kms. in the earth. The 190 km. depth corresponds very closely to the 183 km. depth that Mintrop found in

Europe. They calculated the depths using the velocity-depth curves given by Jeffreys and Gutenberg (Jacobs, 1953) for the deeper portions of the upper mantle, and they assumed linear ray paths of the energy. The discontinuity at 190 km. seems well supported by reflections, but the others are not so convincing.

Shor in 1955 reported reflections from the Moho at normal incidence from large quarry blasts in Southern California. However, on many other records, he could not see any such reflections because of a high reverberation level. He found that the Moho was 32 km. below sea level in that area.

Berg, Cook, Narans, and Dolan in 1960 published results obtained in Utah from nine quarry blasts and also from two nuclear explosions near Mercury, Nevada. They found the crustal layering in the eastern Basin and Range province as follows: 5. 73 km. /sec. to a depth of 9 kms. ; 6. 33 km. /sec. from 9-25 kms. ; 7. 59 km. /sec. from 25-72 kms. ; and 7. 97 km. /sec. at depths greater than 72 kms.

Narans, Berg, and Cook then used smaller charges in the Rozel Hills of northern Utah in an attempt to record sub-basement reflections. Two of the reflections yielded horizon depths of about 8. 5 kms. and 26. 3 kms. , which agreed very well with the first two horizons found in the refraction work above.

In 1960, Milne and White published the results of a seismic survey in the vicinity of Vancouver Island, B. C. Considerable information was obtained about the area. It seems that a granitic rock with a velocity of 6. 3 km. /sec. forms the basement rock of the area. This rock outcrops at the D. A. O. , at Horseshoe Bay, and possibly at Alberni.

South of Victoria, this rock is covered by a volcanic rock with a velocity of 5. 4 km. /sec. This formation dips to the north. On the west coast of the strait, the velocity seems to be 4. 05 km. /sec.

I wish to discuss the work of only two more groups in this field, the University of Wisconsin and Richards and Walker of Triad Oil Co. The University of Wisconsin has done work in Mexico, Arkansas-Missouri, Wisconsin, and Montana. The work in Montana will be discussed in some greater detail than the others, since it is very close to the work done in Alberta by the University of Alberta.

Four crustal models were constructed as possible interpretations of the seismic results in Mexico. All four models give a velocity for the material below the Moho as 8. 4 km./sec. The models differ by taking into account various possible intermediate layers. On the basis of amplitude study, two of the models were more or less ruled out. Of the other two models, the one given below was selected by the workers, Steinhart, Meyer, and Wallard, as the one best fitting the data.

0-1 km.,	3. 0 ± . 5 km. /sec.
1-4 km.,	4. 95 ± . 15 km. /sec.
4-32. 5 km.,	6. 01 ± . 003 km. /sec.
32. 5 - 43 kms.,	7. 63 ± . 04 km. /sec.
below 43 kms.,	8. 38 ± . 09 km. /sec.

Thus, the depth to the Moho is given as 43 kms., with a sub-Moho velocity of 8. 4 km. /sec.

The other model which is considered almost as reliable as the above, includes a layer with velocity 6. 44 ± . 06 km. /sec. between the 6. 01 km. /sec. layer and the 7. 63 km. /sec. layer. However, depth to

the Moho for this model is 44.5 kms. which is very close to the depth found from the chosen model.

The value for the velocity of the Moho is a little higher than what is normally expected, but apparently velocities of 8.4 - 8.5 km./sec. have been reported in the Caribbean by Officer (1959), using reverse profiles. However, no reverse profile was used here, and some dip is probable.

Five crustal models were constructed as possible interpretations of the results in Arkansas-Missouri, but only two seem to fit the data well, according to the workers (same as above). The velocity below the Moho was found to be 8.2 km./sec. The one model which best fits the data is given below (the other model depends on one very questionable point):

0-2 kms.,	4.64 km./sec.
2-10 kms.,	5.18 km./sec.
10-41 km.,	6.64 km./sec.
below 41 km.,	8.16 km./sec.

Thus, the depth to the Moho is given as 41 kms., with a sub-Moho velocity of 8.2 km./sec.

It was expected that the crust would not be as thick in this region as in Mexico, since the Mexican results were taken on a plateau. The theory of isostasy does not seem well-supported by these two profiles.

A reverse profile was shot in north-central Wisconsin from the Apostle Islands to Lohrville. Two crustal models were chosen, which best fit the data. The model given below is considered the preferred model by the workers, on the basis of amplitude ratios mainly. They found a dip in the layers of about 1/2 degree to the north. The

following information then is true velocity, but average depth across the profile for the layers: 0-3 kms., 5.4 kms./sec.; 3-14 kms., 6.11 kms./sec.; 14-40 kms., 6.51 kms./sec.; and below 40 kms., 8.03 kms./sec. Thus, the depth to the Moho was found to be roughly 40 kms., with a sub-Moho velocity of 8.0 kms./sec.

A single-ended profile was then shot along the Keweenawan Penninsula in Upper Michigan. Two crustal models were constructed for this profile, which fit the data well. The amplitude ratios and the fact of generally less scatter in the results aided the observers to choose a preferred model. This is given below:

0-2 kms., 4.75 kms./sec.; 2-16 kms., 6.44 kms./sec.; 16-37.5 kms., 6.67 kms./sec.; and below 37.5 kms., 8.08 kms./sec.

Thus, the Moho in this region appears to be at a depth of about 37-38 kms., with a sub-Moho velocity of 8.1 kms./sec.

Then, in 1959, Meyer, Steinhart, and Bonini carried out work in Montana for the University of Wisconsin. Since the area in Montana is immediately south of the work in Alberta, I will treat the work there in a little more detail. The results by Wisconsin before 1959 had not supported the idea of isostasy, i.e., the simple variation of crustal thickness as a function of elevation. To further test this theory, the margin of the Rocky Mountains was chosen for study. Two reverse profiles were shot in Montana; the Acme Pond-Ft. Peck reverse profile in eastern Montana, and the Cliff Lake--Sailor Lake reverse profile in Western Montana close to the Rockies. The eastern profile was in a north-south direction, while the western profile was in a N-W, SE direction almost paralleling the continental divide, and lying in the

high mountains. The group used a spread length of 1.5 to 2.0 km. in an attempt to get more accurate apparent velocity data. All cameras were operated at 2 in./sec. and the spacing of traces was 5 mm. Records from eastern Montana were of better quality than the ones from the mountains of Western Montana. In both areas, some of the spreads had to be slightly offset due to topography, available roads, etc. This probably caused some difficulties in phase correlation. Shot size ranged from 50 lb. to 1900 lb.

Despite the reasonably long spread lengths, the group found very many discrepancies with regard to apparent velocities (it will be seen later on that the University of Alberta results show the same type of discrepancy). The apparent velocities were often too high for the line-up of phases with which they seemed to agree. Sometimes, the apparent velocities were too low for the wave to which the arrivals seemed to belong. The workers in the U.S.S.R. (e.g. Veitsman, 1957) found the same problem. The measurements of these velocities, however, were quite accurate in Montana, and it is impossible to explain them on the basis of experimental error. Steinhart et al. mention the possibility that dispersion effects may be present in these body waves, which may cause the apparent discrepancy.

For the eastern Montana profile, 20 models were constructed at first, but after applying the least squares fit and amplitude data, only two models finally remained. It should be noted here that a group from the Carnegie Institution were recording in Montana, at the same time, using the explosions set off by the University of Wisconsin. They used only single-ended profiles, and had only two detectors per station.

Thus, their results may not be as reliable as those of the University. But, they do agree well, and one of the two models of the crustal structure of eastern Montana put forth by the University better agreed with the east-west profile of the Carnegie people than the other. This model was then chosen as the preferred model for eastern Montana. (See Figure 1. for a cross-section of the Acme Pond - Ft. Peck profile according to this model.)

Since the data from Western Montana is not so plentiful as that from eastern Montana, it is possible to fit more models to it. Steinhart and workers accepted the simplest model that satisfied the observations. (See Figure 1. for a cross-section of the Cliff Lake-Sailor Lake profile according to the selected model.)

It is seen at once that a surprising result is indicated. The crust of the earth is thicker in eastern Montana than it is in Western Montana in the mountains! Even if another intermediate layer is included in the Western cross-section (one that doesn't contradict the observations), the crust is still found to be thinner in the northern Rocky Mountains than in Eastern Montana.

According to the two models selected by the University of Wisconsin, the crustal thickness in Southern Montana should increase from 43 km. to 51 km. from west to east. (The Carnegie east-west profile in this area nearer the western profile shows a thickness of 46 kms., which is just what would be expected). But, in northern Montana, the crust should thicken from 37 km. to 54 km. from west to east. The Carnegie east-west profile in this area near the western profile shows a thickness of 55 kms., while the Carnegie east-west profile in the area

near the eastern University of Wisconsin profile shows a thickness of 46 km. This seems to be a contradiction of the work by the University. Steinhart and Meyer state that because the Carnegie profiles were not reversed and contained fewer stations with only two geophones per station, the lack of agreement is not believed to be serious. But, also more work is needed in Western Montana before a definite conclusion on crustal structure in Montana can be reached.

The final work which I wish to discuss is that of Richards and Walker in Southern Alberta in 1959. Their work was a very short reverse profile (only 132 km. long) parallel to the frontal thrust of the Rocky Mountains and about 60 miles east of the thrust. According to the interpretation given by Richards and Walker, the Moho occurs at a depth of 43 km., with a sub-crustal velocity of 8.2 km./sec. They also claim to have found an intermediate layer at a minimum depth of 29 kms., with a velocity of 7.2 km./sec. All of the seismic records that were taken by Richards and Walker have been obtained by the University of Alberta, and were re-examined by us during the summer. Some of the records were of very poor quality. Before discussing this, I will discuss the instrumentation and general layout of the field work done by Richards and Walker. Fifteen different oil companies participated in this work, giving 15 spreads over the length of the profile. Each company had their own equipment, had a different spread length, and ran their cameras at different speeds. This makes interpretation of the records extremely difficult. Even though the profile was in a NW-SE direction, the spreads were all on N-S roads for ease of

accessibility and, as Richards and Walker state, the measured distance to each geophone may be assumed to apply to the straight line joining the shot points with very little error. Spread lengths varied from .29 km. to 5.8 km. Most of the geophones employed by the parties were 6-1/2 c.p.s. phones. Some, however, used 10 c.p.s. phones, and 10 of the 1 c.p.s. Willmore phones were used by the group. All of the conventional amplifiers were operated without automatic gain control, with a minimum of low frequency attenuation and high frequency cut-off of 30 c.p.s. Camera speeds varied from 1 in./sec. to about 10 in./sec. Calibration of the response of the systems was not very well done. A steel ball dropped from a height of 6 inches into a layer of grease on top of a geophone. While this method of calibration did not give a good measure of response, it did show which equipment normally gave up-kicks on the trace and which gave down-kicks. Shot timing was provided by 40 watt Ernest Turner transceivers operating on a frequency of 1652 kcs., from a horizontal half-wave antenna 40 ft. above the ground. The shooting signal was a 250 c.p.s. tone about 10 seconds long, at the end of which the shot went off. The size of the charges used was 875 lb., distributed in five holes at an average depth of 70 ft. and 50 ft. apart.

The two travel time graphs submitted by Richards and Walker are reproduced in this paper. (See Figure 2). It is immediately noted that they have very little support for any arrivals later than the first. The only actual support for the Moho is a strong energy arrival at about 25 secs. at a distance of about 130 kms. This is somewhere near the point where critical reflections from the Moho may be expected from theory, assuming "normal" crustal thickness and velocities. This arrival

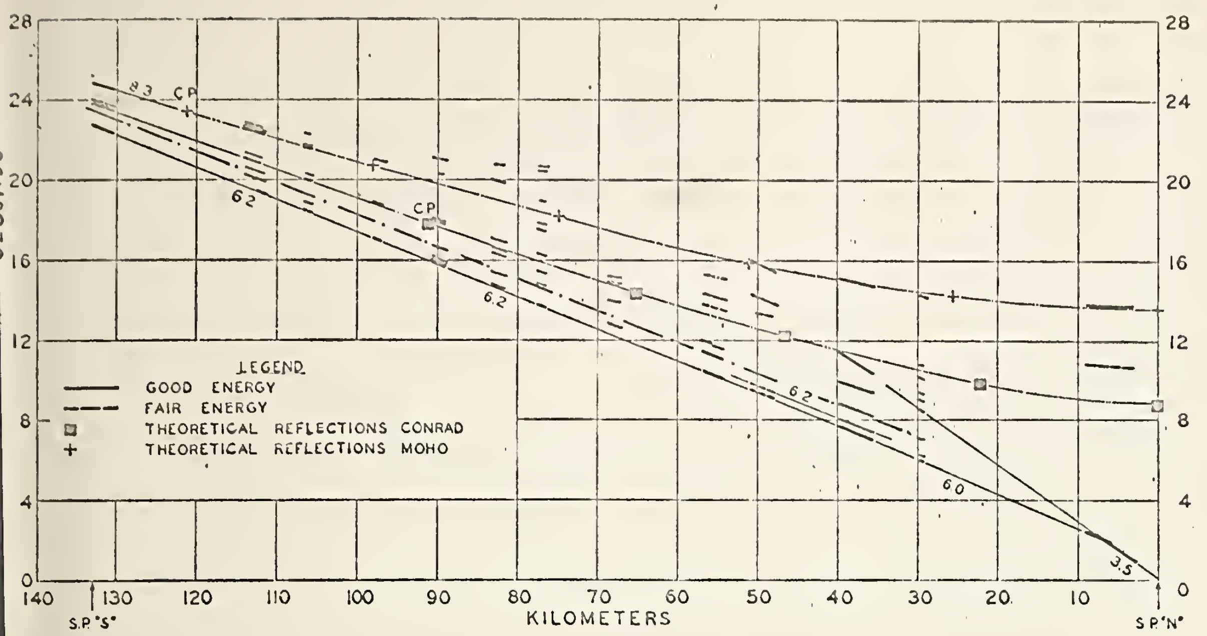

a. Time-distance curves from Shotpoint N.

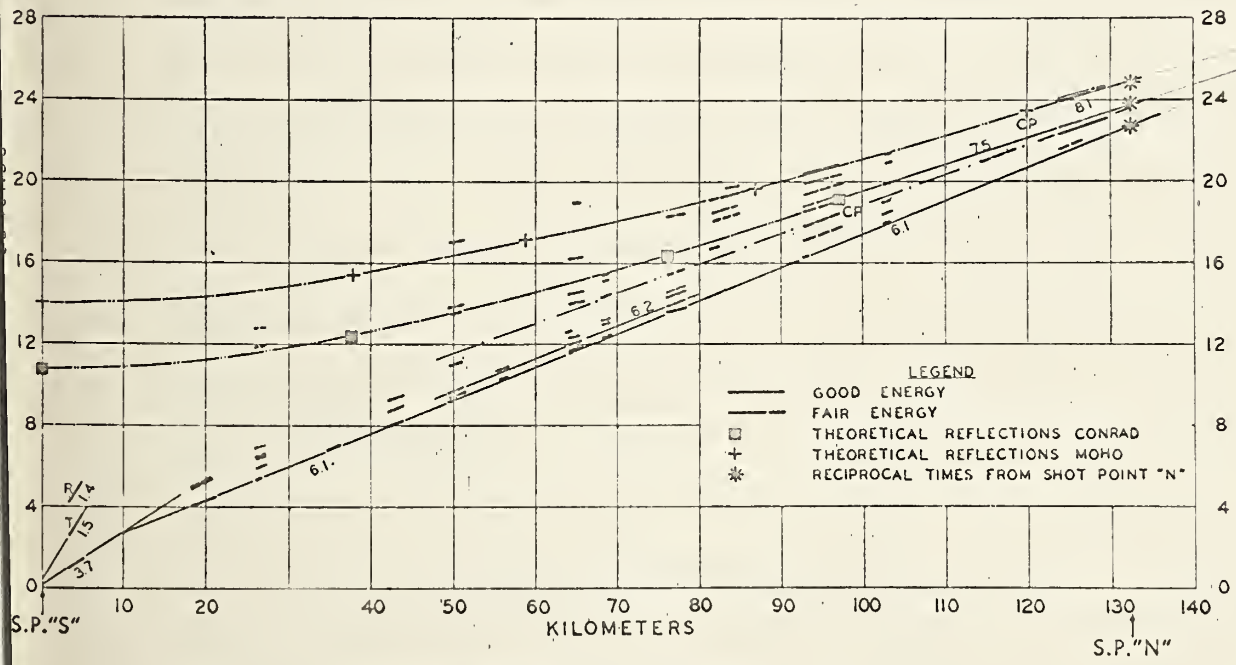

b Time-distance curves from Shotpoint S.

Fig. 2. *(after Richards & Walker, 1959)*

[Reproduced from STEINHART et al.]

is very likely one from the Moho as they have shown. Support for the remainder of the reflection line is extremely poor. Some of the arrivals picked by Richards and Walker seem to be strictly figments of their imagination, when one looks at the records where the arrivals are supposed to be. All the records obtained from the south shot point were repicked by us at the University of Alberta. The graph which we obtained on plotting these arrivals is reproduced in this thesis. (See Figure 3.) Several discrepancies are at once noticeable when our graph is compared with that of Richards and Walker. Several arrivals which they have plotted, we have not plotted, since we feel that such arrivals are not really present on the records, but that Richards and Walker merely correlated some random noise pulses which happened to be present on the record at a place where they expected or needed an arrival. It may also be seen that we have plotted some additional arrivals which Richards and Walker do not show on their travel time graphs. We feel that some of these arrivals are as genuine as some of the others which both we and they have picked. All arrivals which we have picked from these records were first plotted on a very expanded scale to determine as accurately as possible the apparent velocity. The arrivals were then all plotted together on a travel time graph of fairly large scale, which was replotted on a smaller size sheet included in this thesis. Note that the distances from the shot point to each spread were remeasured by us as accurately as possible on National Topographic Survey maps of scale 1 : 250,000. This graph is in reality an independent interpretation of the records by us. Only the records from the south shot were done, as it was not felt

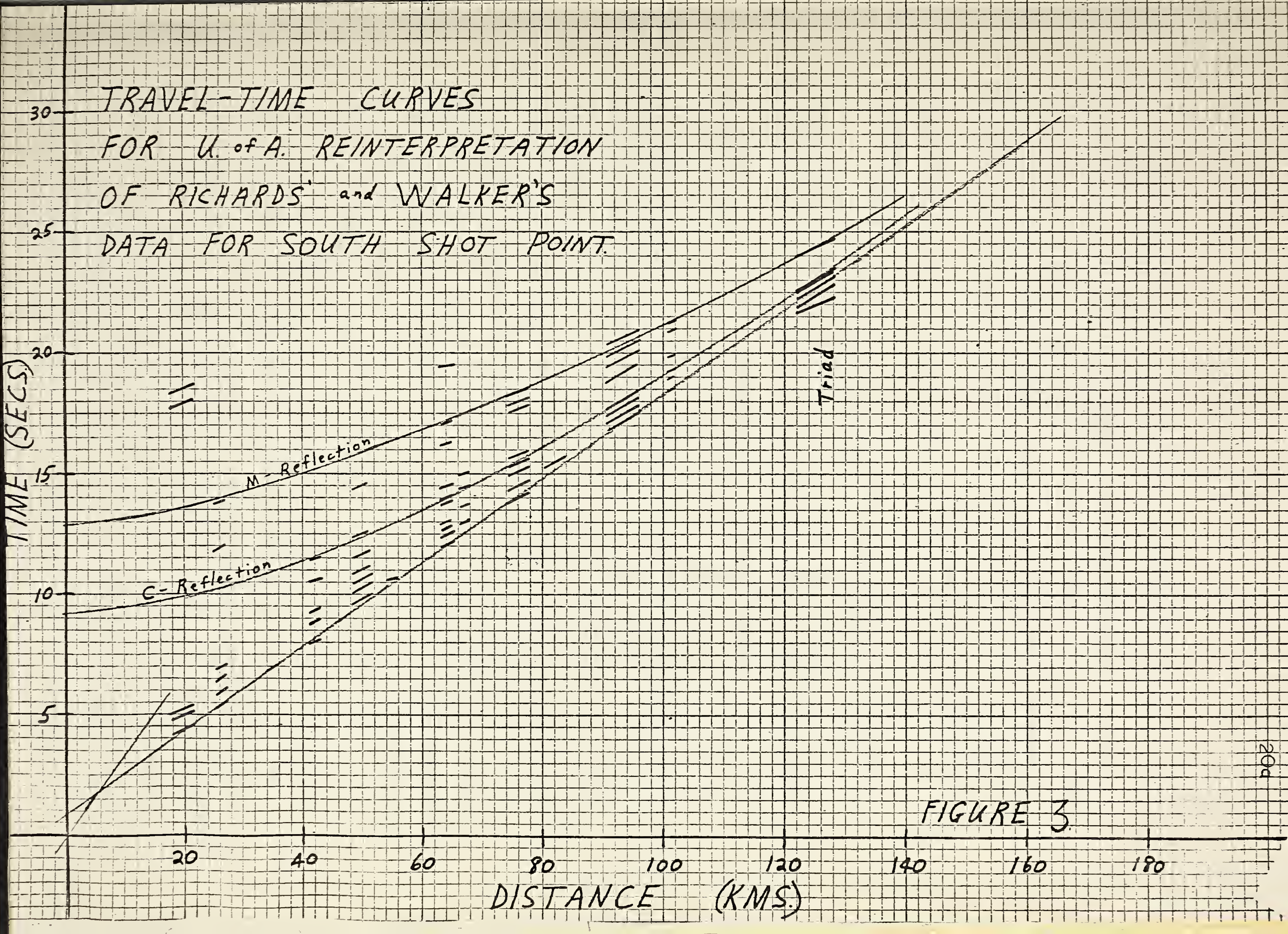

TRAVEL-TIME CURVES
FOR U. of A. REINTERPRETATION
OF RICHARDS' and WALKER'S
DATA FOR SOUTH SHOT POINT.

FIGURE 3.

worthwhile to take the time to do both shots, since this thesis is concerned mainly with our own work at University of Alberta, and not someone else's work. The tables of distances and arrival times have not been included in this thesis because it was not thought necessary, since the graph suffices for the comments that follow. These tables have not been destroyed, however, and are available at the University of Alberta.

The basement velocity from Richards' and Walker's data as calculated by us is 5.7 km./sec. This does not seem as reasonable as the 6.1 km./sec. found by Richards' and Walker, but nevertheless, it seems to be based on more definite arrivals than theirs. It is noted that there are two earlier arrivals shown on our graph for the Triad Spread. But, they are extremely weak, and their very existence is even doubted. However, they may well be real. If so, possibly the line which we have drawn represents the Mississippian layer, and the Precambrian line is a little earlier and faster. With such a short profile, the interpretation is ambiguous. It is seen that the intermediate layer which we have drawn is different from that drawn by Richards and Walker. The line that we have drawn is supported by far more arrivals than that of theoriginal workers. The line drawn for the Moho is almost identical to the one drawn by the original workers. By plotting T^2 vs. X^2 for both the intermediate layer and the Moho, we found the depth to the intermediate layer (possibly the Conrad discontinuity) to be 26 km., and the depth to the Moho to be 43 km. Richards and Walker had found depths of 29 km. and 43 km. respectively. Thus, our reinterpretation yields a Moho depth identical to theirs. But, even so, this reflection line is very indefinite. A longer spread is definitely necessary to obtain

first arrivals for the Moho, or at least, convincing second arrivals, and not merely weak wide-angle reflections. It should also be noted here that this work indicates that the Conrad discontinuity dips slightly to the south-east, while the Moho dips slightly to the north-west, toward the mountains. The dips are small, however, and based on only the single refraction observed from each discontinuity.

CHAPTER III

GENERAL SEISMIC THEORY

The following pages are a general collection of seismic theory from books and papers which are listed in the bibliography. Very little attempt has been made to include the actual development or proof of any theories or methods of interpretation offered in this thesis. It was not thought necessary to do this in order to accomplish the purpose intended (the proofs can be found in the references). The purpose of this section was to collect together various methods of interpretation of seismic results, to summarize these methods for ease of reference, and to establish a uniform set of understandable symbols. I believe that this has been at least partly accomplished. The symbols used are explained adequately, I hope, by the diagrams. At the conclusion of this section on theory, there is a brief discussion on the relative merits of the methods, plus reasons for the fact that only certain of the methods were used in the interpretation of the University of Alberta seismic results.

SEISMIC THEORY

A. Seismic Refraction

1. Horizontal layering:

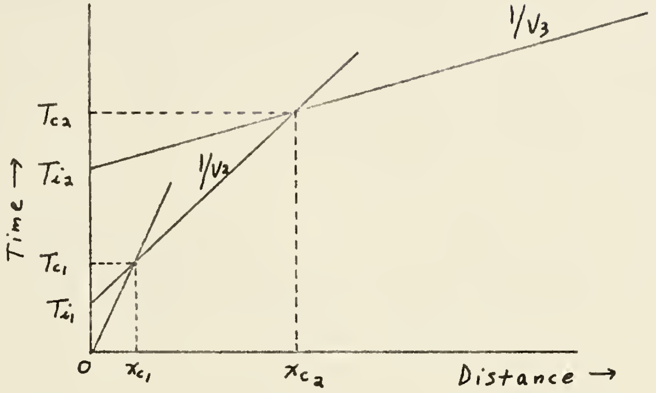

Type graph for a 3-layer case.

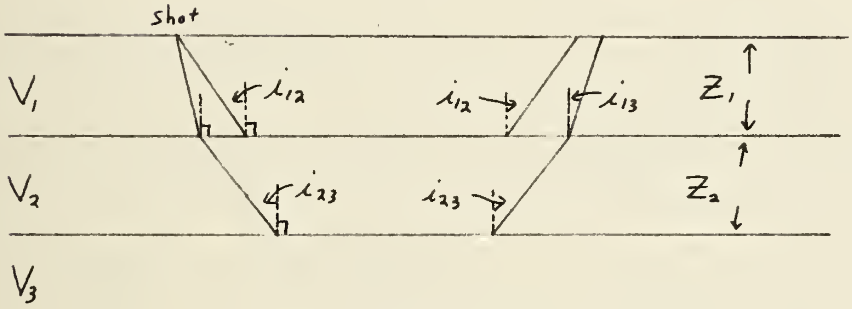

$$V_3 > V_2 > V_1$$

$$\sin i_{13} = \frac{V_1}{V_3}\ , \quad \sin i_{12} = \frac{V_1}{V_2}\ , \quad \sin i_{23} = \frac{V_2}{V_3}$$

n - layer case below:

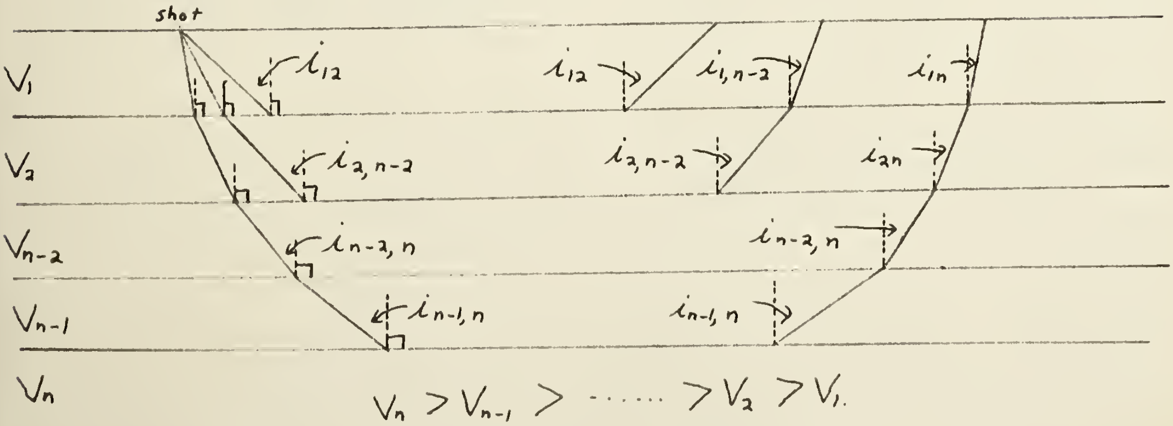

$$V_n > V_{n-1} > \cdots\cdots > V_2 > V_1.$$

$$\sin i_{1,n} = \frac{V_1}{V_n}, \quad \sin i_{2,n} = \frac{V_2}{V_n} \; \ldots\ldots \; \sin i_{n-1,n} = \frac{V_{n-1}}{V_n}$$

$X_{c,n-1}$ = crossover distance for n'th layer.

$T_{i,n-1}$ = intercept time of n'th layer.

Useful formulae:

(a) 2 - layer cases:

$$z_1 = \frac{T_{i1}}{2} \frac{V_1 V_2}{(V_2^2 - V_1^2)^{1/2}}$$

$$\text{or} \quad z_1 = \frac{X_{c1}}{2} \left(\frac{V_2 - V_1}{V_2 + V_1}\right)^{1/2}$$

(b) 3 - layer case:

$$z_2 = \frac{1}{2} \left[T_{i2} - 2z_1 \frac{(V_3^2 - V_1^2)^{1/2}}{V_3 \, V_1} \right] \left[\frac{V_2 \, V_3}{(V_3^2 - V_2^2)^{1/2}} \right]$$

(c) the n - layer case:

$$T_{i,n-1} = 2 \sum_{j=1}^{n-1} z_j \left(\frac{V_n^2 - V_j^2}{V_n^2 \, V_j^2}\right)^{1/2}$$

Solve for z_j as required down to z_{n-1}.

$$\text{or} \quad z_{n-1} = \frac{X_{c,n-1}}{2} \left(\frac{V_n - V_{n-1}}{V_n + V_{n-1}}\right)^{1/2} + \sum_{j=1}^{n-2} z_j \frac{\left(\frac{1}{V_j^2} - \frac{1}{V_{n-1}^2}\right)^{1/2} - \left(\frac{1}{V_j^2} - \frac{1}{V_n^2}\right)^{1/2}}{\left(\frac{1}{V_{n-1}^2} - \frac{1}{V_n^2}\right)^{1/2}}$$

Depth to the n'th layer is $z_1 + z_2 + z_3 + \ldots + z_{n-2} + z_{n-1}$.

(d) Travel time for n - layers:

$$T_{n-1} = \frac{x}{V_n} + 2 \sum_{j=1}^{n-1} z_i \left(\frac{(V_n^2 - V_j^2)}{(V_n^2 V_j^2)}\right)^{1/2}$$

or $$T_{n-1} = \frac{x}{V_n} + 2 \sum_{j=1}^{n-1} \frac{z_j}{V_j} \cos i_{jn}$$

or $$T_{n-1} = \frac{X \sin i_{mn}}{V_m} + 2 \sum_{j=1}^{n-1} \cos i_{jn}$$

where m is any single value from 1 to n-1.

For intercept time for any layer, let $X \to 0$, and get $T_{i,n-1}$

For crossover time, let $X \to X_{c,n-1}$, and get $T_{c,n-1}$.

2. Dipping layers:

A reverse profile must be available for this.

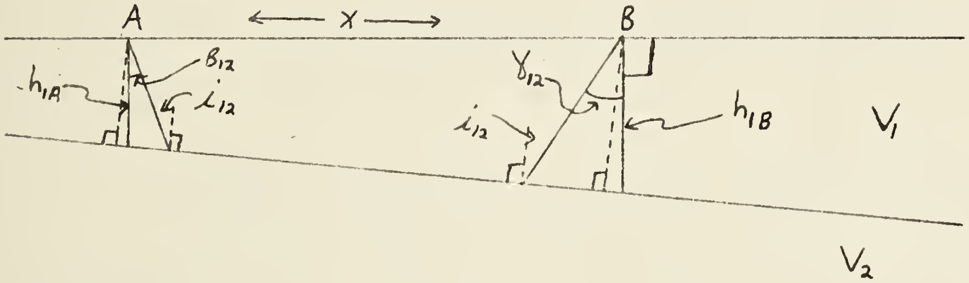

Let us examine the 2 - layer case first, a diagram for which is shown above.

h_{1A} is the vertical thickness under A, while h_{1B} is the vertical thickness under B. α_1 is the angle

of dip, considered positive as shown. β_{12} is the angle between the vertical and the ray at A, while γ_{12} is the angle between the vertical and the ray at B.

$$\beta_{12} = i_{12} - \alpha_1$$

$$\gamma_{12} = i_{12} + \alpha_1$$

Travel time from A to B(downdip) is:

$$T_{1A} = \frac{2\, z_{1A} \cos i_{12}}{V_1} + \frac{X}{V_1} \sin (i_{12} + \alpha_1)$$

Travel time from B to A (updip) is:

$$T_{1B} = \frac{2\, z_{1B} \cos i_{12}}{V_1} + \frac{X}{V} \sin (i_{12} - \alpha_1)$$

Let $X \to 0$, and get intercept times.

$$\therefore \quad T_{i1A} = \frac{2 z_{1A} \cos i_{12}}{V_1} \quad \text{and} \quad T_{i1B} = \frac{2 z_{1B} \cos i_{12}}{V_1}$$

The inverse slope of the downdip segment of the graph gives an apparent velocity of

$$\frac{V_1}{\sin(i_{12} + \alpha_1)} = V_{2A},$$ while the inverse slope of the updip segment gives $$\frac{V_1}{\sin(i_{12} - \alpha_1)} = V_{2B}.$$

V_{2A} and V_{2B} are the apparent velocities that would be found from the travel-time graph, shooting from A and B respectively.

$$\therefore \frac{V_1}{V_{2A}} = \sin(i_{12} + \alpha_1) \quad \text{and} \quad \frac{V_1}{V_{2B}} = \sin(i_{12} - \alpha_1)$$

$$\therefore i_{12} + \alpha_1 = \sin^{-1} \frac{V_1}{V_{2A}} \quad \text{and} \quad i_{12} - \alpha_1 = \sin^{-1} \frac{V_1}{V_{2B}}$$

Add, and get

$$i_{12} = \frac{1}{2}\left[\sin^{-1} \frac{V_1}{V_{2A}} + \sin^{-1} \frac{V_1}{V_{2B}} \right]$$

Subtract, and get:

$$\alpha_1 = \frac{1}{2}\left[\sin^{-1} \frac{V_1}{V_{2A}} - \sin^{-1} \frac{V_1}{V_{2B}} \right]$$

Since, $\sin i_{12} = \frac{V_1}{V_2}$, then true $V_2 = \frac{V_1}{\sin i_{12}}$.

So, now, we can solve for z_{1A} and z_{1B}:

$$z_{1A} = \frac{V_1 T_{i1A}}{2 \cos i_{12}} \quad \text{and} \quad z_{1B} = \frac{V_1 T_{i1B}}{2 \cos i_{12}}$$

and the vertical thicknesses are:

$$h_{1A} = \frac{V_1 \, T_{i1A}}{2 \cos i_{12} \cos \alpha_1} \quad \text{and} \quad h_{1B} = \frac{V_1 \, T_{i1B}}{2 \cos i_{12} \cos \alpha_1}$$

Thus, we have found all the angles, depths, and true velocities for a dipping two-layer case.

If dip is small, one may simply average the apparent velocities from both graphs, and average the intercept times, and use the normal formula for the two-layer, non-dipping case. This will give an average depth between the shot points.

We shall now do the three-layer case, and finally the n-layer case.

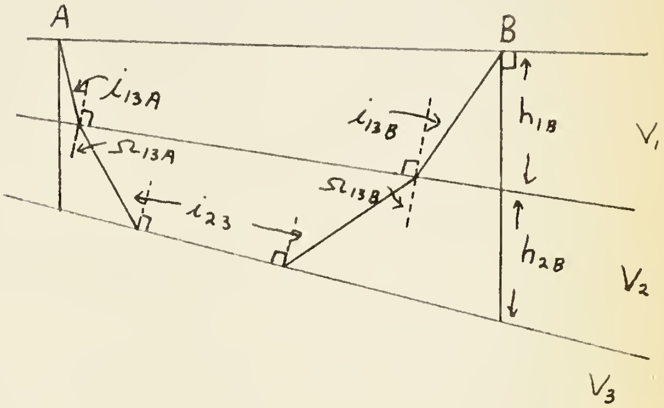

(b) 3 - layer case:

$$\frac{V_1}{V_{3A}} = \sin(i_{13B} + \alpha_1)$$

$$\frac{V_1}{V_{3B}} = \sin(i_{13A} - \alpha_1)$$

$$\therefore \quad i_{13A} = \sin^{-1}\left(\frac{V_1}{V_{3B}}\right) + \alpha_1$$

where α_1 is known from before

$$i_{13B} = \sin^{-1}\left(\frac{V_1}{V_{3B}}\right) - \alpha_1$$

$$\Omega_{13A} = \sin^{-1}\left(\frac{V_2}{V_1}\sin i_{13A}\right)$$

where V_2 is known from before.

$$\Omega_{13B} = \sin^{-1}\left(\frac{V_2}{V_1}\sin i_{13B}\right)$$

$$i_{23} = \frac{\Omega_{13A} + \Omega_{13B}}{2} = \text{the critical angle.}$$

$$\alpha_2 = \frac{\Omega_{13B} - \Omega_{13A}}{2} + \alpha_1 = \text{the dip of the second interface.}$$

$$\text{True } V_3 = \frac{V_2}{\sin i_{23}} .$$

Depths can now be calculated, but will not be included here. They are included for the n-layer case below:

(c) n - layer dipping case:

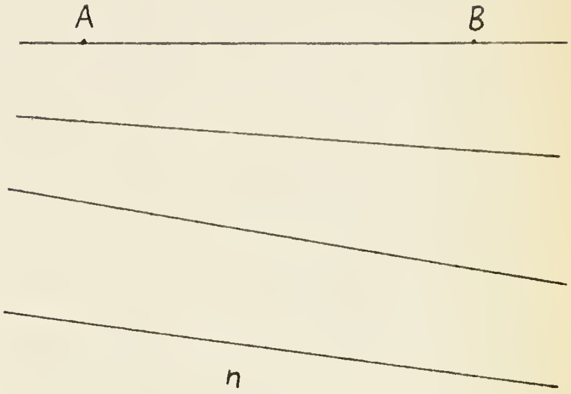

$$\frac{V_1}{V_{nA}} = \sin(i_{1nB} + \alpha_1)$$

$$\frac{V_1}{V_{nB}} = \sin(i_{1nA} - \alpha_1)$$

$$\therefore \quad i_{1nA} = \sin^{-1}\left(\frac{V_1}{V_{nB}}\right) + \alpha_1$$

$$i_{1nB} = \sin^{-1}\left(\frac{V_1}{V_{nA}}\right) - \alpha_1$$

$$\therefore \quad \Omega_{1nA} = \sin^{-1}\left(\frac{V_2}{V_1} \sin i_{1nA}\right)$$

$$\Omega_{1nB} = \sin^{-1}\left(\frac{V_2}{V_1} \sin i_{1nB}\right)$$

And, therefore:

$$i_{2nA} = \Omega_{1nA} + \alpha_2 - \alpha_1$$

$$i_{2nB} = \Omega_{1nB} - \alpha_2 + \alpha_1$$

And, then:

$$\Omega_{m,n,A} = \sin^{-1}\left(\frac{V_{m+1}}{V_m} \sin i_{m,n,A}\right)$$

$$\Omega_{m,n,B} = \sin^{-1}\left(\frac{V_{m+1}}{V_m} \sin i_{m,n,B}\right)$$

And,

$$i_{m,n,A} = \Omega_{m-1,nA} + \alpha_m - \alpha_{m-1}$$

$$i_{m,n,B} = \Omega_{m-1,nB} - \alpha_m + \alpha_{m-1}$$

$$\text{Critical angle} = i_{n-1,n} = \frac{\Omega_{n-2,nB} + \Omega_{n-2,nA}}{2}$$

Angle of dip of the top of the n'th layer is:

$$\alpha_{n-1} = \frac{\Omega_{n-2,nB} - \Omega_{n-2,nA}}{2} + \alpha_{n-2} .$$

And, true velocity in the n'th layer is $V_n = \dfrac{V_{n-1}}{\sin i_{n-1,n}}$.

Thus, we have found all the angles of incidence and refraction, all the angles of dip, and the true velocities in each layer for an n-layer case.

Now, we can very easily find the vertical thicknesses of each layer under point A and point B. From the angles which we now know, we can find the angles between each refracted ray and the vertical. These angles have been mentioned already as β_{in} under the shot point A, and γ_{in} under the point B.

These are found as follows:

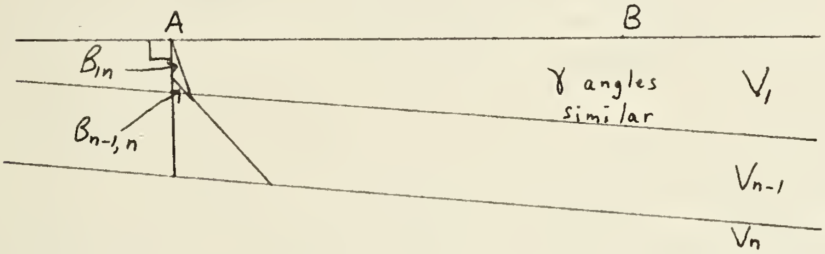

$$\begin{array}{ll}
\beta_{1n} = i_{1nA} - \alpha_1 & \gamma_{1n} = i_{1nB} + \alpha_1 \\
\beta_{2n} = \Omega_{1nA} - \alpha_1 & \gamma_{2n} = \Omega_{1nB} + \alpha_1 \\
\beta_{3n} = \Omega_{2nA} - \alpha_2 & \gamma_{3n} = \Omega_{2nB} + \alpha_2 \\
\cdot \quad \cdot \quad \cdot & \cdot \quad \cdot \quad \cdot \\
\cdot \quad \cdot \quad \cdot & \cdot \quad \cdot \quad \cdot \\
\beta_{n-1,n} = \Omega_{n-2,n,A} - \alpha_{n-2} & \gamma_{n-1,n} = \Omega_{n-2,n,B} + \alpha_{n-2}
\end{array}$$

It may then be shown with difficulty that the intercept of the n'th layer for a shot from A is given as follows:

$$T_{i,n-1,A} = \sum_{j=1}^{n-1} \frac{h_{jA}}{V_j} (\cos \gamma_{j,n} + \cos \beta_{j,n})$$

and for a shot from B as follows:

$$T_{i,n-1,B} = \sum_{j=1}^{n-1} \frac{h_{jB}}{V_j} (\cos \gamma_{j,n} + \cos \beta_{j,n})$$

h_{jA} is the vertical thickness of layer j under shot point A, and h_{jB} is the vertical thickness of layer j under shot point B.

The vertical depth to any layer under a shotpoint is found by adding all the vertical thicknesses down to that layer.

Once the angles are found, these formulae are extremely easy to use to find the depths under each shot point. The only prerequisite is that one have a desk calculator available.

If the dip is very small (i.e. the apparent velocities on the two graphs are not very different), then for an average depth to each layer between the shot points, the values of velocities and intercepts from both graphs may be averaged, and the formulae for horizontal layering used.

B. Seismic Reflection Theory

1. Horizontal layering:

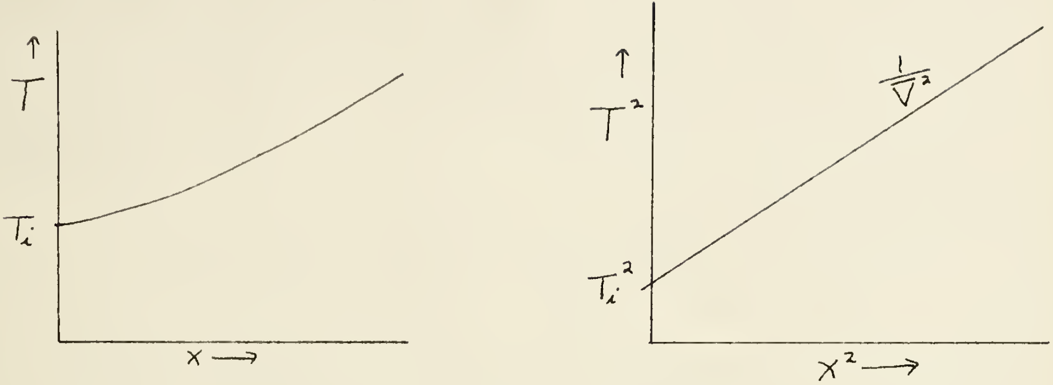

typical reflection curves.

(a) two-layer case:

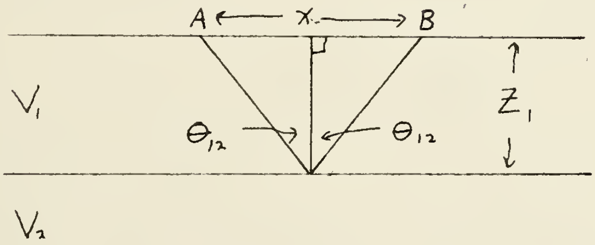

Let θ_{12} be the reflection angle, and let T be the reflection time for distance X.

Then, $(\frac{X}{2})^2 + z_1^2 = (\frac{T}{2})^2(V_1^2)$

Thus, a plot of T vs X will be a hyperbola, while a plot of T^2 vs X^2 will be a straight line.

Thus, the method used is to plot T^2 vs X^2, and find the slope and intercept of the line.

The slope is $\frac{1}{V_1^2}$ and the intercept is

$$T_{i1}^2 = \frac{4z_1^2}{V_1^2}$$

$$\therefore \quad z_1 = \left(\frac{V_1^2 T_{i1}^2}{4}\right)^{1/2} .$$

The critical reflection occurs when $\theta_{12} = i_{12}$, the critical angle. Let X_{k1} be the critical distance.

$$\text{Then,} \quad X_{k1} = \frac{2z_1V_1}{V_2\left(1 - \dfrac{V_1^2}{V_2^2}\right)^{1/2}} ,$$

and the time for this critical reflection is

$$T_{k1} = \frac{2z_1}{V_1\left(1 - \dfrac{V_1^2}{V_2^2}\right)^{1/2}}$$

(b) three-layer case:

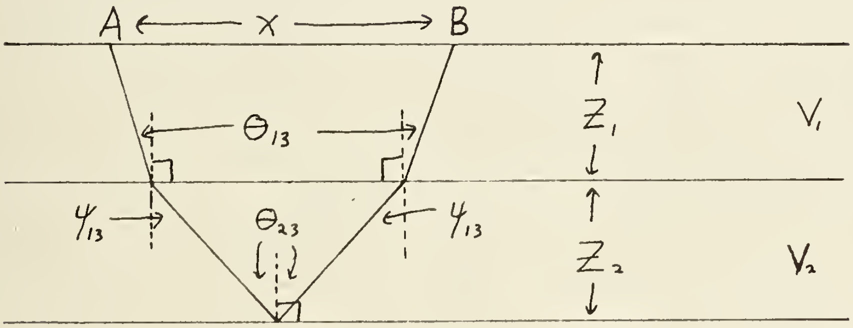

$$\frac{\sin \theta_{13}}{\sin \psi_{13}} = \frac{V_1}{V_2} = \frac{\sin \theta_{13}}{\sin \theta_{23}}$$

Let $1/\lambda$ be a parameter, representing the apparent emergent velocity.

$$\therefore \quad \frac{1}{\lambda} = \frac{V_1}{\sin \theta_{13}}$$

$$\therefore \quad \lambda = \frac{\sin \theta_{13}}{V_1}$$

$$\therefore \quad \sin \theta_{23} = \lambda V_2$$

Total path travelled is: $\dfrac{2z_1}{\cos \theta_{13}} + \dfrac{2z_2}{\cos \theta_{23}}$

Total time $= \dfrac{2z_1}{V_1(1-\lambda^2 V_1^2)^{1/2}} + \dfrac{2z_2}{V_2(1-\lambda^2 V_2^2)^{1/2}}$ for travel time, *in terms of* λ.

And, $\therefore \quad X = \dfrac{2\lambda z_1 V_1}{(1-\lambda^2 V_1^2)^{1/2}} + \dfrac{2\lambda x_2 V_2}{(1-\lambda^2 V_2^2)^{1/2}}$

Knowing λ, z_1, V_1, V_2, and T, we can calculate z_2. Or, if z_2 is also known, we can use the above formulae to calculate the reflection curve.

Consider a critical reflection: For this case, $\theta_{13} = i_{13}$, and $\theta_{23} = i_{23}$ (the critical angle).

Also, $\lambda = \dfrac{\sin i_{13}}{V_1} = \dfrac{1}{V_3}$

$$\therefore \quad X_{k2} = \frac{2z_1 V_1}{V_3\left(1-\frac{V_1^2}{V_3^2}\right)^{1/2}} + \frac{2z_2 V_2}{V_3\left(1-\frac{V_2^2}{V_3^2}\right)^{1/2}}$$

$$\text{and} \quad T_{k2} = \frac{2z_1}{V_1\left(1-\frac{V_1^2}{V_3^2}\right)^{1/2}} + \frac{2z_2}{V_1\left(1-\frac{V_2^2}{V_3^2}\right)^{1/2}}$$

(c) n-layer case:

$$\lambda = \frac{\sin \theta_{1n}}{V_1}$$

$$X = 2 \sum_{i=1}^{n-1} \frac{\lambda z_i V_i}{(1-\lambda^2 V_i^2)^{1/2}}$$

$$\text{and} \quad T = 2 \sum_{i=1}^{n-1} \frac{z_i}{V_i(1-\lambda^2 V_i^2)^{1/2}}$$

For a critical reflection, $\lambda = \frac{1}{V_n}$.

$$\therefore X_{k,n-1} = 2 \sum_{i=1}^{n-1} \frac{z_i V_i}{V_n\left(1-\frac{V_i^2}{V_n^2}\right)^{1/2}}$$

$$\text{and} \quad T_{k,n-1} = 2 \sum_{i=1}^{n-1} \frac{z_i}{V_i\left(1-\frac{V_i^2}{V_n^2}\right)^{1/2}}$$

λ is actually dT/dX of the reflection curve at the distance X which is being considered. An accurate method of finding λ as given by Dix will be discussed later.

(d) Short-cut method of finding depths by reflection data:

This method simply ignores the refractions in the upper layers, and treats the problem as a two-layer case.

In practice, this works as follows:

The valves of X and T for various reflection

arrivals are squared, and plotted on a $T^2 - X^2$ graph. They will not all fall on a straight line, but on a curve which is concave downwards. A least-square straight line, however, may be drawn through the points. This straight line will give a greater intercept than the curve would, and would also give a slightly greater average velocity. Thus, the depth calculated by this method is always slightly greater than the actual depth. The error introduced is, in general, not too significant, and most workers use this short-cut method for finding depths. It is virtually the only method which can be used if no information is obtained by refraction methods down to the reflecting horizon. This is also the method used in the interpretation of reflection data which appears on the seismic records taken by the University of Alberta in Southern Alberta.

(e) Accurate method of determining the parameter λ, and of removing the effect of the upper layer, for a 3-layer case:

This method was given by Dix (1955).

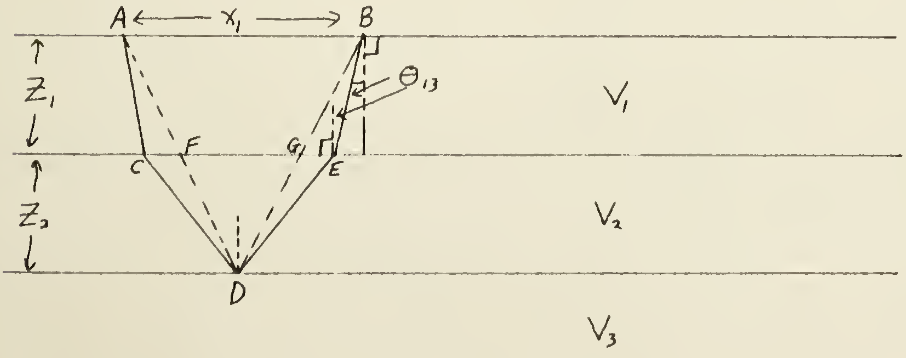

As stated before, the T^2 vs X^2 curve for the reflection path A C D E B will be a curve very slightly concave downwards, because it is a shorter time path than the path A F D G B .

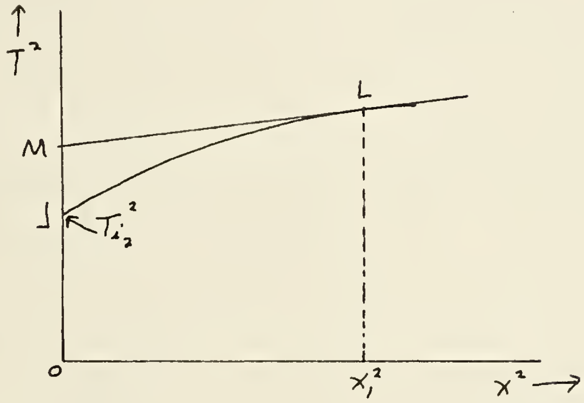

We shall solve the problem by removing the effect of the upper layer.

Firstly, we must determine the angle θ_{13}.

We know that $\lambda = \frac{\sin \theta_{13}}{V_1} = \frac{dT}{dX}$ at the distance considered.

We assume that V_1 is known, and thus, the problem is to accurately determine dT/dX.

A direct determination, but not very accurate, is to use the T - x curve, and set the derivative equal to ΔT/ΔX. But, ΔT must be kept down to about .010 sec. or the chord will not be a good approximation to the tangent. ΔT requires two time measurements, each with a probable error of at least ± 0.001 secs., which would

correspond to an error of ± 0.0014 sec. for ΔT, or about 14%. This is a very large error.

So, instead of the T - X curve, we use the $T^2 - X^2$ curve. We draw the tangent to the $T^2 - X^2$ curve at X_1^2 (the value of X we are considering; i.e., the value of X where the reflection under consideration occurs). The tangent is easy to draw, since the curve is almost straight at this point. The line L M is the tangent.

L M has the equation:

$$T^2 = M + \frac{X^2}{\bar{V}_2^{\,2}(X_1)}$$

[$\bar{V}_2^{\,2}(X_1)$ is the inverse slope of the line]

If we differentiate this equation with respect to X, at $X = X_1$, we get

$$T\,\frac{dT}{dX} = \frac{X_1}{\bar{V}_2^{\,2}\,(X_1)}$$

Thus, $\lambda = \dfrac{X_1}{T\,\bar{V}_2^{\,2}(X_1)}$ at $X = X_1$, where T is the reflection time at $X = X_1$.

Thus, λ can be found accurately this way.

We can also remove the effect of the upper layer, and find the true V_2.

$$\lambda = \frac{X_1}{T\,\bar{V}_2^{\,2}\,(X_1)} = \frac{\sin\,\theta_{13}}{V_1}$$

and $\therefore \quad \sin\theta_{13} = \dfrac{X_1V_1}{T\,\overline{V}_2^{\,2}(X_1)}$.

From θ_{13}, AC and BE are computed.

$$AC = BE = \frac{z_1}{\cos\theta_{13}}$$

From this, we can compute the time to be removed from T to give the time from C to D to E.

The time to be removed is $\dfrac{2z_1}{V_1\cos\theta_{13}}$.

This gives T_R or T reduced.

We can also compute 2EH and subtract this from X to give X_R. $2EH = 2z_1 \tan\theta_{13}$.

Thus, we have effectively removed the upper layer. If we do this for several points X_i, and if we plot T_R^2 as X_R^2, we get a straight line whose equation is:

$$T_R^2 = Ti_{2R}^2 + \frac{X_R^2}{V_2^2}$$

$\sqrt{\text{inverse slope}}$ gives us V_2, and $\sqrt{\text{intercept}}$ gives us Ti_{2R}. The thickness of the second layer is:

$$z_2 = \frac{V_2 Ti_{2R}}{2}$$

This method has been developed for only three layers, but it could be extended to more complicated layering.

In order to use this method, we must know the thicknesses and velocities of the layers above the one we are

interested in. This is not always possible.

2. Dipping Layers:

(a) 2-layer case:

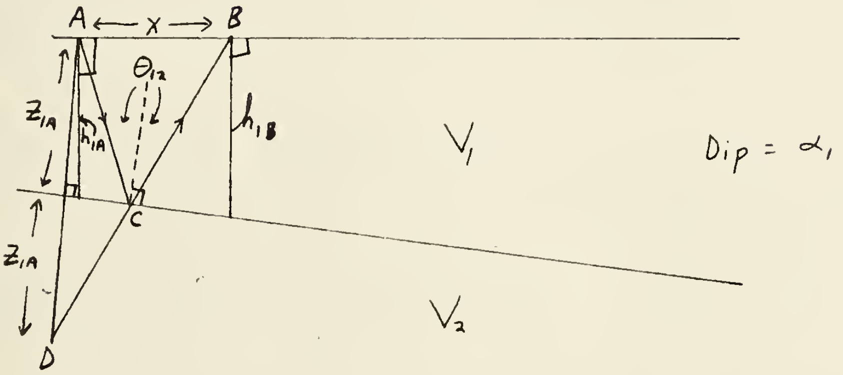

Travel time for shot at A is:

$$T_A = \frac{AC}{V_1} + \frac{CB}{V_1} = \frac{AC}{V_1} + \frac{CD}{V_1} = \frac{BD}{V_1}$$

$$\text{But, } (BD)^2 = (AD)^2 + (AB)^2 - 2\ AD \cdot AB \cos BAD.$$

$$\therefore\ (BD)^2 = 4z_{1A}^2 + X^2 - 4z_{1A}\,X \cos\,(90 + \alpha_1).$$

$$\therefore\ T_A^2 V_1^2 = 4z_{1A}^2 + X^2 + 4Xz_{1A} \sin \alpha_1$$

$$\therefore\ T_A^2 = \frac{4z_{1A}^2}{V_1^2} + \frac{X^2}{V_1^2} + \frac{4Xz_{1A}}{V_1^2} \sin \alpha_1$$

Similarly, for a shot at B,

$$T_B^2 = \frac{4z_{1B}^2}{V_1^2} + \frac{X^2}{V_1^2} - \frac{4Xz_{1B}}{V_1^2} \sin \alpha_1$$

A plot of T vs X is a parabola now, and not a hyperbola.

If we plot T_A vs X, the intercept is $\frac{2z_{1A}}{V_1}$, and if we plot T_B vs X, the intercept is $\frac{2z_{1B}}{V_1}$.

The vertical depth under A is $\frac{z_{1A}}{\cos \alpha_1}$ and under B is $\frac{z_{1B}}{\cos \alpha_1}$.

$$\text{Now,} \quad \frac{dT_A}{dX} = \frac{X}{T_A V_1^2} + \frac{2z_{1A}}{T_A V_1^2} \sin \alpha_1$$

$$\text{and,} \quad \frac{dT_B}{dX} = \frac{X}{T_B V_1^2} - \frac{2z_{1B}}{T_B V_1^2} \sin \alpha_1$$

These values are the reciprocal of the step-out velocity, or apparent velocity at any point X. These are the λ values.

If $\alpha_1 = 0$, the step-out velocity is the same as for a non-dipping layer. If step-out velocity is greater than normal, the signal was recorded downdip. If step-out velocity is less than normal, signal was recorded updip.

These equations are really not very useful, unless α_1 and V_1 are known from a refraction profile.

This method becomes cumbersome for more than two layers.

(b) Method of Steinhart et al:

2-layer case:

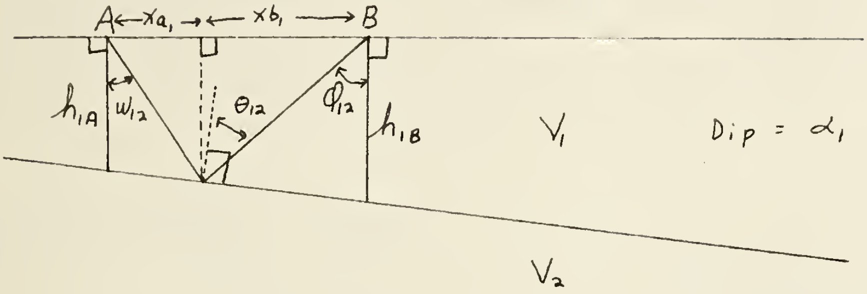

Consider a shot at A.

Use the parameter method.

$\lambda = \dfrac{\sin \varphi_{12}}{V_1}$. We know how to find λ, so we can find φ_{12}, assuming we know V_1.

$$\theta_{12} = \varphi_{12} - \alpha_1$$

$$W_{12} = \theta_{12} - \alpha_1$$

By geometry,

$$X_{a1} = \frac{h_{1A}}{\dfrac{1}{\tan W_{12}} - \tan \alpha_1} \quad \text{and} \quad X_{b1} = \frac{h_{1A} + X_{a1} \tan \alpha_1}{\dfrac{1}{\tan \varphi_{12}}}$$

$$X = X_{a1} + X_{b1}$$

$$t_{1A} = \frac{h_{1A} + X_{a1} \tan \alpha_1}{V_1 \cos W_{12}} \quad \text{and} \quad t_{1B} = \frac{h_{1A} + \tan \alpha_1 (X_{a1} + X_{b1})}{V_1 \cos \varphi_{12}}$$

∴ total travel time for a shot at A is $T_A = t_{1A} + t_{1B}$.

Now, consider a shot at B:

$$\text{in this case, } \lambda = \frac{\sin W_{12}}{V_1}$$

$$\therefore \theta_{12} = W_{12} + \alpha_1$$

$$\varphi_{12} = \theta_{12} + \alpha_1$$

and, by geometry again:

$$X_{b1} = \frac{h_{1B}}{\frac{1}{\tan \varphi_{12}} + \tan \alpha_1} \quad \text{and } X_{a1} = \frac{h_{1B} - X_{b1} \tan \alpha_1}{1/\tan W_{12}}$$

$$X = X_{b1} + X_{a1}.$$

I should note here that I am using one diagram for two things. In other words, for a shot at A, we are not necessarily recording at the other shot point, or vice versa. Thus, X_{b1} for a shot at B may be different than X_{b1} for a shot at A. In short, X and θ_{12} are changing.

$$t_{1B} = \frac{h_{1B} - X_{b1} \tan \alpha_1}{V_1 \cos \varphi_{12}} \quad \text{and} \quad t_{1A} = \frac{h_{1B} - \tan \alpha_1 (X_{b1} + X_{a1})}{V_1 \cos W_{12}}$$

$\therefore$ total travel time for a shot at B is $T_B = t_{1B} + t_{1A}$.

For a critical reflection, θ_{12} becomes i_{12}, the critical angle, and W_{12} becomes β_{12}, and φ_{12} becomes γ_{12}. This simplifies matters a great deal.

In all of these formulae, many of the quantities must be known, before others can be found. If all are known, the formulae can be used to calculate the reflection curve.

(c) n-layer case:

The method given by Steinhart et al., which has been outlined for a two-layer case can easily be extended to a n-layer case. These formulae are most useful when used in conjunction with refraction data to calculate critical distances. Thus, for the n-layer case, the formulae are stated in the form used to find critical distance. If they are to be used for any reflected ray, the parmeter λ must be introduced.

$$\lambda = \frac{\text{sin of the emergent angle}}{V_1}$$

Then, $i_{n-1,n}$ becomes $\theta_{n-1,n}$, and β_{jn} becomes W_{jn}, and γ_{jn} becomes φ_{jn}. Otherwise, the formulae are the same.

Thus, for an n-layer case, the critical distance is found as follows, if the shot is from point A:

$$X_{a1} = \frac{h_{1A}}{\dfrac{1}{\tan \beta_{1n}} - \tan \alpha_1}$$

$$X_{a2} = \frac{h_{2A} + X_{a1}\,(\tan \alpha_2 - \tan \alpha_1)}{\dfrac{1}{\tan \beta_{2n}} - \tan \alpha_2}$$

$$\begin{array}{ccc} \cdot & \cdot & \cdot \\ \cdot & \cdot & \cdot \\ \cdot & \cdot & \cdot \end{array}$$

$$X_{an-1} = \frac{h_{n-1A} + (\sum_{i=1}^{n-2} X_{ai})(\tan \alpha_{n-1} - \tan \alpha_{n-2})}{\dfrac{1}{\tan \beta_{n-1,n}} - \tan \alpha_{n-1}}$$

$$X_{bn-1} = \frac{h_{n-1A} + (\sum_{i=1}^{n-1} X_{ai})(\tan \alpha_{n-1} - \tan \alpha_{n-2})}{\frac{1}{\tan \gamma_{n-1,n}} + \tan \alpha_{n-2}}$$

$$X_{bn-2} = \frac{h_{n-2A} + (\sum_{i=1}^{n-1} X_{ai} + X_{bn-1})(\tan \alpha_{n-2} - \tan \alpha_{n-3})}{\frac{1}{\tan \gamma_{n-2,n}} + \tan \alpha_{n-3}}$$

$$\vdots \qquad \qquad \vdots \qquad \qquad \vdots$$

$$X_{b2} = \frac{h_{2A} + (\sum_{i=1}^{n-1} X_{ai} + \sum_{i=n-1}^{3} X_{bi})(\tan \alpha_{2} - \tan \alpha_{1})}{\frac{1}{\tan \gamma_{2n}} + \tan \alpha_{1}}$$

$$X_{b1} = \frac{h_{1A} + \tan \alpha_{1} \, (\sum_{i=1}^{n-1} X_{ai} + \sum_{i=n-1}^{2} X_{bi})}{\frac{1}{\tan \gamma_{1n}}}$$

All of the X_{ai} and X_{bi} are the projections of the ray paths on the horizontal plane. Thus, the critical distance for the n'th layer is as follows:

$$X_{k,n-1} = \sum_{i=1}^{n-1} (X_{ai} + X_{bi})$$

The time that it takes its ray segment to travel its distance can also easily be found:

$$t_{a1} = \frac{X_{a1}}{V_1 \sin \beta_{1n}}$$

$$t_{a2} = \frac{X_{a2}}{V_2 \sin \beta_{2n}}$$

$$\begin{matrix} \cdot & & \cdot \\ \cdot & & \cdot \\ \cdot & & \cdot \end{matrix}$$

$$t_{an-1} = \frac{X_{an-1}}{V_{n-1} \sin \beta_{n-1,n}}$$

$$t_{bn-1} = \frac{X_{bn-1}}{V_{n-1} \sin \gamma_{n-1,n}}$$

$$\begin{matrix} \cdot & & \cdot \\ \cdot & & \cdot \\ \cdot & & \cdot \end{matrix}$$

$$t_{b2} = \frac{X_{b2}}{V_2 \sin \gamma_{2n}}$$

and $$t_{b1} = \frac{X_{b1}}{V_1 \sin \gamma_{1n}}$$

$\therefore$ total travel time for a shot at point A is :

$$T_A = \sum_{i=1}^{n-1} (t_{ai} + t_{bi})$$

And, since it is the critical ray we are considering this is the critical time for the n'th layer, $T_{k,n-1}$.

I will not restate the formulae for a shot from point B, but I will just indicate the first and the last. The others follow the same pattern.

$$X_{b1} = \frac{h_{1B}}{\dfrac{1}{\tan \gamma_{1n}} + \tan \alpha_1}$$

$$\vdots \qquad\qquad \vdots \qquad\qquad \vdots$$

$$X_{a1} = \frac{h_{1B} - \tan \alpha_1 \left(\sum_{i=1}^{n-1} X_{bi} + \sum_{i=n-1}^{2} X_{ai} \right)}{\dfrac{1}{\tan \beta_{1n}}}$$

These formulae are very useful for calculating the critical distances in both directions for a reverse profile where velocities, depths, angles, and dips are known from the refraction data. This was the method used to calculate the critical distances for the seismic work done by the University of Alberta.

C. Time - Term Method of Seismic Interpretation:

This will be a very brief treatment of the method given by Scheidegger and Willmore.

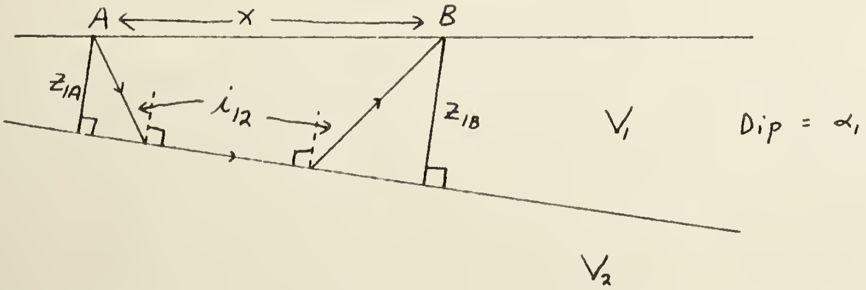

Consider a shot at point A.

From the theory considered earlier, the travel time from A to B is:

$$T_A = \frac{2z_{1A} \cos i_{12}}{V_1} + \frac{X}{V_1} \sin(i_{12} + \alpha_1).$$

$$\therefore T_A V_1 = 2z_{1A} \cos i_{12} + X(\sin i_{12} \cos \alpha_1 + \cos i_{12} \sin \alpha_1)$$

Now, $z_{1B} - z_{1A} = X \sin \alpha_1$

$$\therefore T_A V_1 = 2z_{1A} \cos i_{12} + (z_{1B} - z_{1A}) \cos i_{12} + X \sin i_{12} \cos \alpha_1$$

α_1 is usually very small, and thus we can set $\cos \alpha_1 = 1$, without great error.

$$\therefore T_A = \frac{z_{1A} \cos i_{12}}{V_1} + \frac{z_{1B} \cos i_{12}}{V_1} + \frac{X}{V_2}$$

or $T_A = a + b + \frac{X}{V_2}$ where $a = \frac{z_{1A} \cos i_{12}}{V_1}$

and $b = \frac{z_{1B} \cos i_{12}}{V_1}$

a and b are called time - terms. a is the time - term under the shot point and b is the time - term under the detector.

$$a + b = T_A - \frac{x}{V_2}$$

Suppose now that we have n shots and m detectors. Let i be one of the shot points, and j be one of the detectors. Then, $a_i + b_j = T_{ij} - \frac{X_{ij}}{V_2}$ is the general

equation for a shot at station i and a pickup at station j. Or, in general terms,

$$P_{st}Y_t = M_s \qquad \text{(the observational equations).}$$

where $Y_t = a_i$ or b_j (i.e., all of the time terms),

and $M_s = T_{ij} - \frac{X_{ij}}{V_2}$.

$P_{st} = 1$ when T refers to a shot point or detector for which travel time appears in the s'th equation, and otherwise $P_{st} = 0$.

Apart from V_2, we have (m + n) unknowns. For a unique solution, the value of one time - term must be assumed, and is set equal to zero to simplify calculations. When calculations are completed, the arbitrary term is introduced. So, now we have (m + n - 1) unknowns, that is, the a_i and b_j.

The normal equation s is produced by multiplying each of the k observational equations by P_{st} and adding.

∴ the normal equations can be written: $q_{st}Y_t = \ell_s$.
The problem is to solve this equation!

Cracovians are used to do this. Cracovians are like ordinary matrices, but the multiplication rules are as follows:

$$C_{ik} = a_{ij}\ b_{kj}$$

Thus, C_{ik} is the sum of the products of the pairs of

coefficients which occur in each row of the i'th and k'th columns.

$$a = a_{\overset{\text{column}}{i}\,\overset{\text{row}}{j}}$$

$$q = p \cdot p$$

$$\ell = m \cdot p$$

Cracovian q is square and symmetric.

$$\therefore \quad Y \cdot q = \ell$$

The solution of this system yields the least square solution for the array of unknowns represented by Y.

The solution is $Y^T = q^{-1}\ell$ where Y^T is Y transposed.

Thus, all we have to do is find q^{-1}.

Now, every symmetric cracovian can be represented by the product of two identical triangular cracovians.

i. e. $\quad q = g \cdot g$

i.e. $$\begin{pmatrix} q_{11} & q_{21} \cdots \\ q_{21} & q_{22} \cdots \\ \cdots & \cdots \\ \cdots & \cdots \end{pmatrix} = \begin{pmatrix} g_{11} & g_{21} \cdots \\ 0 & g_{22} \cdots \\ 0 & 0 \; \cdots \\ \cdots & \cdots \end{pmatrix} \begin{pmatrix} g_{11} & g_{21} \cdots \\ 0 & g_{22} \cdots \\ 0 & 0 \; \cdots \\ \cdots & \cdots \end{pmatrix}$$

$$\therefore \; q_{11} = g_{11}^{2} \quad \text{and} \quad \therefore \; g_{11} = \sqrt{q_{11}}$$

$$q_{12} = q_{21} = g_{21}g_{11} \quad \text{and} \quad \therefore \; g_{21} = \frac{q_{12}}{g_{11}}$$

$$q_{22} = g_{21}^{2} + g_{22}^{2} \quad \text{and} \quad \therefore \; g_{22} = \sqrt{q_{22} - g_{21}^{2}}$$

. . . . . .

Thus, the elements of g can be found one by one.

Finally, we find q^{-1} from: $g^{-1} = q^{-1}(g^T)$. For this, only the diagonal elements of g^{-1} are needed, and these are simply $g_{ii}^{-1} = \frac{1}{g_{ii}}$.

The terms of q^{-1} can be calculated one by one beginning with the lower right, and noting that q^{-1} is symmetric.

We know that $\ell = m \cdot p$, and $\therefore$

$$\ell_i = \sum_k t_{ik} - \frac{1}{V_2} \sum_k X_{ik},$$ where k takes all values appropriate to all stations which observed shot i (or to all shots observed at station i).

Time terms $= Y^T = q^{-1}\,\ell$.

We next insert Y into the observational equations;

$a_i + b_j = T_{ij} - \frac{X_{ij}}{V_2}$, and we get a set of expressions of the form: $C_{ik} - \frac{1}{V_2} d_{ik} = \delta_{ik}$, where δ_{ik} is the residual.

$$V_2 = \frac{\Sigma\ d_{ik}^{\ 2}}{\Sigma\ C_{ik}\ d_{ik}}\ .$$

The square of the standard deviation e of Y_i is:

$e_i^{\ 2} = \frac{q_{ii}^{-1}\ \delta^2}{K - L}$ where δ^2 is the sum of the squares of the residuals from the observational equations, K is the number of observational equations, and L is the number of unknowns.

If all n shots have been observed at all m stations, the problem is easier.

In this case,

$$q = p^2 = \begin{pmatrix} mI^1 & E^1 \\ E^{11} & nI^{11} \end{pmatrix}$$

where the E's have one in all positions, and the I's are identity cracovians.

I^1 is square and has n columns.

I^{11} has (m-1) columns (as b for the last station has been set to zero).

E^1 has (m-1) columns and n rows.

$E^{11} = (E^1)^T$.

$$q^{-1} = \left\{ \begin{matrix} \left\{ \begin{matrix} x & y & y & . & . & . & . \\ y & x & y & . & . & . & . \\ y & y & x & . & . & . & . \\ . & . & . & . & . & . & . \end{matrix} \right\} & zE^1 \\ zE^{11} & \left\{ \begin{matrix} \xi & \eta & \eta & .... \\ \eta & \xi & \eta & .... \\ \eta & \eta & \xi & .... \\ . & . & . & .... \end{matrix} \right\} \end{matrix} \right\}$$

$q^{-1}q = 1$ and $\therefore$ $Xm + z(m-1) = 1$

$Ym + z(m-1) = 0$

$X + Y(n-1) + zn = 0$

$nz + \xi n = 1$

$nz + \eta n = 0$

And, $\therefore$ $$X = \frac{m+n-1}{mn}$$

$$Y = \frac{m-1}{mn}$$

$$z = -\frac{1}{n}$$

$$\xi = \frac{2}{n}$$

$$\eta = \frac{1}{n}$$

Next, we have to estimate the value of the time term which we assumed was zero. Once this is done, the actual values of all the time - terms can be found. The value of the time term at any point gives the depth at that point.

This method would be very useful if a large number of shot points and detector locations were used. The subsurface could then be mapped very accurately using the time-term method. But, if only two shot points are used, one at each end of the straight line profile along which detectors are laid out, then this method would not yield that much more useful information than ordinary seismic theory for the work involved. Furthermore, it has only been developed for two layers to date, which is not very practical.

D. The Plus - Minus Method of Interpretation:

This method was developed by J. G. Hagedoorn. If travel times to a number of seismometers are recorded from two shot points, then the surface of the refractor may be outlined by a Huygen construction in reverse. An approximate method based on this theory is the plus - minus method.

The plus values at the surface, that is, the simple addition of the two travel times to each seismometer, minus the constant total travel time between the two shotpoints, will be proportional to the depths, to a degree of accuracy depending on the relief of the refractor surface and on the variation of velocity in the refractor. This plus - value is the same quantity that is usually called the intercept time. It must be multiplied by a scale factor, depending on the velocities, to get the actual depth.

If the minus values (the simple subtraction of the two travel times to each seismometer) are plotted against distance along the surface, then the slopes of the plotted line through the points will give a picture of the varying velocities in the refractor.

In essence, the plus - minus method transforms the two measured variables at each seismometer into two independent variables, the plus values or intercept times at each point, which give the depths or delay times of the over-

burden, and the minus values which give the velocities in the underlying layer.

This method could be very useful if the sqme seismometer locations were used for shots from each end of the profile.

E. Least Square Fitting the Line Segments:

If we have a line whose equation is:

$T = T_i + \frac{X}{V}$, where T_i is intercept time, and if this line is given by N points (X_j, t_j), then the least squares solutions for T_i and V are given by the following:

$$\frac{1}{V} = \frac{\Sigma X_j t_j - \frac{\Sigma X_j \; \Sigma t_j}{N}}{\Sigma X_j^2 - \frac{(\Sigma X_j)^2}{N}}$$

and $$T_i = \frac{\Sigma X_j \; \Sigma X_j t_j - \Sigma t_j \; \Sigma X_j^2}{(\Sigma X_j)^2 - N(\Sigma X_j^2)}$$

These formulae are the normal least squares formulae, and should always be used in refraction seismology to calculate the best straight line through a number of arrivals. These formulae were quoted here simply for ease of reference.

F. Correlation of Seismic Waves:

This is a summary of the paper by Veitsman (1957) dealing with the problem of correlation tracing of seismic waves and wave groups recorded in seismic depth soundings of the earth's crust. On the basis of analysis of a number of stable kinematic and dynamic indications, criteria have been formulated for the separation and identification of wave groups recorded on separate profiles. These criteria for revealing and identifying basic wave groups are given below:

(a) Kinematic criteria:

    (1) Criteria from arrival time:

        (i) the order of arrival of the different wave groups determined as a function of the distance from explosion point.

        (ii) an approximately rectilinear form of the hodograph drawn for the first waves of each group. A hodograph is simply a graph of the arrival times vs. distance for a wave group, with each point joined, rather than the best straight line through them drawn. For a genuine arrival, the hodograph should be approximately a straight line.

        (iii) an approximately prallel relation between successive hodographs constructed according to the first waves of one and the same group.

(iv) fulfilment of the principle of reciprocity: that is, the equality of arrival times at reciprocal points on reversed hodographs. In other words, the interchange of shot and detector should yield the same arrival time for a particular wave group.

(2) Criteria for apparent velocities:

(i) similar apparent velocity values for the majority of waves of one group, and very different values for the other groups.

(ii) similar apparent velocity values for waves of a group determined from phase hodographs on continuous profiles.

(b) Dynamic criteria:

(1) Criteria from intensity:

(i) the presence of a relative maximum for each wave group on the amplitude curve $A = A(t)$, inside the interference zone; that is, where the wave groups are separated.

(ii) a determined regularity in the variability of the relative intensity of the waves of the different wave groups as a function of distance from the shot point. An example is shown below:

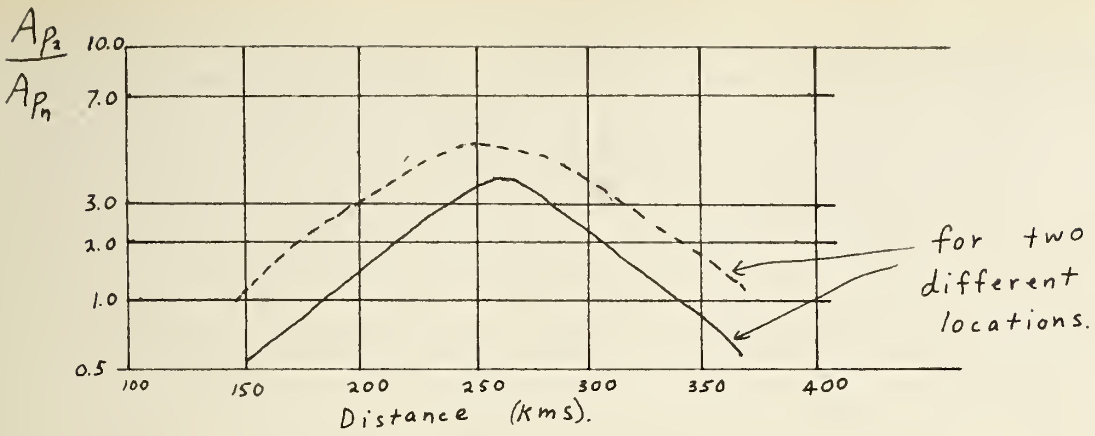

(2) Criteria from form of the trace:

This means stability of the form of trace for each wave group on the separate profiles.

(3) Frequency criterion:

There should be a small difference in the prevailing values of the frequencies recorded for the difference wave groups.

Those were the criteria which can be used to correlate groups of waves recorded on various spreads at different distances from the shot, with ten to twenty kilometres or more between spreads. The fact that P_2 (intermediate layer) and P_n (Moho) waves recorded on earthquake traces as individual waves appear as wave groups on SDS seismograms (Seismic Depth Sounding) is probably the result of the greater distinguishing capacity of the SDS method in comparison with the ordinary methods of seismology. The first waves of each group are single refracted head waves connected with the main and clearest seismic boundaries in the earth's crust. The nature of

the subsequent waves is still not clear, but they may be due to a thin-layered transition region between layers with different seismic-wave propagation velocities. Veitsman states that on their records, at least, there is no basis for thinking that among these waves there are any which travel along refraction boundaries as transverse waves.

I will now just briefly state here the characteristics of the basic wave groups found on the seismograms taken in Russia. Waves of the P_1 group (granite layer) were traced as first arrivals out to 200 kms. from the shot point. On the SDS seismograms, they are rather weak, and dampen rapidly with distance. The apparent velocity values are 5 - 6 kms./sec. and the oscillation frequencies are 9 - 12 c.p.s. Waves of the P_2 group (basalt layer) were traced up to a maximum distance of 430 kms. At distances greater than 300 kms. (after the zone of interference with P_n group waves), the P_2 waves are never first arrivals. For a large distance, including the zone of interference with the P_n group, P_2 waves are dominant, having much larger amplitudes, with much less dampening than the P_1 group waves. The waves of the P_2 group seem to have a simple and stable form. The apparent velocity values are 6 - 7 kms./sec., and the oscillation frequencies are 9 - 10 c.p.s. Waves of the P_n group (Mohorovicic dis-

continuity) which are recorded after the interference zone are stable in form and undergo considerably less damping with distance than P_1 or P_2. Apparent velocity values are 7.5 - 8.5 kms./sec. and oscillation frequencies are 10 - 14 c.p.s. Mean boundary velocity by reversed profiles is 8.1 kms./sec.

The principles of correlation discussed here were used extensively in the interpretation of the work done by the University of Alberta.

G. Distance Calculation

Very little is found in the literature on the calculation of distance between shot points and detectors. If large accurate maps of the region in which one is working are available, then distances can usually be scaled off the map accurately enough. This was the method used by us at the University of Alberta. The most accurate method, however, is to use the formula for distance involving latitudes and longitudes of the shot point and detector location. These latitudes and longitudes should be obtained from the local Survey Department. The latitudes which they will give, however, (and those found on the map), are the geographic latitudes, that is, the angles between the normal to the geoid and the equatorial plane. The formula requires the geocentric latitude, that is, the angle between the

radius from the centre of the earth to the point and the equatorial plane. Thus, the latitudes from the map all require a correction to be applied in order that they may be used in the formula. This correction can be obtained from tables. At a latitude of 50^{o}N, the correction to the geographic latitudes is about - 11.3 minutes.

Let θ, and ϕ be the geographic latitude and longitude respectively. Then, a correction is applied to θ to get the geocentric latitude θ^{1}. The distance formula is then given by:

$$\cos \Delta = \sin \theta_1{}^1 \sin \theta_2{}^1 + \cos \theta_1{}^1 \cos \theta_2{}^1 \cos (\phi_1 - \phi_2).$$

Δ is the angle subtended at the centre of the earth by the two points (shot and detector). Then, the distance between the shot and detector is: $X = R\Delta$ where R is the radius of the earth at the latitude at which one is working and Δ is the angle found above, in radians.

This is probably the most reliable method of finding distances in seismic work.

H. Air - Coupled Waves:

I just wish to mention very briefly what air-coupled waves are, and when they should be observed. Air-coupled waves refer to two phenomena, a ground wave producing an air wave, or an air wave producing motion of the ground. In most investigations of elastic wave propa-

gation in solids in contact with the air, the effect of the atmosphere may be neglected. But, the intensity of signal of a particular frequency transferred may be very great due to constructive interference. To a first approximation, we may follow Lamb's treatment of the effect of a disturbance produced by a travelling line source. The travelling impulse may be replaced by a series of infinitesimal impulses placed at equal intervals of time along the path of the disturbance. Each impluse initiates a train of dispersive waves, and constructive interference is possible only for those waves of such a frequency whose phase velocity c = the speed of the travelling disturbance. The energy thus transferred from the air to the ground will form a train of constant frequency waves. The length of time that the wave train will last at any distance will be proportional to $(\frac{1}{c} - \frac{1}{u})$ where u is the group velocity corresponding to phase velocity, c. The ground waves will extend ahead of the air pulse if $u > c$, otherwise they will lag behind. Generally, $u < c$, and the ground waves follow the air pulse.

The properties of the air enter into the phase velocity equation only through a term of this form:

$$\frac{\rho a}{\rho \sqrt{1 - (\frac{c}{Va})^2}}$$

where ρ_a is density of air,

ρ is density of solid medium,

Va is velocity of sound in air,

c is phase velocity of the surface waves in the solid medium.

Since $\rho a/\rho \stackrel{.}{\approx} 10^{-3}$, this term is small when c is very different from Va. But, if for a particular frequency $c \longrightarrow Va$, then the term is large, and the form of the dispersion curve in the neighbourhood of that frequency will be greatly dependent on the associated air wave.

Compressional wave velocities less than that of sound in air are common in the uppermost part of the low velocity surface layer, and shear wave velocities much less than Va are the rule. Thus, it is to be expected that the surface waves on such a medium will be strongly dispersed, with the phase velocity decreasing from values greater than that of sound in air at low frequencies to values less than Va at higher frequencies. Therefore, some part of the surface motion should be accompanied by an air-coupled wave.

Mathematical theory on air-coupled waves will be omitted here, but results can be summarized as follows:

(1) For a buried shot in a layered medium, a geophone records ground roll as an orderly sequence of dispersive Rayleigh waves.

(2) For a hole shot, an air microphone records a constant frequency train of waves following the abrupt arrival transmitted with the speed of sound in air.

(3) Ground roll from an air shot recorded by a geophone predominates after the arrival of the direct air wave, and then only as a train of waves having constant frequency and phase velocity. The character of the seismogram after the arrival of the air wave is independent of the height of the charge above the surface.

(4) In areas where a high speed surface layer occurs such that the Rayleigh wave velocity in the surface layer is greater than V_2, coupling of the ground roll to the air cannot exist.

From this, it can be concluded that air-coupled waves should be seen in Southern Alberta, and, in fact, they were observed. This will be discussed in the chapter on Interpretation.

I. Theory used in the Interpretation of the results of Southern Alberta:

The seismic theory which has just been presented has, ofcourse, not all been used in the interpretation of the results taken by the University of Alberta. Since the travel - time graphs indicated almost no dip, seismic refraction theory for horizontal layering was used

extensively in the preliminary testing of models. Seismic refraction theory for dipping layers was then applied to the preferred model to obtain the dips of the layers, and the thicknesses under each shot point.

Seismic reflection theory for horizontal layering only was applied to the University results. The method which I have called the short-cut method was used exclusively. This is the method used by most workers in the field, and gives an approximate depth to a horizon (a depth which is independent of any other data). The depth, however, will be slightly greater than the true depth for reasons stated before. Since the dip was so small in Southern Alberta, it was felt that theory for horizontal layering was sufficient. The reflections are used for checking the seismic data, to see if the preferred model is at least reasonable. It happens that for the data taken in southern Alberta, the reflections agree extremely well with refraction data. But, this is discussed later. Dipping theory was used, however, to calculate the critical point for a shot from both east and west, from the refraction data for the final model chosen.

The time - term method of calculation was not used at all by the University. This method would be useful where more than two shot locations were used, but, in our case, for the additional work involved, it just

does not yield that much more information. Furthermore, it appears that the method has been developed for only two layers, while our preferred model at the University of Alberta for Southern Alberta includes six layers. Thus, the time - term method is of little use.

The method outlined by Veitsman (1957) for correlation of seismic waves in seismic depth soundings of the earth's crust was used in the work done by the University. The method provides a basis for correlation of energy bursts on records other than the experience and intuition of the seismologist.

These theories of interpretation will be referred to again in the chapter on Interpretation.

CHAPTER 4 - FIELD EQUIPMENT

Field equipment consisted of two sets of very low frequency refraction apparatus which the University purchased from Texas Instruments. Each set consisted of 12 two cycle per second geophones, a power supply, an amplifier, 3 rolls of cable, and a recording oscillograph and developing tank. Two extra geophones were purchased in case one or two of the other phones became unserviceable. One complete set of equipment was installed in each of two panel trucks owned by the University, which were used for transportation throughout the summer. When the trucks were moving from one location to another, the equipment was all fastened securely to the floor of the truck. The cables were tied down with rope. The geophone box was bolted to the floor. The amplifiers were tied securely to the table (which was permanently affixed to the floor) with rope. The camera was held steady by means of a wooden support across the top. Furthermore, the batteries were covered with a specially made wooden box. All of these rather elaborate precautions proved their worth during the summer, since the trucks were each involved in an accident in which they were rolled. None of the equipment, however, was damaged, as it had been fastened down securely.

When a location was selected for setting up, the cables were immediately untied, and then unrolled one at a time, by setting the reel on the geophone box and driving forward slowly with the truck. One person guided the cable off the reel as smoothly as possible. Then, on the way back to the beginning of the spread, a geophone was carefully dug into the ground at each takeout on the cable. When the truck arrived back at the point from which it started, the geophone box, now empty of phones, was removed. This provided ample working space in the truck, as the cables were , of course, gone also. The rest of the equipment was then set up in the truck, and the shot recorded. Following the shot and the development of the record, the equipment was once more tied down, and the geophone box was replaced. Then, the cable was rewound by backing the truck slowly along the line, as one person in the back reeled in the cable, with the reel itself resting on the top of the geophone box. As each take-out on the cable was reached, the geophone was pulled from the ground, clamped, and replaced in the box. When the end of the line was reached, the three rolls of cable were tied to the floor, and the truck was ready to move to its next location.

The timing of the shots will be discussed later, after the specifications of each piece of seismic equipment

is discussed. The amplifier was a very low frequency system developed by Texas Instruments. The camera was an RS-8u recording oscillograph, and the geophones were the S-36 VLF detectors, sold by Texas Instruments.

I will discuss the Power Supply and amplifier first. The power supply is a fairly standard D.C. power supply designed to deliver about 100 + volts of D.C. voltage. The 12 volt D.C. input is inverted to A.C. by the transistorized inverter, amplified, then rectified and filtered to give 300 volts of D.C. The 300 volts is then put through a tube-type regulator, and is finally brought to the output as a carefully regulated D.C. voltage of 100 + volts. A difference from conventional regulators should be noted, however. This unit clamps the grid and puts the D.C. voltage sensing on the cathode. Thus, a change in plate voltage looks like a change in the D.C. output voltage. This design can cause some problems. If the voltage is changed from a higher value down to a lower value, oscillations with a period of approximately one second occur in the output voltage. If the voltage, however, is moved up to a desired operating level from some lower level, this usually does not occur. The oscillation, if it occurs, can be seen on the voltmeter (on the amplifier). We did not have much trouble with this type of oscillation, however, but we did have considerable difficulty with another type of oscillation to be discussed later.

A photograph of the VLF amplifier appears in figure 4. The amplifier consists of 12 channels, with 2 channels in each bank. An amplifier bank can be removed very simply by freeing the four Dzus fasteners with a screwdriver and pulling the unit out. This is very convenient for servicing. Each channel has an attenuation control calibrated in decibels from 0 to 66 db. Each amplifier bank (2 channels) has a high cut frequency control, with possible cut-off frequencies of 8, 12, 16, 24, 32, or 48 cycles per second. Note that each channel has a line balance control. This control is simply a 10 K potentiometer across the input circuits with a switch in the arm to ground. With the knob turned to off, the switch is open. The control, when it is not off, serves as a resistive line balance, and is used in conjunction with a filter network to attenuate any input signal above 60 cps. It can be used effectively to balance out 60 c.p.s. Note also that there are two input jacks. Plugging into the second input simply reverses the order of the traces, so that the phone which was being recorded on #1 trace is now being recorded on #12 trace, and so on. The operate-parallel-test control serves as a function switch and is in the signal input circuit. When on operate, the signal is connected directly to the amplifier input as is required for normal operation. When on parallel, the signal from phone #3 is fed to each amplifier input. This position

is used for testing the phase and amplification of each amplifier. When on test, a metering circuit is available to test the continuity of each seismometer circuit. To do this, the spring - switch marked 90V - ohmmeter must be held in the ohmmeter position, and the metering switch is rotated from 1 through 12 to check each seismometer in turn. The resistance of each should be about 4000 ohms. If the meter reads infinity, the seismometer is either disconnected or the wires to that seismometer in the cable are broken.

The characteristics and response of this amplifier as listed in the manual are given below.

Frequency response: 0.7 to 33 c.p.s. for high cut filter setting at 48 c.p.s. Figure 5 shows the response curves for various filter settings including filter insertion loss.

Phase response: figure 6 gives the phase response in milliseconds.

Distortion: distortion is below 1% at 7 c.p.s., for inputs below 2 millivolts, with the gain adjusted to give 1 inch peak to peak deflection.

Gain: An input of 15 uv., with zero attenuation and high cut filters at 48 c.p.s., will give a 1 inch peak to peak deflection with an RS-8U recording oscillograph using 200 c.p.s. galvanometers. Instrument gain (including

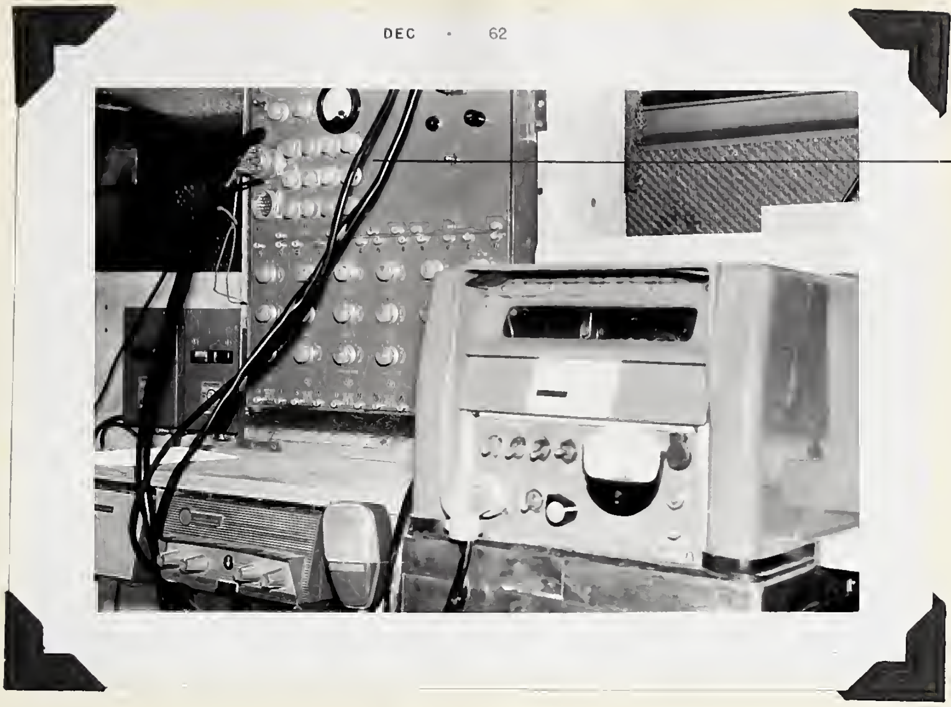

FIG 4

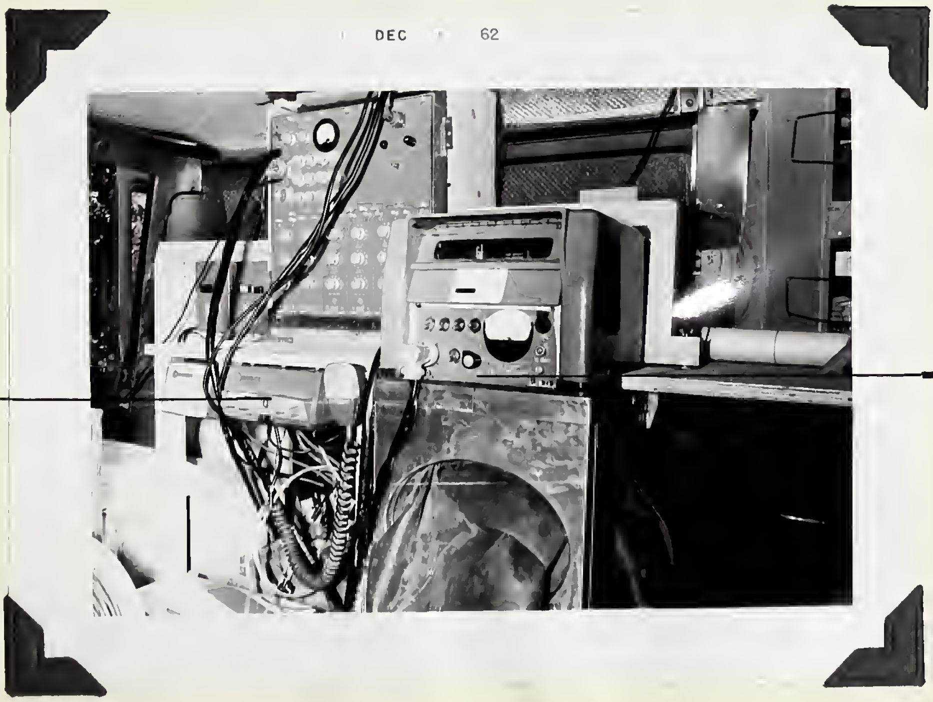

FIG 8

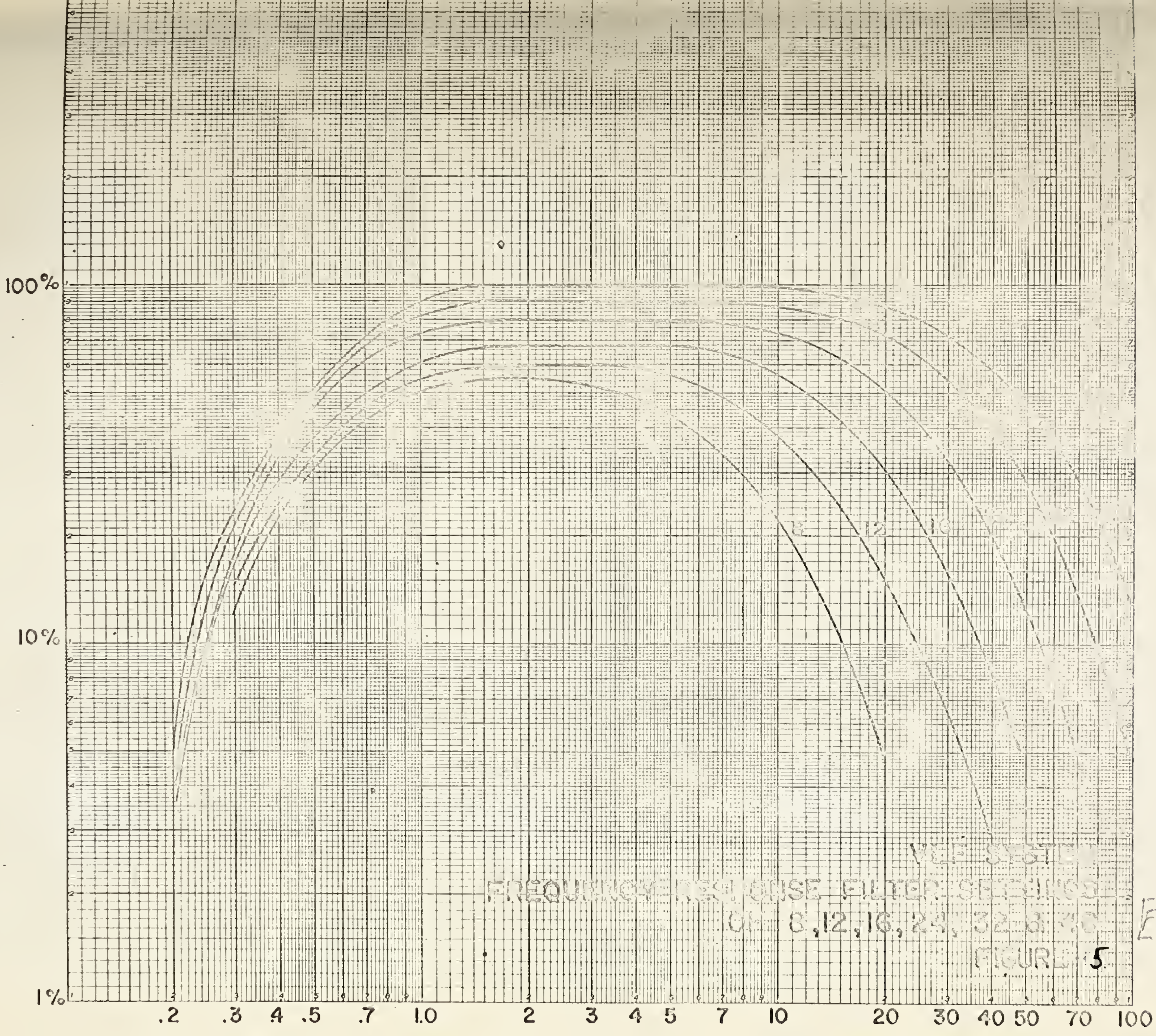

VLF SYSTEM
FREQUENCY RESPONSE FILTER SETTINGS
OF 8, 12, 16, 24, 32 & 48
FIGURE 5

[FROM MANUAL]

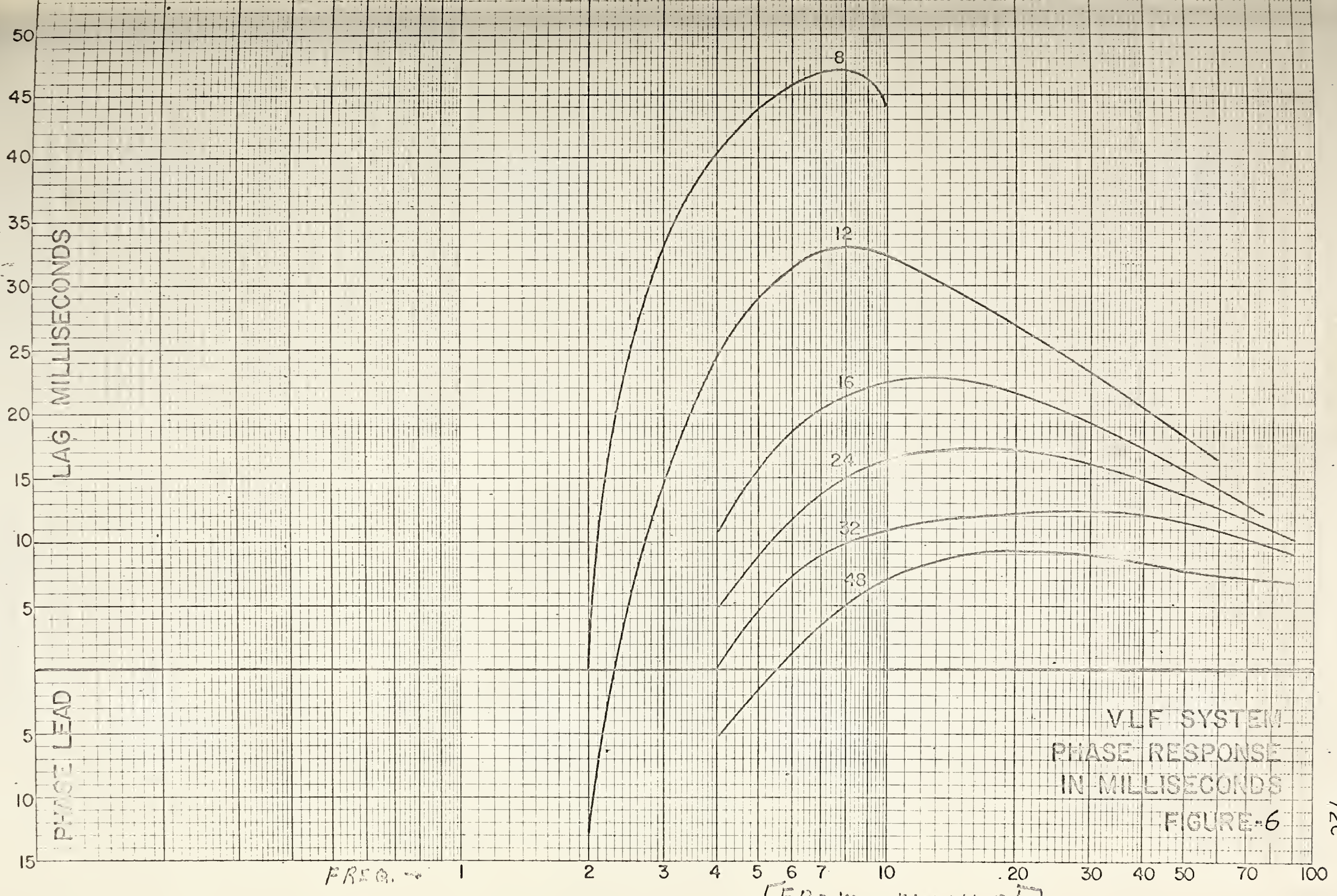

V.L.F SYSTEM
PHASE RESPONSE
IN MILLISECONDS
FIGURE-6

[FROM MANUAL.]

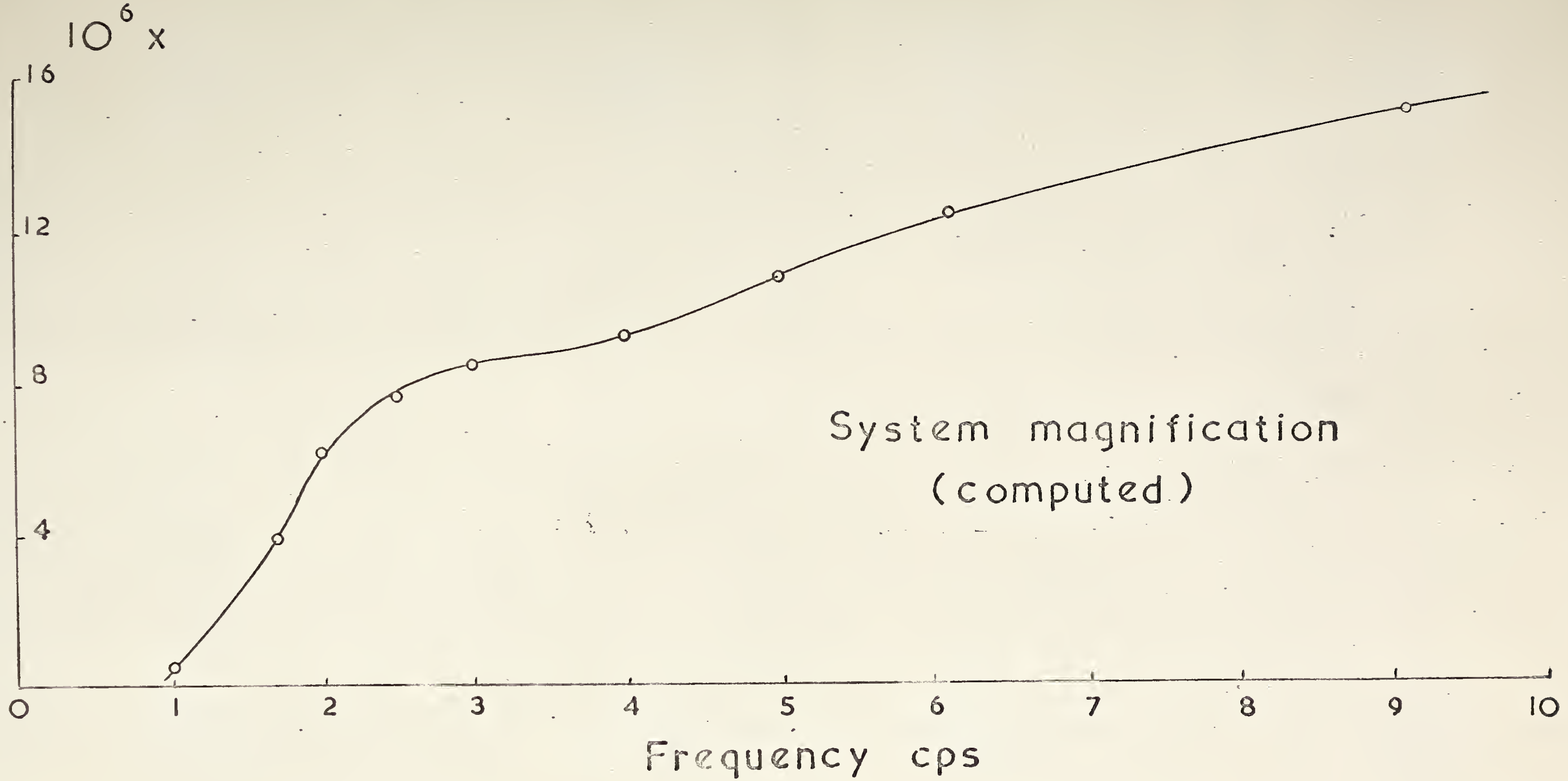
10^6 x
16
12
8
4
0
1
2
3
4
5
6
7
8
9
10
Frequency cps
System magnification
(computed)

FIG. 7.

geophones) has been calculated by Dr. Garland and is shown in figure 7 as function of frequency.

Noise: The internal noise of the instrument is equivalent to an input signal of three microvolts.

Input: the input impedance is 10,000 ohms, and the line is balanced. No input transformer is used.

Output: two outputs, having a deflection ratio of 4 to one are provided. This is accomplished simply by dropping the signal over a resistor. No output transformer is used, and the outputs are unbalanced with one grounded.

A number of test records made in the laboratory are discussed in the next chapter.

A photograph of the RS-8U recording oscillograph appears in figure 8. The RS-8U recording oscillograph is a self-contained unit containing an optical system, timing system, recording galvanometers, and paper transport system. The galvanometers are all 200 c.p.s. galvanometers. Three paper speeds are provided in the ratios of approximately, 1 : 2 : 5, designated as slow, medium, and fast. For our work, we set the slow speed at approximately 2 1/2 inches per second. Medium speed was then 5 in./sec., and fast speed was about 12 in./sec. Most of our records were taken at the slow speed, and a few were taken at medium speed. The brightness of the

lamps is also automatically changed when the speed is changed. The lamps are brightest on fast speed and weakest on slow speed. This is accomplished by resistors. It was found that in one of the cameras, two of the resistors were interchanged when the unit was received from Texas. This caused a very intense light on medium speed and a weaker light on fast speed. These resistors were changed to their correct positions by our technician, Mike Burke. The camera takes a paper size of 6" or 8" x 200 ft. Eight inch paper is better, as it allows wider spacing of the galvanometer traces. The lamp switch turns on the trace and timing lamps, and puts the voltmeter across the battery terminals. The fork switch provides power to the fork to keep it vibrating, and to the timing moter which turns a slotted cylinder between the timing lamp and the paper. The motor is started by pulling out the starting rod on the lower right of the camera and pushing it swiftly in to give the motor a spin. The timing motor is governor controlled so that its speed is constant. To verify this, galvo 50 monitors the field of the fork coil. The fork has a frequency of 100 c.p.s. The whole timing circuit has an accuracy of ± 1 part in 10,000 parts for any temperature between -40°F. and $+140^{\circ}$F., and any supply voltage between 10.5 volts and 15 volts D.C., according to the manual. The outputs from the VLF amplifier plug into the back of the recording oscillograph. When these are not

connected, the damping blocks should be inserted to protect the galvos. The galvo block should also be clamped when the camera is moved. Note that the brightness and sharpness of the traces can be controlled by adjustment of the galvos forward or back. If the light reflected from a certain galvo can be seen on looking into the camera, but does not appear on the developed record, the galvo is probably out of adjustment. Similary, the brightness and sharpness of the timing lines can be adjusted by changing the tilt on the mirror. The adjustment for this is at the left front of the camera unit. The records can be easily developed in the developing box. One arm is inserted through each of the rubber sleeves in order to work inside. But, since the sleeves are of very stiff rubber, one must be very careful that light does not enter around one's arm. We found it convenient to darken the trucks as much as possible when developing. We found that the easiest and safest way to develop records was to leave the lids on the developing cans until the camera was turned off. Then, the arms are inserted through the sleeves and the paper is torn off and rolled up. This rolling up is absolutely necessary for long records (anything longer than 8 to 10 ft.). Then, the lid is removed from the can of developing solution, and the record is unrolled and rolled up through the solution twice. Then, the lid is

removed from the water and the record is briefly washed. Then, the lids are placed back on those two cans and the lid is removed from the fixing solution. The record is unrolled and rolled up through the solution once. Then, the can of fixer with the record can be taken out of the developing box into the daylight. There, the record can be rolled through the solution once again. Records up to 100 ft. long were developed by us at the University of Alberta by using the method outlined here. It is a very tedious job, but the records are always good if developed this way. Drying long records in the field can be a problem, especially if it is windy. But, if one is staying at a hotel, he can unroll the records in the corridor, and they dry very quickly!

A photograph of an S-36 seismometer appears in figure 14. The detector has a double coil system wound as a "hum-bucking" device. The coils are centered in the magnet assembly by a pair of springs at each end of the assembly. The natural frequency is 2 c.p.s. ± 0.5 c.p.s. The coil resistance is 4000 ohms. The frequency response characteristics of the S-36 are shown in figure 9. It is seen that the internal damping resistor is 15K. Since we did not add any external resistance, the damping which we used was 0.311, critical. Note that it is essential to clamp the coil when the geophone is moved. The clamping

RESPONSE OF THE S-36 SEISMOMETER

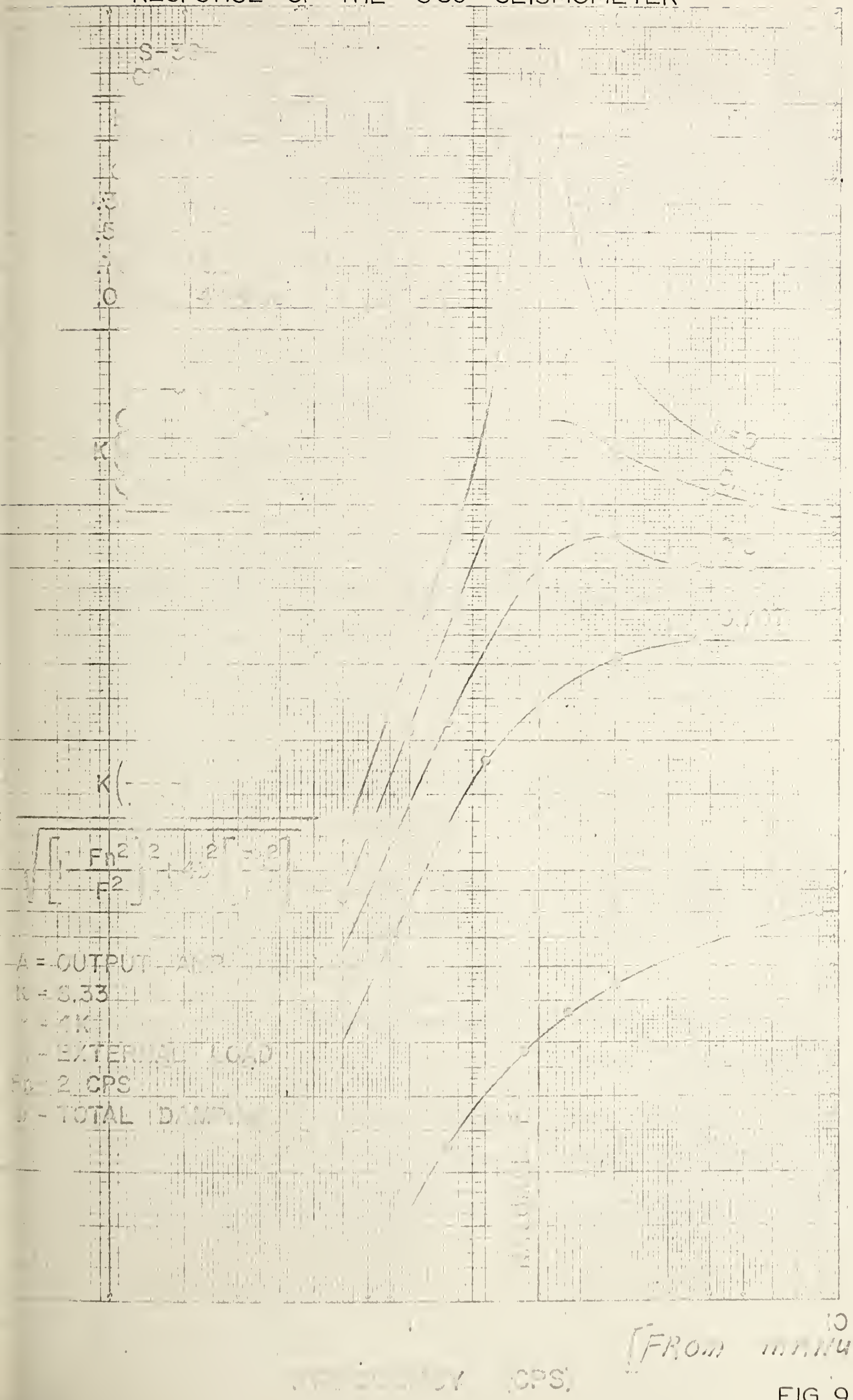

[From manual]

FIG. 9.

screw is on the bottom. It should be clamped at all times except while making a record. The seismometers are quite rugged as long as they are clamped. In particular, in one of the truck accidents during the University of Alberta field season, the top was torn from the geophone box, and geophones were scattered all over the truck. All worked perfectly when tested later in the lab. One fault is noted in the geophones. They have a tendency to come unclamped slightly during transportation by vibration of the truck. However, this does not seem to cause them any harm. The geophones were generally buried to a depth of slightly over a foot. Usually the tops of the phones were just deep enough to cover with 2 or 3 inches of earth. This depth was found to be quite suitable in keeping wind noise to a minimum.

This completes a description of the actual seismic equipment used. It should be noted here that a separate battery must be used for each unit, power supply, amplifier, and recording oscillograph. Furthermore, the batteries must be isolated from each other, that is, a common ground cannot be used. This particular fact was discovered by the University of Alberta at the cost of much valuable time. Another fact discovered at the same time was that the battery connections must be as tight as possible and as clean as possible. If all of these precautions are not

taken, the system will oscillate. These oscillations were not seen in the laboratory before the equipment was taken into the field. I presume that they were not seen because all battery connections were tight and clean. But, once in the field, the trouble began. The oscillations were intermittent and usually occurred just at the time an arrival was expected, thus spoiling the record. The frequency of oscillation was about 6 cycles per second, and varied if the high cut filters on the amplifier were varied. This oscillation could not usually be seen on the voltmeter which monitored the power supply voltage, indicating that these oscillations were different from those mentioned earlier. An example of these oscillations is seen in figure 10. Sometimes actual oscillations did not take place, but severe voltage "kicks" occurred which affected all traces. See figure 11. Clearly we could not operate under these conditions. A technician from Texas Instruments was called up, and he too was somewhat puzzled. He suggested, however, that we isolate the batteries, solder all connections firmly, and clean all dust and other foreign material off the batteries, especially near the terminals. This we did, and had no further trouble. From that time on, we found that, if small random voltage kicks began to occur, when the batteries were cleaned and all connections tightened, the trouble disappeared.

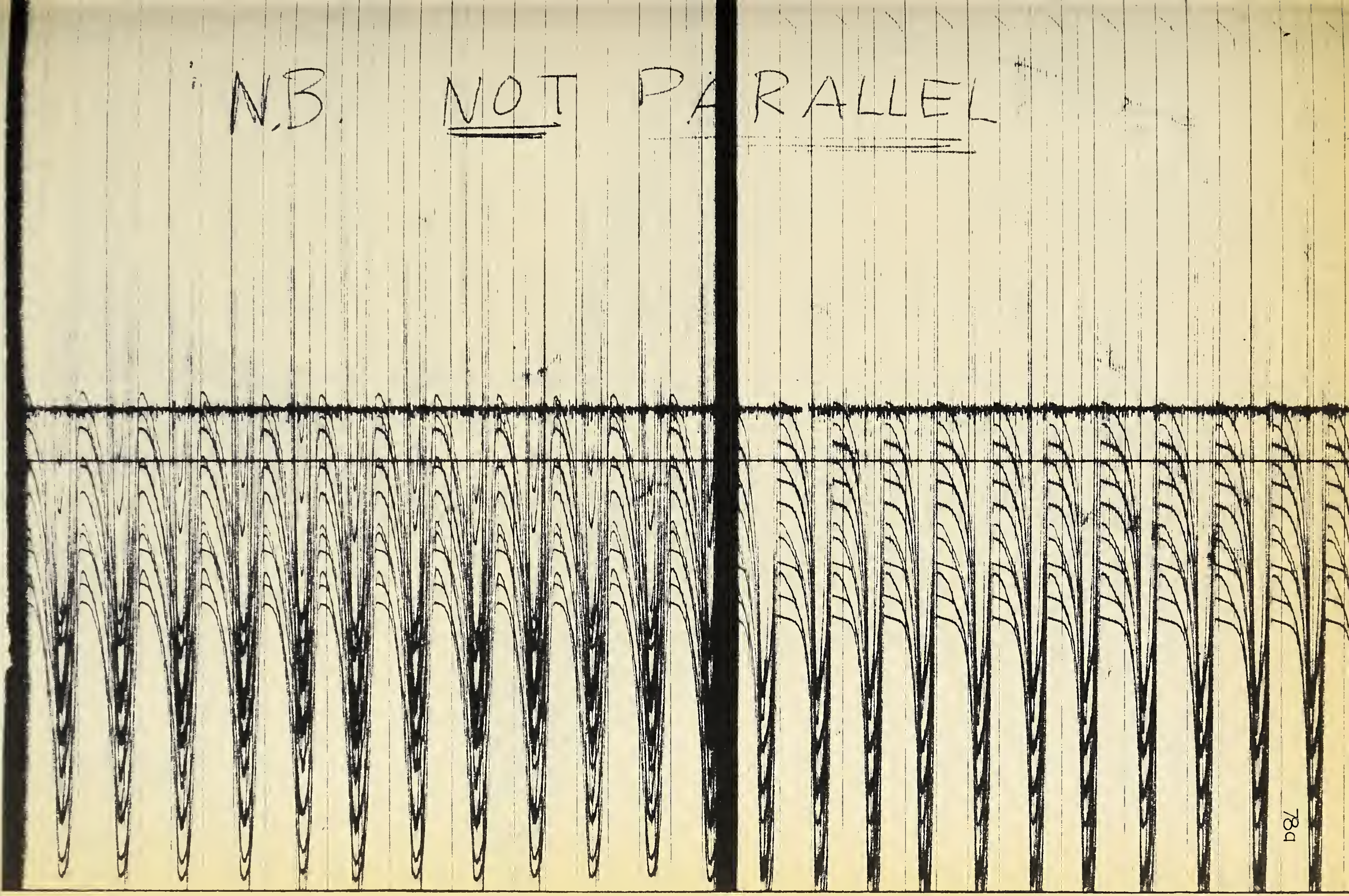

OSCILLATIONS. Figure 10.

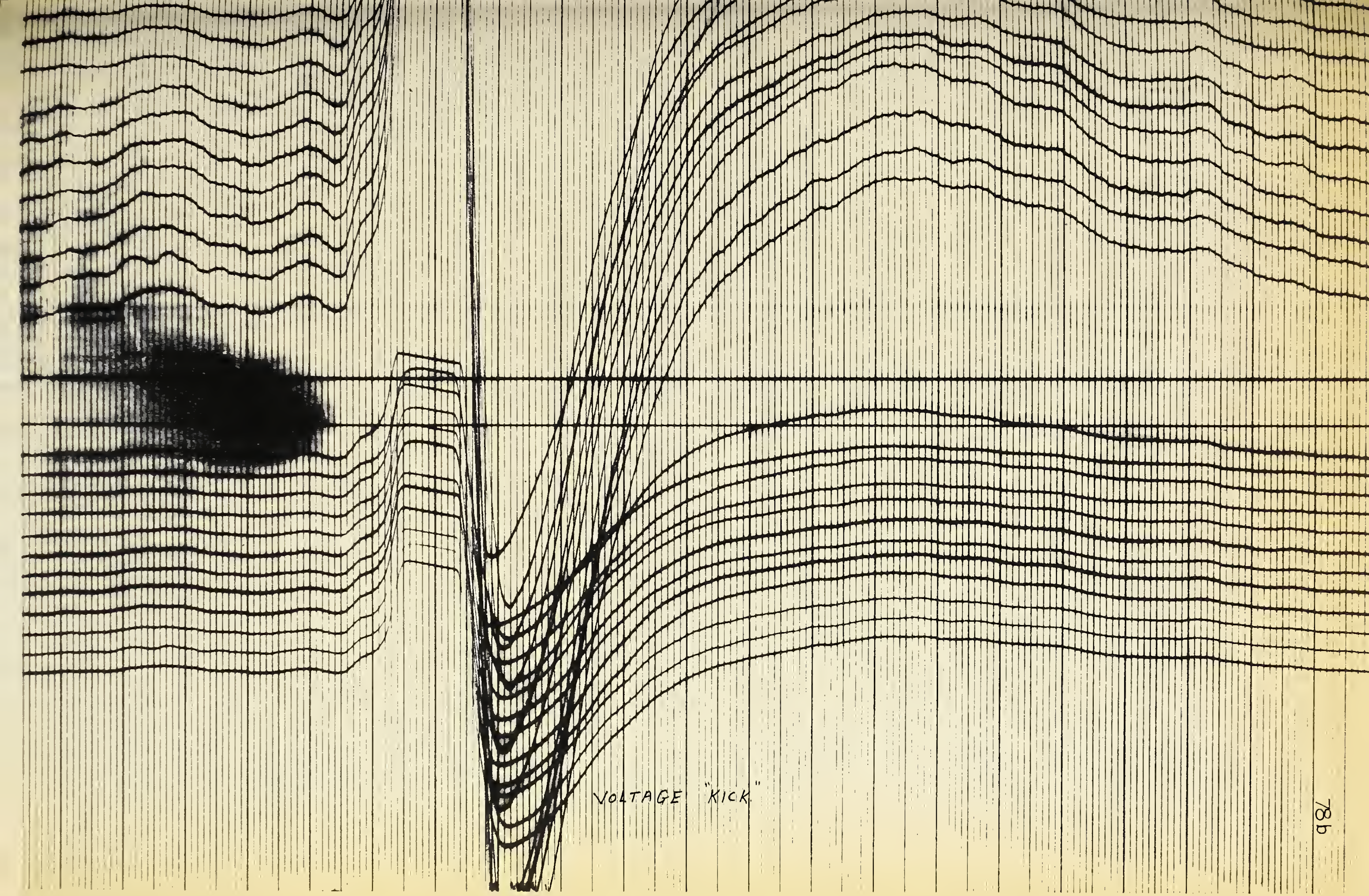

Figure 11.

This cross-feed is a peculiar phenomenon, but apparently other groups have the same problem with other equipment as well. One can waste valuable time if he doesn't know how to handle the difficulty.

It should be noted here that the University of Alberta used a spread length of 1.42 km., (4670 ft.). Three cables were used, and placed end to end. Each cable had 4 take-outs. Take-out spacing was 410 ft. But, the ends of the cables were 245 ft. long, making the spacing between phones 4 and 5 (where two cables join) 490 ft., and the spacing between phones 8 and 9 also 490 ft. The three cables end to end measured 5160 ft. The cable was a 24 conductor shielded type.

Besides the seismic equipment in each truck, there was installed a General Electric Transistorized Progress Line two-way portable radio. These were two-channel units designed to operate at very high frequencies (150 mc. or so). The Suffield Experimental Station, who were setting off the charges for us, were supplied with a console, a device which delivers a one second 1000 cycle per second tone from time minus 1 second to zero, and then fires the shot on zero (at the end of the tone). The seismic trucks recorded this tone on one of the galvanometer traces in the camera, thereby providing the shot time on the seismic records. In order to receive the radio signal from Suffield out to High River, two repeater stations were set up, one at Rainier and one at Buffalo

Hill, 12 miles north of Vulcan. By equipping the mobiles in the trucks with the appropriate crystals, we could talk to and receive Suffield either through Rainier, through Buffalo Hill, or directly, depending on our location. The second channel of the mobiles was never used. It was supposed to have been used for communication from mobile to mobile, but the correct crystals for the frequencies assigned by D. O. T. were never received. It is a nuisance both to the personnel of the trucks and also to the personnel at the shot point if messages between trucks have to be relayed by the people at the shot point.

At the recording trucks, the radio signal from Suffield was rectified, integrated and placed directly on one of the spare galvanometers by means of one of the extra inputs on the back of the camera. The one-second tone then gave a sharp break at the beginning and ending on the trace, and the shot instant could be fixed on the record to within 1 or 2 milliseconds. See figure 12 for an example of a good tone break. The exact length of the tone determined in the laboratory at Suffield was .999835 secs. ± 1 millisec., and the shot was always fired in 1.003018 secs. ± 1 millisec. after the beginning of the tone break. This method of timing proved quite successful once it was operating. Many difficulties and delays were encountered at the beginning of the summer, however, in setting up the repeater

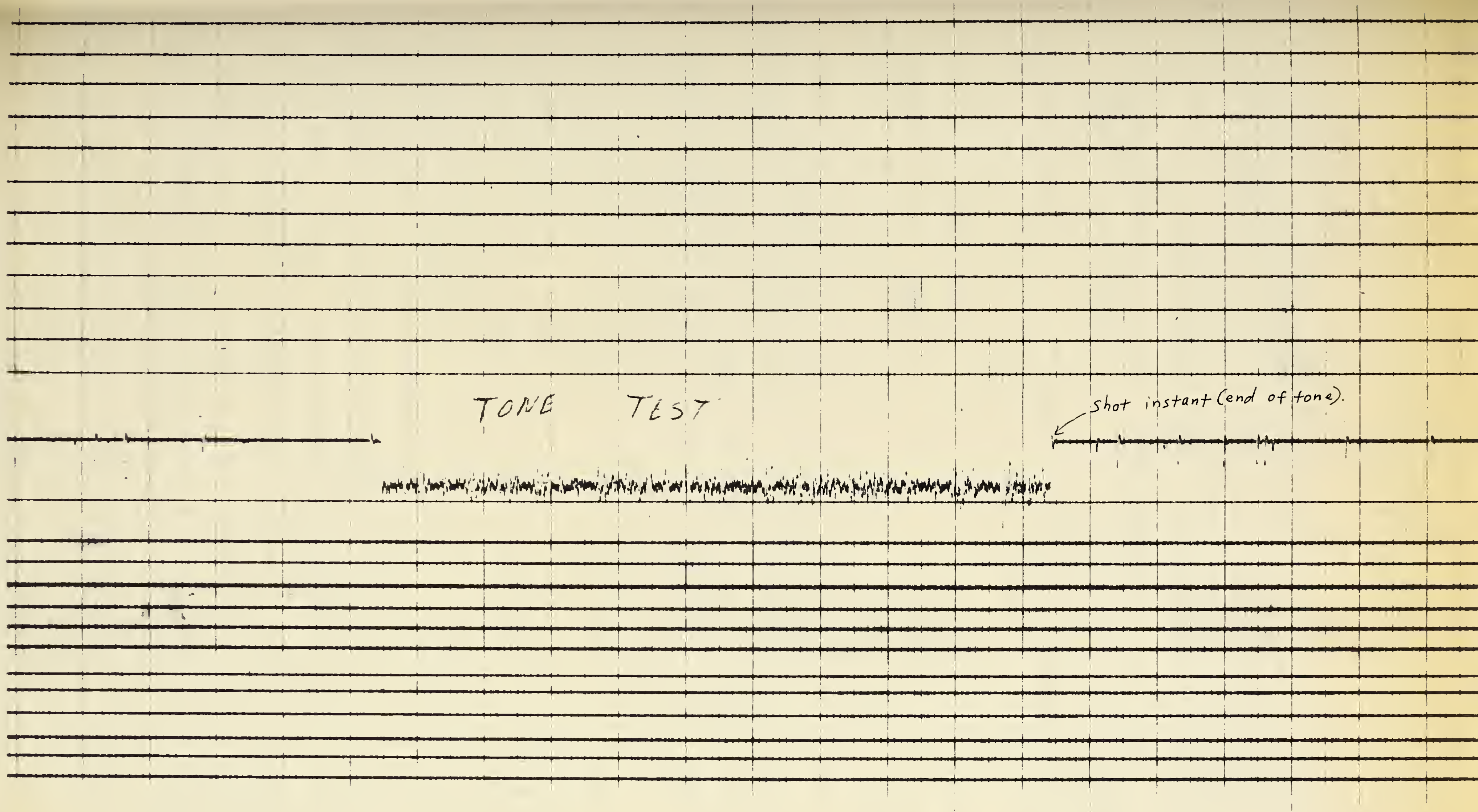

Figure 12.

stations, obtaining proper crystals, and generally ironing the "bugs" out of the system. But, once the repeaters were up and tuned properly, and the crystals installed in the mobiles and they were tuned properly, the timing system was very effective. On any occasions when one of the mobiles was not working, a standard broadcast radio station was used to time the second truck. The first truck put the tone break on one trace and the radio station on another trace (also rectified and integrated). The second truck put on only the radio station. It is then a simple matter to correlate the radio station's signal on both traces, and thereby provide the timing for the second truck.

It will be seen that shots 2 and 3 for the University of Alberta were not fired by Suffield. They were fired from the west by the Century Geophysical Company. Thus, the radio link was not used for timing. In these cases, the WWV and CBC time signals were used. The recording trucks each recorded the CBC time signal (the beginning of the CBC long dash marks 10:00 A.M.). At the shot point, a two channel brush recorder was used. On one channel, the WWV time signal was recorded. On the other channel, the shot instant was recorded, by recording the discharge of the capacitor in the firing circuit. Thus, the exact time after the hour of the shot was determined. It was then an easy matter to pick off this time on the records obtained

by the recording trucks. Shot # 7 was also fired from the west, and in this case, the timing was provided by WWV and a chronometer. Since WWV was usually rather difficult to receive, a chronometer would be rated against WWV when the signal was good, by recording the chronometer clicks on one trace and WWV on an adjacent trace. Then, when the shot was fired, the chronometer was recorded on one trace and the shot instant (discharge of capacitor) on another . This proved quite effective. All these shots from the west were also recorded for us by some American groups, the USGS and the USCGS. Timing on the USGS records was provided by WWV only. Since we recorded the absolute time of the shot for all shots from the west, it was an easy matter to pick the shot time on the American records. See figure 13 for an example of a chronometer signal, and a WWV signal.

The next chapter deals with various tests performed in the laboratory prior to the field work, with the seismic equipment that has been specified in this chapter.

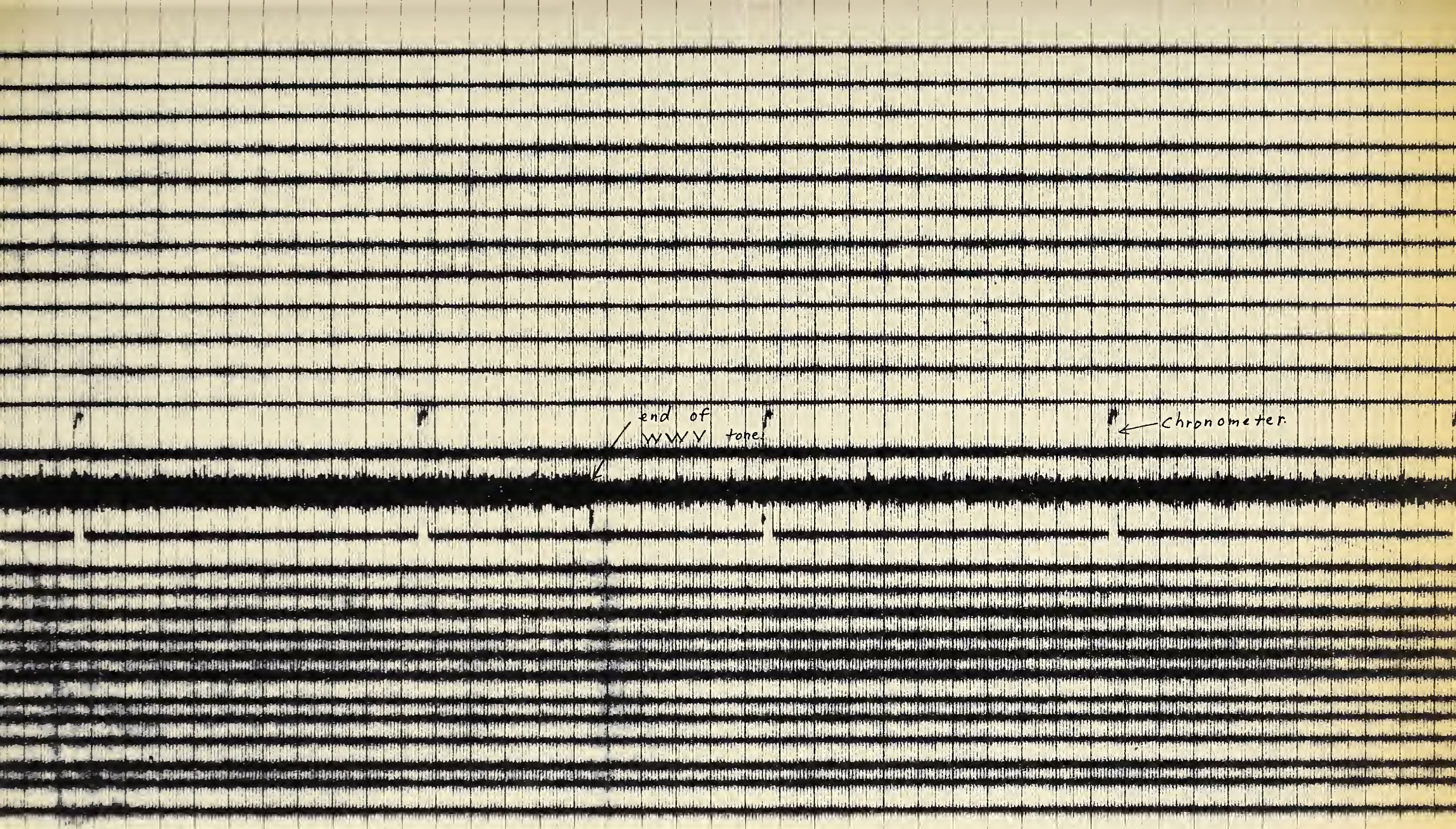

Figure 13.

CHAPTER 5 - LABORATORY TESTING OF EQUIPMENT

Before going into the field, extensive tests were carried out in the laboratory using the VLF refraction system. A wooden frame was built (see figure 14) to hold twelve seismometers upright with their bases resting on the cement floor. The rest of the equipment, including the three batteries, was set up on the laboratory table. Impulses were given to the geophones by jumping on the floor. In this way, various tests on amplitude and phase of the amplifiers, phase of the phones, etc., as described below were carried out in the lab.

The portion of the test record in figure 15 illustrates a typical amplitude and phase test of the amplifiers. The amplifier was set on Parallel which means that the same signal (from phone #3) is being fed into each amplifier input. All attenuations were set at 60 db. down, and the camera was operated on fast speed. The amplitudes of the traces were measured as below:

trace no.	amplitude(peak to peak) (mm)
1	8.9
2	9.5
3	9.0
4	10.4
5	10.0
6	10.0
7	10.0
8	10.2
9	10.3
10	9.6
11	9.4
12	10.2

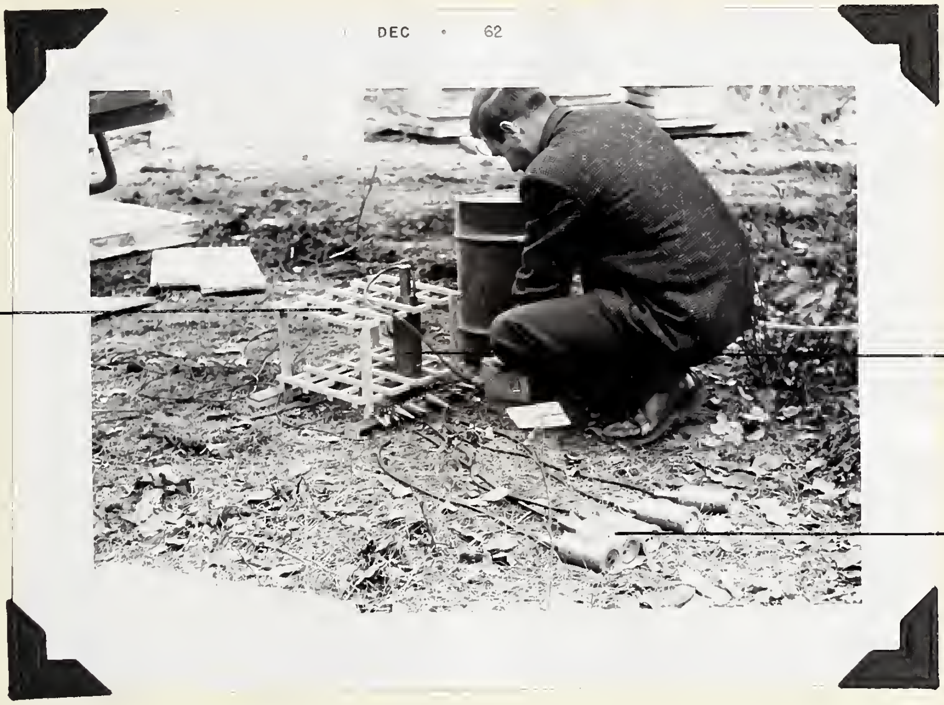

FIG 14

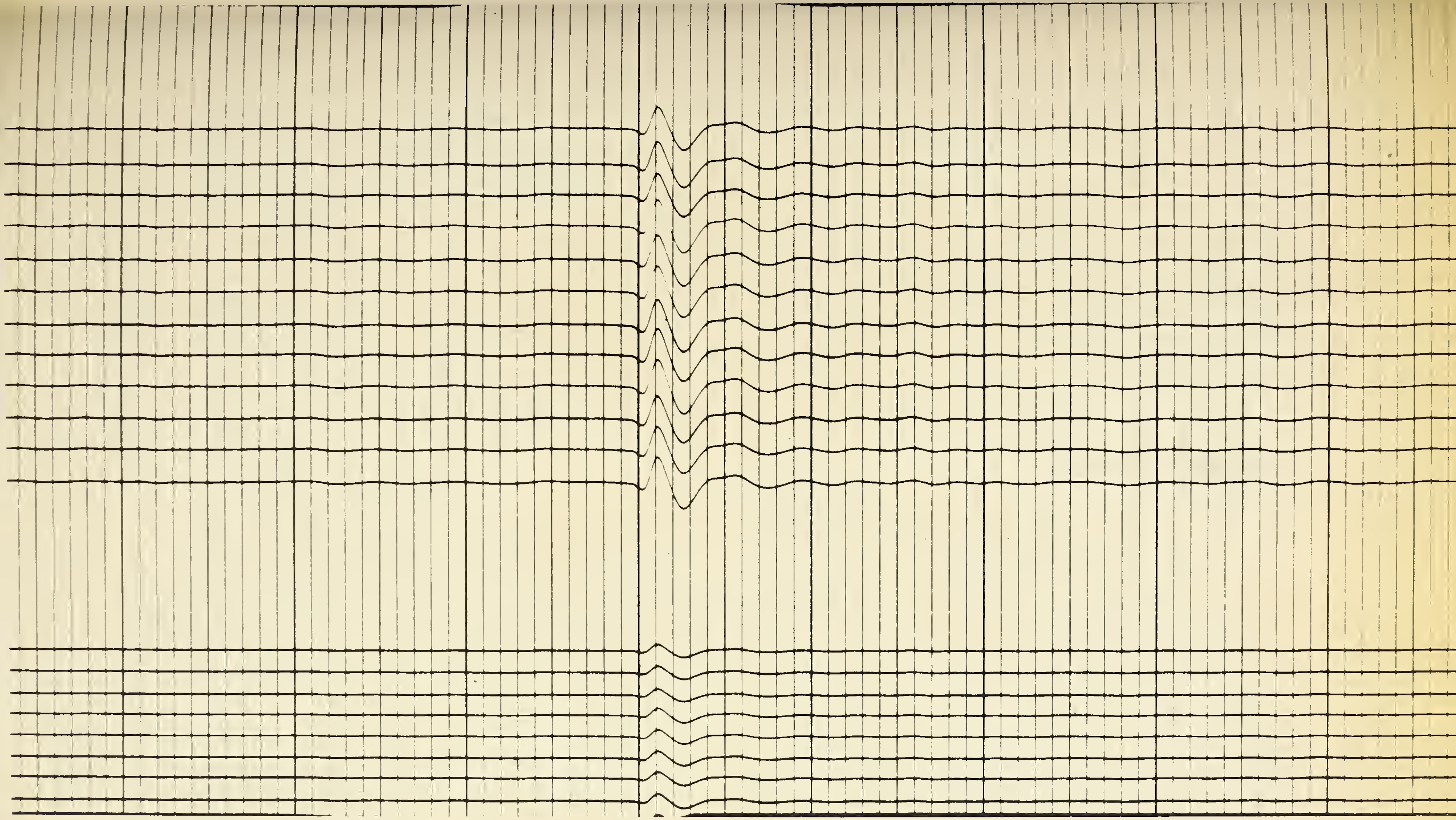

Figure 15.

The average amplitude was 9.8 mm. Greatest deviation from the average was $\frac{0.9}{9.8} \times 100 = 9.2\%$.

Thus, the amplitudes are within ± 10%. This is the maximum allowable deviation according to the manual.

The phase of the pulse on each trace is also within ± 1 millisecond. This is satisfactory. When the Willmore 1 c.p.s. seismometer was substituted for one of the S-36 phones in an "operate" test, it was found that the Willmore is not as sensitive as the TI phones. The energy output of the Willmore seems to be about only 1/4 the output of the TI phones, since an attenuation 6 db. less makes the amplitude of the Willmore trace only very slightly more then that of the TI phones.

Various tests were performed to determine the correct lamp intensity for the recording and timing lamps. Other tests were performed to determine to what extent time of developing affected the final record. It was found that a developing time of 30 sec. was insufficient, although the record could probably be interpreted with extreme difficulty. A developing time of one minute resulted in a clear, bright record. A developing time of 4 minutes also resulted in a clear, bright record, very little different from the record developed in one minute. Thus, overdeveloping does not seem to harm the record in anyway.

Figure 16 shows a portion of another very important test record. This record was a parallel check on medium speed. It shows that the 6 db. steps on the attenuation are not all identical. Each 6 db. step should increase the energy output of the amplifiers by 4 times, and therefore, should increase the amplitude of the traces by two. This was not always the case as seen from the measurements below:

trace	atten. db.	ampl.(peak to peak of pulse)(mm)	expected ampl. inc. over #1	no. of times increase over previous	no. of times increase over # 1
1	66	2.0	1.0	1.00	1.00
2	60	3.2	2.0	1.60	1.60
3	54	4.9	4.0	1.53	2.45
4	48	10.0	8.0	2.04	5.00
5	42	19.8	16.0	1.98	9.90
6	36	37.4	32.0	1.89	18.7
7	36	38.0	32.0		19.0
8	42	30.0	16.0		10.0
9	48	10.1	8.0		5.05
10	54	5.0	4.0		2.50
11	60	3.3	2.0		1.65
12	66	2.2	1.0		1.10

The deviation from the expected increase is quite noticeable. If any amplitude studies of seismic energy were to be attempted, much more testing along this line should done. In this thesis, however, very little is done on amplitude studies.

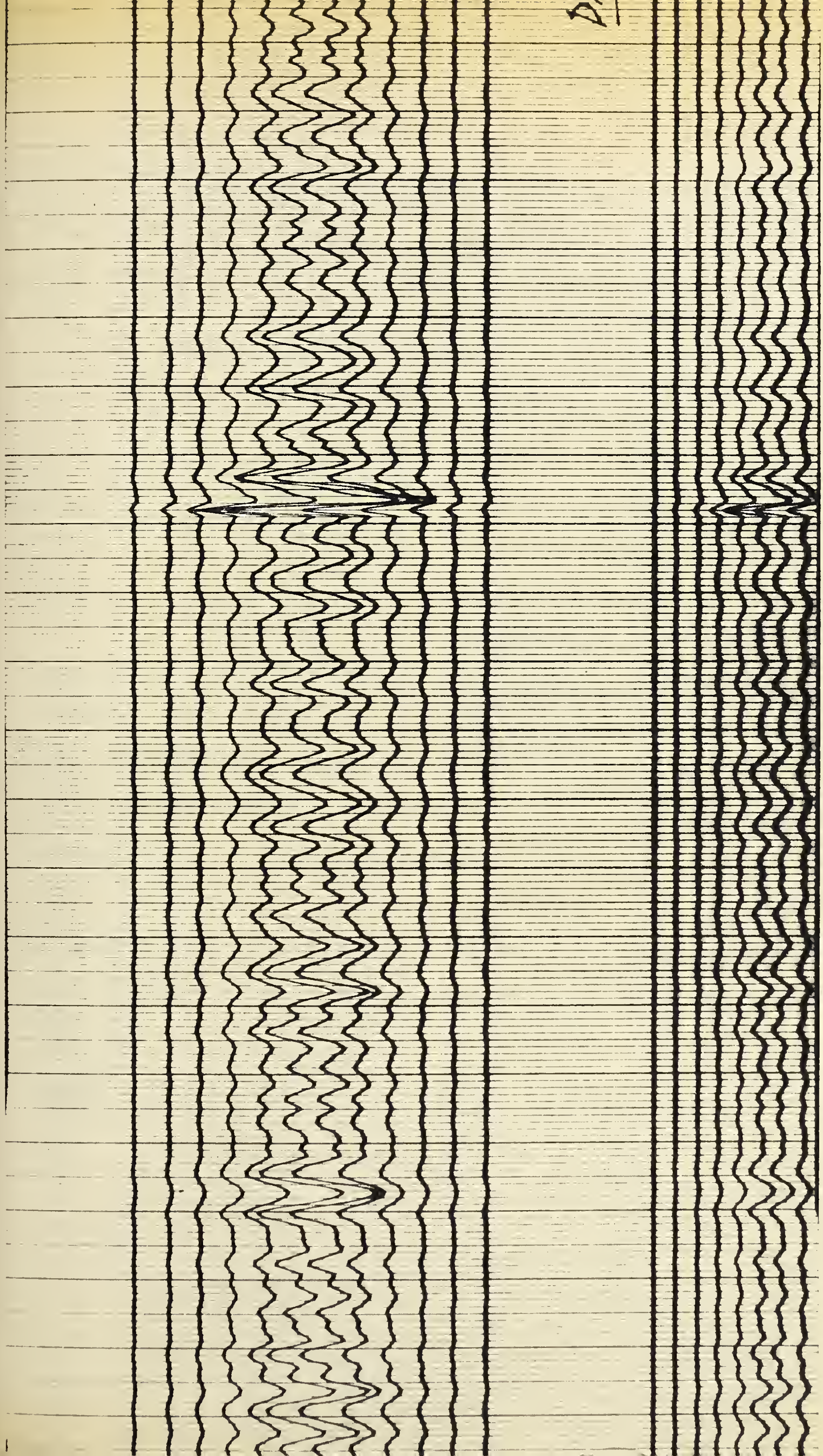

Figure 16.

Figure 17 shows 6 short portions of a test record. The test was run on parallel on medium speed. The high-cut filter settings and attenuations are given below:

part	H.C.F.(c.p.s.)	atten.(db)
1	48	54
2	32	48
3	24	42
4	16	36
5	12	30
6	8	24

This record actually proves very little since no strict control of the magnitude of the pulses was made. It does show though that the high cut filters do reduce the high frequency components, and it indicates that a 6 db. decrease in attenuation slightly more than compensates for the attenuation due to filter loss.

Figure 18 shows part of another important test record. This record was also taken on parallel, but on fast speed. Attenuation for the various traces is shown below:

trace	atten.(db)	trace	atten.(db)
1	66	7	30
2	60	8	24
3	54	9	18
4	48	10	12
5	42	11	6
6	36	12	0

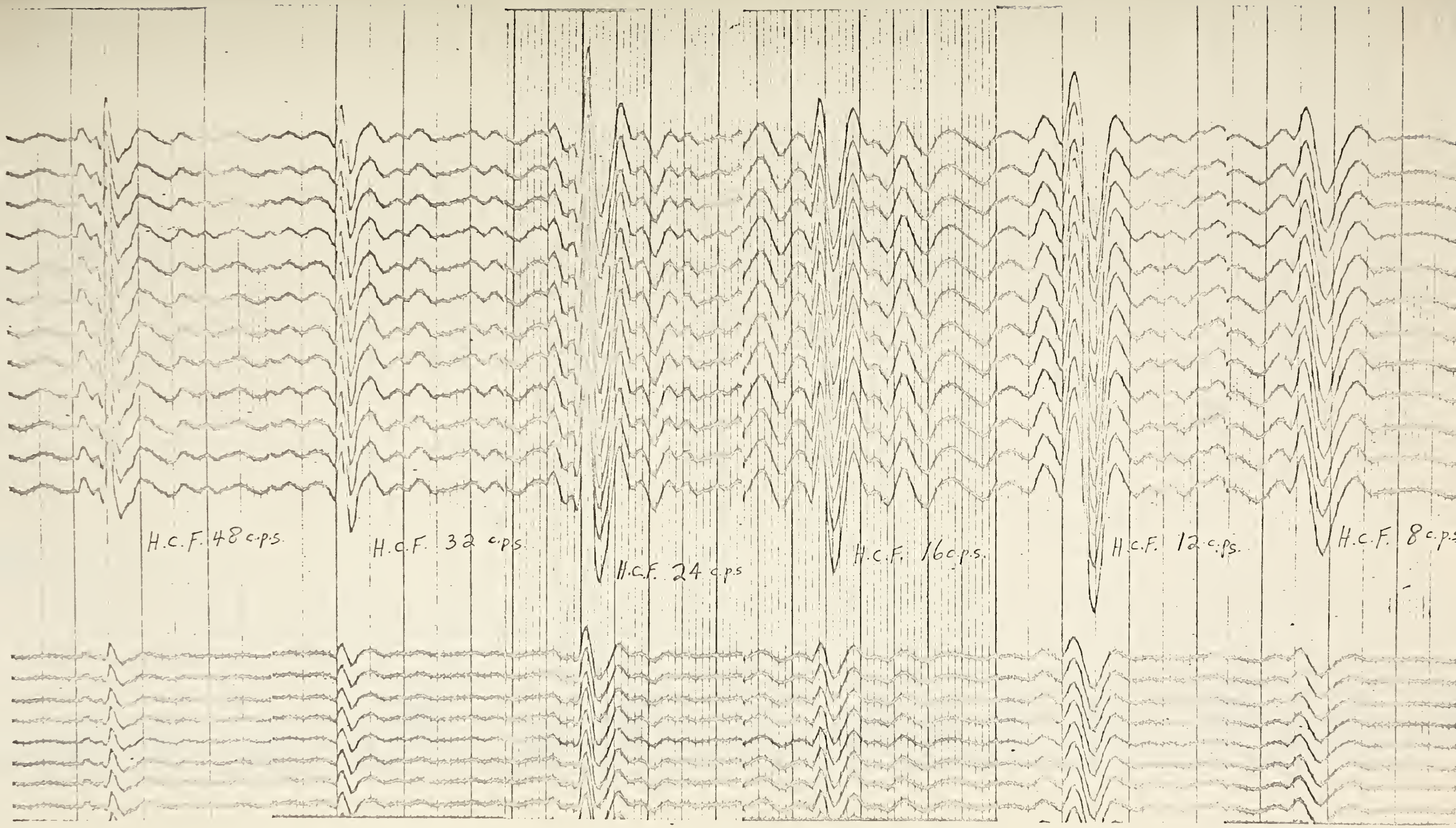

Figure 12.

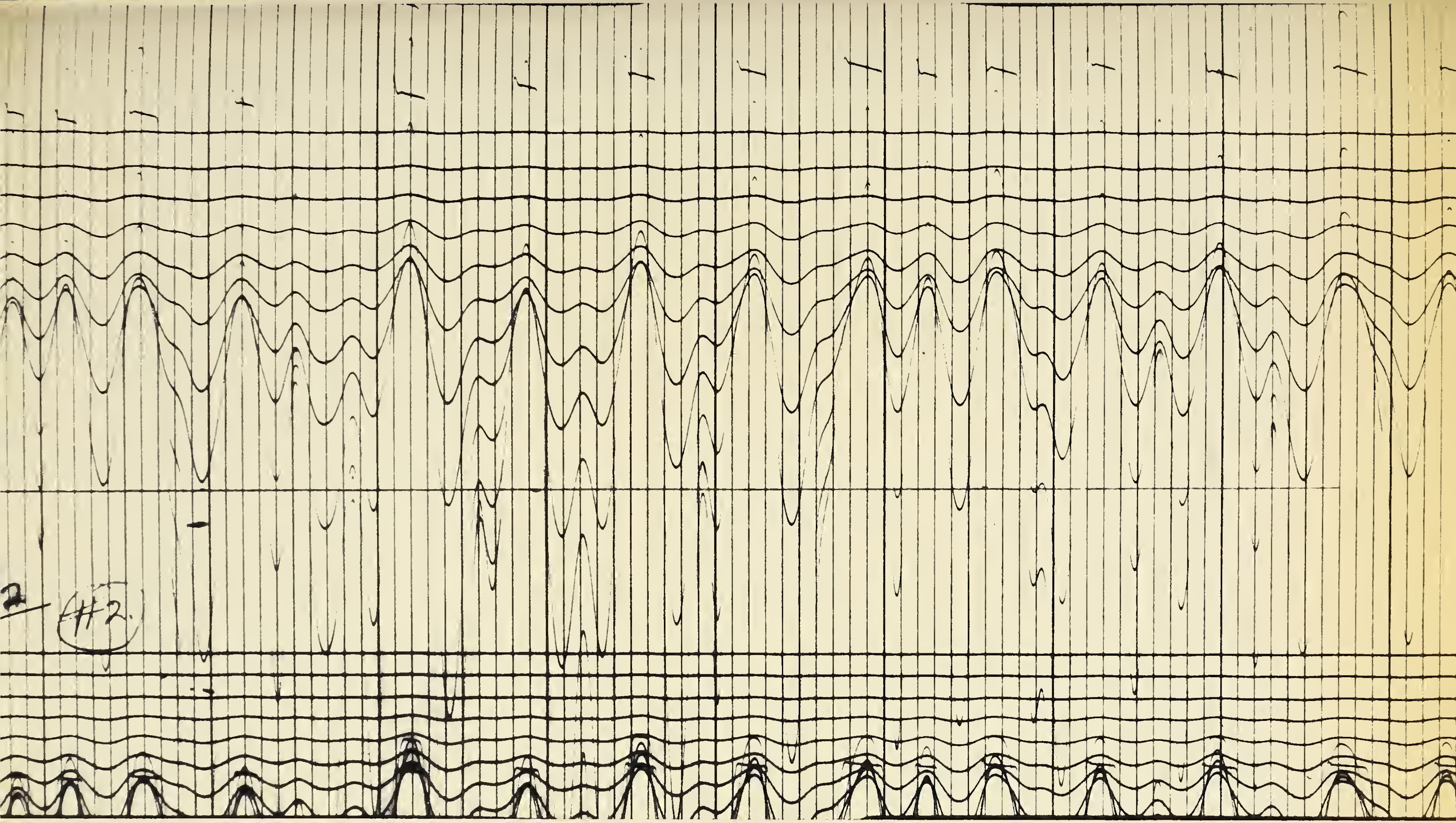

AMPLIFIER DISTORTION.

Figure 18.

A fairly large pulse was delivered to the phones. Note the distortion on the upper peaks of the traces with low attenuation. I think it can be concluded that the distortion is caused by the amplifier and not by the fact that the galvanometers have reached their limit of swing. By examining the record, one can see that roughly speaking distortion occurs on the upper traces at an amplitude of 7 1/2 cm., and on the lower traces at an amplitude of 2 cm. Now, the lower traces are 12 db. down from the upper traces, meaning that they should have 1/4 the amplitude. The difference is provided by resistors. Thus, the signal for both upper and lower traces has gone through the same amplification by the amplifiers. And, as we see, distortion occurs at about 1/4 the amplitude in the lower traces, indicating that the amplifiers are the cause. Furthermore, there is no difference at all between the galvanometers making the upper traces and those making the lower traces. This was proven by reversing the connections at the back of the camera and putting the signal of 1/4 amplitude on the upper traces. Thus, if the cause of distortion were the galvos, we would expect to see the distortion on the traces of high amplitude and not on the traces of 1/4 amplitude. Thus, the distortions are caused by the amplifiers. This is useful, actually, as it prevents the galvos from becoming overloaded. Note, however, that the peaks

seem to be amplified more than the troughs, since none of the troughs show distortion. This is a curious point.

Figure 19 shows two interesting points. The record was run on operate so that there is a separate geophone on each trace. The speed was medium. The Willmore phone is on #1 trace with an attenuation of 54 db. All the other traces are Texas S-36 phones, all at an attenuation of 60 db. No. 12 geophone is resting on a double thickness of foam rubber, while all the others are resting on the cement floor. Trace # 2 was connected to a strong 60 cycle source. This record shows crossfeed between adjacent channels. The 60 cycle source on the second trace affects the first trace very much (it is in the same amplifier bank) and the third trace to some extent. The amplifier manual does not give the channel separation, but it doesn't seem to be as much as it might be. The second noticeable point about this record is that the noise level of trace #12 (#12 phone is on the foam rubber) is much higher than that of the other traces. Also, when a pulse is applied, this phone oscillates at a frequency of between 30 and 35 c.p.s. This is probably the natural frequency of the particular kind of rubber used. This fact means that a geophone needs to be planted firmly in solid ground.

The next test was designed to check the phase of the geophones. Does an upmotion of the ground produce an

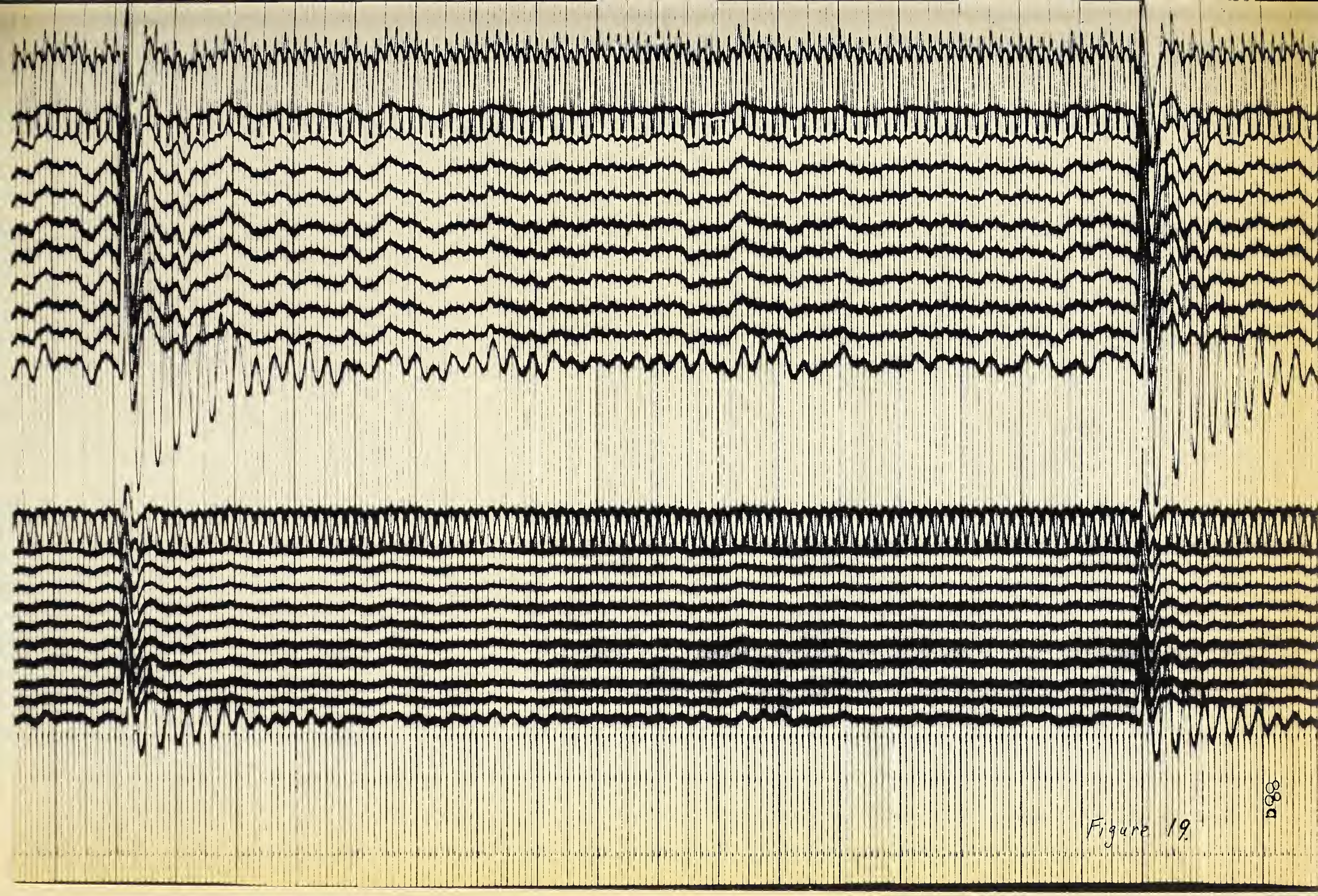

Figure 19.

up-kick or a down-kick on the seismic record? A weight (a coil of paper) on a string was used. The record was run on operate a low speed. Phone #12 was the one used for testing, and it was placed on a double thickness of foam rubber. Figure 20 shows the record produced. The first pulse was produced by setting the weight on the phone. This causes a down motion of the phone which caused an up-kick on the record. The next pulse was produced by lifting the weight off again. The phone would move up and this produced a down-kick on the record. Thus, it is concluded that an up-motion of the ground produces a down-kick on the record, when the phones are connected in the normal way (black on black, and red on red). This is conventional for exploration work.

Figure 21 shows a dynamic test of the geophones. This test is designed to determine whether the geophone is swinging properly (that is, whether it is clamped or unclamped.). This test is useful in the field to determine if a geophone, which checks out perfectly on the resistance test but produces only a dead trace, is clamped or not. If it is not clamped, then the trouble is probably at the recording truck. It can save a long useless walk! The test is carried out by setting the high cut filters on 48 c.p.s. and the attenuation at 66 db. Low speed is best. The amplifier is set on test. The camera is

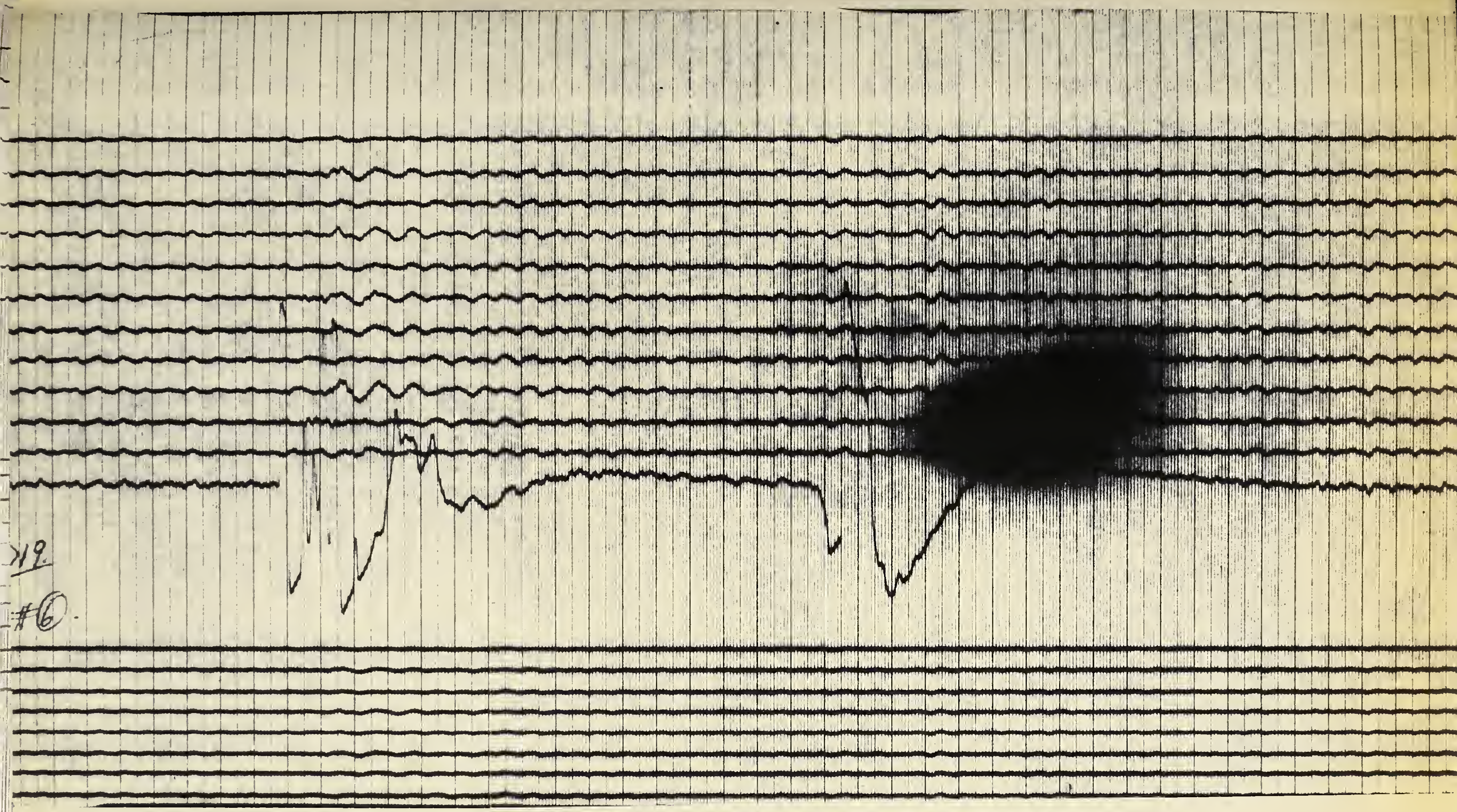

Figure 20.

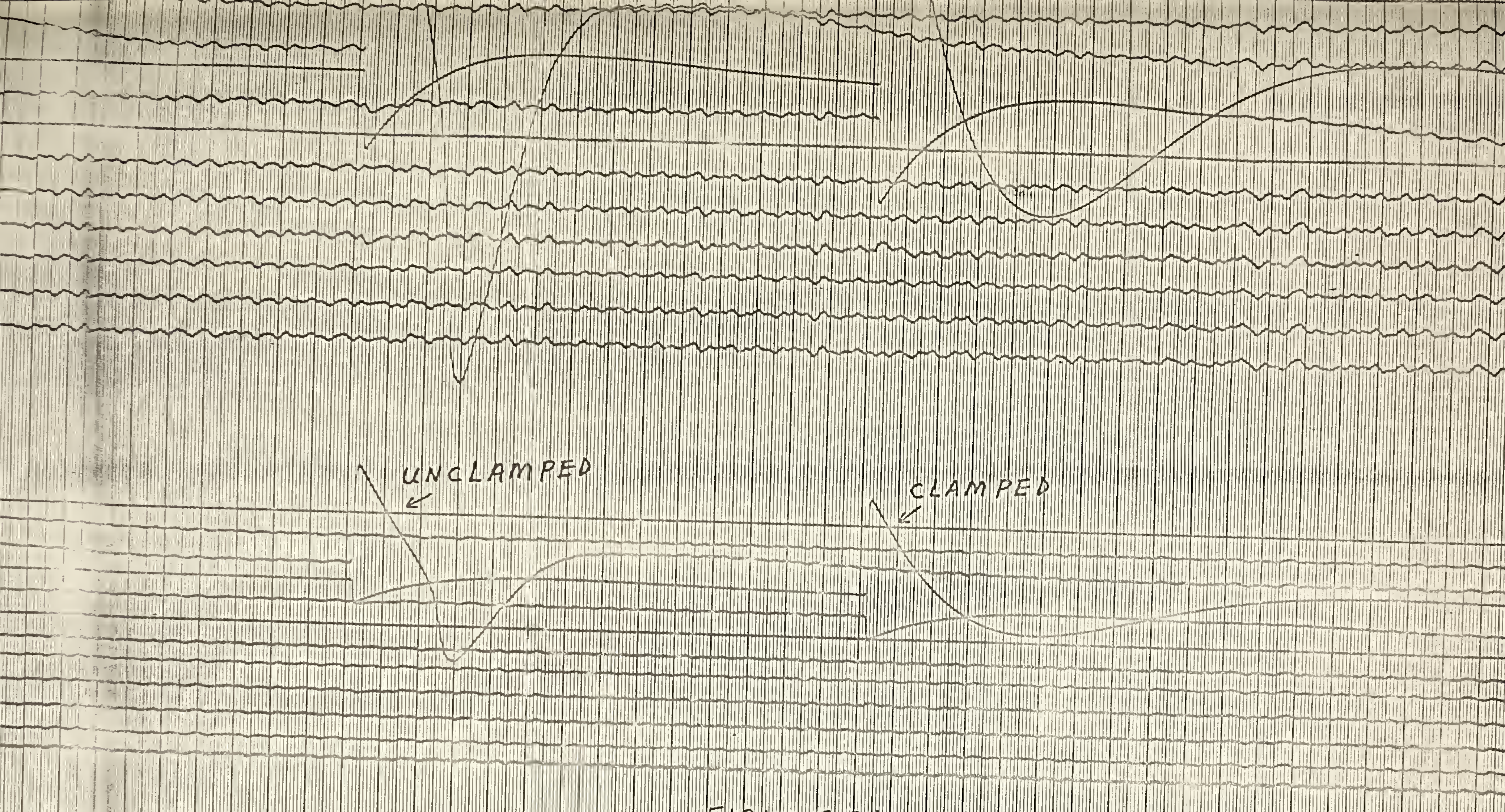

FIGURE 21

started, and the meter switch on the amplifier is rotated clockwise through 1, 2, 3, ... 12, one step per second or so. This applies a pulse to each phone in turn. The record is then developed. An unclamped phone will swing freely and damp slowly. A clamped phone damps out very quickly as shown in the figure. This test cannot show the polarity of the phone, however, that is, if the connections on the phone have been connected to the cable in reverse order or not.

Another test which was performed was designed to check the accuracy of the timing motors in the cameras. A chronometer was put on one galvo trace of the camera. Then, a short record was run to rate the chronometer against the timing lines produced by the timing motor in the camera. The timing motor and chronometer were then allowed to run for a few hours. Each hour, a short record was taken to rate the chronometer and timing lines again. Assuming that the chronometer is correct, it was found that one timing motor (on the S6 unit) was drifting .019 sec./hr. and the one on the other unit (the S3) was drifting .035 sec./hr. This is less accuracy than that quoted in the manual (1 part in 10,000). Here, we have approximately 3 parts in 10,000 and 6 parts in 10,000 respectively. But, we cannot be sure that the chronometer was not drifting. In any event, the accuracy is far more

than that required for our field work.

This would be a good place to include information on the cables. Part of this was discovered in the laboratory and part in the field. The table below gives the distances of the various take-outs on the cable (i.e., three shorter cables connected together).

Geophone #	Ft.	Kms.	Geophone #	Ft.	Kms.
female end	0	0	7	2785	.850
1	245	.0746	8	3195	.974
2	655	.199	9	3685	1.124
3	1065	.325	10	4095	1.248
4	1475	.450	11	4505	1.372
5	1965	.599	12	4915	1.499
6	2375	.724	male end	5160	1.572

The actual spread length (from phone 1 to phone 12) is 4670 ft. or 1.424 kms.

Take-out #1 (Geophone #1) can become the upper trace in two different ways: (1) plugging the female end of the cable into input #2 of the amplifier, (2) plugging the male plug into the reversing connector and plugging the reversing connector into input #1 of the amplifier.

Similarly, take-out #1 can become the lower trace by: (1) plugging the female plug into input #1, (2) plugging the male plug into the reversing plug and plugging the reversing plug into input #2.

To put all this very simply: the take-out nearest the truck becomes the #1 trace if input #2 is used (whether or not a reversing plug is needed).

In all our work at the University of Alberta, we made it a convention to have the phone nearest the shot on the #1 trace.

This concludes a description of the series of tests performed in the laboratory with the equipment before the field season began.

CHAPTER 6. GEOLOGY OF THE AREA AND THEORETICALLY PREDICTED SEISMIC ARRIVALS.

Although the main interest is not in the sedimentary section, an account must be taken of this section in order to accurately determine the thicknesses and depths of the crustal layers. This chapter explains how the effect of the sedimentary section was found.

Reflection records and velocity well-logs for Southern Alberta were obtained from various oil companies for the purpose of determining as accurately as possible the geology of the area in which the seismic survey was to be carried out. Five well-logs were found in the general area of Southern Alberta between High River and the East shot point on the Suffield Range. These wells were not in a straight line along our profile, of course, but it was assumed that a well survey a few miles off the seismic line could be used to represent conditions along the line without great error. Three of these wells penetrated the Precambrian basement. The various layers with their velocities as identified by the wells were plotted on the profile shown in figure 22. Then, the reflection records for the general area between High River and Suffield were carefully picked for reflections from the various layers down to and including the Precambrian basement. Depths to any reflecting layer were calculated

using the standard method employed where well data is available. From the well data, average velocity versus depth curves are prepared. Then, from the basic reflection formula: $T^2 = x^2/V^2 + 4h^2/V^2$, time versus depth curves can be prepared for various values of x. Then, the times for the various reflections on the reflection records are used in conjunction with the above set of curves to read off the depths to the various reflecting layers. This method of calculating depths from reflections is actually the short-cut method described in the theory with one refinement, and that is, that here the average velocity to various depths is known from well data. If this is not known, then the T^2 versus x^2 curve must be plotted and the slope taken. In this case, for calculation of depths to the various layers down to the basement, the average velocity from the well nearest the point where the record was taken was always used. The various depths that were calculated were then plotted on the profile in figure 22. Then, in conjunction with the well data previously plotted on the profile, it was a relatively easy matter to correlate the various reflecting horizons. The Solid lines indicate layers which are well supported by both reflection and well data. Thus, the profile in figure 22 is considered to be a reasonably accurate representation of the cross-section down to the basement

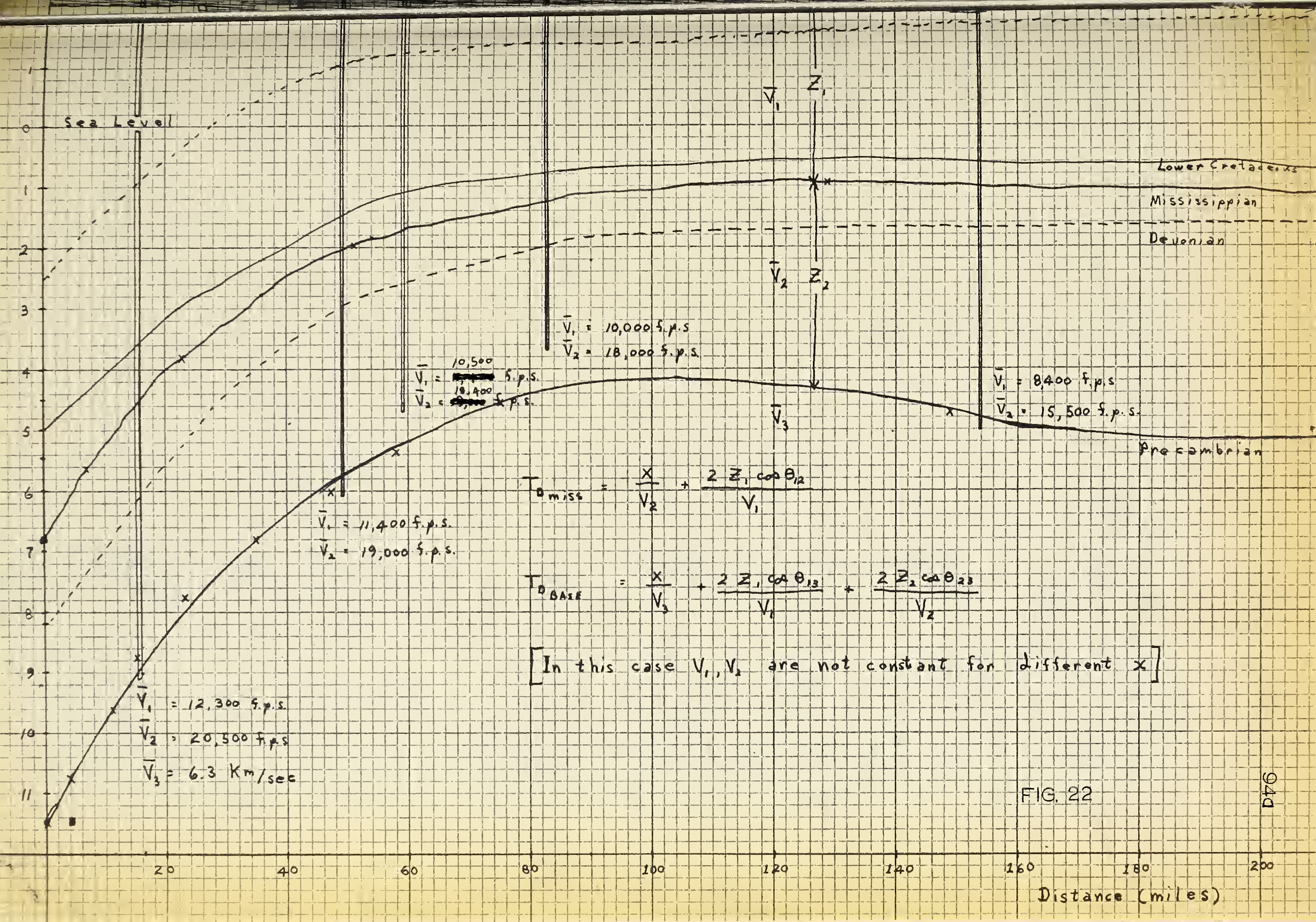

$$T_{0_{miss}} = \frac{X}{V_2} + \frac{2 Z_1 \cos\theta_{12}}{V_1}$$

$$T_{0_{BASE}} = \frac{X}{V_3} + \frac{2 Z_1 \cos\theta_{13}}{V_1} + \frac{2 Z_2 \cos\theta_{23}}{V_2}$$

[In this case V_1, V_2 are not constant for different X]

FIG. 22

in the region of Southern Alberta where the seismic survey was taken, calculated from all the latest reflection and well data in the area. It is seen from the well data that the velocity within each of the horizons increases to the west. It is also seen that all the horizons begin a very gentle slope to the west, at the western end of the profile, towards the mountains. This slope appears quite steep in the cross-section because of the vertical exaggeration of about 50 times. The actual slope at the western end is about 1.3 degrees. The velocity in any layer down to the Mississippi-an is very little different from that in any other layer. Therefore, these layers are grouped together and the various values of $\overline{V}_1$ stated on the profile are the average values of the velocity in this "first layer" at each well. Similarly, the Mississippian and Devonian layers (and any other layers between the Mississippian and Precambrian which did not show up on the reflection records) are grouped together and the values of $\overline{V}_2$ stated on the profile are the average values of the velocity in this "second layer" at each well. Since only 3 wells penetrated the Precambrian and then only very slightly, it could not be determined very accurately whether or not the velocity in this layer increased from east to west. $\overline{V}_3$ is an average velocity in this layer from all well data and is about 6.3 km./sec. If we assume that the velocity in the upper layer and in the

Mississippian layer increases linearly from east to west (and this appears to be roughly true), then since well #4 is about at the midpoint between the shot points, we can say that the velocities found at well #4 are average values for the profile. Therefore, average values of velocities are:

$$\bar{V}_1 = 10{,}000 \text{ ft./sec.} = 3.05 \text{ km./sec.}$$
$$\bar{V}_2 = 18{,}000 \text{ ft./sec.} = 5.48 \text{ km./sec.}$$
$$\bar{V}_3 = 20{,}650 \text{ ft./sec.} = 6.30 \text{ km./sec.}$$

Thus, average velocity in the upper (Cretaceous) layers is 3.1 km./sec.

Average velocity in the Mississippian layer is 5.5 km./sec., and the average velocity in the basement (Precambrian) is 6.3 km./sec. These average values are useful to keep in mind as orders of magnitude of the velocities, but for any calculations, the fact that the velocity does increase from east to west must be taken into consideration.

The upper layers (Cretaceous) are generally sandstones and shales. The Mississippian layer is high-speed limestone. The Precambrian is generally known as the top of the granite layer. It consists of a complex of igneous and metamorphic rocks.

The next section discusses the calculation of theoretical refraction arrivals from both the Mississipian and the Precambrian basement. Since it is not very certain

that the velocity in the Precambrian increases from east to west, a fixed velocity of 6.3 km./sec. was used for this layer in all calculations. However, for refraction time through the Mississippian and Precambrian, the increase in velocity in the limestone was definitely considered. Figure 23 shows a plot of 1/V in the Mississippian from east to west (top) and from west to east (bottom). This figure also indicates how the travel time was calculated through the Mississippian by integrating these graphs. From the seismic theory chapter, travel time for two layers is

$$T = \frac{X}{V_2} + 2z_1\left(\frac{V_2^{\,2} - V_1^{\,2}}{V_1^{\,2}\ V_2^{\,2}}\right)^{1/2}$$

This can also be written as

$$T = \frac{X}{V_2} + \frac{2z_1 \cos i_{12}}{V_1}$$

The first term X/V_2 is calculated by integrating the graph of $1/V_2$ versus X (figure 23). The second term $(2z_1 \cos i_{12})/V_1$ can be called a time-delay term. This term is composed of two parts, the travel time from the shot to the Mississippian and the travel time from the Mississippian to detector. These two times are the same if the depth z_1 is constant (i.e., if the layer is horizontal) and if V_1 is also constant. Neither is true here. Thus, we calculate a delay time for the shot point and one for the detector and

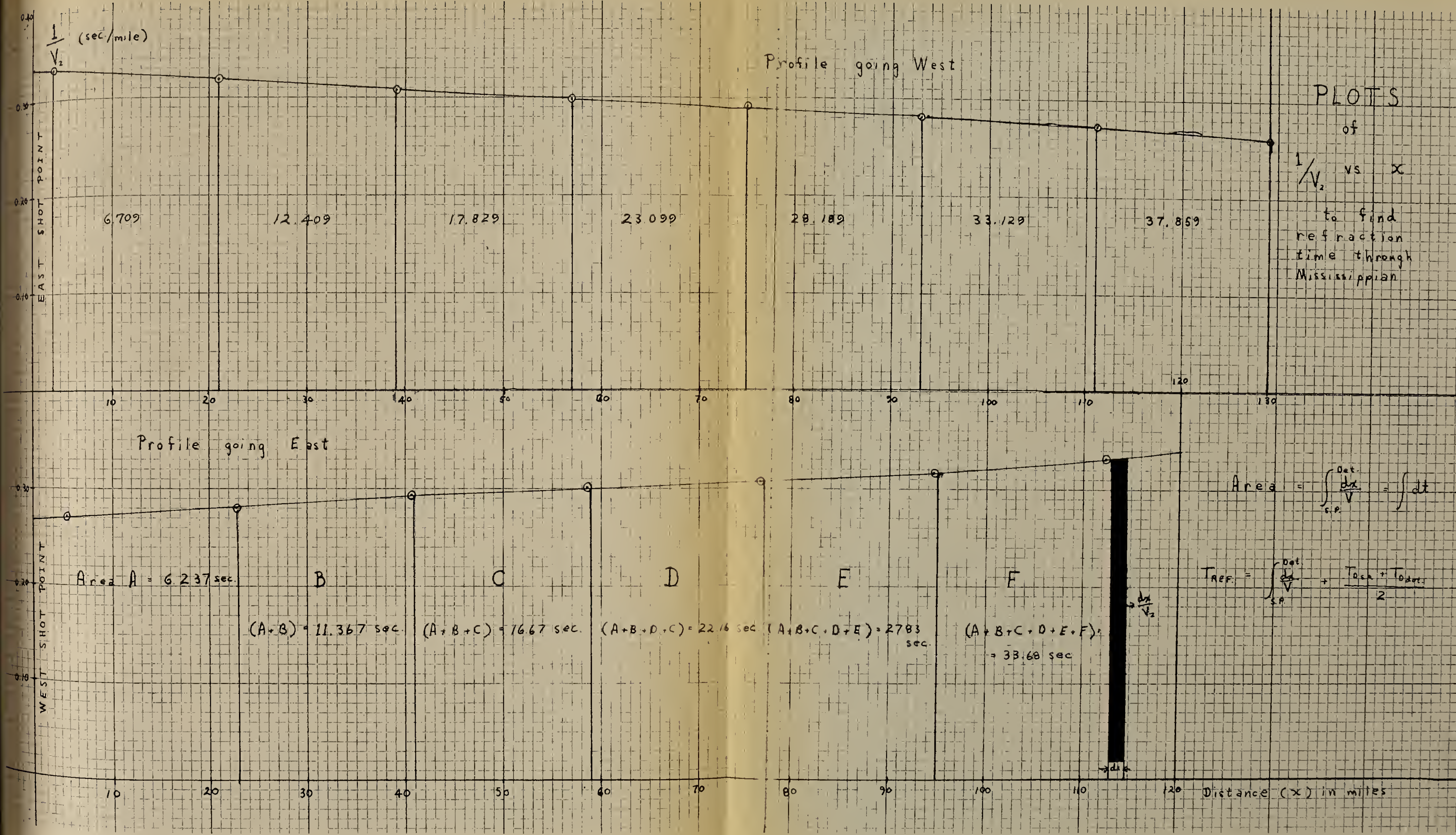

PLOTS
of
1/V₂ vs x
to find refraction time through Mississippian
1/V₂ (sec/mile)
Profile going West
EAST SHOT POINT
0.40
0.30
0.20
0.10
6.709
12.409
17.829
23.099
28.189
33.129
37.859
10
20
30
40
50
60
70
80
90
100
110
120
130
Profile going East
WEST SHOT POINT
Area A = 6.237 sec.
B
C
D
E
F
(A+B) = 11.367 sec.
(A+B+C) = 16.67 sec.
(A+B+D+C) = 22.16 sec
(A+B+C+D+E) = 27.83 sec.
(A+B+C+D+E+F) = 33.68 sec
dx/V₂
dx
Area = ∫_{S.P.}^{Det.} dx/V = ∫dt
T_REF. = ∫_{S.P.}^{Det.} dx/V + (T_0sh + T_0det.)/2
Distance (x) in miles

divide by two to get the total delay time. Thus, for any shot - detector distance X, the appropriate delay time is calculated and added to the appropriate integral from the graph to give the total travel time for that refraction from the Mississippian. Using this method, the theoretical refraction lines from the Mississippian were calculated for both the west shot point and the east shot point. Similarly, theoretical refraction times from the Precambrian were calculated for both the west shot point and the east shot point; More complicated delay terms are involved in this case, but integration on a velocity - distance graph is not necessary since we are considering (for lack of data) a uniform velocity of 6.3 km./sec . at the top of the Precambrian.

These theoretical refraction arrivals for the Mississippian are shown plotted on the same time - distance graphs as our field results (figures 26 & 27). More will be said about them later in the chapter on Interpretation of the Field Results.

The calculations are not included in this thesis, since the details are not pertinent to the results. They are, however, available at the University of Alberta. The theoretical arrival times for the Precambrian are not shown on our graphs, since the times are very close to those actually found in the field, and their inclusion would have made the graphs difficult to read.

CHAPTER 7 - ORGANIZATION OF THE FIELD WORK

The seismic work by the University of Alberta was carried out in Southern Alberta for a number of reasons. The area is open, flat, prairie with no trees and only an occasional farm house. One can drive almost anywhere on the prairie, as long as one remembers to open and close the numerous cattle gates. Invariably, any spot picked on the map as a suitable place for a set-up, will be possible to reach by truck. Power lines are about the only source of trouble on the prairie. But, if 60 cycle power lines are found on reaching the chosen site, another site can always be found within a mile or so which will be suitable and free of power lines. Map reading must be done very carefully on the prairie, or one will very quickly become lost, since there are almost no landmarks (except a microwave tower and the occasional grain elevator of a small village) to follow. Another reason for choosing Southern Alberta for the work is that Richards and Walker carried out a short refraction profile in south-western Alberta parallel to the Rocky Mountain trench in 1958, and this work is very useful to compare to our own. This work has already been discussed, and will be referred to again. Thirdly, the Suffield experimental station agreed to cooperate with us fully by setting off the charges for us. It was thought

that this would save us valuable time and money. Unfortunately, it did neither. This was certainly not the fault of the Suffield people, however, since I believe that they worked very hard for us, in fact, harder than necessary, and we are deeply indebted to them. But, it is, difficult for large organizations such as the University of Alberta and the Suffield Experimental Station to work together efficiently. Very often, when we were ready for a shot, Suffield was not in a position to set one off for us, due to pressure of their own work. Then, when they were ready to set off a charge for us, we were often not ready for them. Also, communication between officials of Suffield and officials of the University was not always the best, and a number of unnecessary trips from Edmonton to Southern Alberta were made. In future, it would probably be better to hire a Geophysical Company to set off the shots whenever they were desired. Another reason for choosing Southern Alberta is that the area is reasonably close to Edmonton, the location of the University. Calgary is only a three hour drive from Edmonton. Thus, if field problems occurred, the trucks could always return to Edmonton to avoid unnecessary hotel bills and living expenses. These are the chief reasons that Southern Alberta was chosen for the work. The exact location of the seismic profile is shown on the map in figure 24.

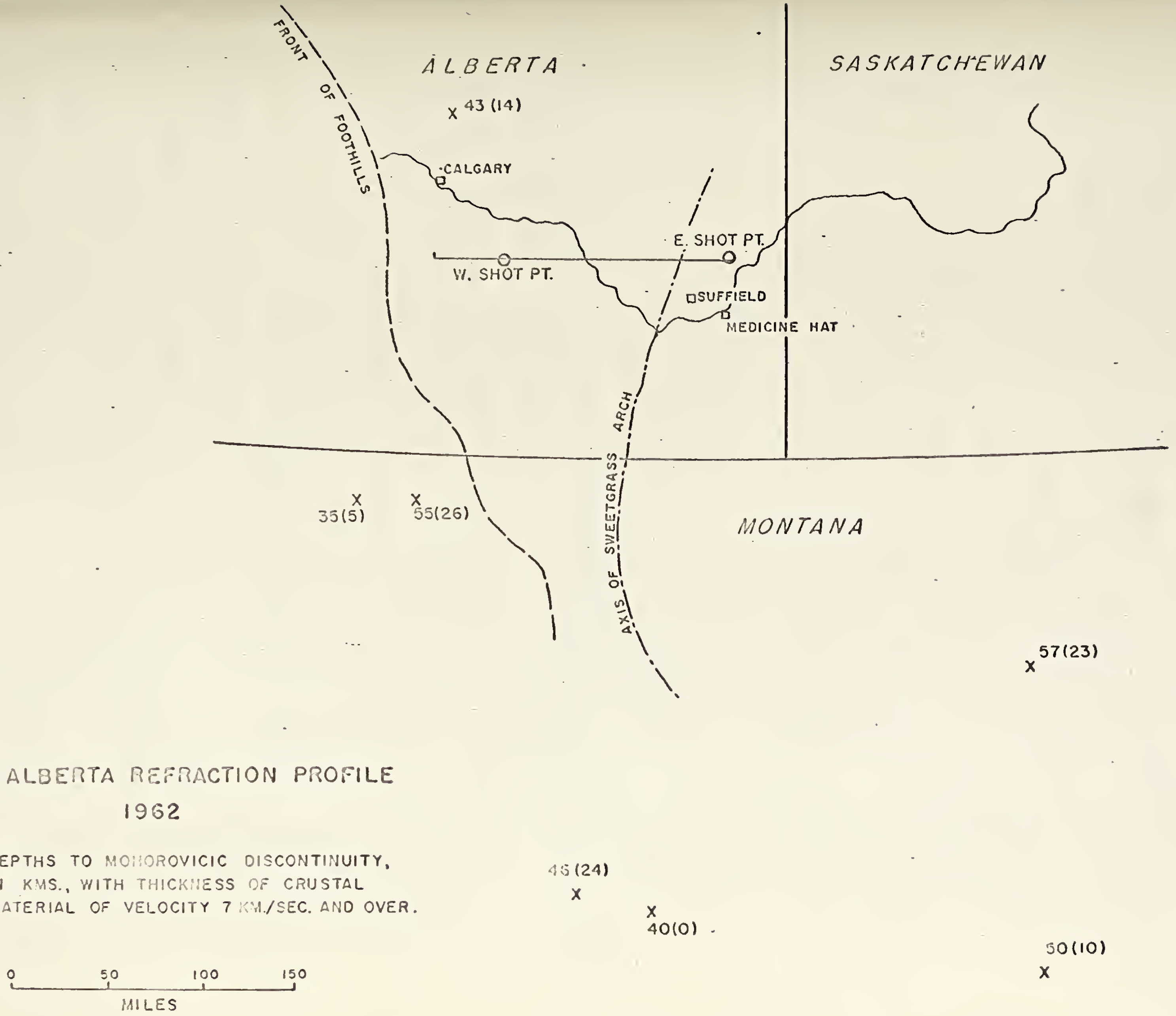

SOUTH ALBERTA REFRACTION PROFILE

1962

57(23) : DEPTHS TO MOHOROVICIC DISCONTINUITY, IN KMS., WITH THICKNESS OF CRUSTAL MATERIAL OF VELOCITY 7 KM./SEC. AND OVER.

FIG. 24

A very important part of the field operations was the setting-up and operation of the very high frequency radio link from Suffield to High River. This was discussed earlier in the chapter on equipment. The radio link, of course, enabled us to communicate directly with the shot point (Suffield), and enabled us to put the exact shot timing on our records. This radio link consisted of two repeater stations (one at Rainier and one north of Vulcan on Buffalo Hill) and the mobile units for each truck (besides, of course, all of Suffield's own radio equipment). The setting-up and operation of this link cost us much valuable time. The General Electric Company was on contract to have the repeater stations operating early in May. They were not operating until mid-June. The fault of the delay, however, does not lie entirely with General Electric. Several unforeseen events occurred to hinder the progress, such as a truck strike in Ontario, which made it impossible to get towers for a certain period. Even after the link was operating, many problems occurred throughout the summer. Either one repeater or the other or one of the mobiles was usually malfunctioning. The service from General Electric in correcting our difficulties was extremely good, however, and I must commend them for that. The fact that all the equipment was new and a link such as this one had not been set up before caused most of the difficulty. Next year,

the same repeater stations (but not the same locations) will be used and the same mobile units will be used. Since most of the "bugs" have been worked out of the system, it should prove very efficient next year. When working properly, the system is one of the best. It provides direct communication with the shot point, and if one runs into difficulty at the recording trucks, he can always delay the shot. Furthermore, the tone break provides the shot instant time on the records to an accuracy of about 1 to 2 milliseconds.

All of the shot information is contained in the table on the next page. This table includes the location, date, time, type, size, and depth of each shot, and the number of useful seismic records obtained from the shot. Diagrams of the exact locations of all the shots and spreads appear in the Appendix III.

The next section will deal with the interpretation of the seismic records taken in Southern Alberta by the University of Alberta.

Seismic Program, Summer, 1962
University of Alberta
List of Shots

Shot No.	Location	Date	Time (hrs)	Type	Approx. (lb) charge size	No. of useful records obtained	Approx. depth of charge (ft)
1	East	June 1	1400	Buried	100	0	100
2	West	June 10	1000	Buried	1,000	4	190
3	West	June 11	1000	Buried	1,000	2	190
4	East	June 13	1400	Buried	200	1	180
5	East	June 20	1400	Buried	1,000	1	150
6	East	June 20	1600	Surface	1,000	0	0
7	West	June 21	1400	Buried	500	2	120
8	East	June 25	1340	Buried	240	2	120
9	East	July 16	1400	Buried	800	0	80 - 90
10	East	July 17	1530	Buried	800	2	40 - 50
11	East	Aug. 1	1330	Surface	10,000	2	0
12	East	Aug 15	1400	Surface	40,000	2	0
13	East	Sept. 10	1015	Surface	10,000	2	0
14	East	Sept. 27	1400	Buried	1,000	2	50
15	East	Sept. 28	1035	Buried	1,000	2	50
16	East	Sept. 28	1530	Buried	1,000	2	50

CHAPTER 8

INTERPRETATION OF THE SEISMIC RECORDS

Distances:

The distances from each shot to each spread were determined by scaling with a good metre rule from large scale maps. The scale given on the maps from the Department of Mines and Technical Surveys was 1:250, 000. This scale was found to be incorrect, probably due to map shrinkage. The distance across several townships on each map, Gleichen and Medicine Hat, was measured in centimetres as accurately as possible several times using the metre rule. This distance in centimetres was then divided into the actual distance in kilometres, calculated by knowing that in an east-west direction, each section is one mile plus a road allowance of 66 ft. Using this method, the scale factor on the Gleichen map was found to be 1:251, 700 and on the Medicine Hat map sheet to be 1:252, 300. These factors would no doubt be different if a different metre stick were used and/or if different copies of the same map were used. Thus, for any accuracy at all in scaling map distances, the scale factors must be checked. The distances from each shot to each spread are given in the table of arrival times in the Appendix II. Two of these scaled distances were checked by scaling the latitudes and longitudes of the points and then using the distance formula given in section G of chapter three. Each of these distances agreed with the scaled distances to ± 0. 30 kilometers. Thus, the error in the distances at 30 kms. is about ± 1%, while for greater distances, the percentage error is much less.

Times:

After each record was dried, and usually after arrival back in the

laboratory at Edmonton, the shot instant was marked on the record in ink. In all cases where the tone break was employed (the majority of records), the shot instant was merely one second and three milliseconds after the beginning of the tone break. In other cases, (shots from the west), shot instants were known in absolute time, and thus were easy to mark on the records, since absolute time had also been recorded on them. Following this, the next heavy timing line after the shot instant was called zero, and the appropriate correction time to shot instant was marked on the record. Then, starting at the zero mark, the timing in seconds was marked along the entire length of each record. Once this was completed, the time for any event on any trace on any particular record could be very quickly determined. The error in the shot instant is about ± one millisecond. The error in the reading of the time for any particular event depends on the quality of that event. For a trace of average quality, however, and a record taken at slow speed (2-1/2 in./sec.), the error in reading a time is probably about ± 2 milliseconds, giving an overall error in the time of ± 3 milliseconds. Even at very small times such as 1 second, this represents an error in the time of only ± 0.3%. But, if the step-out time across the record is only 0.20 seconds, then this timing error could result in an error of ± 1.5% in the apparent velocity of an arrival. These percentage errors which I am giving do not represent any sort of confidence limits, but rather represent worst possible cases.

Picking of Arrivals and Plotting of Them:

The picking of separate energy events on records is more of an art than a science. It depends mostly on the experience and intuition of the seismologists. The records must be studied again and again in order to make sure that all the separate energy events have been picked, and that no second or later cycle of one event has been picked as a separate

event. Time-distance tables for all arrivals correlated on each record can be found in Appendix II. These tables also contain the apparent velocity values for each arrival. These apparent velocity values were found by plotting each arrival on very large scale time-distance graphs. Figure 25 shows one of these graphs for the first few arrivals on the record taken by truck two for shot number ten.

Then, all of these arrivals were plotted in their correct places on very large travel time graphs (actual size 4 ft. by 4-1/2 ft.), one graph for each shot point (east and west). These arrivals were then correlated on these graphs from spread to spread, using data such as energy, frequency, character, etc. , (as given in section F of Chapter 3), and straight lines were drawn through all arrivals believed to be refractions from the same horizon. Each particular set of travel-time lines represents an earth model. Once an earth model has been chosen, calculations must be done to find out if the model is reasonable, and if the calculated critical points are not in contradiction to the appearance of strong energy arrivals on the graphs. In all, more than twenty earth models were tested, before a preferred model was chosen. Since none of the models tested indicated very much dip in any of the layers, the velocity and intercept values were averaged from both graphs, and refraction theory for horizontal layering was used in the preliminary testing of all models. When the preferred model was finally chosen, refraction theory for dipping layers was applied in order to find the actual depths under each shot-point, and the dips of the layers. The travel-time graphs for the preferred model are shown in figures 26 and 27. Figure 26 is the travel time graph for the east shot point and figure 27 is the graph for the west shot point.

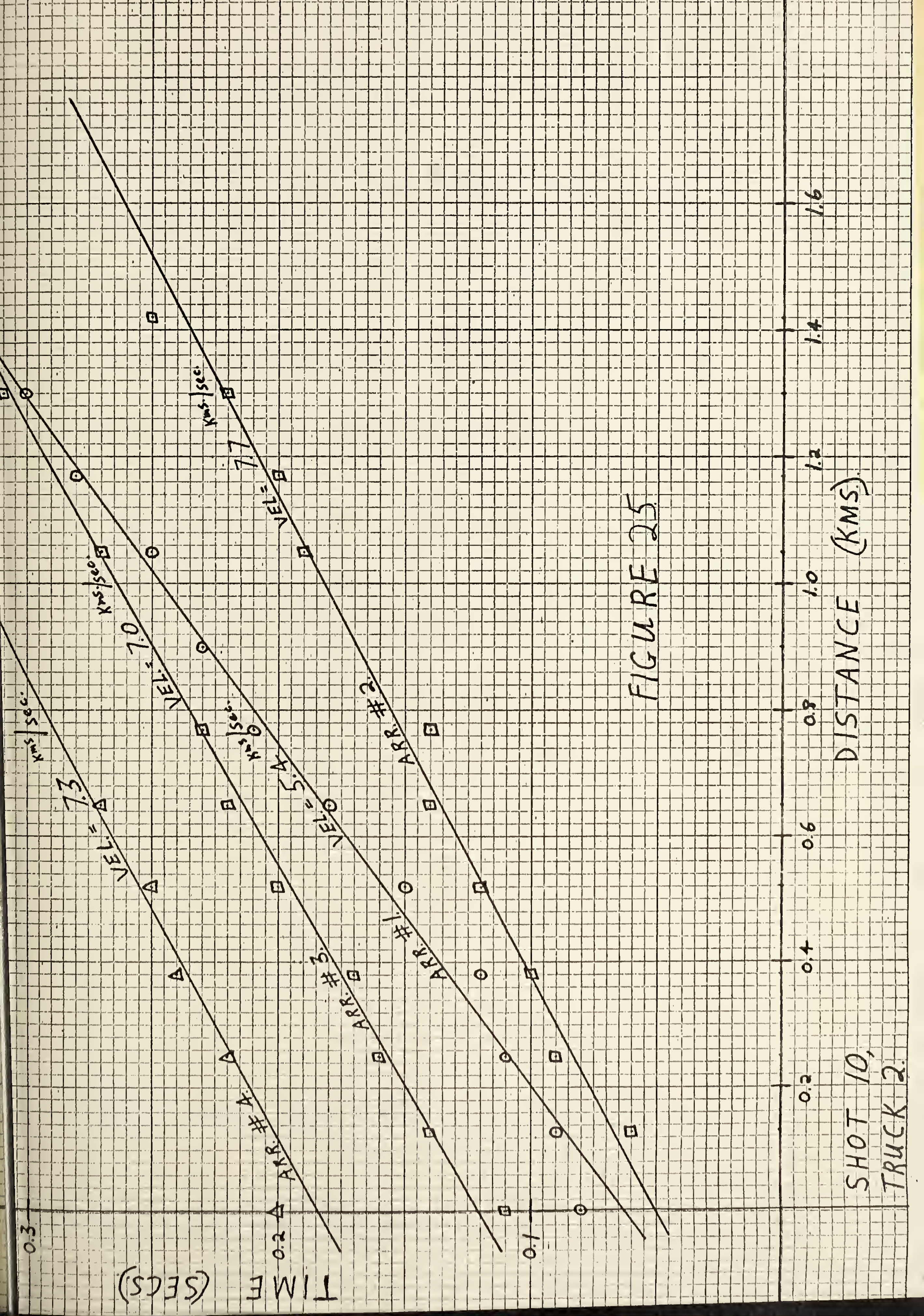

FIGURE 25

SHOT 10,
TRUCK 2.

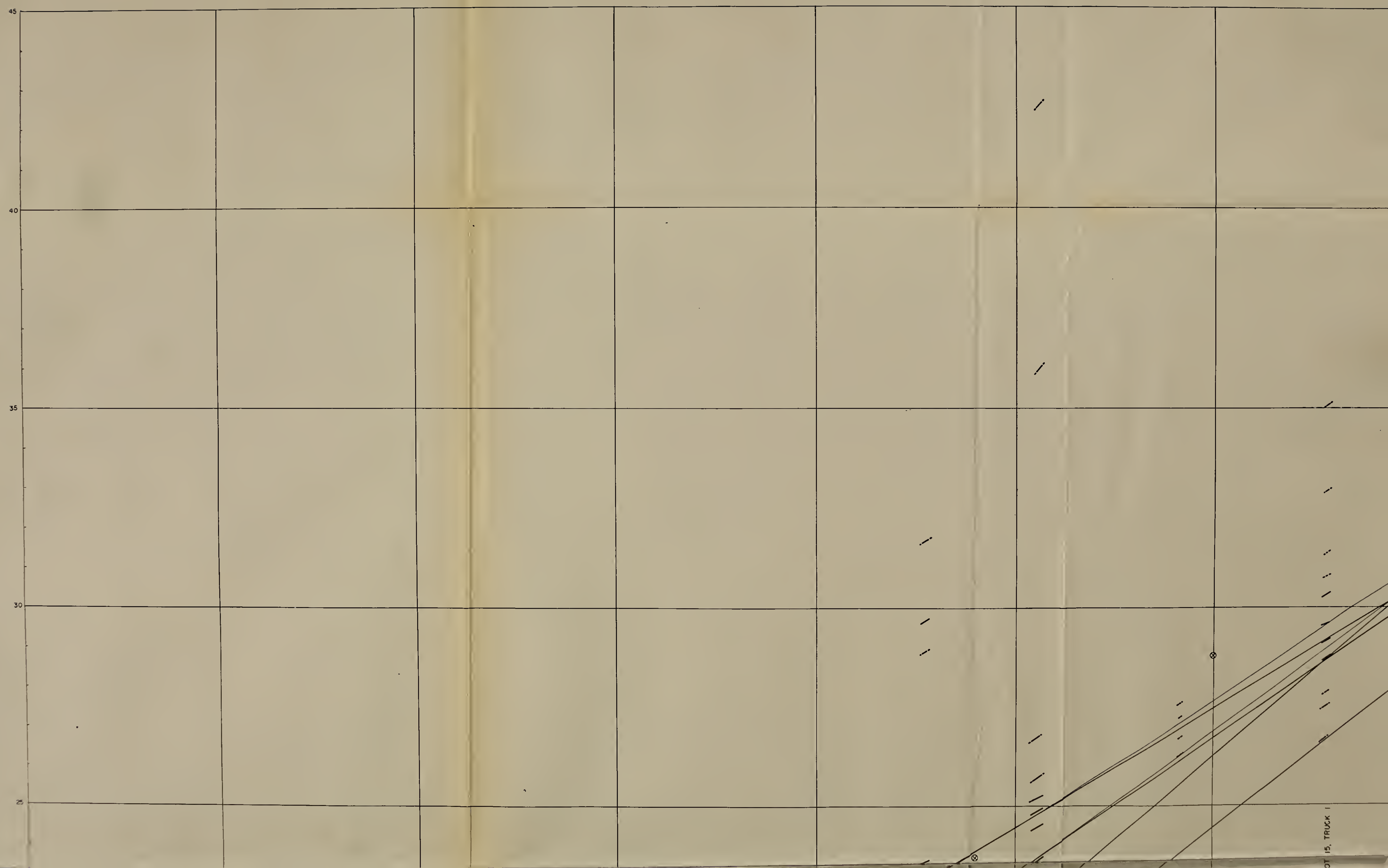
45
40
35
30
25
OT 15, TRUCK 1

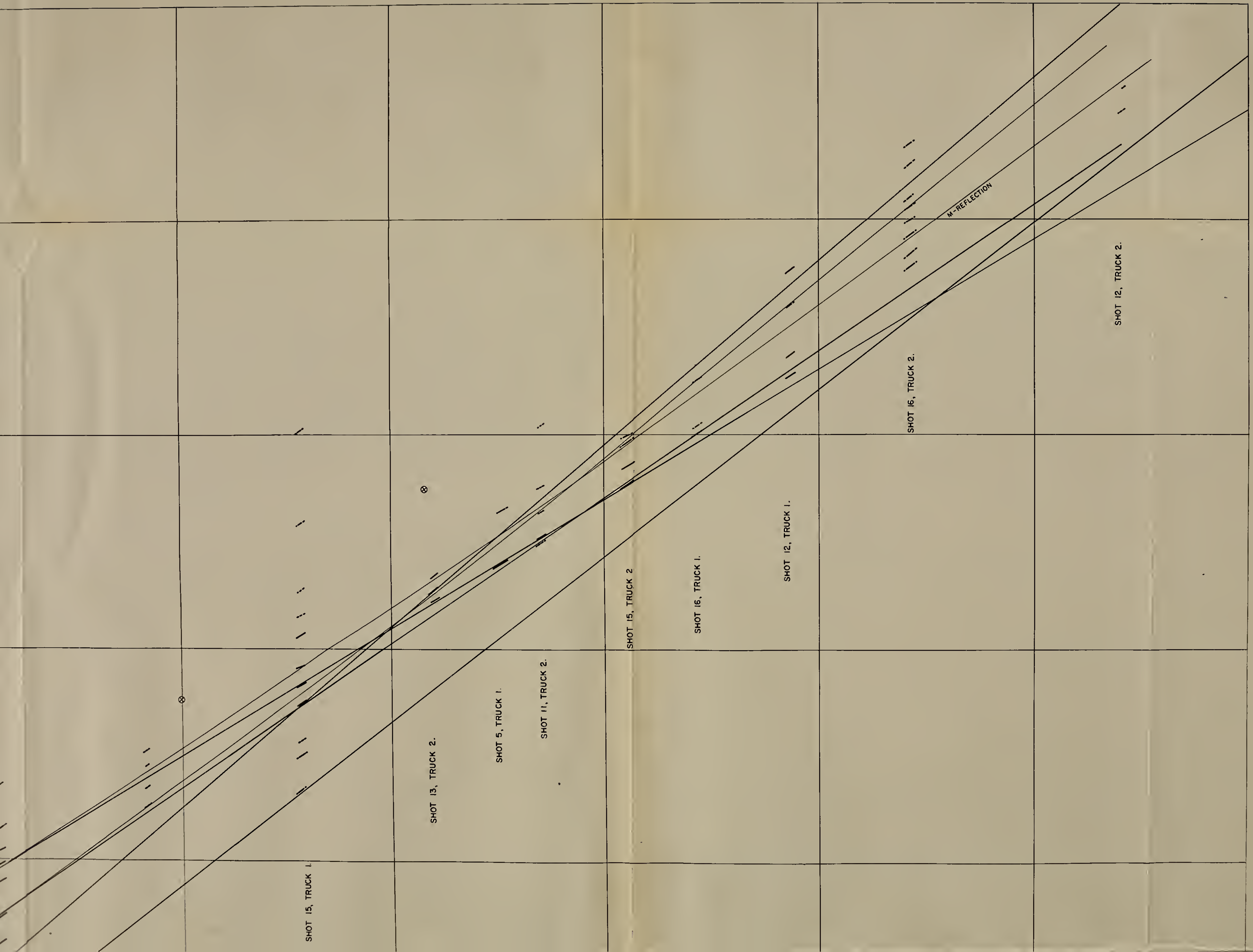
SHOT 15, TRUCK 1.
SHOT 13, TRUCK 2.
SHOT 5, TRUCK 1.
SHOT 11, TRUCK 2.
SHOT 15, TRUCK 2
SHOT 16, TRUCK 1.
SHOT 12, TRUCK 1.
SHOT 16, TRUCK 2.
SHOT 12, TRUCK 2.
M-REFLECTION

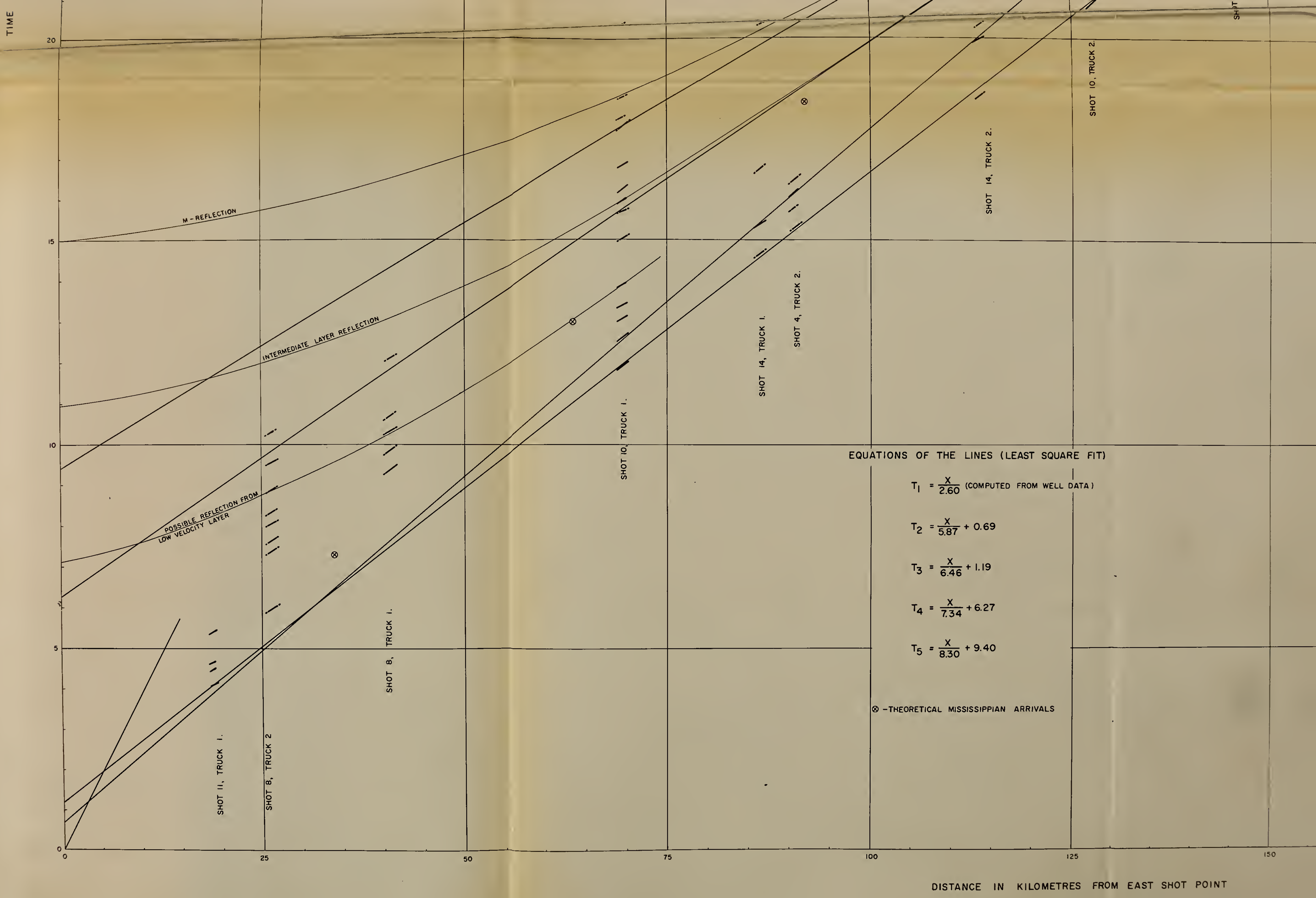

EQUATIONS OF THE LINES (LEAST SQUARE FIT)

$T_1 = \frac{X}{2.60}$ (COMPUTED FROM WELL DATA)

$T_2 = \frac{X}{5.87} + 0.69$

$T_3 = \frac{X}{6.46} + 1.19$

$T_4 = \frac{X}{7.34} + 6.27$

$T_5 = \frac{X}{8.30} + 9.40$

⊗ -THEORETICAL MISSISSIPPIAN ARRIVALS

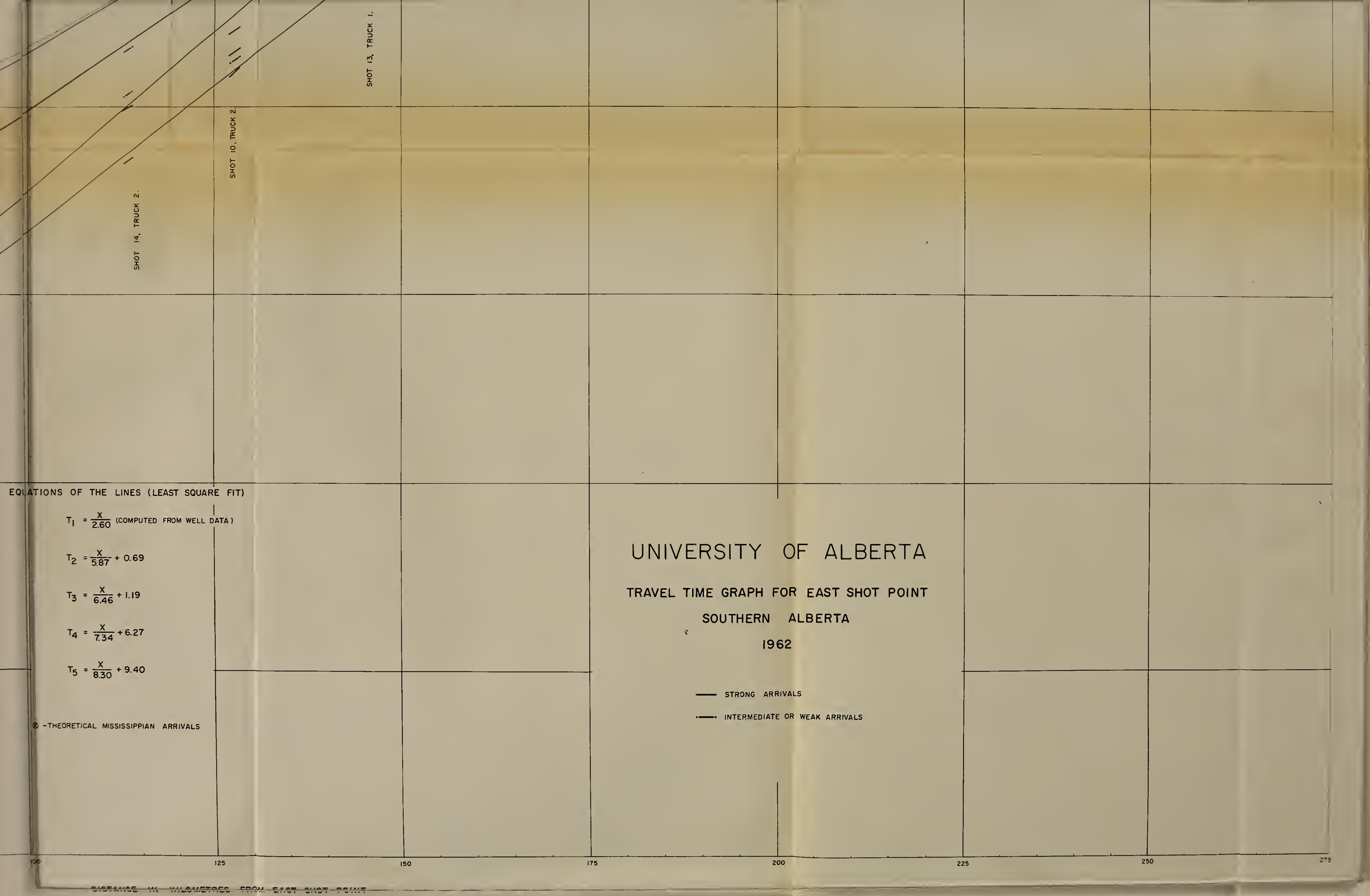

EQUATIONS OF THE LINES (LEAST SQUARE FIT)

$T_1 = \frac{X}{2.60}$ (COMPUTED FROM WELL DATA)

$T_2 = \frac{X}{5.87} + 0.69$

$T_3 = \frac{X}{6.46} + 1.19$

$T_4 = \frac{X}{7.34} + 6.27$

$T_5 = \frac{X}{8.30} + 9.40$

⊗ -THEORETICAL MISSISSIPPIAN ARRIVALS

UNIVERSITY OF ALBERTA

TRAVEL TIME GRAPH FOR EAST SHOT POINT

SOUTHERN ALBERTA

1962

—— STRONG ARRIVALS

·—· INTERMEDIATE OR WEAK ARRIVALS

WEST TRAVEL TIME GRAPH.

FIG. 27

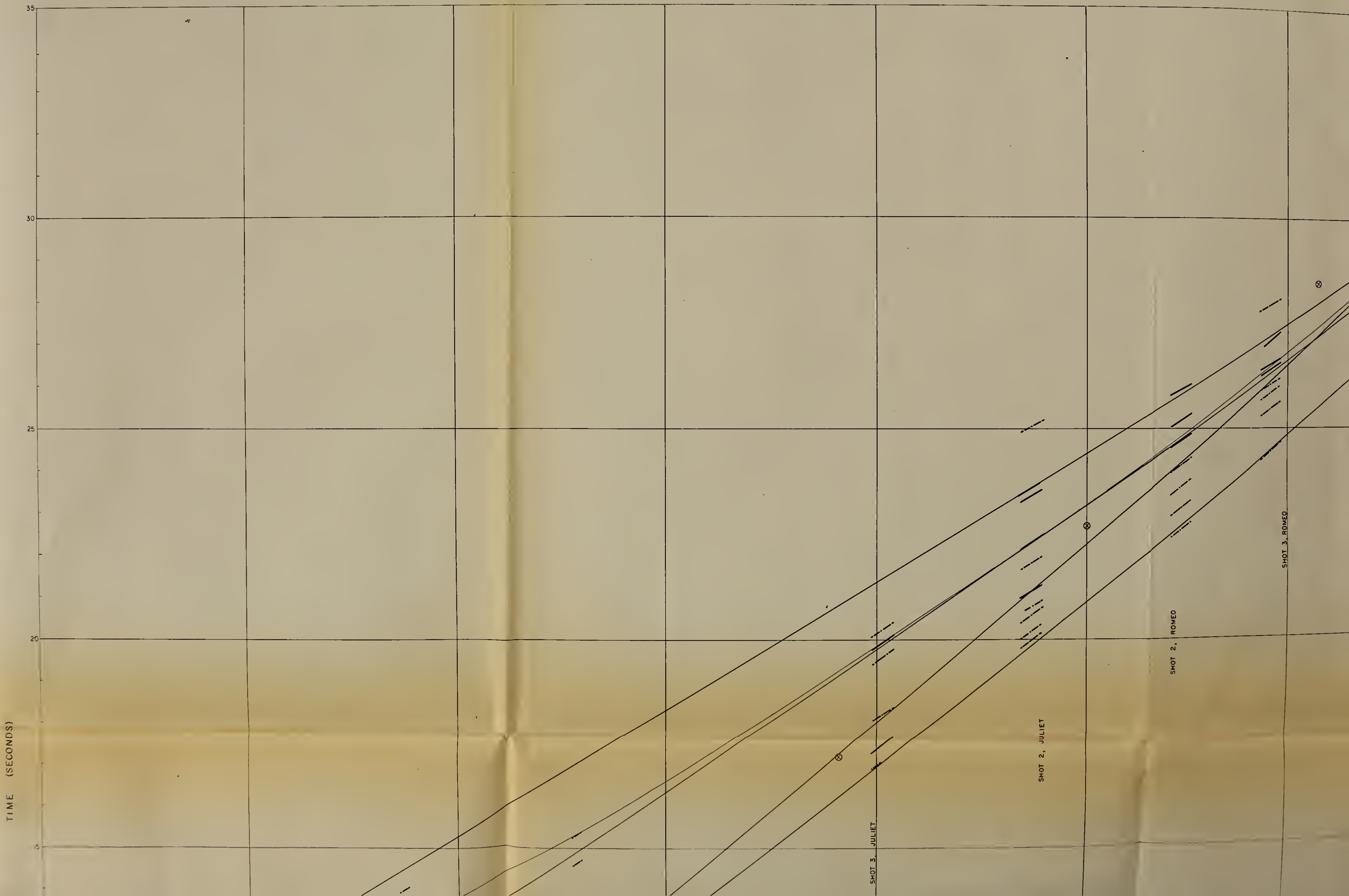
35
30
25
20
15
TIME (SECONDS)
SHOT 3, JULIET
SHOT 2, JULIET
SHOT 2, ROMEO
SHOT 3, ROMEO

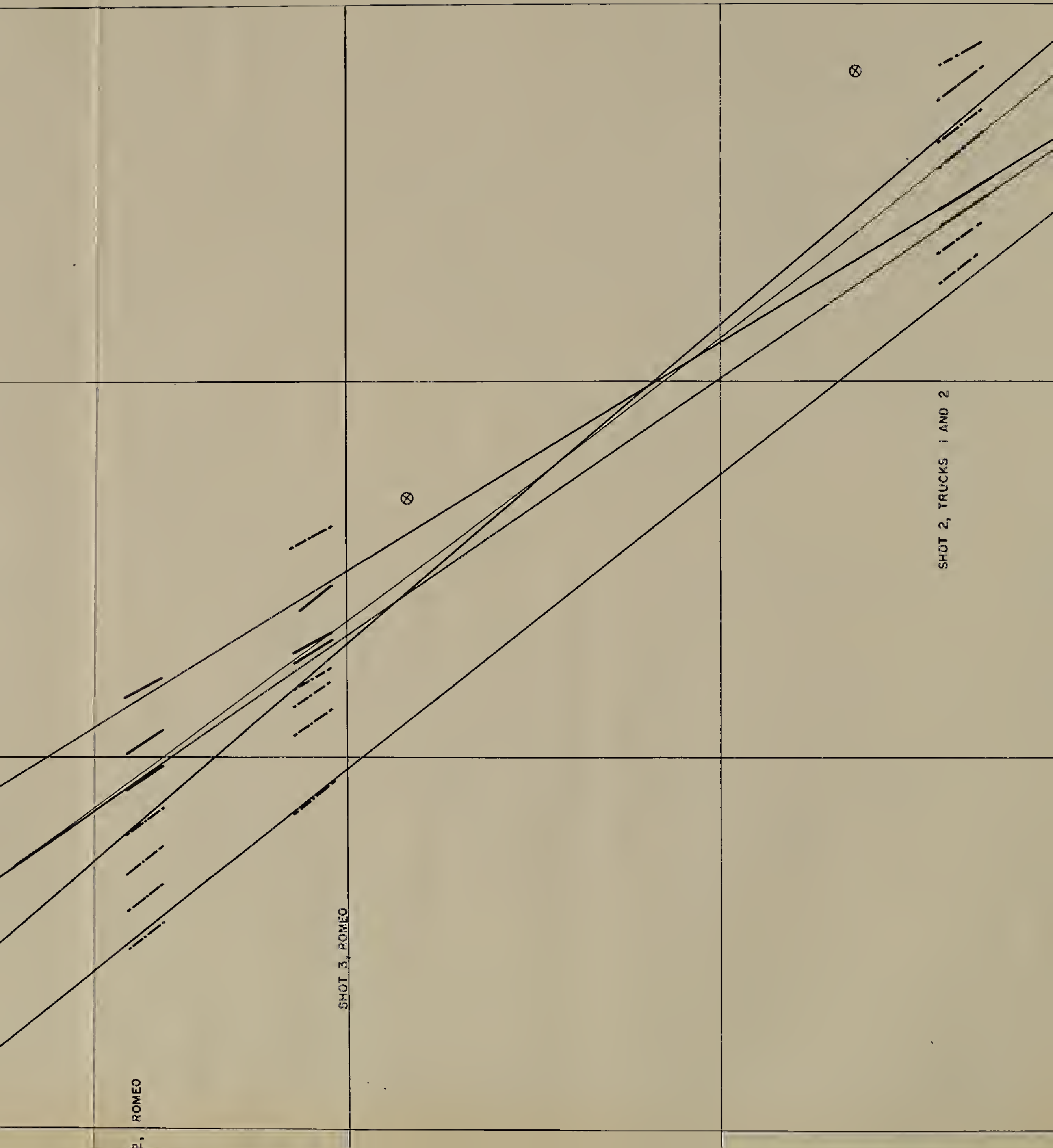
SHOT 2, TRUCKS 1 AND 2
SHOT 3, ROMEO
ROMEO

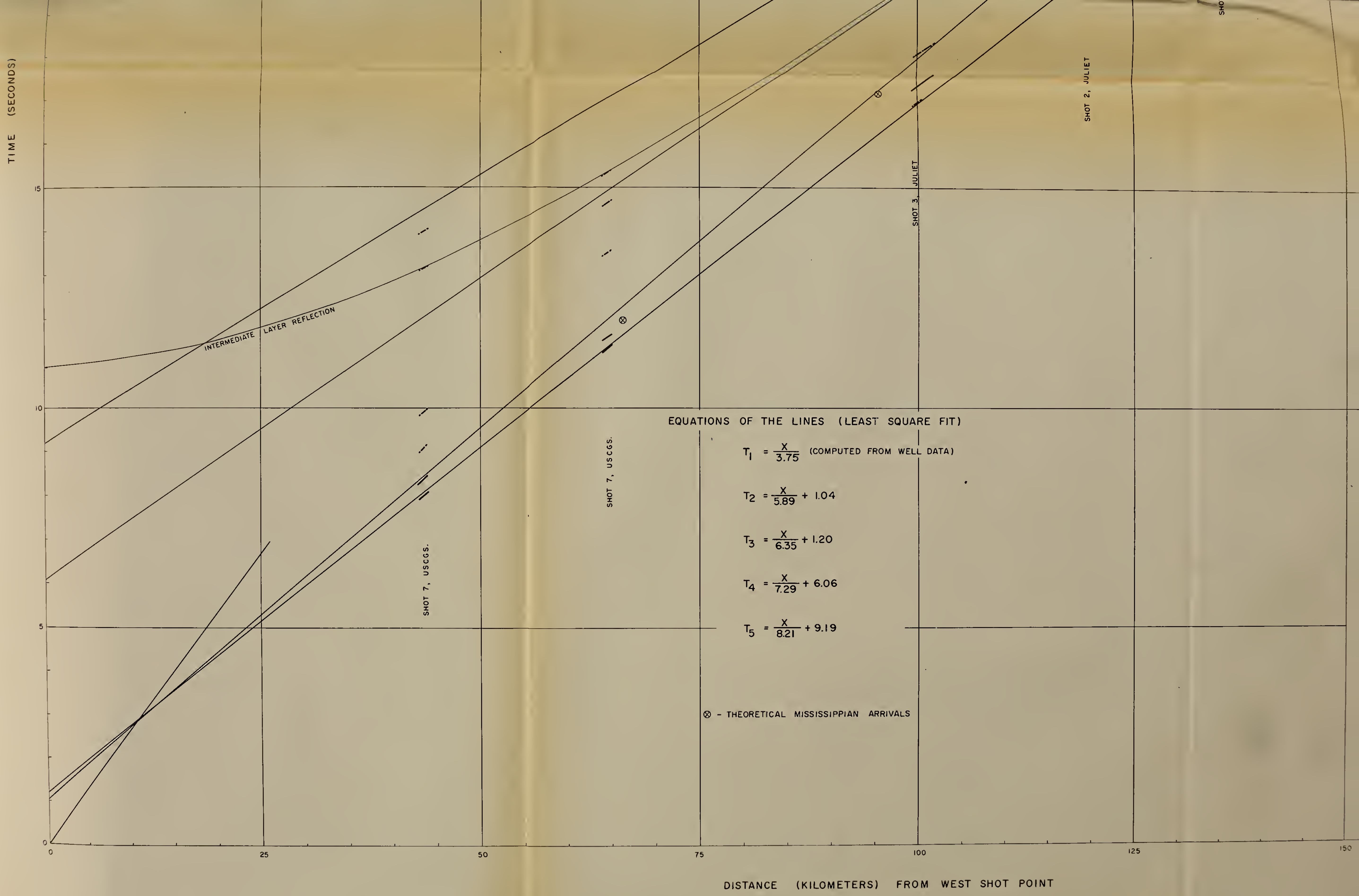

EQUATIONS OF THE LINES (LEAST SQUARE FIT)

$T_1 = \frac{X}{3.75}$ (COMPUTED FROM WELL DATA)

$T_2 = \frac{X}{5.89} + 1.04$

$T_3 = \frac{X}{6.35} + 1.20$

$T_4 = \frac{X}{7.29} + 6.06$

$T_5 = \frac{X}{8.21} + 9.19$

⊗ - THEORETICAL MISSISSIPPIAN ARRIVALS

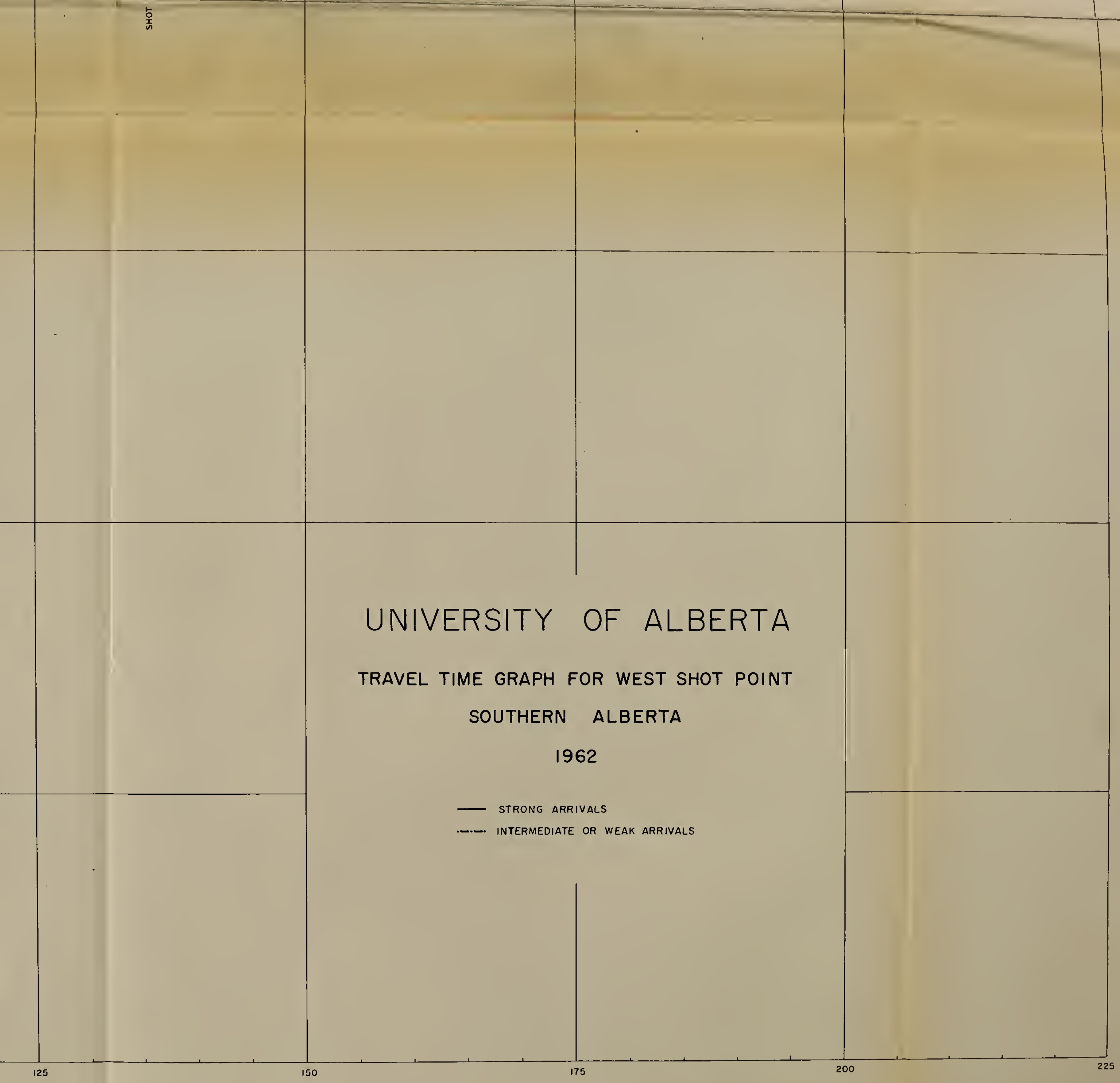

UNIVERSITY OF ALBERTA

TRAVEL TIME GRAPH FOR WEST SHOT POINT

SOUTHERN ALBERTA

1962

Summary of the more important models, and reasons for rejection of them:

Model 1:

This was a four-layer case (omitting the intermediate layer). The average velocities of the four layers were 3.16, 5.95, 6.42, and 8.35 kms./sec. respectively. The depth to the Moho was found to be 44.6 kms. This model was rejected, because there are good arrivals from an intermediate layer, which we simply cannot ignore.

Model 2:

This was a five-layer case, which included a layer of velocity 7.05 kms./sec. just above the base of the crust. The depth to this intermediate layer was found to be 35.8 kms. For this model, the depth to the Moho by the crossover and intercept methods did not agree. The crossover method gave a depth of 44.7 kms., while the intercept method gave 47.1 kms. This model was rejected on the basis of this discrepancy. The seismic records were examined again for both shot points and several errors were found in the picking of events. Several events had been picked on a second cycle. These events were then replotted, and a new model was drawn up.

Model 3:

This was also a five-layer case, with the average velocities of the five layers as: 3.16, 5.88, 6.42, 7.05, and 8.30 kms./sec. respectively. The depth to the intermediate layer was found to be 36.2 kms., and the depth to the Moho was found to be 46.4 kms. This time, the crossover and intercept methods did agree. Critical points for both the intermediate layer and for the Moho were calculated, and it was found that they did not agree with the first appearance of strong arrivals for these layers. The critical distance for the intermediate layer was much too great, plotting at 150 kms., while strong arrivals began at about 120 kms. This model

was ruled out on this basis.

The concept of a low velocity layer above the intermediate layer was then introduced in order to make the critical points agree with the actual data. Calculations were then performed for various thicknesses of the layer with velocity 6. 42 kms. /sec. The thickness of this layer must be assumed, since no refraction arrivals are possible from the top of the low velocity layer. The velocity of this low velocity layer must also be assumed, and was chosen as 6. 0 km. /sec. This is a more "normal" velocity for the top of the Precambrian, the 6. 4 km. /sec. velocity being anomalous. Thus, it was thought reasonable to assume that a layer with the more usual lower velocity might well be present under the higher-velocity layer. The most reasonable model of this series is the one given below.

Model 4:

This was a 6-layer case, with the average velocities of the six layers as: 3. 16, 5. 88, 6. 42, 6. 00, 7. 05, and 8. 30 km. /sec. respectively. The thickness of the layer with velocity 6. 42 km. /sec. was assumed to be 16. 50 kms. The depth to the low velocity layer was found to be 20. 9 km. ; the depth to the intermediate layer was 32. 3 kms. ; and depth to the Moho was 45. 3 kms. Critical distances to the intermediate layer and to the Moho were calculated to be 119. 5 kms. , and 112. 6 kms. , respectively. Both of these values fit the graphs reasonably well. Of all the models tried up to this point, this model, which I have called model 4 here, satisfied the data the best.

Validity of the assumption of a low velocity layer:

There are several facts which support the assumption of a low velocity layer. See figure 28 for a plot of the Bouguer gravity anomaly

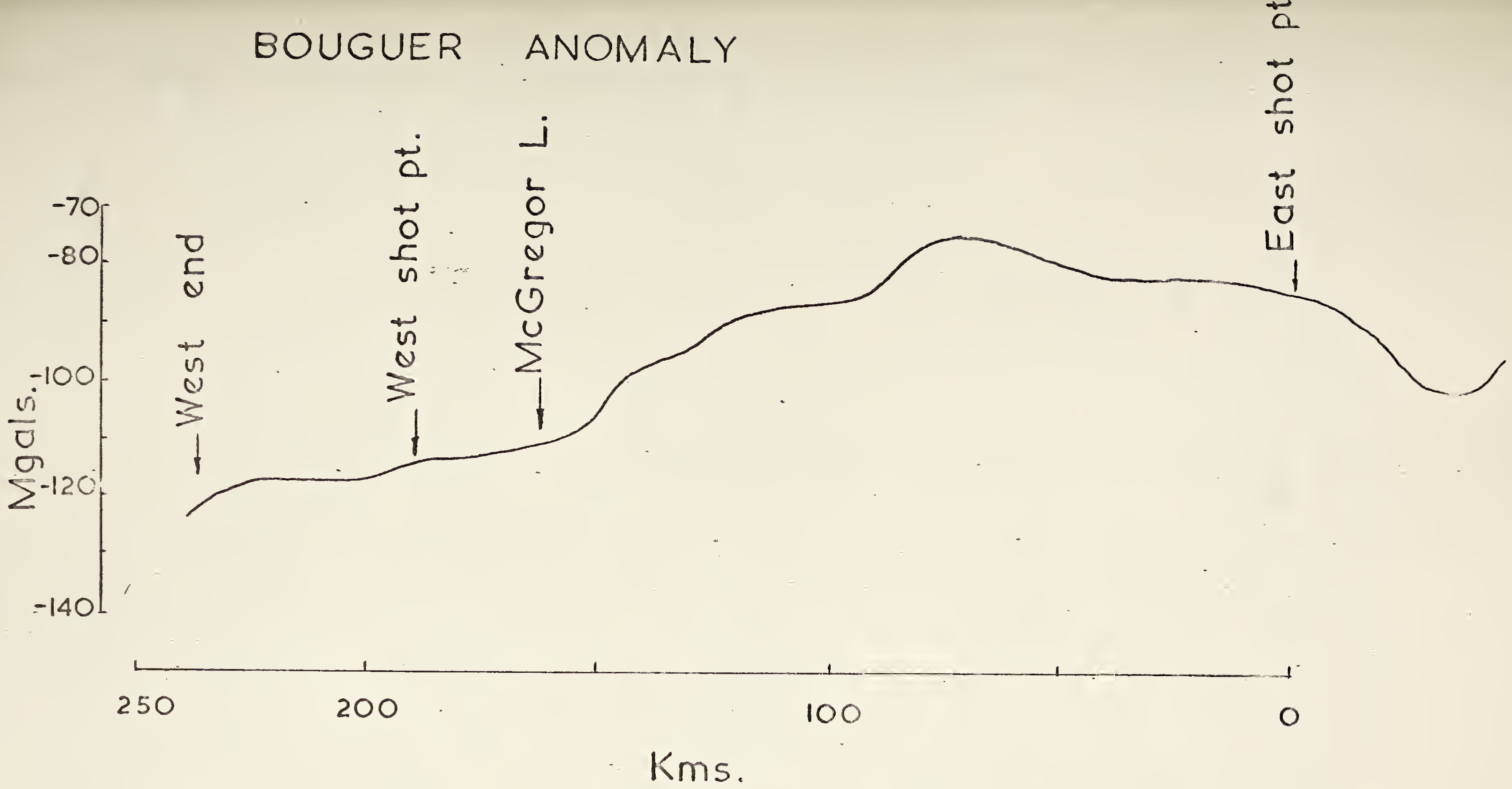
BOUGUER ANOMALY
Mgals.
-70
-80
-100
-120
-140
West end
West shot pt.
McGregor L.
East shot pt.
250
200
100
0
Kms.

FIG. 28.

against distance across Southern Alberta. It is seen that there is a more negative Bouguer anomaly both west and east of our seismic line. In other words, between our two shot points, the Bouguer anomaly is less negative than it is to either side of our profile. This is consistent with what we have assumed. There is an anomalous high-velocity layer (velocity of 6.4 kms./sec.) between our two shot points over the layer with the more normal lower velocity of around 6.0 kms./sec. The difference in Bouguer anomaly, however, does not indicate that the higher-velocity layer is as thick as we have assumed it to be. The gravity data indicates a maximum thickness of around 2 kms. This thickness, however, is inconsistent with our data, and there must be some other unknown factors influencing the gravity results. But, at least, the Bouguer anomaly does not contradict our assumption. In further support of the anomalous higher-velocity layer overlying the lower velocity layer between our shot points, it is noted that arrivals from the 6.4 km./sec. layer are damped out beyond 165 kms., for a shot from the east. This is again consistent with this layer pinching out beyond the west shot point. Furthermore, Richards and Walker did not record arrivals from a layer with velocity 6.4 kms./sec. The velocity they found was 6.1 kms./sec.

Bott, in a paper in 1961, suggests that because of negative Bouguer anomalies over granites, the upper part of the upper crustal layer may well be more basic than the lower part.

Thus, the concept of a higher velocity layer overlying material of a lower velocity between our shot points is very reasonable, and has much support.

Model 5:

As stated before, model 4 was the best fit to our data up to this

point. Then, the records were re-examined, and it was decided that where control exists, the reciprocal times must agree. Reversed control exists for both intermediate and Moho arrivals. In order to make the reciprocal times agree, the correlation on the graph for the west shot point had to be changed. For model 4, arrival 3 on the records taken by trucks 1 and 2, shot 2, was considered to be the Moho refraction arrival, while arrival number 4 was considered to be from the intermediate layer. In order to make the reciprocal times agree, however, arrival 3 must be that from the intermediate layer while arrival 4 must be that from the Moho. This change increases the velocity of the intermediate layer and decreases that of the material below the crust. The character of these two arrivals is very little different in this record, except that number 3 is slightly stronger. On the record taken by truck 2 for shot 11, which is the reverse record, the Moho arrival is the strongest. This would tend to support the previous correlation. But, there seems to be no valid reason for doubting the reciprocal times. The distances and times for both records have been checked and rechecked, and were found to be correct. But, it should be recalled that shot 11 was a surface burst, whereas shot 2 was a distributed buried charge. This fact could account for the difference in character of the two records. For great accuracy in checking the reciprocal times, even the relative elevations of shot point and detectors and the depth of burial of shot 2 were considered. If reciprocal times have any meaning, the new correlation must be the correct one.

Besides this change in correlation on the graph for the west shot point, which remains the same in all subsequent models, some changes were made on the east travel-time graph as well for this model (#5). An earlier arrival on the record taken by truck 2 for shot 10 was considered

as a possible Moho arrival for this model.

This model was the 5-layer case, with no low velocity layer. The velocities of the layers were: 3.16, 5.88, 6.42, 7.15, and 7.96 km./sec. respectively. The depth to the intermediate layer was found to be 35.6 kms., and the depth to the Moho was 45.6 kms. It may be noted here that the depth to the Moho has not varied very much in any of these models. For this model, the critical point for the Moho was calculated to be 133.5 kms., while the critical distance for the intermediate layer was found to be 137.6 kms. Both of these values are much too great to be consistent with the data on the field records. Thus, the low velocity layer was again introduced, and several thicknesses of the 6.4 kms./sec. layer were tried. No matter how much low velocity material was introduced, the Moho critical point could not be made low enough to agree with the strong arrivals on the record taken by Juliet 2. On the other hand, the critical point for the intermediate layer becomes rapidly too low. Thus, this model was rejected as being unsatisfactory. The changes which were made on the eastern travel-time graph were really not very convincing in any case. They were made more or less to convince ourselves that they were incorrect, and that the previous correlation was more correct. The new correlation on the western graph must remain, however, if reciprocal times are to be believed.

Model 6:

At this point, all of the records for both shot points were re-examined to make sure that the beginning of each separate arrival was picked, and that no late cycles were mistakenly used. Then, the character of the arrivals, the strength of arrivals, the reciprocal times, and other features (given in the section on theory) were all re-examined to obtain

the most convincing correlation of arrivals from spread to spread on both travel-time graphs. The best straight lines through these arrivals were then drawn by eye (least square solution was done later). The velocity of the low velocity layer was assumed to be 6. 1 kms. /sec., rather than the 6. 0 kms. /sec. which had been assumed before. This change makes very little difference, but the new velocity agrees more with that found by Richards and Walker. That is about the only reason for changing it. Calculations for model 6 were performed, however, without including the low velocity layer. The velocities of the layers were: 3. 18, 5. 88, 6. 41, 7. 32, and 8. 26 kms. /sec., respectively. The depth to the intermediate layer was found to be 35. 6 kms., and the depth to the Moho was calculated to be 48. 0 kms. The critical point for the Moho was 129. 9 kms., and the critical point for the intermediate layer was 122. 7 kms. Both of these critical distances are too great. Furthermore, other information as stated before supports the existence of a low velocity layer under the anomalous higher velocity material. Thus, this model was rejected. Then, various thicknesses of the 6. 4 km. /sec. layer were tried, and a value of 20. 00 kms. seemed most satisfactory. With this thickness, the critical point for the intermediate layer was found to satisfy the data on both graphs. The critical distance for the Moho satisfied the eastern graph, but plotted after the very strong arrival of Juliet 2 on the western travel-time graph. But, no matter how thin the higher velocity material is made, the Moho critical point cannot be made to agree. The reason for this is not clear. Perhaps there is a thin layer above the Moho with a velocity less than 7. 32 km. /sec. Or, perhaps the velocity in the intermediate layer decreases gradually from 7. 32 km. /sec. to a lower value. Both of these factors would tend to reduce the critical distance for the Moho.

Preferred Crustal Model:

At this point, all of the records were re-examined, and correlation from spread to spread was rechecked. A reduced travel-time plot made by Dr. G. L. Cumming of the University of Alberta was also studied. No reason could be found to reject the earth model number 6, with a low velocity layer included. The field data indicates that this is the only model to use. An amplitude plot made by Dr. G. D. Garland of the University of Alberta, and shown in figure 29, was also considered, and shows that there definitely is a maximum in the amplitude of the Moho reflection curve near the critical point. This reflection curve will be discussed later. There is only one discrepancy in this model, and that is, that the calculated critical point for the Moho does not agree with the presence of strong energy on the graph for the west shot point. But, there seems to be no other convincing way to correlate the arrivals. Thus, model 6 with a low velocity layer included was chosen as the final model.

A least square fit was then carried out for each refraction line; the limestone, the Precambrian, the intermediate layer, and the Mohorovicic discontinuity, for both graphs. These least square fitted lines are the ones shown on our final travel-time graphs included in this thesis, figures 26 and 27. It is seen at once that the reciprocal times for the arrival from the top of the Precambrian (6. 4 kms. /sec.) just do not agree. But it must be remembered that there is no control for this arrival at the reciprocal distance. The arrival is damped out before that time. Thus, there is really nothing which can be done about this, until more data are taken next year.

The equations of the least square lines are given below (they are

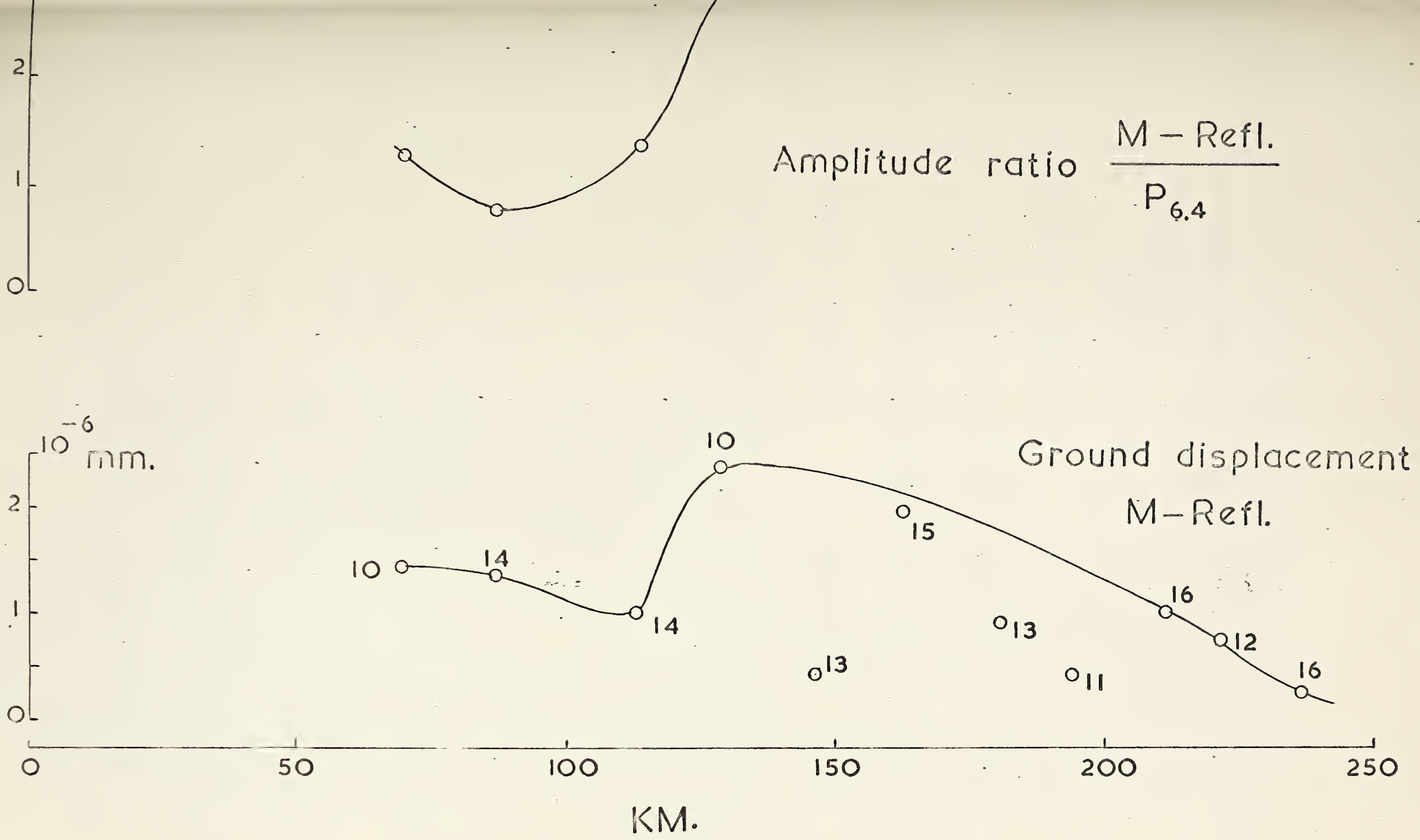
Amplitude ratio $\frac{\text{M - Refl.}}{P_{6.4}}$
2
1
0
Ground displacement
M-Refl.
10^{-6} mm.
2
1
0
10
14
14
10
15
16
12
16
13
13
11
0
50
100
150
200
250
KM.

FIG. 29.

also given on the travel-time graphs). The first one is actually assumed from the well-data. The others are least-square fits.

East Shot Point		West Shot Point
$T_1 = \frac{X}{2.60}$	(upper sediments)	$T_1 = \frac{X}{3.75}$
$T_2 = \frac{X}{5.87} + 0.69$	(limestone)	$T_2 = \frac{X}{5.89} + 1.04$
$T_3 = \frac{X}{6.46} + 1.19$	(Precambrian)	$T_3 = \frac{X}{6.35} + 1.20$
$T_4 = \frac{X}{7.34} + 6.27$	(Intermediate layer)	$T_4 = \frac{X}{7.29} + 6.06$
$T_5 = \frac{X}{8.30} + 9.40$	(Moho)	$T_5 = \frac{X}{8.21} + 9.19$

An important point can be seen from this immediately. The limestone appears to dip west, while the other layers seem to dip east, but only very slightly. For the Precambrian arrival, the intercept times do not agree with the apparent velocities. The velocities indicate a dip east, whereas the intercept lines indicate no dip, in fact, or an extremely small dip west. It must be remembered that this is the arrival with no reciprocal time control. I believe that this stresses the importance of good reciprocal time control. It should also be noted that in the calculations for all the models so far, the depths to the limestone and Precambrian layers were greater than those found on the cross-section in figure 22. The reason for this is not clear. But, it appears that there is something wrong with the Precambrian arrivals, since, as stated before, the velocities, intercepts, and reciprocal times for the Precambrian are not consistent with each other. This arrival is always very weak, and perhaps some or all of the refracted events from this layer have been unknowingly picked on a second or third cycle, the first cycle not being visible. There may also

be some low velocity layers in the sedimentary section (in fact, the well logs do show some such very thin layers), which would cause the calculated depth to be greater when they are not considered. Furthermore, the cross-section was prepared from well data taken to the south of our line, and the layers may well be slightly deeper along our seismic line. Another consideration is that the arrivals which we have correlated on our graphs may not be the Mississippian or top of the Precambrian arrivals as shown on the cross-section. Perhaps the arrival which we are calling the Mississippian is really the Devonian, and perhaps the arrival we are calling the top of the Precambrian (as shown on the cross-section) is really an arrival from a more distinct horizon slightly deeper. The theoretical Mississippian arrivals are shown on the travel-time graphs. They do not agree with the field arrivals. It is possible that the base of the sedimentary section and the top of the Precambrian contain material of about the same velocity, 6.0 km./sec., followed by a more abrupt velocity change to 6.4 km./sec., followed again by material of the lower velocity, 6.0 or 6.1 kms./sec. But, we cannot determine the true facts from the data which we have at the present time.

We cannot ignore completely the data for the sedimentary section on our travel-time graphs, nor can we ignore the cross-sectional data. Thus, we combined both sets of data to give a most reasonable picture of the sedimentary section, roughly satisfying both our graphs and the well data. Furthermore, in calculations it is necessary to assume a single average velocity for the uppermost layer, that average velocity being 3.18 kms./sec.

The travel-time graphs indicate a dip west for the limestone layer. From the cross-section, the maximum allowable dip west for this layer

(which also considers the greater elevation of the west shot point than the east) is 8 minutes. This was the dip value used in further calculations. The travel-time graphs indicate a dip east for the top of the Precambrian, indicated by the velocities, and no dip indicated by intercept times. The cross-section indicates that a slight dip east is possible since the axis of the Sweetgrass Arch is between the shot points, and the portion of this layer directly under the west-shot point which dips west is not sampled by the seismic waves. The maximum allowable dip east by the cross-section is about 6 minutes. This was the dip used in further calculations. It may be noted here that theory now gives a much smaller thickness of the Precambrian under the west shot point than that shown on the cross-section, since theory assumes that the dip east carries on under this point. Now, the thicknesses as calculated by theory, assuming the above dips and using the travel-time information were averaged with the thicknesses as measured on the cross-section (but assuming that the 6 minute dip east of the Precambrian carries on under the west shot point). Thus, thicknesses and dips for the sedimentary section were found which do not violently disagree with either the information on the travel-time graphs, or that on the cross-section. It will be shown that this change does not affect the depth to the Moho. It merely makes the thicknesses in the sedimentary section more reasonable.

Refraction theory for dipping layers was then applied to the data, using a thickness of the 6.4 kms./sec. layer of 20.00 kms. It will be recalled that this proved to be the most reasonable thickness in the preliminary calculations. One more assumption had to be made, and that

was the dip of the top of this low velocity layer. It was assumed that it dipped 6 minutes east, the same as the top of the 6.4 km./sec. layer. The dips are so small that they really make very little difference in any case.

Final calculations on preferred crustal model:

The final calculations yielded the following information:

WEST	Dips and Velocities	EAST
vertical thicknesses		vertical thicknesses
h_1 = 1.70 kms.	α_1 = 8' W.	h_1 = 1.17 kms.
h_2 = 0.82	α_2 = 6' E.	h_2 = 1.70
h_3 = 20.00	α_3 = 6' E.	h_3 = 20.00
h_4 = 10.53	α_4 = 34' E.	h_4 = 12.36
h_5 = 13.69	α_5 = 29' E.	h_5 = 12.93

Depths under shot point W.		Depths under shot point E.	
to limestone	= 1.70 kms.	to limestone	= 1.17 kms.
to Precambrian	= 2.52	to Precambrian	= 2.87
to low velocity layer	= 22.52	to low velocity layer	= 22.87
to intermediate layer	= 33.05	to intermediate layer	= 35.23
to Moho	= 46.74	to Moho	= 48.16

True velocities in the layers

V_1 = 3.18 kms./sec.	V_4 = 6.10 kms./sec.
V_2 = 5.88	V_5 = 7.32
V_3 = 6.40	V_6 = 8.25

Critical distance for intermediate layer for a west shot is: 109.8 kms.

Critical distance for Moho for west shot is: 128.8 kms.

Critical distance for intermediate layer for an east shot is: 113.9 kms.

Critical distance for Moho for an east shot is: 128.9 kms.

Below is a comparison of the thicknesses and depths averaged between the shot points from the last table, and the thicknesses and depths as calculated in the preliminary testing of the model when dips were not considered, and no corrections had been on the thickness of the sedimentary section.

Averages between shot points from last table		Averages from preliminary testing	
thicknesses		thicknesses	
h_1	= 1.44 kms.	h_1	= 1.64 kms.
h_2	= 1.26	h_2	= 2.25
h_3	= 20.00	h_3	= 20.00
h_4	= 11.45	h_4	= 9.76
h_5	= 13.31	h_5	= 13.56
Depths		Depths	
to limestone	= 1.44 kms.	to limestone	= 1.64 kms.
to Precambrian	= 2.70	to Precambrian	= 3.89
to low velocity layer	= 22.70	to low velocity layer	= 23.89
to intermediate layer	= 34.15	to intermediate layer	= 33.65
to Moho	= 47.46	to Moho	= 47.21

Thus, it can be seen that the consideration of the small dips and the corrections to the upper layers have almost no effect on the average depths to the intermediate layer and the Moho.

The list of all the incident and refracted angles at each layer for each shot point will not be included here. Figure 30 is a scale diagram of the cross-section down to the mantle in Southern Alberta as given by our preferred model. The critical rays for the intermediate layer and for the Moho are shown, indicating the amount of reversed coverage we have for each layer. We have 80 kms. of reverse coverage on the intermediate layer, and 63 kms. of reverse coverage on the Moho. Thus, even though the dips which we find for these layers are east dips, we cannot say that our data proves that these layers dip away from the mountains. Just west of the sections which have reverse coverage, these horizons may begin a gentle dip toward the mountains. This dip may well become greater and greater as the mountains are approached. More work is necessary in the area, west of our profile, to determine whether the crust is thicker or thinner under the mountains, than it is along our profile.

Apparent velocity data:

It can be seen from our travel-time graphs or from the tables of arrival times in Appendix two that the apparent velocities are often too high for the line-up of arrivals with which they have been correlated. But this is not always true, as some of the apparent velocity values are too low. It will be remembered that Steinhart and Meyer found the same situation in Montana. In our case, if all the apparent velocity values for any one arrival (on both graphs) are averaged, this average apparent velocity is very close to that found from the slope of the travel-time line. The results are given below:

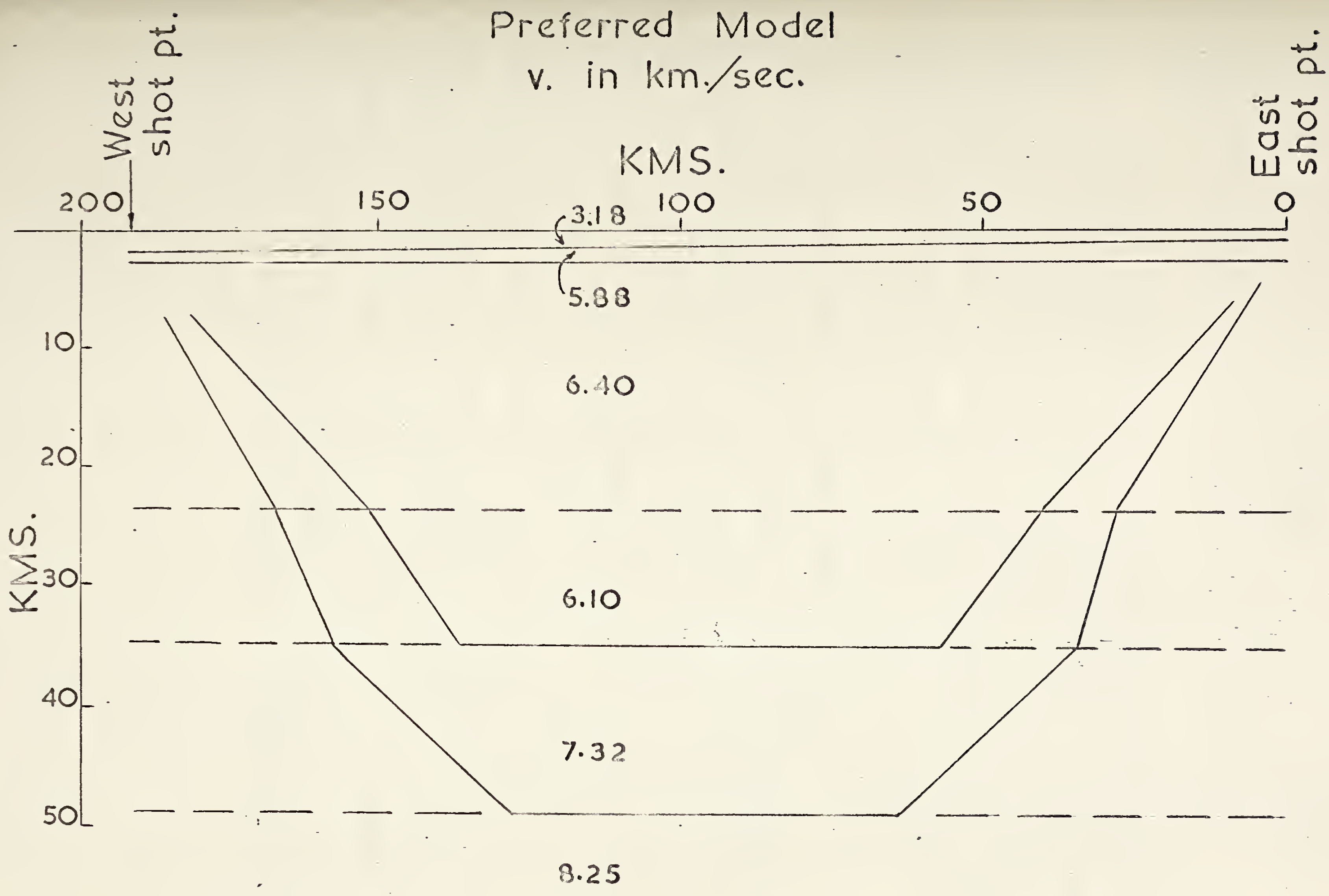
Preferred Model
v. in km./sec.
West shot pt.
East shot pt.
KMS.
200
150
100
50
0
3.18
5.88
6.40
6.10
7.32
8.25
KMS.
10
20
30
40
50

FIG. 30.

Layer	Average App. Vel.	True velocity in the layer
Limestone	7.00	5.88 kms./sec.
Precambrian	6.43	6.40
Intermediate Layer	7.62	7.32
Moho	8.25	8.25

Thus, the apparent velocity for the limestone layer is the only one that is appreciably different from the group velocity. Possibly dispersion effects are causing the difference in this layer. The thickness of the layer is comparable to the wave length of the waves being recorded. Thus, the energy may be travelling through this layer as some dispersive type of wave, whose phase velocity is being influenced by the layer below.

Support for the preferred model from reflection data:

Arrivals which appear to be reflections from the Mohorovicic discontinuity were correlated on the travel-time graph for the east shot point, and the reflection locus is shown on this graph. As stated in the theory chapter, the method of plotting T^2 vs. X^2 was used in the interpretation of reflections. Arrivals were correlated on both graphs which appear to be reflections from the intermediate layer. These curves are shown on the graphs. Finally, on the eastern graph a curve is drawn through three strong arrivals with similar character, and this curve is considered as a possible reflection from the top of the low velocity layer. Calculations were performed on all these reflection curves, and depths to the layers are shown below, compared to the average depths found by the refracted arrivals.

Depths by reflection		Depths by refraction	
to Low velocity layer	= 23. 2 kms.	to Low velocity layer	= 22. 70 kms.
to Intermediate layer	= 34. 2	to Intermediate layer	= 34. 15
to Moho	= 48. 9	to Moho	= 47. 46

Thus, it is seen that the reflection data supports the refraction data very well, giving depths slightly greater than that given by the refraction technique. It has been shown earlier that the method of calculation used on the reflection data will tend to give greater depths than the true depths. Thus, the reflection data from our records is considered to be very good indeed. Even the low velocity layer, which we have assumed, is supported by the reflection data.

Portions of field records: -

Five examples of the actual field records have been included in this thesis. Figure 31 is a portion of the field record taken by Juliet 2, for a shot from the west. It shows the strong arrivals which have been attributed to the Intermediate layer and to the Moho. Figure 32 is a section of the record taken by truck #2 for shot #10. It shows the strong arrivals which have been attributed to the intermediate layer and to the Moho respectively for this spread. This record, being from a distributed charge, may be compared with the record taken by the same truck for shot #11, which was a 5-ton surface burst. A portion of this latter record, showing the very strong Moho arrival, is reproduced as figure 33. It is immediately seen that there are a great many more apparent line-up of phases on the record from the distributed charge, that is, the 800 pound shot, distributed in five holes 50 ft. apart. The reason for this difference is not known. Perhaps interference between the distributed portions of the charge and/or

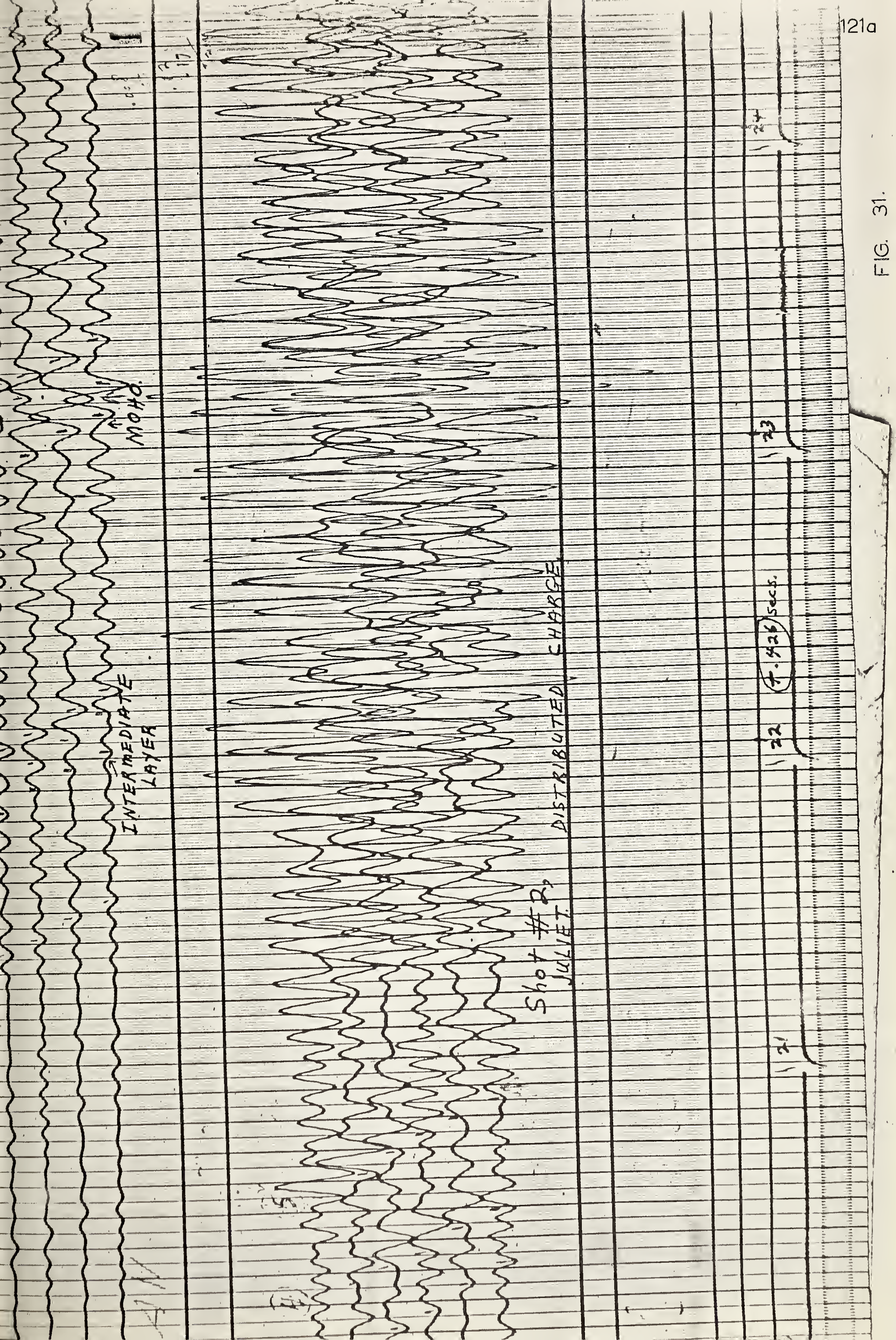
INTERMEDIATE LAYER
MOHO
Shot #2, JULIET. DISTRIBUTED CHARGE
21
22
7.426 secs.
23
24

FIG. 31.

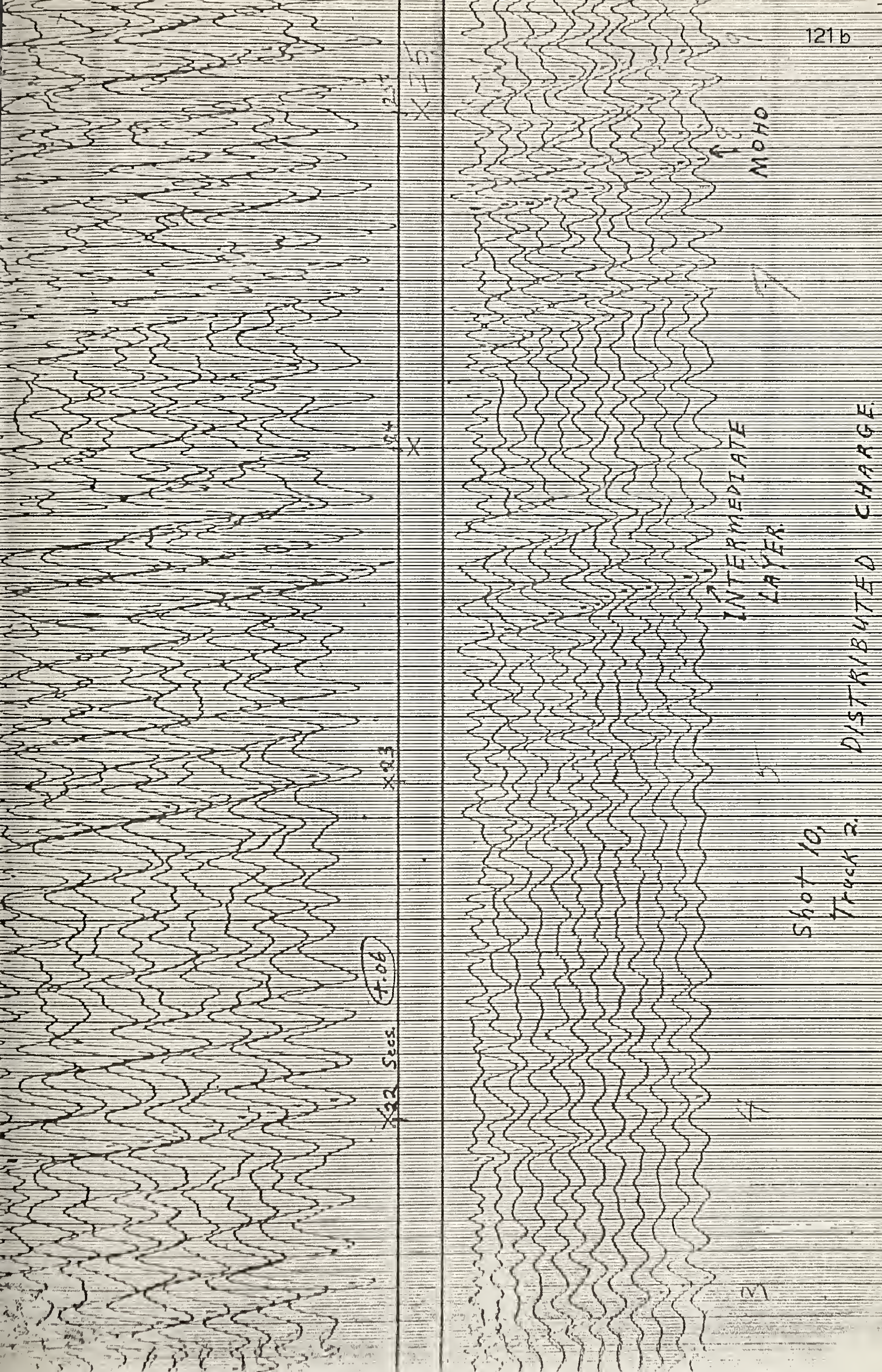
MOHO
INTERMEDIATE LAYER
DISTRIBUTED CHARGE
Shot 10, Track 2.
X 2.2 Secs.
+.06
X 2.3
X 2.4
X 2.5

FIG 32

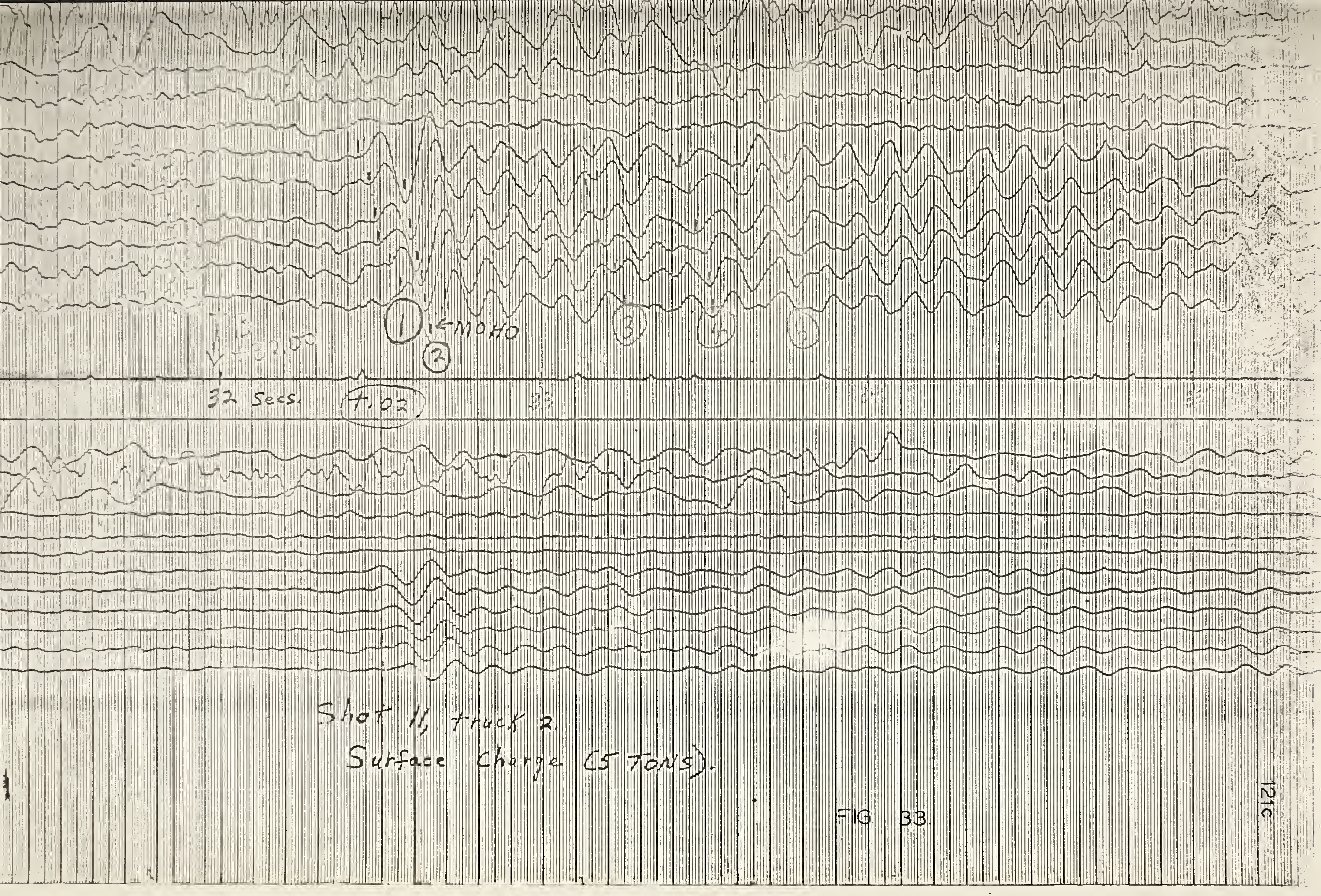

Shot 11, truck 2.
Surface Charge (5 Tons).

FIG 33.

different filtering action of the ground are responsible for the difference. Both of these records may be compared with the record taken by truck #1 for shot #15, which was a non-distributed buried charge. This record is shown in figure 34. (Note that this record was recorded on medium speed. Several dead traces are apparent, due to a faulty cable). This record is similar in appearance to the one recorded from the surface burst. Thus, for some reason, the distributed charge tends to produce a record with a very large number of line-ups. The energy seems to be attenuated very little for a considerable length of record. On the other hand, a non-distributed charge or a surface burst tends to produce a record with very few line-ups, but with strong clear arrivals from the discontinuities. The energy is damped out much more quickly along the length of a record, (i.e. arrivals do not persist at any one point for as long a time). Some interesting work could be done to determine the cause of this difference. Certainly the records from a non-distributed charge or a surface charge are much easier to interpret, as far as isolating waves from discontinuities is concerned. A further point may be made concerning charge types. It was determined from a study of amplitude ratios (shown in figure 29 as plotted by Dr. Garland) that a 20 ton surface shot is approximately equivalent to a 1000 lb. buried charge, with regard to delivering energy to the ground. Thus, coupling to the ground for a surface burst is very poor.

The possibility of other refracted phases on the records, besides P phases was considered. Rough travel-time calculations were made for phases such as PSP for the Moho (that is, a shear wave along the boundary and a P wave the rest of the distance), PPS and SPP for the Moho. Some

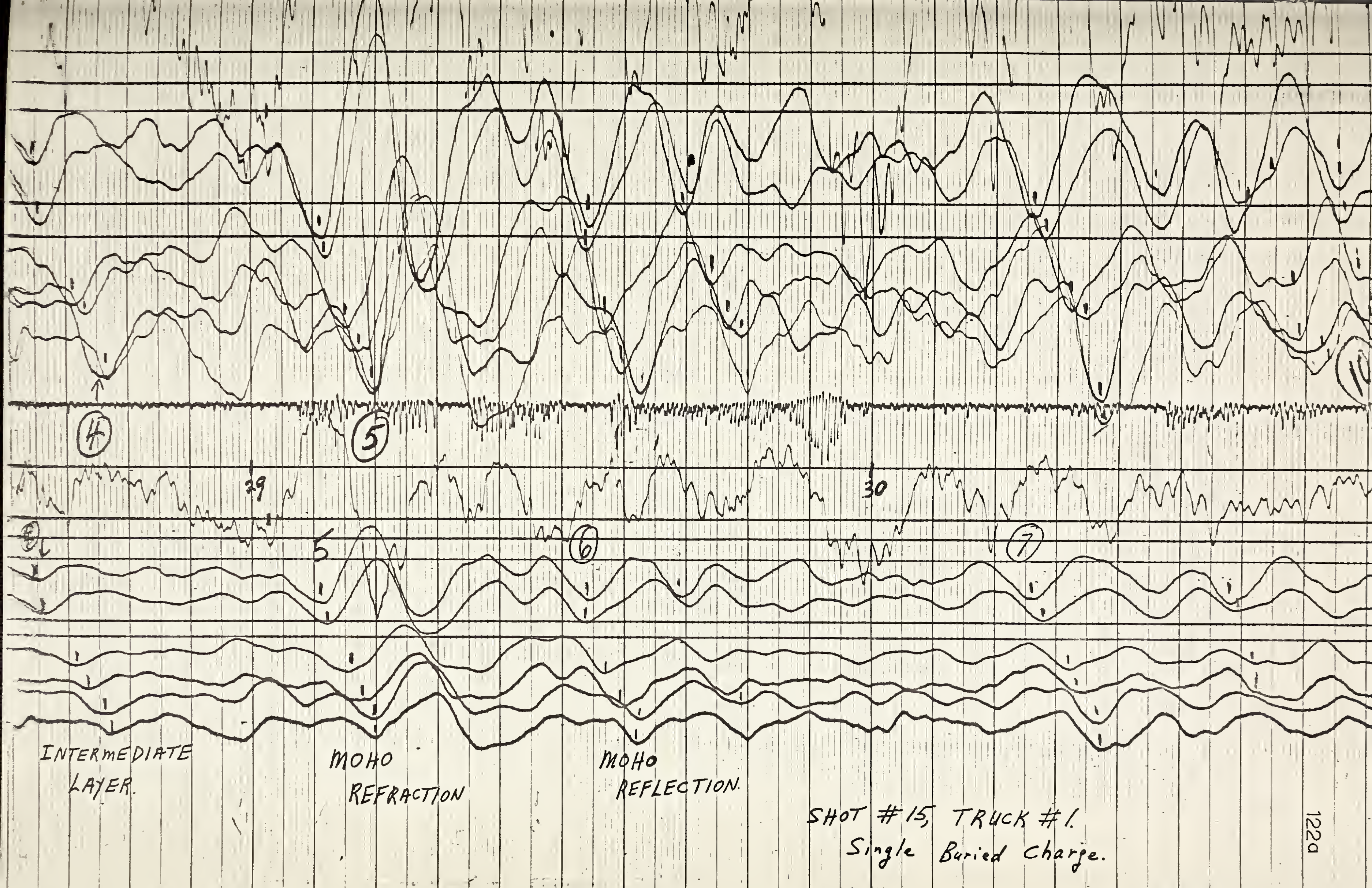
4
5
6
7
10
29
30
5
INTERMEDIATE LAYER.
MOHO REFRACTION
MOHO REFLECTION.
SHOT #15, TRUCK #1.
Single Buried Charge.

FIG. 34

late arrivals on Shot #10, truck #2 did fall on the calculated lines for some of these phases, but the apparent spread velocities were incorrect by a large amount. Similar phases were considered for other layers, with no success. However, one very late arrival on the record taken by truck #2 for Shot #10 appears to be an S-wave refracted from the Precambrian (that is, S down, along the boundary, and back again). The apparent spread velocity is also consistent with this phase. Figure 35 shows this arrival. If two horizontal seismometers (such as two Willmores) had been used on each field record taken, it may have been possible to see more S arrivals.

One further point may be stated here. It seems that the mean frequency of all our arrivals is about 7 c.p.s. Thus, it appears that geophones with a resonant frequency of around 7 c.p.s. would give as good a result as our bulkier 2 c.p.s. phones.

Air-coupled waves:

No interpretation has been done yet on the air-coupled waves which we find on our records. Other people are presently working on the data. I merely wish to say that we did observe air-coupled Rayleigh waves on our records, when the energy source was a surface charge. For all surface charges, 6 of the geophones were replaced by 6 pressure phones, and the records were allowed to run for very long periods of time (up to 14 minutes) in order to pick up the sound wave. Erhard Reinelt is using these sound wave arrivals for his work on the upper atmosphere. It so happens that each sound arrival was accompanied by a ground wave which was recorded on the 6 geophones. An example of this air-coupled wave is shown in figure 36. This is a portion of the record taken by truck #1 for Shot #11. The ground wave has the same apparent velocity

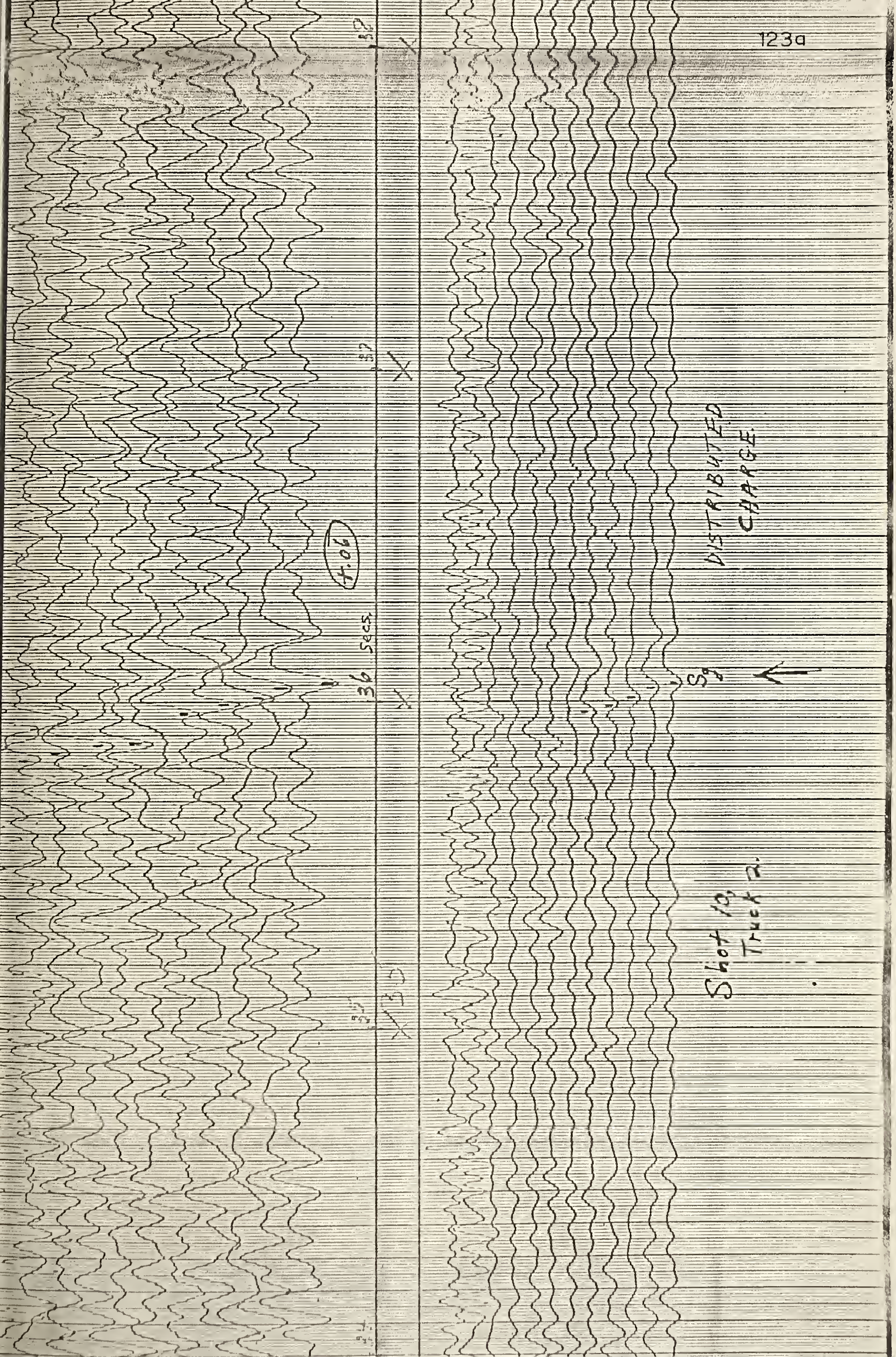
38
37
36 Secs.
+.06
35
34
Sg
DISTRIBUTED CHARGE
Shot 10,
Truck 2.

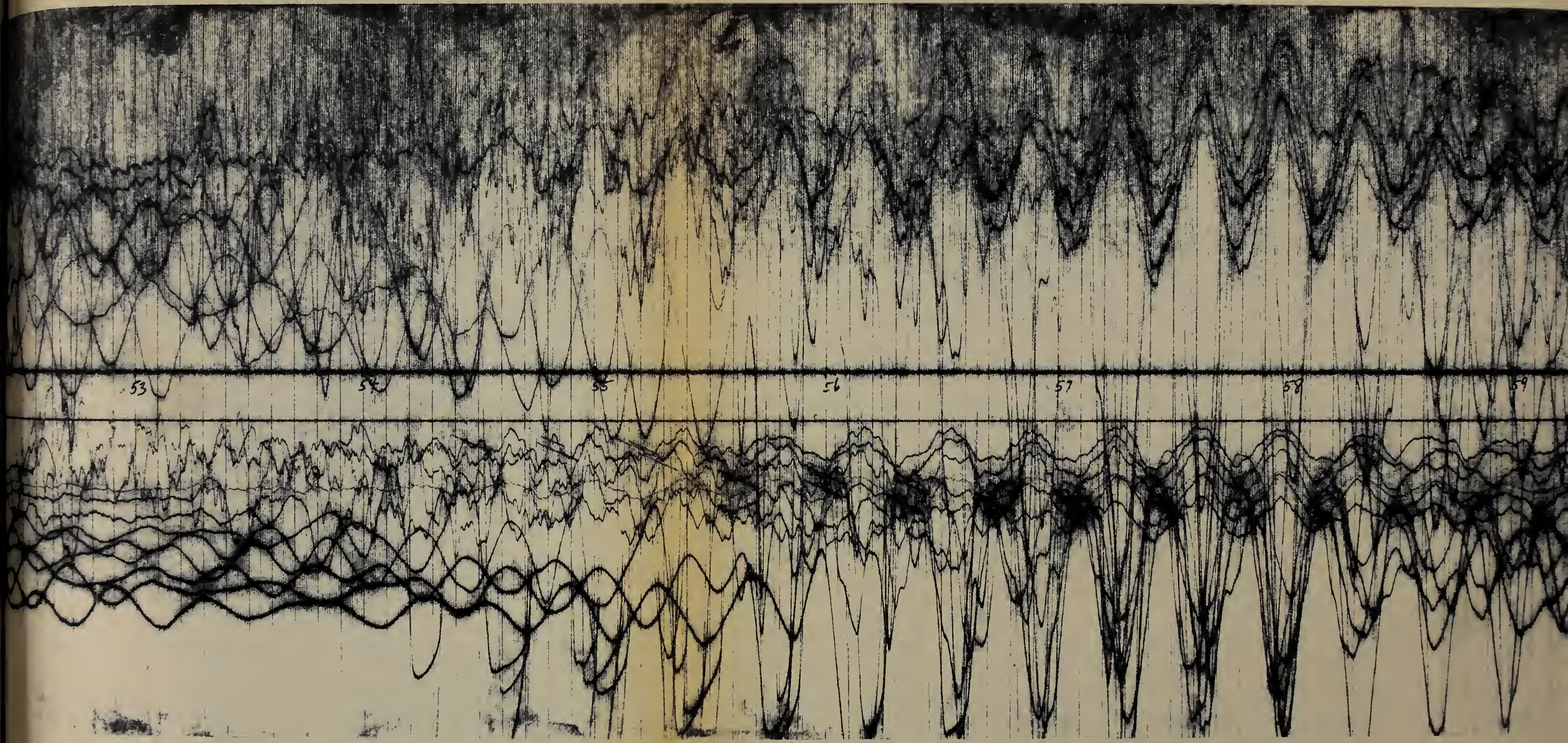

1st six Press. Phones.
Last six Geophones.

AIR-COUPLED WAVES

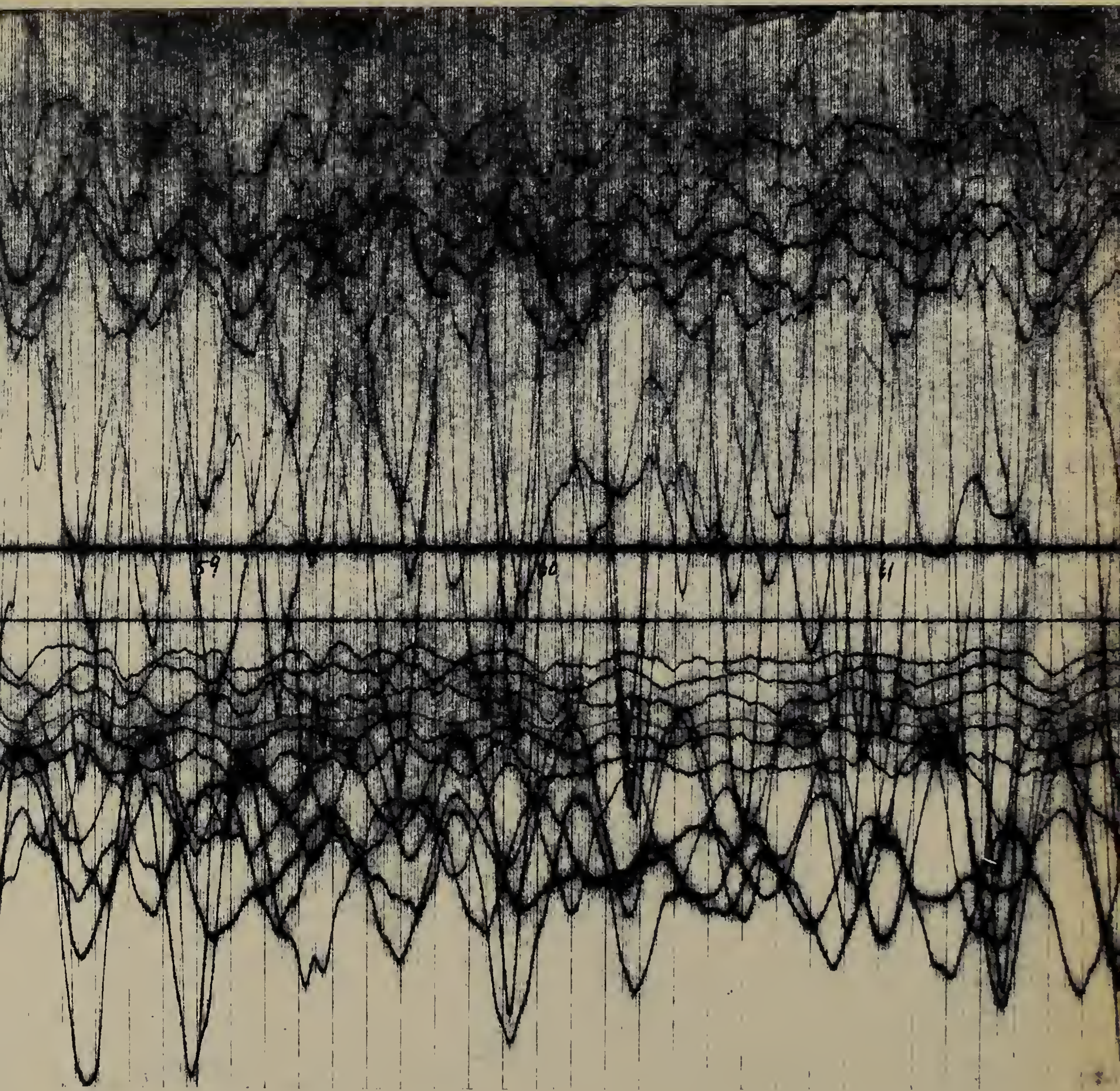

Figure 36.

as the air wave (velocity of sound in air) and has greater amplitude on the records. The frequency is approximately constant as expected from theory. For the record included, the frequency is about 3-1/2 c. p. s. Thus, this is the frequency for which the phase velocity of the Rayleigh wave is the same as that of sound in air.

No more will be said here about air-coupled waves. It seems that if records are allowed to run long enough, an air-coupled ground wave will be observed from a surface charge.

CHAPTER 9

CONCLUSIONS AND SUGGESTIONS FOR FUTURE WORK

The seismic work carried out by the University of Alberta which has been analyzed in this thesis certainly yielded much useful information, but left many problems still to be solved. Because fewer records were taken from the west shot point, the statistical error in the slopes and intercepts on this graph are much greater. For the refracted arrival from the Mohorovicic discontinuity on this graph, the error in the slope is about ± 6 per cent, while the error in the intercept is about ± 1 second (for 90% confidence limits). For the refraction line from the Moho on the east travel-time graph, the error in the intercept is only about ± 0.23 seconds (for 90% confidence limits). Thus, the error in depth to the Moho for information from the west travel-time graph is much greater than that from the east, simply because of a lack of sufficient number of points. The actual error is probably not as great as it seems from the statistical calculation, since the points are good, although there are few of them. Recalling the last chapter, it will be remembered that the average depth to the Moho derived from the preferred model was 47.5 kms. It will also be recalled that all models tried gave a depth to the Moho of over 44.5 kms. and under 48.9 kms. Thus, it seems that the maximum limits of error in the depth to the Moho as determined from our field work would be ± 3 kms. These would be also valid maximum limits of error in the depth to the intermediate layer, if the results are recalled. These errors are not statistical errors, but represent the limits of error which cover the depths as determined by all models tried. For this reason, I believe these errors have some meaning.

Conclusions:

(1) The average depth to the Mohorovicic discontinuity in southern Alberta between Vulcan and Suffield is 47.5 ± 3 kms., with a small dip to the east. The velocity in the upper mantle is 8.25 kms./sec. The boundary seems to be a sharp one, as strong, clear arrivals were observed. No vertical reflections were seen, however. No definite statement can be made as to whether the discontinuity dips under the mountains or not, as data has not been taken for enough west as yet. Richards and Walker found a shallower depth which supports our eastern dip, but they found a dip west. Thus, the Moho may well continue to dip east until a distance from the mountains of that of Richards' and Walker's profile, and then begin to dip west. More data are necessary to determine whether this is true or not.

(2) The existence of an intermediate layer in Southern Alberta was definitely shown. The average depth to this layer between Vulcan and Suffield is 34.2 ± 3 kms. The velocity at the top of the intermediate layer is 7.32 kms./sec. The dip of the interface is about 1/2 degree to the east. This discontinuity also seems to be a sharp one, as several strong, clear arrivals were observed from it. No vertical reflections were seen, however. Richards and Walker also noted this discontinuity farther west at a depth of 29 kms. (reinterpreted as 26 kms.), still with a slight dip to the east (actually south-east). The shallower depth and the dip both support our data. Thus, the intermediate layer is thinner over The Sweetgrass Arch (our profile) than it is farther west. More data will need to be taken closer to the mountains to determine if this discontinuity continues to dip away from the mountains or not.

(3) There is an anomalous high velocity layer (6.4 kms./sec.) below the sedimentary section between Vulcan and Suffield. This layer overlies the more normal lower velocity material.

(4) The location map in figure 24 shows the locations of other crustal thickness determinations relative to our own. The results of most of these determinations were discussed in chapter 2. But, the depth to the Moho and the thickness of crustal material with velocity over 7 kms./sec. are shown on the map for these other locations. Nothing definite can be really concluded from this, as the results seem very random. The depth to the Moho does, however, seem to be generally over 40 kms., and becoming deeper toward Saskatchewan or the Dakotas. Nothing can be said about whether the Moho dips under the mountains or not, as more work is necessary in both Montana and Alberta to show this. Some crustal material with velocity over 7 kms./sec. is shown in all cases but one. Thus, the base of the crust does appear to be composed of denser, higher velocity material than the upper part. This material is probably of basaltic composition. The upper boundary of this layer may well be the discontinuity discovered by Conrad. This Conrad discontinuity may well be more universal than some workers believe, (e.g. Steinhart).

Many more crustal thickness determinations are needed before any definite conclusions may be drawn as to what these discontinuities do under the mountains and what they do under the Sweetgrass Arch. The east-west profile of this year will be extended next year by the University of Alberta.

Suggestions for Future Work:

(1) No shots less than 800 to 1000 pounds buried or 5 tons surface are sufficient for this type of work.

(2) The VHF radio link as used by the University of Alberta is excellent for communication and shot timing, when it is working properly. But, getting the "bugs" out of such a link can be time consuming.

(3) For any one shot, recording trucks should be in spreads adjacent to one another, not one close to the shot and one 200 kms. away. This would probably aid correlation, as any source effects would be common and easy to correlate.

(4) Reversed profiles are definitely necessary in order to get good reciprocal time control. All precautions should be taken to get the best reciprocal control possible. The size and type of charge used should be the same; amplifier settings and camera speeds should be the same; and one detector location should become precisely the next shot location. This would prevent any ambiguities whatsoever in reciprocal times.

(5) An attenuation setting of zero should always be used on the amplifiers. The lower traces are always attenuated by 12 db. in any case. If wind noise is too great to operate on zero db. attenuation, the shot should be postponed.

(6) A filter setting on the amplifier of about 24 c. p. s., if possible, should be used. The dominant frequency in the arrivals seems to be 7 c. p. s.

(7) For great accuracy, distance calculations should be made by the formula, the latitudes and longitudes having been obtained from the local survey branch.

(8) Two horizontal component Willmore seismometers in each spread

might enable more S phases to be identified.

(9) The detection of near vertical reflections should be attempted again.

(10) The possibility of an anomalous higher velocity layer overlying a lower velocity layer should always be kept in mind.

(11). For anyone interested in air-coupled waves, they may be studied very easily by using a few pressure phones in conjunction with the geophones, and allowing the records to run for a longer period of time.

(12) If long records are not necessary, medium speed (5 inches per second) is the best camera speed to use. Events are easier to sort out at this speed; 2-1/2 inches per second is sufficient, however, but any slower speed is just not enough.

(13) An extension of this summer's profile west towards the Rocky Mountains would prove most interesting.

BIBLIOGRAPHY

Bath, Markus,: "Shadow Zones, Travel Times, and Energies of Longitudinal Seismic Waves in the Presence of an Asthenosphere Low-Velocity Layer," Trans. Am. Geophysical Union, Vol. 38, No. 4, pp. 529-538, (1957).

Berg, and Cook,: "Ground Motion Measurements Near Quarry Blasts at Promontory Point, Utah", Bull. Seism. Soc. Am., Vol. 49, No. 4, (1959).

Berg, Cook, Narans, and Dolan: "Seismic Investigation of Crustal Structure in Eastern Part of Basin and Range Province", Bull. Seism. Soc. Am., Vol 50, No. 4, (1960).

Bott, M. H. P.,: "The Granitic Layer," Geophysical Journal of the Royal Astronomical Society, Vol. 5, No. 3, pp. 207 - 216, (1961)

Bullen, K. E.: "Introduction to the Theory of Seismology", Cambridge University Press, 2nd ed., (1953).

Dix, C. H.,: "Seismic Velocities from Surface Measurements", Geophysics, Vol. 20, pp. 68-86, (1955).

Dobrin, Milton B.,: "Introduction to Geophysical Prospecting", 2nd ed., McGraw-Hill, (1960).

Eve and Keys,: "Applied Geophysics", Cambridge University Press, 4th ed., (1956).

Ewing, Press, and Jardetsky,: "Elastic Waves in Layered Media", McGraw-Hill, (1957).

Garland, G. D., and R. A. Burwash,: "Geophysical and Petrological Study of Precambrian of Central Alberta, Canada," Bull. of Am. Assoc. of Petroleum Geologists, Vol. 43, No. 4, pp. 790 - 806, (1959).

Hagedoorn, J. G.,: "The Plus-Minus Method of Interpreting Seismic Refraction Measurements", - - - -

Hoffman, John P., Joseph W. Berg, Jr., and Kenneth L. Cook,: "Discontinuities in the Earth's Upper Mantle as Indicated by Reflected Seismic Energy", Bull. of Seism. Soc. of Am., Vol. 51, No. 1, pp. 17 - 27, (1961).

Howell, B. F., Jr.,: "Introduction to Geophysics", McGraw-Hill, (1959).

Jacobs, J. A., Russell, R. D., and Wilson, J. T.,: "Physics and Geology", Toronto, McGraw-Hill, (1959).

Jakosky, J. J.,: "Exploration Geophysics", Trija Publ. Co., 2nd ed., Newport Beach, Calif., (1950).

Jardetzky, W. S., and F. Press,: "Rayleigh Wave Coupling to Atmospheric Compressional Waves", Bull. Seism. Soc. Amer., Vol. 42, pp. 135-144, (1952).

Jeffreys, H.,: "The Earth, Cambridge University Press, 2nd ed., (1952).

Milne, W. G., and White W. R. H.,: "A Seismic Survey in the Vicinity of Vancouver Island, B. C.", Pubs. of Dom. Observ., Ottawa, Ont., Vol. XXIV, No. 7, (1960).

Mintrop, L.,: "On the Stratification of the Earth's Crust According to Seismic Studies of a Large Explosion and Earthquakes", Geophysics, Vol. 14, pp. 321-336, (1949).

Mota, L.,: "Determination of the Dips and Depths of Geological Layers by the Seismic Refraction Method", Geophysics, Vol. 19, pp. 242-254, (1954).

Narans, Berg, and Cook,: "Sub-Basement Seimic Reflections in Northern Utah", Journal Geophys. Research, Vol. 66, No. 2, (1961).

Poldervaart, Arie,: "Crust of the Earth", a Symposium, Geol. Soc. of Amer., Special Paper No. 62, (1955).

Press, Frank,: "Determination of Crustal Structure from Phase Velocity of Rayleigh Waves, Part I", Bull, Geol. Soc. Am., Vol. 67, pp. 1647-1658, (1956).

Press, F., and Ewing, M.: "Ground Roll Coupling to Atmospheric Compressional Waves", Geophysics, Vol. 16, pp. 416-430, (1951).

Richards, T. C., and Walker, D. J.,: "Measurement of Thickness of the Earth's Crust in the Alberta Plains of Western Canada". Geophysics, Vol. 24, pp. 9- , (1959).

Scheidegger, A., and Willmore,: "The Use of a Least Squares Method for the Interpretation of data from Seismic Surveys", Geophysics, Vol. 22, No. 1, (1957).

Shor, George G., Jr.,: "Deep Reflections from Southern California Blasts"., Trans. Am. Geophys. Union, Vol. 36, No. 1, (1955).

Steinhart and Meyer,: "Explosion Studies of Continental Structure", Carnegie Instit. of Wash. Pub., No. 622,(1961).

Veitsman, P. S.,: "The Correlation of Seismic Waves in Seismic Depth Soundings of the Earth's Crust," Bull. of Acad. of Sciences of the U. S. S. R., No. 12, pp. 9-28, (1957).

Wyrobek, S. M.,: "Application of Delay and Intercept Times in Interpretation of Multilayer Time-Distance Curves"., Geophys. Prospecting, Vol. 4, pp. 112-130, (1956).

Billings Geological Society,: "Sweetgrass Arch", Sixth Annual Field Conference, (1955).

APPENDIX I

THE NATURE OF THE MOHOROVICIC DISCONTINUITY

APPENDIX I. THE NATURE OF THE MOHOROVICIC DISCONTINUITY

A knowledge of the nature of the Mohorovicic discontinuity is essential to the solution of certain problems regarding the surface and subcrustal structure of the earth. Some of these problems are solved if the discontinuity is considered as a phase transition. Most workers, however, still feel that the Moho represents a change in chemical composition from basaltic type rocks to peridotite or dunite. This chapter will treat the relative merits of these two ideas, based on the most important of the existing literature on the subject.

The existence of the Mohorovicic discontinuity, marking the boundary between the earth's crust and mantle, is generally accepted by everyone. Geophysicists, in general, agree that the composition of the continental crustal rock is essentially that of an igneous rock intermediate between granite and basalt while oceanic crustal rocks are usually basaltic in composition. But, there is much less agreement on the nature of the material under the crust in both oceanic and continental regions.

Another discontinuity, above the Moho, has been suggested by Conrad, but its existence is not very well supported in most regions. It is considered to represent a discontinuity under the continents between rocks of a more granitic nature and rocks of a basaltic composition. It is generally accepted that rocks in the "upper" crust are more granitic in composition while those in the "lower" crust are more basaltic, but whether there is an actual discontinuity or a more gradual change has never been confirmed. The summer's work by the University of Alberta

seems to indicate a discontinuity, but many ambiguities are still present.

An important test of the sharpness of discontinuities is the observation of deep reflections from them. If the physical properties change abruptly at a discontinuity, then reflections at near vertical angles of incidence should be detected. Thus, the sharpness of the discontinuities is measured by the wavelength of the waves recorded. This fact is very important. It could well provide the answer to the question of whether the velocity increase in the crust is due to a continuous functional increase or whether there are one or more discontinuities in the crust. It could also provide the answer to the question of the sharpness of the Moho. This, in turn, would aid in determining whether the Moho should be considered as a phase transition or as a chemical change. Kennedy states that unless the reflected waves can be observed, it is difficult to be sure whether the Moho is due to an abrupt change in chemical composition and density of crustal rocks, or whether it is a result of a phase transition within the rock itself, spread over a range of depth of a few kilometres. This seems reasonable that a phase transition would probably not be as sharp as a compositional change. Steinhart and Myer, however, profess the opposite point of view. They state that if the reflections are observed, it would indicate that the M is probably a phase change boundary, whose position is governed by pressure and temperature, because it is hard to imagine a knife-sharp compositional change that is both universal and stable through long stretches of geologic time. I believe that they are mistaken in this point of view. I feel that, by its very nature, a phase change could never be knife-sharp, at least not a two component phase change as this one would be. Turner and V rhoogen state this very definitely when they say that

the pressure-induced transition from gabbro to eclogite would not be a sharp one, as in a system of one component; in a multicomponent system, it would be spread over a certain pressure interval. The two components of eclogite are a pyroxene omphacite and a lime-bearing almandine pyrope type of garnet. The chemical equivalence of olivine gabbro and bimineraltic eclogite can be shown by the following simple equation:

$$3Ca\,Al_2\,Si_2\,O_8 + 2Na\,Al\,Si_3\,O_8 + 3\,Mg_2\,SiO_4 + n\,Ca\,Mg\,(Si\,O_3)_2$$

labradorite olivine diopside

$$= 3\,CA\,Mg_2\,Al_2\,(SiO_4)_3 + 2\,Na\,Al\,(Si\,O_3)_2 + n\,Ca\,Mg\,(Si\,O_3)_2 + 2\,Si\,O_2$$

garnet omphacite quartz

We will now have a short aside and discuss phase rules and components. Gibbs phase rule may be expressed as follows:

$f = c + 2 - \Phi$, where f = no. of degrees of freedom,

c = no. of components,

Φ = no. of phases.

This phase rule is determined simply by counting the number of unknowns and the number of relations to determine them. Consider a system of c components in Φ phases. For equilibrium, the chemical potential of each component should be the same in all phases in which it is present, so we have $c\ (\Phi - 1)$ equations of the type

$$\begin{array}{l} U_1^{\alpha} = U_1^{\beta} = \dots = U_1^{\Phi} \\ \cdots\cdots\cdots\cdots\cdots\cdots \\ U_c^{\alpha} = U_c^{\beta} = \dots = U_c^{\Phi} \end{array}$$

(Note that chemical potential is the free energy per mole of a pure component. An expression for free energy is $G = E + PV - TS$,

where E is the internal energy,

P is the pressure,

V is the volume,

T is the temperature,

S is the entropy.

A necessary condition for a component i to migrate spontaneously from phase α to phase B is that its chemical potential should be greater in phase α than in phase B.)

Now, the chemical potential depends on the intensive variables P, T, and N_1^1, N_1^2 .... N_c^Φ, where N_c^Φ are molar fractions of component c in phase Φ. Thus, there are $2 + c\varphi$ variables. But, the molar fractions are not all independent, for we know that for each phase $\sum_i Ni = 1$ and thus we have Φ more relations of this type. Therefore, there are $c(\Phi - 1) + \varphi$ relations between $C\Phi + 2$ variables. Thus, if we assign arbitrary values to $f = c\varphi + 2 - (c(\Phi - 1) + \Phi) = f = c + 2 - \Phi$ variables, we can determine all the other variables. This is Gibbs' phase rule as stated before. It merely states that the state of any system is defined by f of these intensive variables P, T, N_1^1 ... N_c^Φ. Note that if a component j is not present in any phase γ, there is no equilibrium condition involving U_j^γ, and thus there is one equation less; but also $N_j = O$, and the number of degrees of freedom stays the same.

If we consider the phase change gabbro ⟶ eclogite, we have $c = 2$, $\varphi = 2$, and therefore $f = 2$. Thus, we have two degrees of freedom, P and T.

Let us consider Duhem's theorem for a moment. This theorem states that in a closed system (no masses added or subtracted in the course of the transformation), the state of the system is completely defined by two independent variables only. In a closed system, these can be either intensive or extensive. This theorem follows from Gibbs' rule by considering that the state is only completely defined by knowing all the variables, extensive or intensive. But, all the extensive variables

are known if all the intensive variables plus the mass of each phase are known. Therefore, we need Φ more variables. But, we also have c more equations of constancy of mass to show that the system is closed, and thus $f = c + 2 - \Phi - c + \Phi = 2$, and this is Duhem's theorem.

Thus, if the phase change gabbro ⟶ eclogite is considered a closed system, which it probably is, it still has 2 degrees of freedom, such as P and T.

This has been a slight digression from the main point that I was making, and that is : that the phase change gabbro ⟶ eclogite would not be a sharp one, but would take place over a certain pressure interval. But, I digressed to illustrate that the phase transformation consisted of 2 components, could be represented by 2 degrees of freedom, and could be considered as a closed system. I should like to state one further point regarding the meaning of the word component. The choice of components (for use in the phase rule) should be such that the chemical composition of each and every phase of the system can be stated in terms of these components. This is done by taking all the S chemical species present in the system, and subtracting the number of reactions possible between these species (since each reaction reduces the variance or number of degrees of freedom by one). Thus, $c = s - r$. A simple example is that of a system containing : brucite $Mg(OH)_2$, periclase MgO, and water H_2O. Here, $s = 3$, but $r = 1$ because $MgO + H_2O = Mg(OH)_2$. Therefore, $c = 2$ (MgO and H_2O). In the case of the gabbro ⟶ eclogite change, there are four species present, but two reactions are possible, and hence $c = 2$, as stated before.

Now, vertical reflections have never been detected from the Moho.

Some workers, such as Shor, Hart, and Reich claim to have observed such reflections, but the evidence is not very convincing. Their records contain other arrivals very close to the ones chosen, which tends to make one doubt the validity of the chosen ones. Furthermore, extensive research by the Carnegie group, the Research Group for Explosion Seismology in Japan, and workers in the Soviet Union, have not produced any evidence for near vertical reflections from the Moho. There is one exception. One record from Japan shows what may be a deep vertical reflection. But, on the same record, an arrival just as strong about 1.5 seconds later is simply ignored in the interpretation. The work of the University of Alberta in Southern Alberta does not show any vertical reflections. A possible reflection is present at about 70 kms. on the eastern profile, but this would indicate an angle of reflection some 40° from vertical. Unfortunately, one record which was taken very close to the shot (18 kms.) in an effort to record a vertical reflection does not show any such reflection because of a great deal of power supply noise on the record at the expected time for the arrival. Other negative evidence comes from Mead (1956) who worked on a project specifically designed to look for deep reflections. He concluded that any arrivals he observed were not due to deep reflections. Thus, I think it can be safely stated that no conclusive evidence for vertical reflections from the Moho has been found. Thus, at present, it appears that the Mohorovicic discontinuity may not be as sharp as it was previously thought to be. This fact tends to support the idea of a phase change.

Before we discuss the phase change hypothesis any further, let us first consider what it means to have the Moho represented by a

chemical change. Gravity measurements over major mountain ranges, continental areas, and over the ocean basins have shown that the mountains do not represent extra loads of rock upon the earth's crust, but rather that they are masses of lighter rock "floating" in a denser substrate. An analogy to this is an iceberg floating in water. Thus, all the major features of relief of the surface of the earth show mirror image features within the crust. This gave rise to the concept that there were two contrasting materials in the "crust" of the earth; sialic material making up the continents and simatic material, making up the denser rocks below the floor of the ocean and lying under the sial of the continents. Then, the Moho was discovered, and indicated an abrupt change in rock type at a few tens of kms. under the continents and a few kms. under the oceans. Since the Moho was found to be much deeper under the continents than under the oceans, and much deeper under the mountains than anywhere else, it was believed that the Moho represented the change in rock type from sial (granitic) to sima (basaltic). Prior to and along this general picture, the concept of isostasy developed. This is just the floating hypothesis mentioned before. Three models were developed, by Pratt, Airy, and Heiskanen. Pratt felt that the crust was everywhere at the same depth below sea level, with its base everywhere supporting a uniform weight per unit area. Under the mountains, these conditions would call for a deficiency in density of the crustal rocks, while under the oceans, the density of the crustal rocks must be greater. Airy postulated that the surface rocks of the earth may be likened to a series of logs of different diameter, but the same density floating in water. Thus, he supposed that the earth's crust was composed of blocks

of one density but different thicknesses floating in a heavier substratum. The weight of the block above sea level is held up by the buoyancy of a root extending below the normal depth of the low density surface material. Heiskanen's model is like Airy's, except that he considered the density to vary up and down the columns or blocks, with denser rocks near the lower end of the blocks. Obviously, Heiskanen's theory best fits the known structure of the crust. Seismic evidence shows that the crust is thicker in general in mountainous regions, and also that the density is greater towards the base of the crust (becoming so either continuously or discontinuously). But, while the Moho was first thought to represent a chemical change between the sial and the sima, it is now believed to represent a chemical change between sima and ultrasima. Seismic velocity data indicates that the velocity below the Moho is everywhere greater than that of ordinary simatic rock such as gabbro or basalt. The velocities found are too high to fit laboratory data on rocks other than dunite, peridotite, or eclogite. We are considering a chemical change here, so let us disregard the possibilities of eclogite.

Turner and Verhoogen state that the probable density of the material below the Moho, from considerations of isostatic balance between continents and oceans is about 3.3 gm/cm^3. They further state that peridotite (or possibly dunite) is the best choice for the rock below the Moho because: (1) the density is approximately 3.3 gm/cm^3; (2) there is a very widespread occurrence in basaltic volcanic ejecta, all over the world, of peridotite nodules of astoundingly uniform composition (olivine, enstatite, chromium diopside, spinel) which are also very similar to the widely distributed dunites and associated intrusive rocks. Bullen also believes that peridotite is the rock type below the Moho for the same reasons.

Very briefly, I want to discuss how such a rock type could have been formed by magmatic differentiation. Magmatic differentiation includes all processes by which a broadly homogeneous parent magma breaks up into contrasted fractions which ultimately form rocks of different compositions. I do not intend to say anything here about the origin of the magmas themselves. But, Turner and Verhoogen give a very good treatment of the possible origin of various types of magma. The mechanism of differentiation which could well produce such a layer is crystal fractionation. This is the separation of successive crystal fractions from the remaining liquid fractions. From a great deal of research on crystallization of various minerals, it has been found that minerals which tend to be associated together in igneous rocks are those which crystallize over the same range of temperature (e.g. olivine-diopside, olivine-labradorite). Likewise, crystals such as orthoclase and diopside, which have a very different range of crystallization, are never found together. All this suggests fractional crystallization. The type of fractional crystallization which is most likely to produce a layer of peridotite or dunite is gravitational differentiation. Being high temperature minerals, the magnesian, olivines and the pyroxenes are among the first minerals to crystallize out. These heavy minerals then sink in a less dense liquid, because at this early stage, the liquid phase is still dominant and is not yet too viscous to prevent the settling of crystals. A full treatment of differentiation of all possible parent magma types is given in Turner and Verhoogen. But, this method seems to me to be a reasonable explanation of how an ultrabasic layer could be formed.

Now, let us summarize what we have stated regarding the Moho

being a chemical change. It does not contradict in any way the principle of isostasy. The seismic velocities below the Moho, and the calculated density there, do not disagree with the chemical change hypothesis. Peridotite nodules of a rather uniform composition are very common. And, gravitational differentiation of a parent magma could well produce such an ultrabasic layer.

But, the following four facts sharply contradict this idea of a more sialic crust floating on an ultrabasic substratum of different chemical composition.

(1) Large areas of continents, long near sea level, have been uplifted many thousands of feet in the air. Furthermore, this uplift seems to have taken place very rapidly in terms of geologic time.

(2) Sediments of low density, filling troughs along the margins of continents, apparently are able to subside into this higher density substratum.

(3) Radioactive, heat-producing elements are associated with sialic rocks. Therefore, one should expect that the heat flow through the thicker parts of the earth's crust to be much greater than through the thinner parts of the crust. This, however, is not found. To a first approximation, heat flow through the crust is the same through continents, mountain ranges, and ocean basins.

(4) The lifetime of continents and mountain ranges is vastly greater than the rates of erosion would suggest. (Kennedy, 1959).

Let us briefly examine each of these apparent facts in the light of the chemical change we have been speaking of.

Problem (1): Regions near sea level may, over a short time such

as a few million years, be uplifted several thousands of feet. A good example is the Colorado Plateau. This is an area of about 250,000 square miles that stood at sea level for hundreds of millions of years, and then was vertically uplifted one mile about forty million years ago (in mid-Tertiary time) and is still a high plateau. What mechanism could cause such an uplift? In addition, gravity and seismic evidence shows that the Colorado Plateau is in isostatic balance. Thus, the Colorado Plateau grew downwards at the same time as it grew upwards. Convection currents could account for some of the uplift, but seem inadequate to account for the transfer of some 2,500,000 cubic miles of sialic rock. And, where did all this light rock come from? The region from which the light rock was moved should have been spectacularly downwarped, but no large neighboring depressions are known.

This uplift and sinking of large crustal blocks, while the blocks remain in isostatic equilibrium, cannot be explained by a chemical change at the Moho.

Problem (2): Why are low density sediments, filling troughs, able to subside into the higher density substratum? The fundamental laws of Physics are violated on a large scale if this downwarping is produced directly by continued loading of sediments. Some of these troughs contain 50,000 to 100,000 feet of sediments and may be 1000 miles long and 100 miles wide. These troughs, like the plateaus, always seem to be in isostatic balance. Thus, dense rock must automatically be removed from below these troughs at the same rate as they receive sediments. Furthermore, these thick lenses of sediment are then slowly folded and uplifted to form mountain ranges which may stand 20,000 feet high. The mystery then is heightened, and cannot be satisfactorily explained by a chemical change at the Moho.

Problem (3): We expect the heat flow through regions with a thicker crust to be greater. This is not found to be true. It is known that most of the heat escaping from the earth is radiogenic, and is not primary heat from an initially hot earth. It has been found that uranium, thorium, and potassium are 10 to 100 times more abundant in light silica rich rock as in denser simatic material, rich in Mg and Fe, and low in silica. Hence, we expect the heat flow under oceans to be only a small part of that under continents. But, Bullard (1952) determined that the heat flow under oceans, continents, and mountain ranges was almost identical. Thus, either the concentration of radioactive minerals under the oceans is the same as that under continents (in which case the idea of sial and sima or ultrasima seems to be in error) or else heat is transferred by some other method (such as convection currents) from deep down in the earth to near-surface places beneath the ocean. It is certainly difficult to explain by considering the Moho as a chemical change.

Problem (4): This problem of the long lifetime of continents and mountain ranges is very difficult to explain. Calculations by Gilluly, Waters, and Woodford (1952) show that the rate of erosion for the whole United States is about one foot in 10,000 years. At this rate, all the land masses of the world would be eroded to sea level in a time interval of the order of 1 - 25 million years. But, land animals and plants are known to have existed for over 300 million years. Sedimentary geology indicates land masses extending back two billion years. Why has not all the sial of the continents been distributed evenly throughout the ocean basins? The rates of erosion of mountain ranges are much greater than for continents. The lifetime of a mountain should then be much less than the 25 million years estimated for the continents. But, the Appalachian mountain range

appears to have existed much as it is for the last 200 million years. Thus, there are orders of magnitude discrepancy between the estimated lifetime (based on known rates of erosion) and the lifetime shown by the geologic record, of both continents and mountain ranges. Even when we take into account the fact that we assume the mountain ranges and continents are floating on denser sima, and that they would float up as they are eroded, the presumed depth of roots and thicknesses of the light continental rocks allow an extension of the previously estimated lifetime of continents by no more than ten times. (Kennedy, 1959).

These four problems are extremely difficult to explain if the discontinuity between the crust and the mantle of the earth is considered to be a chemical change. Thus, there seems to be much more evidence against a chemical change than there is for such a change. As we shall soon see, a phase change could quite easily answer the above problems.

Now, that we have briefly discussed the pros and cons of a chemical change at the Moho, let us deal with the concept of a phase change. As stated earlier, this is a 2-component phase change with two degrees of freedom, P and T. Basalts and eclogites which have sharply contrasting mineralogy, have essentially identical composition. This is illustrated by the following table.

	Eclogite (MacDonald, 1959)	Plateau Basalt (Daly, 1933)
SiO_2	48.12 %	48.80 %
TiO_2	.85	2.19
Al_2O_3	10.42	13.98
CaO	9.99	9.38
MgO	14.22	6.70
FeO	13.92	13.60
Na_2O	1.45	2.59
K_2O	.58	.69

Eclogite, however, contains no feldspar, instead it is made up of a jadeitic pyroxene (omphacite) and garnet. The average density of eclogite is generally given as 3.3 gm/cm^3 or 3.4 gm/cm^3, tending to be slightly higher than that of peridotite. The mean density of gabbro is about 2.95 gm/cm^3. Since eclogite is the denser of the two phases, it is the rock which must exist at the higher pressures.

Lovering states that the theory of a phase transition has been supported by recent experiments in the determination of the composition of stony meteorites. This composition is generally believed to be analogous to the composition of the earth's mantle. The stony meteorites can be considered as samples of the silicate mantle of the parent meteorite--thus the analogy to the earth's mantle. The chondritic and polymict brecciated stony meteorites are excluded. The latest meteoritic evidence suggests that the outer zone of the mantle of the parent meteoritic body is formed of basaltic or euchritic achondrites, with compositions very near those of basalts and norites of the earth. Thus, we see that if the greater part of the earth's upper mantle were composed of material similar in composition to the euchritic achondrites (as was the upper mantle of the parent meteoritic body), then such a material would have a composition nearly identical with rocks such as basalt which probably form the major components of the earth's lower crust. Thus, there is no evidence to indicate that the discontinuity between the crust and the mantle (the Moho) is due to a chemical change.

The equivalence of olivine basalt and eclogite chemically was shown earlier when the equation of transformation was written. This is restated below.

$$\underset{\text{labradorite}}{(3Ca\,Al_2\,Si_2\,O_8 + Na\,Al\,Si_3\,O_8)} + \underset{\text{olivine}}{3\,Mg_2\,Si\,O_4} + \underset{\text{diopside}}{n\,Ca\,Mg\,(SiO_3)_2}$$

$$\longrightarrow \underset{\text{garnet}}{3Ca\,Mg_2\,Al_2\,(SiO_4)_3} + \underset{\text{omphacite}}{2Na\,Al\,(SiO_3)_2 + n\,Ca\,Mg\,(SiO_3)_2} + \underset{\text{quartz}}{2\,Si\,O_2}$$

A similar equation can be written to show the equivalence of euchritic achondrites and eclogites:

$$\underset{\text{Bytownite}}{4Ca\,Al_2\,Si_2\,O_8 + Na\,Al\,Si_3\,O_8} + \underset{\text{pigeonite}}{8\,Mg\,SiO_3 + n\,Ca\,Mg\,(SiO_3)_2}$$

$$\rightarrow \underset{\text{garnet}}{4Ca\,Mg_2\,Al_2\,(Si\,O_4)_3} + \underset{\text{omphacite}}{Na\,Al\,(SiO_3)_2 + n\,Ca\,Mg\,(Si\,O_3)_2} + \underset{\text{quartz}}{5\,SiO_2}$$

There is much evidence from petrology to show that eclogites are very unstable rocks and that reactions transforming them to the less dense rock type can take place in geologically short times.

Now, why should the phase change take place at a shallower depth beneath the oceans than beneath the continents? To explain this, Lovering has made a re-estimation of the pressure-temperature curve for the basalt to eclogite phase change. From this, he came to the conclusion that because the temperature at the bottom of the ocean is lower than the temperature beneath the continents where the pressure is the same, the temperature at any given pressure beneath the oceans must generally be lower than under the continents. And, since the pressure at which a phase change takes place increases as the temperature increases, it follows that the basalt-eclogite phase change will take place at a greater depth under the continents.

To get values for this postulated pressure-temperature curve, temperatures were calculated at the Moho from surface heat flow and an assumed distribution of radioactivity. As we stated before, the average value of heat flow under the oceans is about the same as that on land,

i. e., about 1.2×10^{-6} cal/cm^2/sec.

Let Ko = thermal conductivity,

Po = density, and Ao = rate of radioactive heat generation/

per unit mass.

Then, if H is the heat flux at the ocean bottom with temperature O°C., the temperature θ at depth x below the ocean floor is given by:

$$= (Hx - 1/2 \; Po \; Ao \; X^2)/K_o.$$

Using typical values of $H = 1.2 \times 10^{-6}$ cal. cm.$^{-2}$ sec.$^{-1}$ (Bullard, 1956),

$Ao = 3.5 \times 10^{-14}$ cal. gm.$^{-1}$ sec.$^{-1}$ (Jacobs, 1956),

$Ko \doteq .0057$ cal. cm.$^{-1}$ sec.$^{-1}$ deg.$^{-1}$

$Po = 2.97$ gm./cm.^{3},

and using 6 kms. as the depth of the Moho, under the ocean floor, the temperature at this depth under the ocean floor is found to be 123°C, while the pressure at this depth is about 2200 bars. This gives point O on curve I. (temperature vs depth as calculated in the above equation).

Now, we make the same calculation for the continents.

Let X_1 be the depth of the sialic layer,

K_1 be the thermal conductivity of sial,

P_1 be the density of sial,

A_1 be the heat production/unit mass of sial, and under the sial is

basalt with K_o = thermal conductivity

P_o = density

A_o = heat production/unit mass.

Then, the temperature at depth X is given by:

$$\theta = (H - 1/2 \; A_1 \; P_1 \; X) \; (X/K_1) \qquad \text{for } O < x < X_1$$

$$\theta = (2H - P_1 \; A_1 \; X_1) \left(\frac{X_1}{2K_1}\right) + \frac{(H - P_1 \; A_1 \; X_1)(X - X_1)}{K_o} - \frac{Po \; Ao \; (X - X_1)^2}{2Ko} \quad \text{for } X > X_1.$$

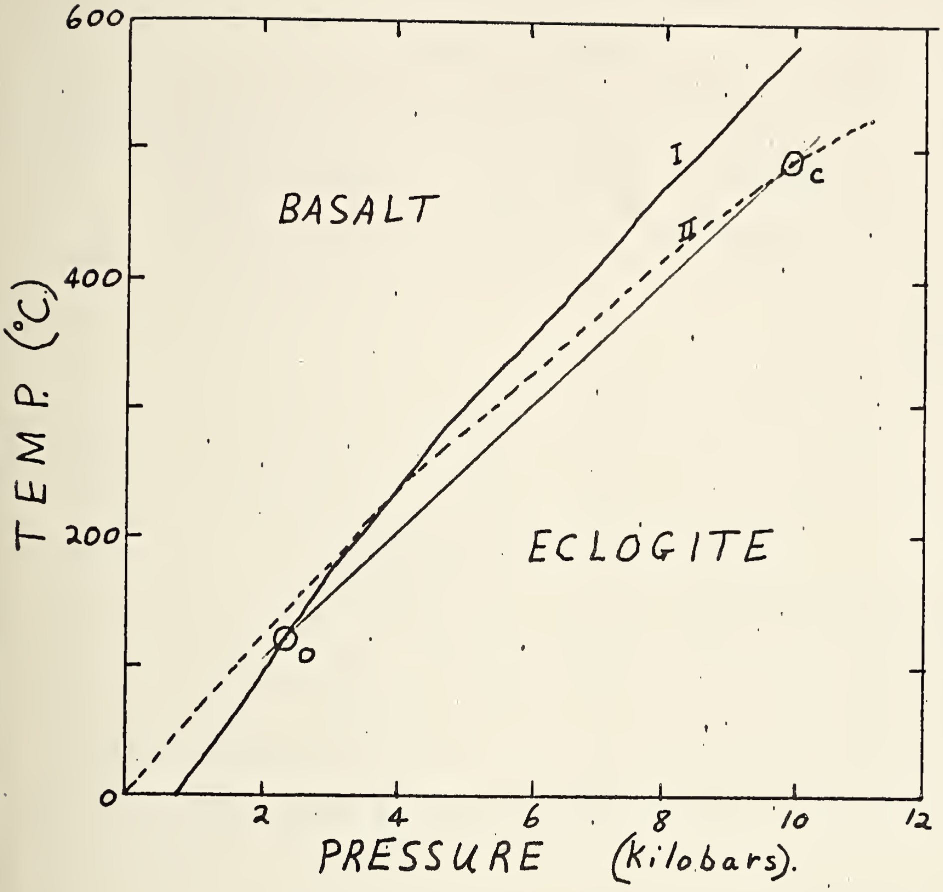

Lovering's Curves.

I = oceanic curves
II = continental curve

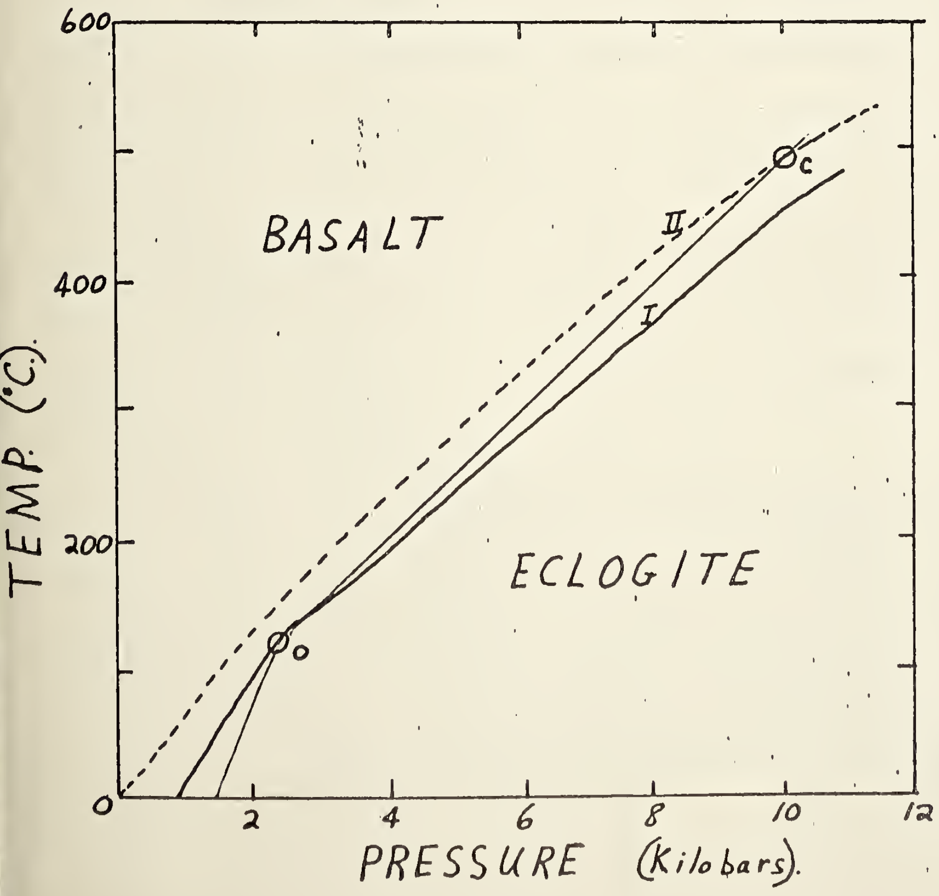

More Probable Curves.

FIG. 37

where the temperature at the surface is taken as $0^{o}C$.

Typical values are again used, as follows:

depth of sial = 10 kms (Gutenberg, 1951) with $P_1 = 2.76$

$A_1 = 1.2 \times 10^{-13}$ (Jacobs, 1956).

$K_1 = .0065$ (Birch, 1942),

and with the values for basalt used before, the temperature at a depth of 35 kms. is found to be 480°C., while the pressure is calculated to be about 10,000 bars. This gives point c on curve II.

From these calculations, we may assume that the pressure-temperature curve for the transformation basalt to eclogite lies roughly along the line Oc. If we assume that it is the straight line Oc, then it can be represented by the equation $p = 21.8\theta - 488$ where p is in bars and θ in °C.

Robertson and others (1957) have concluded that the pressure needed to form an omphacite pyroxene is probably less than that needed to form jadeite, but they also conclude that the equilibrium line for the formation of jadeite from albite and nepheline is close to the line Oc on the graph, estimated as the equilibrium line for the formation of eclogite from basalt. We must note that the use of the single line Oc to separate these stability fields is not really true, as 2 components (or maybe more according to Lovering) are involved here.

Now, let us examine these graphs as made by Lovering. Basalt is stable on the upper side of the Oc line and eclogite is stable below this line. We also recall at this point that Lovering made the statement that the temperature at any pressure under the oceans must be lower than that at the same pressure under the continents. We notice immediately that

his graphs do not support his statements. The continental curve seems to be satisfactory, as when it crosses the transition line, it remains in the region of the graph where eclogite is stable as it should. But, the oceanic curve runs from the field of stability of eclogite into the field of stability of basalt. It also crosses the continental curve. Thus, it shows that for any pressure, the temperature under the oceans is warmer than the temperature at the same pressure under the continents, contrary to Lovering's statement. I have recalculated some of the points on this curve from the equation, and the curve is correct. Why the discrepancy or contradition? The following reasons may be at least part of the cause of trouble. First of all, the equation for temperature under the oceans could only be used down to the Moho as it stands, without some modification. The modification would be the taking into account of the fact that at the Moho (about 6 kms. below the ocean floor), the density changes from 2.97 to about 3.3 gm/cm^3 and the thermal conductivity no doubt changes. Lovering, however, used the same equation for temperature under the oceans, even below the Moho. The modification might cause quite a change in the curve. Even if we just take into account the density change with regard to the increased pressure, we note that the curve is brought down. Secondly, the phase transition curve is very likely not to continue in a linear manner or even in a regular manner at low temperatures and pressures. The following graphs (lower graph, p. 16, a) as I have redrawn them may well be closer to the truth. More work will have to be done along these lines. In any event, the points O and C are reasonable, and give a reasonable pressure-temperature line between them for the phase transition. The

continental temperature-pressure curve supports the idea of a phase change and the oceanic curve may well do so if the equation is modified for the greater depths.

Several people have done work on the correlation of continental and oceanic phase transitions, by beginning with the assumption that the phase transition is at equilibrium. Two of these workers were MacDonald and Ness. I do not intend to include any of their mathematical calculations here, as I already feel I have included too much detail in this supposedly brief general discussion of the possible nature of the Moho. But, in order to point up the fact that there are also difficulties involved in assuming that the Moho is a phase change, I wish to state that after extensive mathematical work, they concluded that the same phase change can produce both the oceanic and continental Moho only if the phase transition has very special properties and somewhat unreasonable crustal models are used.

Simple mathematical calculations for the phase transition under equilibrium conditions can also be used to attempt to predict the movement of the phase transition due to surface perturbations. MacDonald and Ness also did work on this. They devised a typical model, as before, and then analysed it mathematically. Once again, I do not intend to include any of their analysis here. However, this analysis shows that amplitudes for the movement of the crust that are in general agreement with geological observations can be found, assuming the Moho is a phase change. But, they state that much more work along this line is needed.

Let us review what we have found so far. We know that basalt and eclogite have about the same composition, and that the change from

one to the other can be represented by a simple equation. The density of eclogite is approximately equal to that of the material believed to be below the Moho. The seismic velocities also correspond. Furthermore, the upper mantle of parent meteoritic bodies (by study of story meteorites) is composed of euchritic achondrites of composition similar to eclogites. And, Lovering offers a reasonable explanation of why the transition would occur at a greater depth under continents (even though his graphs as he has drawn them do not show this). Mathematical calculations of transition boundary movement due to surface perturbations give reasonable results, but it is very difficult to correlate mathematically the continental and oceanic transitions. Taken as a whole, there is no direct evidence to show that the Moho cannot be a phase change.

Let us assume that it is a phase change, and see how well it answers the four problems of the surface of the earth posed before.

(1) Large areas of continents, at sea level once upon a time, could be elevated to a high plateau just by warming the rocks near the discontinuity by a few tens of degrees. This would cause the eclogite to change to basalt, and the phase change would migrate downwards. The volume increase when the dense rock turned to light rock would float the continents to higher levels. Thus, convection currents are not needed to explain the transport of millions of cubic miles of light material to uplift continents. But, convection currents may well be the cause of the rise in temperature needed to bring about this uplift.

(2) The downsinking of sediments into troughs is also easily explained by a phase transition. The initial effect of depositing sediments

in troughs would be to increase the pressure at the discontinuity with little or no change in temperature. Thus, basalt would change to eclogite, and the phase change would migrate toward the surface. The decrease in volume would cause the trough to sink. Thus, the short-time effect of rapid sedimentation is one of sinking. But, in a sufficient amount of time, since the new sediments would be of low thermoconductivity and probably richer in radioactive material, the temperature at the base of the trough would slowly rise. Then, the eclogite would change to basalt and the discontinuity would migrate downward. The consequent increase in volume would cause great uplift. Thus, troughs may sink for considerable time and then be uplifted to form mountain ranges as the roots of the trough migrate downward.

(3) The phase transition also explains the problem of a rather uniform heat flow to the surface of the earth. If the bulk composition of the rocks under the continents were not much different from the bulk composition of oceanic rocks (basalt and eclogite), then we would expect relatively uniform heat flow. This is what we find, of course.

(4) The long lives of mountain ranges can be similarly explained by a phase change. As the tops of mountains are eroded away, the pressure at the discontinuity is decreased. This causes eclogite to change to basalt, and the volume increase would keep the mountains floated to a high elevation.

Thus, the four problems which we had much difficulty explaining in terms of a chemical change are very easily answered by treating the Moho as a phase change. More work is needed to determine for certain

the exact nature of the Moho. While the concept of a phase change seems to solve more problems of the earth's crust than does a chemical change, it also creates some problems as we have seen. But, no evidence directly contradicts the idea, and much evidence supports it. I believe that there will be no way of deciding on a definite answer until Project Mohole is complete. Until such time, I prefer to believe the concept of a phase change at the Moho.

Much work remains to be done in the world to determine the exact depth and attitude of the Moho at all places. This thesis is concerned with that aspect of research on the Moho. The second chapter was a brief summary of former work done by other workers in other places. Following this, a detailed interpretation of the work in Southern Alberta by the University of Alberta was given.

I wish to mention here, that, following the writing of this section, a paper by Bullard and Griggs was brought to my attention by Dr. Garland. They conclude that the Mohorovicic Discontinuity represents a chemical change rather than a phase change. They have three major objections to the theory of a phase change.

(1) The oceanic and continental transitions cannot both result in the high pressure form lying beneath the Moho. This is the fact that I have discussed already when I was speaking about Lovering's curves. But, I did offer a possible explanation for some of the difficulty, but there would probably be still some discrepancy even if this were considered.

(2) The variations in Moho depth from place to place are less than would be expected from variations of heat flow. As stated before,

the mean heat flow under both oceans and continents is the same. But, variations occur under both. To date, however, Moho depth determinations have not been made extensively in anomalous areas. But, as Bullard and Griggs state, measurements that have been made indicate that changes in depth are not as great as those expected. More work definitely should be done.

(3) The third objection raised by Bullard and Griggs to the idea of a phase change is that a phase change boundary would not be sharp. They feel, that, since some workers claim to have observed vertical reflections from the Moho, it is a sharp boundary. But, I have already discussed such reflections, and showed that they are not very convincing.

Certainly there are objections to the theory of a phase change. But, since it explains so many difficulties, I believe that the Mohorovicic discontinuity must represent a phase change.

BIBLIOGRAPHY

Bullard, E. C., and Griggs, D. T.,: "The Nature of the Morhorovicic Discontinuity", Geophys. Journal, Vol. 6, No. 1, pp. 118-123, (1961).

Harris, P. G., and Rowell, J. A.,: "Some Geochemical Aspects of the Mohorovicic Discontinuity", Journ. Geophys. Research, Vol. 65, pp. 2443-2459, (1960).

Kennedy, G. C.,: "The Origin of Continents, Mountain Ranges, and Ocean Basins"., Am. Scientist, Vol. 47, pp. 491-504, (1959).

Lovering, J. F.,: "The Nature of the Mohorovicic Discontinuity", Trans. Am. Geophys. Union, Vol. 39, pp. 947-955, (1958).

MacDonald, G. J. E., and N. F. Ness,: "Stability of Phase Transitions Within the Earth", Journ. Geophys. Research, Vol. 65, pp. 2173-2190, (1960).

Turner and Verhoogen,: "Igneous and Metamorphic Petrology", McGraw-Hill, 2nd ed., (1960).

APPENDIX II

TABLES

OF

ARRIVAL TIMES

Distances are in Kilometres.

Times are in Seconds.

App. vel. = apparent velocity in kms. /sec.

EAST SHOT POINT

ARRIVAL TIMES (Secs.)

SHOT #4, TRUCK #2. (Poor Record)

Geoph. No.	Dist.	Arr. #1, Precambrian, app. vel. 6.6.	Arr. #2, app. vel. 6.4.	Arr. #3, limestone refraction, app. vel. 5.7.	Arr. #4 app. vel. 6.3
1.	90.04	15.22	15.69	16.05	16.39
2.	.17	--	.71	.08	.42
3.	.29	.24	--	--	--
4.	.42	.25	.76	.11	.46
5.	.56	--	.77	.13	.47
6.	.69	.30	.79	.16	--
7.	.81	--	.83	.18	--
8.	.94	.35	.83	.21	--
9.	91.09	.37	--	.22	--
10.	.21	.38	.86	.23	.58
11.	.34	--	--	--	--
12.	.46	.41	--	--	.62

EAST SHOT POINT

ARRIVAL TIMES (Secs.)

SHOT #5, TRUCK #1. (Fair Record)

Geoph. No.	Dist.	Arr. #1, Moho refraction, app. vel. 8.2.	Arr. #2, app. vel. 9.4.
1.	187.20	31.93	--
2.	.33	.95	--
3.	.45	.94	33.19
4.	.58	.94	.20
5.	.72	--	.21
6.	.85	--	.23
7.	.97	32.00	--
8.	188.10	.02	.25
9.	.25	.05	--
10.	.37	--	.27
11.	.50	.07	.30
12.	.62	.08	.31

EAST SHOT POINT

ARRIVAL TIMES (Secs.)

SHOT #3, TRUCK #1. (Poor Record)

Geoph. No.	Dist.	Arr. #1 app. vel. 6. 6	Arr. #2 app. vel. 7. 0	Arr. #3 app. vel. 8. 8	Arr. #4 app. vel. 7. 2	Arr. #5 app. vel. 8. 5
1.	40. 17	9. 28	9. 75	10. 24	10. 60	--
2.	. 29	. 30	. 76	. 26	. 61	--
3.	. 42	. 32	. 79	. 27	. 62	--
4.	. 54	. 36	. 81	. 28	. 64	--
5.	. 69	. 38	. 83	. 31	. 67	12. 09
6.	. 82	. 40	. 86	. 32	. 69	. 10
7.	. 94	. 42	. 87	. 33	. 70	. 11
8.	41. 07	--	--	. 35	--	--
9.	. 21	. 46	. 90	. 36	. 74	. 15
10.	. 34	. 46	. 92	. 38	. 75	. 16
11.	. 46	--	. 94	--	--	--
12.	. 59	. 49	. 95	. 40	. 79	. 19

EAST SHOT POINT

ARRIVAL TIMES (Secs.)

SHOT #8, TRUCK #1. (Poor Record)

Geoph. No.	Dist.	Arr. #1 app. vel. 8.0	Arr. #2 app. vel. 7.8	Arr. #3 app. vel. 8.1	Arr. #4 app. vel. 9.5
1.	25.64	5.89	7.30	7.57	8.00
2.	.76	.90	.34	.58	.03
3.	.89	.90	.35	.61	.04
4.	26.01	.94	.36	.62	.05
5.	.16	.96	.38	.64	.07
6.	.29	--	.38	.65	.07
7.	.41	--	.42	.66	.08
8.	.54	--	.44	.67	.10
9.	.68	6.02	.45	.70	.12
10.	.81	.03	.47	.72	.14
11.	.93	.05	.49	.74	--
12.	27.06	.07	.50	.75	--

EAST SHOT POINT

ARRIVAL TIMES (Secs.)

SHOT #8, TRUCK #1. (Poor Record)

(Continued)

Geoph. No.	Dist.	Arr. #5 app. vel. 8.7	Arr. #6 app. vel. 8.7	Arr. #7 app. vel. 10.3	Arr. #8 app. vel. 8.7
1.	25.64	8.27	8.82	9.50	10.21
2.	.76	.29	.84	.52	.24
3.	.89	.30	.85	.52	.26
4.	26.01	.31	.87	.54	.27
5.	.16	.33	.87	.54	.29
6.	.29	.35	.88	.55	.30
7.	.41	--	.90	.56	.31
8.	.54	.37	--	--	--
9.	.68	.38	--	--	--
10.	.81	.40	.96	.60	.36
11.	.93	.43	.97	.63	--
12.	27.06	--	--	.65	--

EAST SHOT POINT

ARRIVAL TIMES (Secs.)

SHOT #10, TRUCK #1 (Good Record)

Geoph. No.	Dist.	Arr. #1 Precambrian refraction, app. vel. 6.5	Arr. #2 limestone refraction, app. vel. 6.6	Arr. #3 app. vel. 8.5	Arr. #4 app. vel. 9.1
1.	68.85	--	--	--	--
2.	.97	11.83	12.51	13.00	13.34
3.	69.10	.86	--	.02	.35
4.	.22	--	--	.03	.36
5.	.37	.89	.56	.04	.38
6.	.50	.90	.58	.06	.39
7.	.62	.92	.59	--	.40
8.	.75	.94	.62	.09	.42
9.	.89	--	.64	.11	.44
10.	70.02	.99	.66	.12	.45
11.	.14	12.00	.68	.14	.46
12.	---.27	--	--	--	--

EAST SHOT POINT

ARRIVAL TIMES (SECS.)

SHOT #10, TRUCK #1 (Good Record)

(Continued)

Geoph. No.	Dist.	Arr. #5 app. vel. 9.1	Arr. #6 app. vel. 8.2	Arr. #7 app. vel. 12.3	Arr. #8 app. vel. 7.5
1.	68.85	--	--	--	--
2.	.97.	13.82	14.96	15.64	--
3.	69.10	.83	.97	--	15.89
4.	.22	--	.99	.66	.89
5.	.37	.86	15.00	.67	.91
6.	.50	.88	.03	.63	.93
7.	.62	.89	.04	--	--
8.	.75	.90	.05	.70	.96
9.	.89	--	.06	--	.98
10.	70.02	.93	.09	.74	16.00
11.	.14	--	.10	--	--
12.	.27	--	.11	.75	.03

EAST SHOT POINT

ARRIVAL TIMES (Secs.)

SHOT #10, TRUCK #1 (Good Record)

(Continued)

Geoph. No.	Dist.	Arr. #9, app. vel. 6.3	Arr. #10 app. vel. 8.7	Arr. #11 app. vel. 6.5	Arr. #12 app. vel. 8.9
1.	68.85	--	--	--	--
2.	.97	--	--	17.69	17.93
3.	69.10	--	16.76	--	.94
4.	.22	16.15	.77	.73	--
5.	.37	.18	.78	.75	.97
6.	.50	.20	.80	.77	.99
7.	.62	.22	.81	.78	--
8.	.75	.24	.82	--	--
9.	.89	.26	.84	.83	18.02
10.	70.02	--	.86	.85	--
11.	.14	--	.87	.87	--
12.	.27	.33	.89	.90	--

EAST SHOT POINT

ARRIVAL TIMES (Secs.)

SHOT #10, TRUCK #1 (Good Record)

(Continued)

Geoph. No.	Dist.	Arr. #13, Moho reflection, app. vel. 11.4	Arr. #14, app. vel. 9.1
1.	68.85	--	--
2.	.97	18.45	20.31
3.	69.10	.46	.33
4.	.22	.47	.35
5.	.37	.48	.37
6.	.50	.49	.39
7.	.62	.50	.40
8.	.75	.52	.41
9.	.89	.53	.42
10.	70.02	.54	.44
11.	.14	.56	--
12.	.27	--	--

EAST SHOT POINT

ARRIVAL TIMES (Secs.)

SHOT #10, TRUCK #2 (Good Record)

Geoph. No.	Dist.	Arr. #1, Precambrian refraction, app. vel. 5.4	Arr. #2, app. vel. 7.7	Arr. #3, app. vel. 7.0	Arr. #4, app. vel. 7.3
1.	127.01	--	--	21.36	21.95
2.	.14	20.79	21.16	.39	--
3.	.26	.81	.19	.41	.97
4.	.39	.82	.20	.42	.99
5.	.53	.85	.22	.45	22.00
6.	.66	.88	.24	.47	.02
7.	.78	.91	.24	.48	--
8.	.91	.93	--	--	--
9.	128.06	.95	.29	.52	.08
10.	.18	.98	.30	.54	.09
11.	.31	21.00	.32	.56	.11
12.	.43	.03	.35	.58	.13

EAST SHOT POINT

ARRIVAL TIMES (Secs.)

SHOT #10, TRUCK #2, (Good Record)

(Continued)

Geoph. No.	Dist.	Arr. #5, app. vel. 7. 4	Arr. #6, Intermediate layer refraction app. vel. 7. 7	Arr. #7, app. vel. 9. 1	Arr. #8, Moho refraction energy, app. vel. 8. 7
1.	127. 01	--	--	--	24. 78
2.	. 14	--	23. 52	24. 39	. 79
3.	. 26	22. 93	. 55	. 40	. 79
4.	. 39	. 96	. 56	. 41	. 81
5.	. 53	. 98	. 58	. 43	. 83
6.	. 66	. 99	. 59	. 45	. 84
7.	. 78	23. 00	. 62	. 46	. 84
8.	. 91	. 02	. 63	--	--
9.	128. 06	. 05	. 64	. 48	. 88
10.	. 18	. 06	. 66	. 50	. 90
11.	. 31	. 08	. 68	. 52	. 92
12.	. 43	23. 10	. 70	. 53	. 93

EAST SHOT POINT

ARRIVAL TIMES (Secs.)

SHOT #10, TRUCK #2 (Good Record)

(Continued)

Geoph. No.	Dist.	Arr. #9, app. vel. 10.1	Arr. #10, app. vel. 6.9	Arr. #11, app. vel. 7.4
1.	127.01	--	25.60	26.64
2.	.14	25.13	.62	.66
3.	.26	.15	.64	.67
4.	.39	.16	.66	.68
5.	.53	.18	--	.71
6.	.66	--	.71	.73
7.	.78	.20	.72	--
8.	.91	--	.73	.76
9.	128.06	.22	.75	.78
10.	.18	--	.77	.80
11.	.31	.24	.79	.81
12.	.43	.27	.81	--

EAST SHOT POINT

ARRIVAL TIMES (Secs.)

SHOT #11, TRUCK #1 (GOOD RECORD).

Geoph. No.	Dist.	Arr. #1, Precambrian refraction app. vel. 10.5	Arr. #2, app. vel. 8.2	Arr. #3, app. vel. 11.3	Arr. #4, app. vel. 8.3
1.	17.88	--	--	--	--
2.	18.01	--	--	--	--
3.	.13	--	--	--	--
4.	.26	--	--	--	--
5.	.40	--	--	--	--
6.	.53	--	--	--	--
7.	.65	4.08	4.44	4.62	5.37
8.	.78	.09	.45	.63	--
9.	.93	.12	--	--	--
10.	19.05	--	.49	--	.41
11.	.18	.13	.50	.66	.42
12.	.30	.14	.51	.68	.45

EAST SHOT POINT

ARRIVAL TIMES (Secs.)

SHOT #11, TRUCK #2 (Good Record)

Geoph. No.	Dist.	Arr. #1, Intermediate layer refraction, app. vel. 7.1	Arr. #2, Moho refraction, app. vel. 8.1	Arr. #3, Moho reflection, app. vel. 8.7	Arr. #4, limestone refraction, app. vel. 5.4
1.	191.56	--	--	--	--
2.	.69	--	--	--	--
3.	.81	--	--	--	--
4.	.94	--	--	--	--
5.	192.08	--	--	--	--
6.	.21	--	--	--	--
7.	.33	32.47	32.60	33.18	33.44
8.	.46	.49	.61	.19	.47
9.	.61	.51	.63	.21	.49
10.	.73	.52	.64	.22	.52
11.	.86	.55	.66	.24	.54
12.	.98	--	.68	--	.55

EAST SHOT POINT

ARRIVAL TIMES (Secs.)

SHOT #11, TRUCK #2 (Good Record)

(Continued)

Geoph. No.	Dist.	Arr. #5, app. vel. 9.6	Arr. #6, app. vel. 7.5
1.	191.56	--	--
2.	.69	--	--
3.	.81	--	--
4.	.94	--	--
5.	192.08	--	--
6.	.21	--	--
7.	.33	33.77	35.17
8.	.46	.78	.19
9.	.61	.79	.21
10.	.73	.80	.22
11.	.86	.80	.24
12.	.98	.81	.26

EAST SHOT POINT

ARRIVAL TIMES (Secs.)

SHOT #12, TRUCK #1

Geoph. No.	Dist.	Arr. #1, Intermediate layer refraction app. vel. 7.4	Arr. #2, app. vel. 6.5	Arr. #3, app. vel. 6.3	Arr. #4, app. vel. 6.6
1.	221.21	--	--	--	--
2.	.33	36.31	36.79	37.92	38.74
3.	.46	--	--	--	--
4.	.58	.35	.82	--	.78
5.	.73	--	--	--	--
6.	.86	.38	.87	.99	.82
7.	.98	--	--	--	--
8.	222.11	.39	.90	38.04	.86
9.	.25	--	--	--	--
10.	.38	--	--	--	--
11.	.50	--	--	--	--
12.	.63	--	--	--	--

EAST SHOT POINT

ARRIVAL TIMES (Secs.)

SHOT #12, TRUCK #2

Geoph. No.	Dist.	Arr. #1, app. vel. 8. 1	Arr. #2, Moho reflection app. vel. 6. 9
1.	259. 59	--	--
2.	. 72	--	--
3.	. 84	42. 44	--
4.	. 97	--	--
5.	260. 11	--	--
6.	. 24	. 49	43. 03
7.	. 36	--	--
8.	. 49	. 52	. 05
9.	. 64	--	--
10.	. 76	--	--
11.	. 89	--	--
12.	261. 01	--	--

EAST SHOT POINT

ARRIVAL TIMES (Secs.)

SHOT #13, TRUCK #1, (Poor Record)

Geoph. No.	Dist.	Arr. #1, app. vel. 6.5	Arr. #2, app. vel. 7.7	Arr. #3, Moho refraction app. vel. 7.3	Arr. #4, Moho reflection app. vel. 6.5	Arr. #5, app. vel. 7.3
1.	145.52	--	--	--	--	--
2.	.64	26.24	26.70	26.92	27.21	27.57
3.	.77	.26	.71	.94	.23	.60
4.	.89	--	--	--	--	--
5.	146.04	.30	.75	.96	.27	.61
6.	.17	--	--	--	--	--
7.	.29	--	--	--	--	--
8.	.42	--	--	--	--	--
9.	.56	--	.83	--	--	--
10.	.69	--	--	--	--	.71
11.	.81	--	--	--	--	--
12.	.94	--	--	27.10	--	--

EAST SHOT POINT

ARRIVAL TIMES (Secs.)

SHOT #13, TRUCK #2, (Fair Record)

Geoph. No.	Dist.	Arr. #1, Moho refraction app. vel. 9.3	Arr. #2, limestone refraction app. vel. 6.3	Arr. #3, Moho reflection app. vel. 6.0
1.	179.01	--	--	--
2.	.13	--	--	--
3.	.26	--	--	--
4.	.38	--	--	--
5.	.53	--	--	--
6.	.66	--	--	--
7.	.78	31.11	31.36	31.68
8.	.91	.14	.37	.71
9.	180.05	.15	.39	.73
10.	.18	.17	.41	.78
11.	.30	.18	.43	.79
12.	.43	.19	.45	.80

EAST SHOT POINT

ARRIVAL TIMES (Secs.)

SHOT #14, TRUCK #1 (Good Record)

Geoph. No.	Dist.	Arr. #1, Precambrian refraction, app. vel. 7.1	Arr. #2, limestone refraction, app. vel. 8.3	Arr. #3, app. vel. 5.4	Arr. #4, Moho reflection, app. vel. 10.7
1.	85.76	14.57	15.31	16.65	--
2.	.89	--	--	--	--
3.	86.01	--	--	--	--
4.	.14	--	--	--	--
5.	.28	14.65	15.39	16.75	20.33
6.	.41	.67	.40	--	--
7.	.53	--	.42	--	.37
8.	.66	.69	--	--	--
9.	.81	.72	.43	.79	.38
10.	.93	.75	.45	.81	.39
11.	87.06	--	.46	.84	--
12.	.18	.77	.48	.86	--

EAST SHOT POINT

ARRIVAL TIMES (Secs.)

SHOT #14, TRUCK #2 (Good Record)

Geoph. No.	Dist.	Arr. #1, Precambrian refraction, app. vel. 7.6	Arr. #2, limestone refraction app. vel. 8.9	Arr. #3, app. vel. 7.6	Arr. #4, app. vel. 8.5
1.	112.61	--	--	--	--
2.	.74	--	--	--	--
3.	.86	--	--	--	--
4.	.99	18.50	19.93	20.28	21.49
5.	113.13	.52	.94	.30	.50
6.	.26	--	.96	.31	.52
7.	.38	.54	--	--	--
8.	.51	.56	.99	.33	.53/
9.	.66	.57	20.01	.35	.56
10.	.78	.61	.02	.38	.58
11.	.91	.62	.03	.40	.60
12.	114.03	.64	.05	.41	.61

EAST SHOT POINT

ARRIVAL TIMES (Secs.)

SHOT #14, TRUCK #2 (Good Record)

(Continued)

Geoph. No.	Dist.	Arr. #5, app. vel. 13.1	Arr. #6, app. vel. 8.7	Arr. #7, app. vel. 7.7	Arr. #8, app. vel. 7.6
1.	112.61	--	--	--	--
2.	.74	--	--	--	--
3.	.86	--	--	--	--
4.	.99	23.54	28.86	29.63	31.58
5.	113.13	.55	.89	--	.59
6.	.26	.55	.90	.64	.60
7.	.38	--	--	--	.63
8.	.51	.58	.93	.68	--
9.	.66	.59	.94	.71	.74
10.	.78	.60	.95	.72	--
11.	.91	.61	--	.73	.77
12.	114.03	.62	.99	--	.80

EAST SHOT POINT

ARRIVAL TIMES (Secs.)

SHOT #15, TRUCK #1 (Good Record)

Geoph. No.	Dist.	Arr. #1, Precambrian refraction, app. vel. 6.4	Arr. #2, app. vel. 7.5	Arr. #3, app. vel. 8.4	Arr. #4, Intermediate layer refraction app. vel. 7.2
1.	163.25	--	--	--	--
2.	.38	--	--	--	--
3.	.50	--	--	--	--
4.	.63	--	--	--	--
5.	.77	26.63	27.43	27.80	28.65
6.	.90	--	.44	--	.66
7.	164.02	--	--	--	--
8.	.15	--	--	--	--
9.	.30	.70	.49	.86	.71
10.	.42	.75	.52	.88	.73
11.	.55	--	.53	.89	--
12.	.67	--	--	--	.77

EAST SHOT POINT

ARRIVAL TIMES (Secs.)

SHOT #15, TRUCK #1 (Good Record)

(Continued)

Geoph. No.	Dist.	Arr. #5, Moho refraction app. vel. 9.5	Arr. #6, Moho reflection app. vel. 11.3	Arr. #7, app. vel. 7.8	Arr. #8, app. vel. 11.0
1.	163.25	--	--	--	--
2.	.38	--	--	--	--
3.	.50	--	--	--	--
4.	.63	--	--	--	--
5.	.77	29.12	29.54	30.26	30.75
6.	.90	.12	--	.28	.76
7.	164.02	--	--	--	--
8.	.15	--	--	--	--
9.	.30	.16	.57	.32	.78
10.	.42	.18	.59	.34	.80
11.	.55	.20	--	.37	.82
12.	.67	.20	.62	.38	.83

EAST SHOT POINT

ARRIVAL TIMES (Secs.)

SHOT #15, TRUCK #1 (Good Record)

(Continued)

Geoph. No.	Dist.	Arr. #9, app. vel. 7.7	Arr. #10, app. vel. 7.8	Arr. #11, app. vel. 6.3
1.	163.25	--	--	--
2.	.38	--	--	--
3.	.50	--	--	--
4.	.63	--	--	--
5.	.77	--	32.88	35.06
6.	.90	31.31	.91	.09
7.	164.02	--	--	--
8.	.15	--	--	--
9.	.30	31.34	.94	.10
10.	.42	.37	.96	.12
11.	.55	.39	.98	.14
12.	.67	.41	.99	.16

EAST SHOT POINT

ARRIVAL TIME (Secs.)

SHOT #15, TRUCK #2 (Good Record)

Geoph. No.	Dist.	Arr. #1, Moho refraction app. vel. 7.4	Arr. #2, Intermediate layer refraction app. vel. 8.7	Arr. #3, Moho reflection app. vel. 6.9	Arr. #4, app. vel. 11.0
1.	202.12	33.76	34.22	34.72	34.92
2.	.24	.80	.22	.75	.93
3.	.37	.80	.24	.76	.96
4.	.49	.83	.25	.77	.97
5.	.64	--	--	--	--
6.	.77	.86	.29	.82	--
7.	.89	.89	.31	.83	35.00
8.	203.02	--	.32	.84	--
9.	.16	.93	--	--	--
10.	.29	--	.34	.89	.02
11.	.41	--	--	--	.04
12.	.54	.94	.37	.94	.07

EAST SHOT POINT

ARRIVAL TIMES (Secs.)

SHOT #16, TRUCK #1 (Fair Record)

Geoph. No.	Dist.	Arr. #1, Intermediate layer refraction app. vel. 7.7	Arr. #2, app. vel. 7.4	Arr. #3, app. vel. 8.4
1.	--	--	--	--
2.	--	--	--	--
3.	--	--	--	--
4.	--	--	--	--
5.	210.37	34.96	35.13	36.21
6.	.50	--	--	--
7.	.62	.98	.17	.25
8.	.75	--	--	--
9.	.90	35.03	.20	.26
10.	211.02	--	.21	.31
11.	.15	.05	--	.31
12.	.27	.10	.26	.32

EAST SHOT POINT

ARRIVAL TIMES (Secs.)

SHOT #16, TRUCK #2 (Fair Record)

Geoph. No.	Dist.	Arr. #1, app. vel. 6.8	Arr. #2, app. vel. 6.4	Arr. #3, Moho reflection app. vel. 7.0	Arr. #4, app. vel. 8.4
1.	234.89	38.78	39.07	39.50	39.88
2.	235.01	.79	.09	.52	.89
3.	.14	.79	.10	.52	.90
4.	.26	.82	.10	.55	.92
5.	.41	--	--	.57	.93
6.	.54	--	.16	.62	.96
7.	.66	.88	.18	--	--
8.	.79	--	.21	.66	.98
9.	.93	.95	.23	--	40.00
10.	236.06	--	--	--	.01
11.	.18	--	--	--	--
12.	.31	.98	.30	.70	--

EAST SHOT POINT

ARRIVAL TIMES (Secs.)

SHOT #16, TRUCK #2, (Fair Record)

(Continued)

Geoph. No.	Dist.	Arr. #5, app. vel. 6.5	Arr. #6, app. vel. 6.1	Arr. #7, app. vel. 5.8	Arr. #8, app. vel. 6.9
1.	234.89	40.19	40.38	41.13	41.62
2.	235.01	.21	--	.14	.65
3.	.14	.23	.41	.15	.66
4.	.26	--	.44	.19	.68
5.	.41	.25	.45	--	--
6.	.54	.29	--	.23	.72
7.	.66	--	--	.26	.74
8.	.79	--	--	--	--
9.	.93	--	.55	.30	.78
10.	236.06	.32	--	.35	.79
11.	.18	--	--	--	--
12.	.31	--	--	--	--

WEST SHOT POINT

ARRIVAL TIMES (Sec.)

SHOT #2, TRUCKS #'s 1 and 2

Geoph. No.	Dist.	Arr. #1, app. vel. 6.8	Arr. #2, app. vel. 7.5	Arr. #3, Intermediate layer refraction app. vel. 7.6	Arr. #4, Moho refraction app. vel. 8.1
1.	189.46	31.28	31.69	32.03	32.26
2.	.58	--	31.72	.05	.28
3.	.71	31.32	31.74	.07	.30
4.	.83	.32	31.76	.08	.32
5.	.98	.38	.78	.11	.35
6.	190.11	--	.79	.12	.36
7.	.23	.39	.81	.13	.37
8.	.36	--	.82	.15	.39
9.	.51	.43	.84	.16	.40
10.	.63	.46	.86	.19	.42
11.	.76	--	.87	.21	.44
1. &12.	.88	.49	.90	.23	.46
2.	191.00	--	.91	.24	.47
3.	.13	--	.93	.26	.49
4.	.25	--	.95	.27	.50
5.	.40	--	--	--	--
6.	.53	--	.98	.31	.54
7.	.65	--	--	.33	.55
8.	.78	--	--	.34	.57
9.	.93	--	--	.36	.58
10.	192.05	31.66	32.07	.37	.60
11.	.18	--	.10	.39	.60
12.	.30	--	.09	.41	.63

WEST SHOT POINT

ARRIVAL TIMES (Secs.)

SHOT #2, TRUCKS #'s 1 and 2

Geoph. No.	Dist.	Arr. #5, Intermed. layer reflection app. vel. 6.0	Arr. #6, limestone refraction app. vel. 6.5	Arr. #7 app. vel. 6.4	Arr. #8, app. vel. 8.1
1.	189.46	32.81	33.16	33.72	34.20
2.	.58	.84	.18	.74	.21
3.	.71	.85	.20	.75	.22
4.	.83	.87	.21	--	.22
5.	.98	.90	--	.81	--
6.	190.11	--	.28	--	.26
7.	.23	--	.30	--	.32
8.	.36	--	.32	--	.32
9.	.51	33.04	.33	.88	.35
10.	.63	.05	.35	.90	.37
11.	.76	.08	.37	.92	.40
1. & 12.	190.88	.12	.38	.94	.40
2.	191.00	.13	.44	--	.43
3.	.13	.14	.46	--	.43
4.	.25	.15	--	--	.44
5.	.40	--	--	--	--
6.	.53	.18	.49	--	.47
7.	.65	.20	.52	--	.49
8.	.78	.22	.53	--	.51
9.	.93	.22	.54	--	.52
10.	192.05	.24	.57	--	.54
11.	.18	.26	.58	34.14	.55
12.	.30	.28	.60	.16	.57

WEST SHOT POINT

ARRIVAL TIMES (Secs.)

SHOT #2, Juliet #2 (Good Record)

Geoph. No.	Dist.	Arr. #1, Precambrian refraction app. vel. 6.7	Arr. #2 app. vel. 6.9	Arr. #3 app. vel. 7.2	Arr. #4, app. vel. 8.6
1.	117.20	19.80	20.00	20.39	--
2.	.70	19.88	.09	.47	20.70
3.	118.20	19.97	.16	.55	.75
4.	.70	--	.22	.60	.79
5.	119.20	20.10	.30	.68	.87
6.	.70	20.18	.37	.75	.93

Geoph. No.	Dist.	Arr. #5, limestone refraction app. vel. 8.3	Arr. #6, app. vel. 8.3	Arr. #7, Intermediate layer refraction app. vel. 7.6	Arr. #8, app. vel. 8.0
1.	117.20	20.98	21.64	22.11	23.24
2.	.70	21.05	.73	.20	.31
3.	118.20	21.12	.80	.26	.37
4.	.70	.17	.85	.33	.42
5.	119.20	.23	.92	.40	.50
6.	.70	.29	.97	.45	.55

WEST SHOT POINT

ARRIVAL TIMES (Secs.)

SHOT #2, Juliet #2 (Good Record)

(Continued)

Geoph. No.	Dist.	Arr. #9, Moho refraction app. vel. 8.9	Arr. #10, app. vel. 8.6
1.	117.20	23.43	24.93
2.	.70	.50	.98
3.	118.20	.55	25.02
4.	.70	.60	.10
5.	119.20	--	.14
6.	.70	.63	.21

WEST SHOT POINT

ARRIVAL TIMES (Secs.)

SHOT #2, Romeo #2 (Good Record)

Geophone No.	Dist.	Arr. #1, Precambrian refraction app. vel. 6.5	Arr. #2, app. vel. 6.7	Arr. #3, app. vel. 6.6	Arr. #4, limestone refraction app. vel. 6.9
1.	135.14	22.42	22.94	23.42	23.96
2.	.64	.48	23.00	.50	24.03
3.	136.14	.56	.07	.57	.10
4.	.64	.65	.14	.64	.17
5.	137.14	.70	.22	.72	.25
6.	.64	.80	.31	.80	.32

Geoph. No.	Dist.	Arr. #5, Int. layer refraction app. vel. 7.4	Arr. #6, app. vel. 7.2	Arr. #7, Moho refraction app. vel. 9.2
1.	135.14	24.54	25.03	25.79
2.	.64	.60	.08	.83
3.	136.14	.67	.14	.89
4.	.64	.73	.21	.94
5.	137.14	.80	.28	26.00
6.	.64	.88	.36	.05

WEST SHOT POINT

ARRIVAL TIMES (Secs.)

SHOT #3, Juliet #3 (Good Record)

Geoph. No.	Dist.	Arr. #1, Precambrian refraction app. vel. 12.4	Arr. #2, app. vel. 6.5	Arr. #3, limestone refraction app. vel. 8.1	Arr. #4 app. vel. 7.1
1.	99.39	16.94	17.29	18.13	19.42
2.	.89	--	17.38	.15	.50
3.	100.39	17.02	.44	.19	.57
4.	.89	--	.57	.28	.64
5.	101.39	--	.61	.33	.71
6.	.89	--	.67	.39	.76

Geoph. No.	Dist.	Arr. #5, app. vel. 7.2	Arr. #6, app. vel. 7.8
1.	99.39	19.76	20.09
2.	.89	.85	.16
3.	100.39	.89	.21
4.	.89	--	.28
5.	101.39	20.05	.34
6.	.89	.11	.42

WEST SHOT POINT

ARRIVAL TIMES (Secs.)

SHOT #3, Romeo #3 (Good Record)

Geoph. No.	Dist.	Arr. #1, Precambrian refraction app. vel. 6.1	Arr. #2, app. vel. 7.4	Arr. #3, app. vel. 7.3	Arr. #4, limestone refraction app. vel. 8.3
1.	146.37	24.26	25.30	25.68	25.90
2.	.87	--	.35	.75	.97
3.	147.37	.39	.46	.76	26.00
4.	.87	.47	.49	.88	.05
5.	148.37	.59	.57	.96	.11
6.	.87	.64	.62	.98	.18

Geoph. No.	Dist.	Arr. #5, Intermediate layer refraction app. vel. 7.8	Arr. #6, Intermediate layer reflection app. vel. 8.9	Arr. #7, Moho refraction app. vel. 6.0	Arr. #8, app. vel. 9.1
1.	146.37	26.27	26.46	--	27.79
2.	.87	.33	--	26.99	.85
3.	147.37	.35	.49	27.01	--
4.	.87	.41	.53	27.11	.96
5.	148.37	.47	.58	.20	28.01
6.	.87	.54	.66	.26	.07

WEST SHOT POINT

ARRIVAL TIMES (Secs.)

SHOT #7, U. S. C. G. S. (305) (Fair Record)

Geoph. No.	Dist.	Arr. #1, Precambrian refraction app. vel. 5.6	Arr. #2, limestone refraction app. vel. 4.6	Arr. #3, app. vel. 4.7	Arr. #4, app. vel. 6.0
Cl.	43.02	7.92	8.27	8.98	9.82
1.	.32	.96	.33	9.05	.85
2.	.63	8.03	.41	.12	.92
3.	.93	.08	.47	.17	.95

Geoph. No.	Dist.	Arr. #5, app. vel. 8.7	Arr. #6, app. vel. 7.7
Cl.	43.02	13.10	13.93
1.	.32	.13	.96
2.	.63	.17	14.01
3.	.93	.19	.04

WEST SHOT POINT

ARRIVAL TIMES (Secs.)

SHOT #7, U. S. C. G. S. (307) (Bow River) (Fair Record)

Geoph. No.	Dist.	Arr. #1, Precambrian refraction app. vel. 6.2	Arr. #2, app. vel. 7.9	Arr. #3, app. vel. 7.7	Arr. #4, app. vel. 7.7
Cl.	63.96	11.27	11.53	13.45	14.58
1.	64.26	.33	.58	.50	.64
2.	.57	.37	.61	.53	.68
3.	.87	.43	.66	.58	.72

Geoph. No.	Dist.	Arr. #5, app. vel. 7.7
Cl.	63.96	15.28
1.	64.26	.32
2.	.57	.36
3.	.87	.40

APPENDIX III

SHOT AND RECORDING LOCATION DIAGRAMS

SHOT NO. FOUR, TRUCK TWO

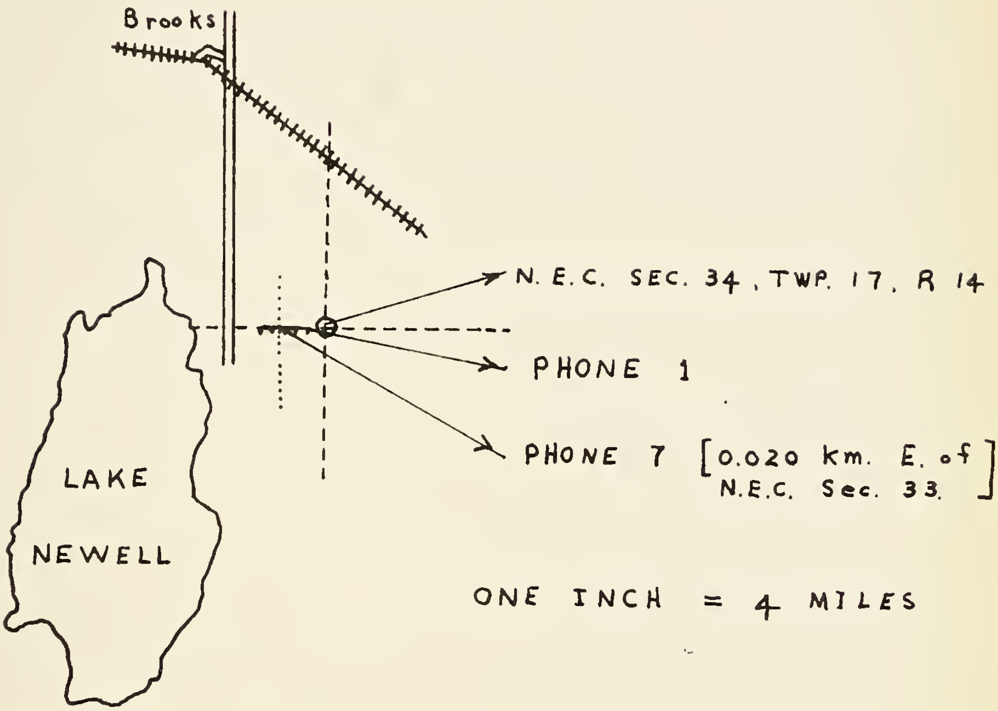
Brooks
N. E. C. SEC. 34, TWP. 17, R 14
PHONE 1
PHONE 7 [0.020 km. E. of N.E.C. Sec. 33.]
LAKE NEWELL
ONE INCH = 4 MILES

SHOT NO. 5, TRUCK ONE

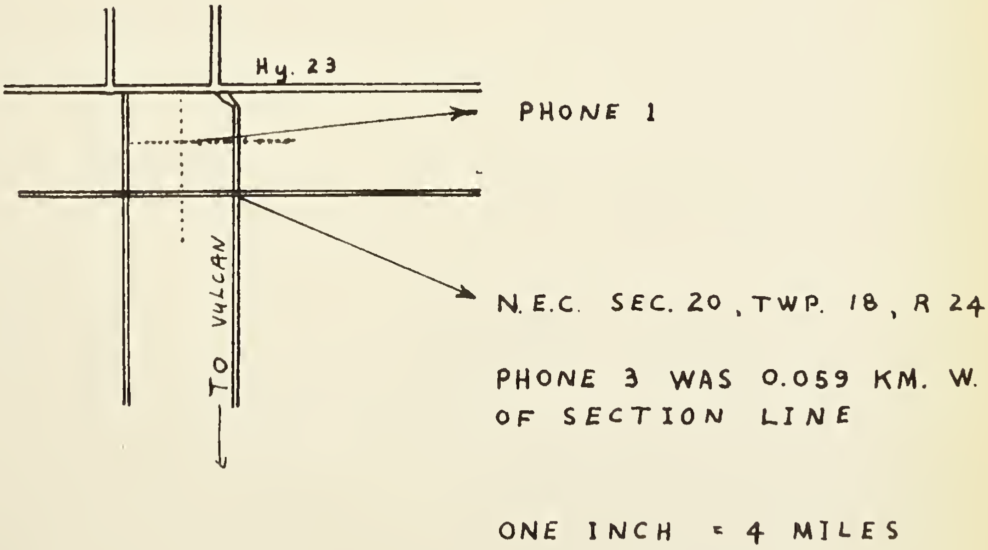
Hy. 23
PHONE 1
TO VULCAN
N. E. C. SEC. 20, TWP. 18, R 24
PHONE 3 WAS 0.059 KM. W. OF SECTION LINE
ONE INCH = 4 MILES

DR.

SHOT NO. EIGHT, TRUCK ONE

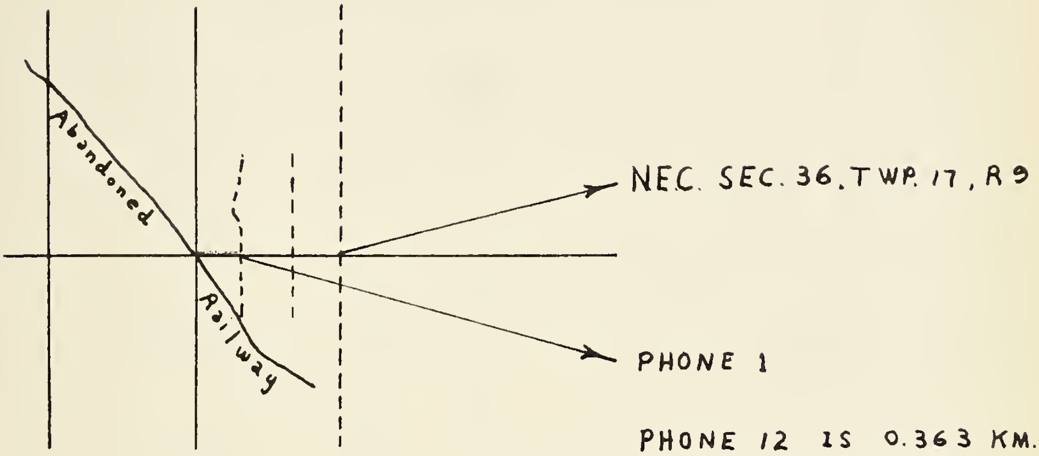

PHONE 12 IS 0.363 KM.
E. OF N.E.C. SEC. 33

ONE INCH = 4 MILES

SHOT NO. EIGHT, TRUCK TWO

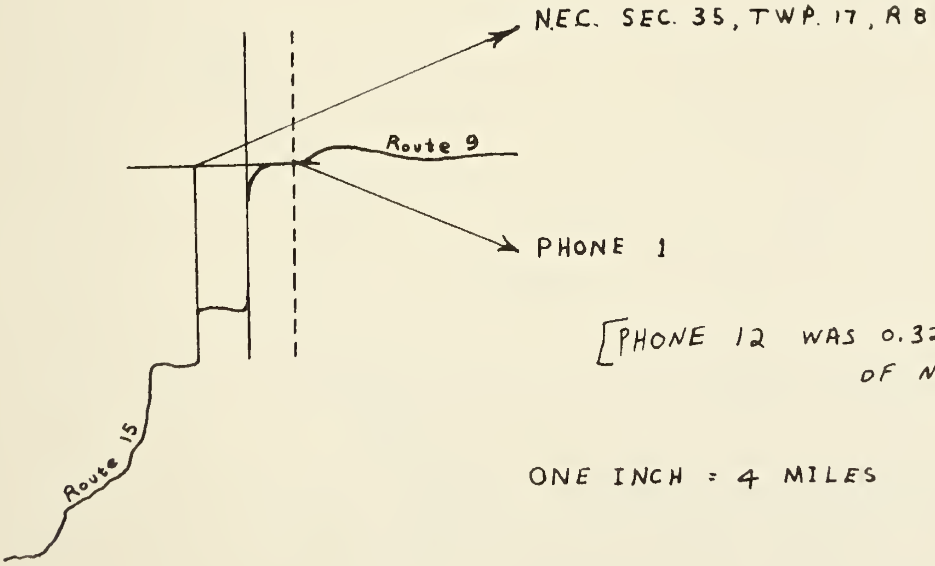

[PHONE 12 WAS 0.320 Km. EAST
of NEC. SEC. 36.]

ONE INCH = 4 MILES

DR.

SHOT NO. 10, TRUCK ONE

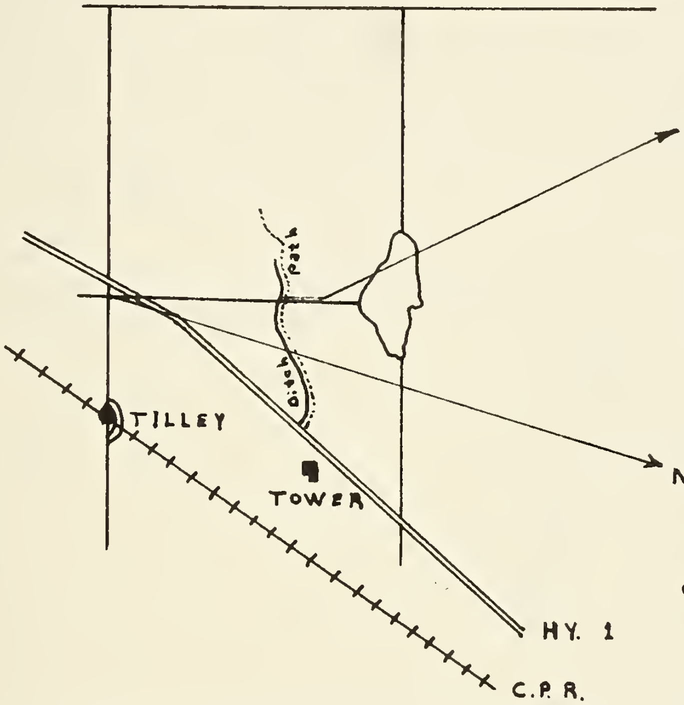

PHONE 12 ON DITCH BANK

ONE INCH = 4 MILES

SHOT NO. 10, TRUCK [redacted] TWO

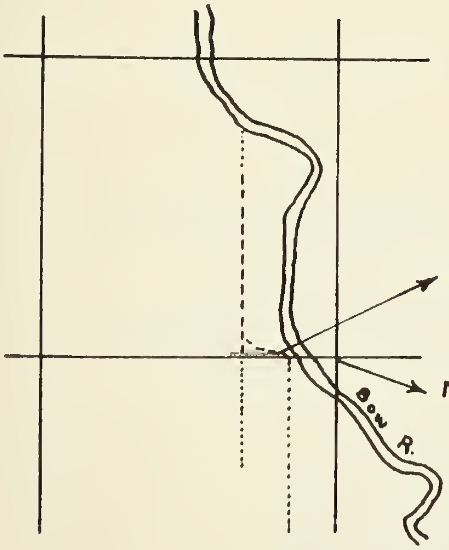

PHONE 10 WAS 0.022 KM. E.
OF N.E.C. SEC. 34.

OR.

SHOT NO. 11, TRUCK ONE

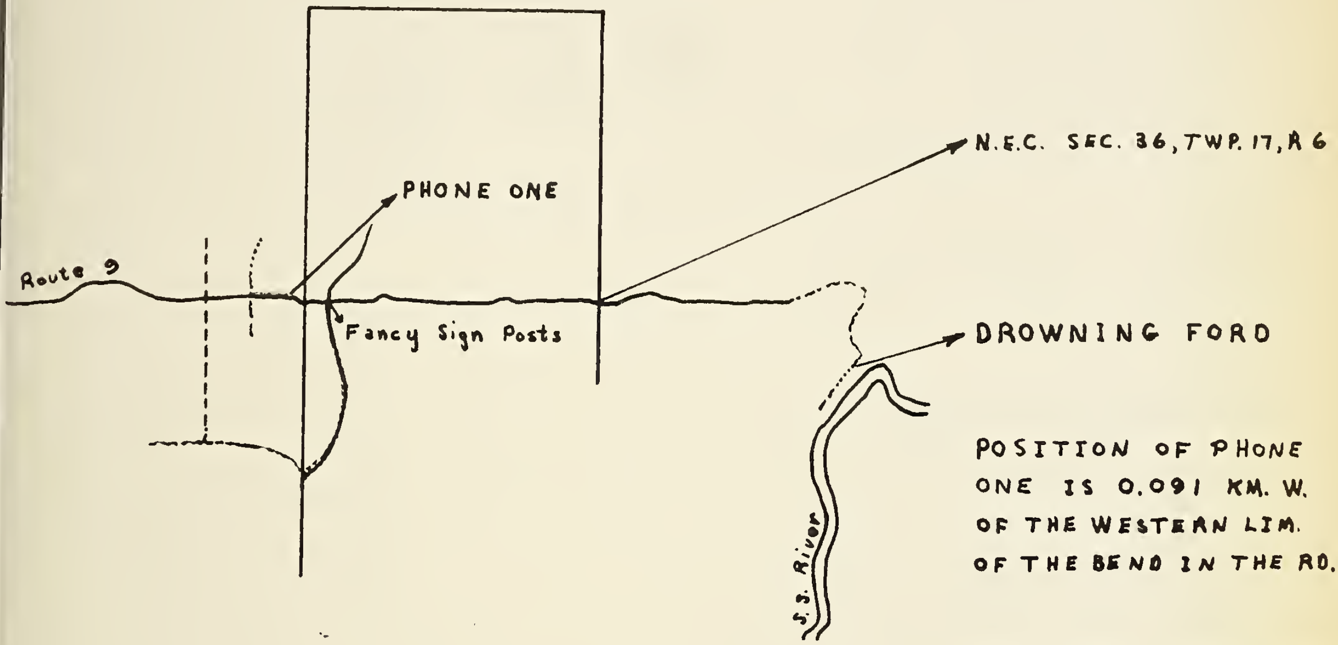

POSITION OF PHONE ONE IS 0.091 KM. W. OF THE WESTERN LIM. OF THE BEND IN THE RD.

ONE INCH = 4 MILES

SHOT NO. 11, TRUCK TWO

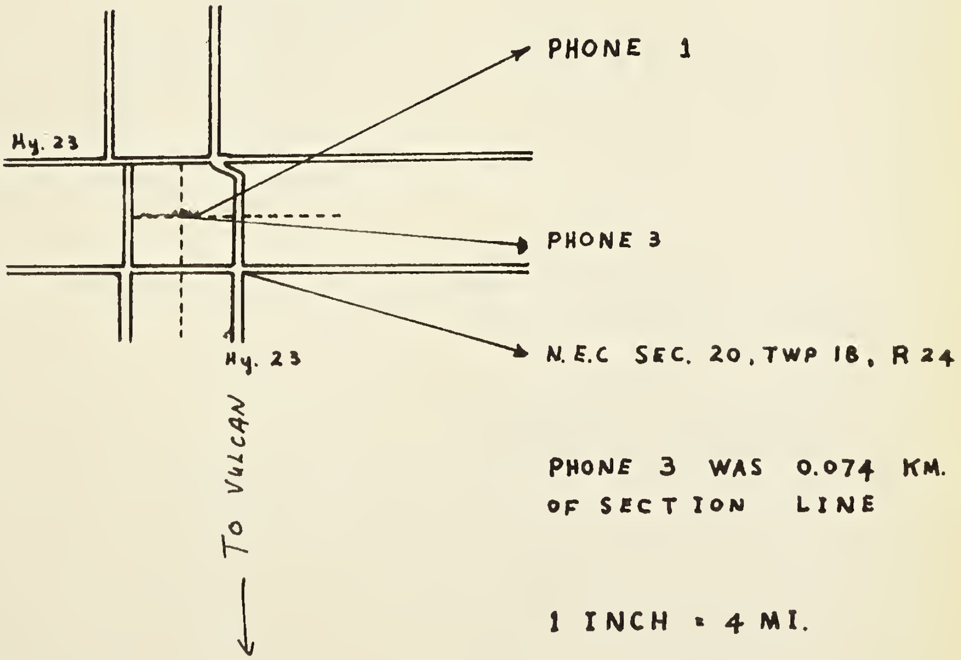

PHONE 3 WAS 0.074 KM. W. OF SECTION LINE

1 INCH = 4 MI.

DR.

SHOT 12, TRUCK ONE

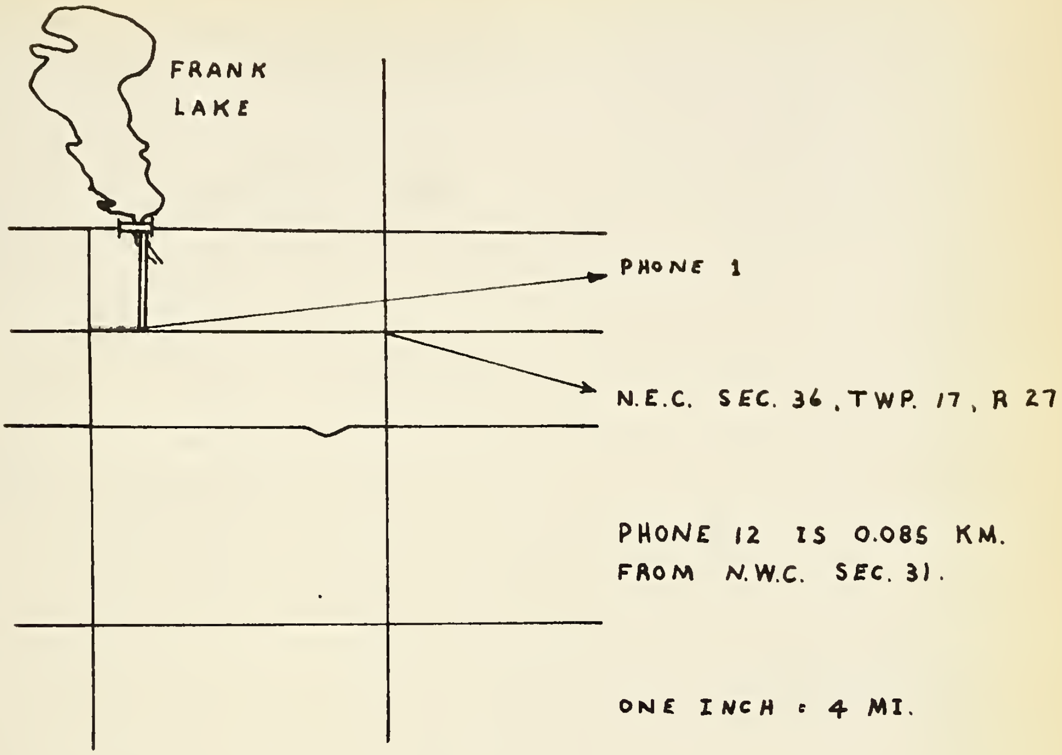

PHONE 12 IS 0.085 KM.
FROM N.W.C. SEC. 31.

ONE INCH = 4 MI.

SHOT 12, TRUCK TWO

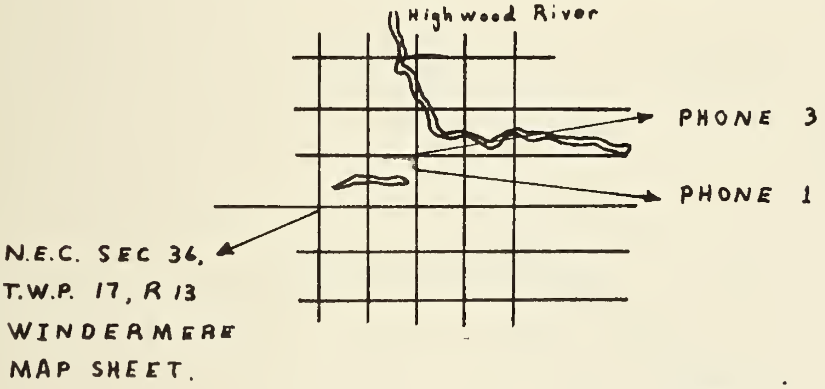

PHONE 3 IS AT N.E.C.
SEC. 5, TWP. 18, R 2 W5.

ONE INCH = 4 MILES

DR.

SHOT NO. 13 , TRUCK ONE

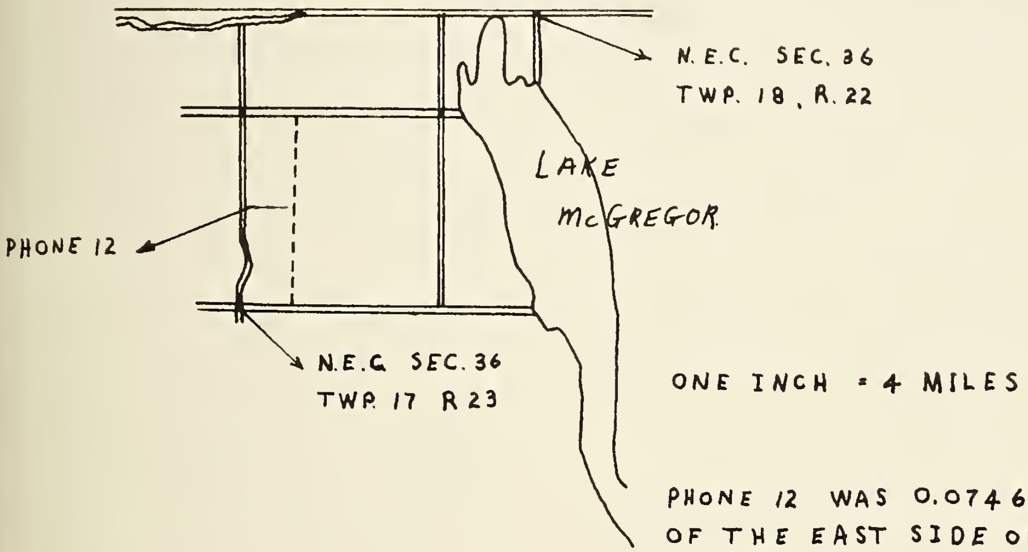

PHONE 12 WAS 0.0746 KM. EAST OF THE EAST SIDE OF THE ROAD ALLOWANCE.

SHOT NO. 13 TRUCK 2

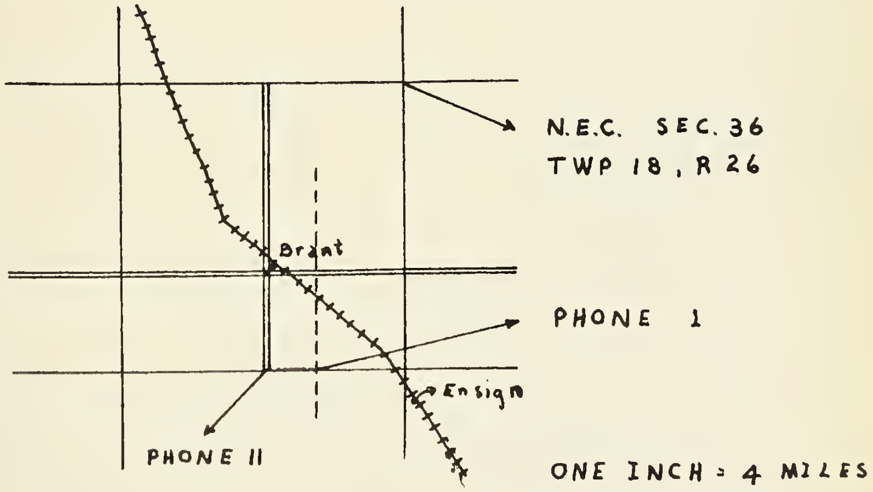

PHONE 11 WAS 0.118 KM. FROM EAST EDGE OF ROAD ALLOWANCE

SHOT 14, TRUCK ONE

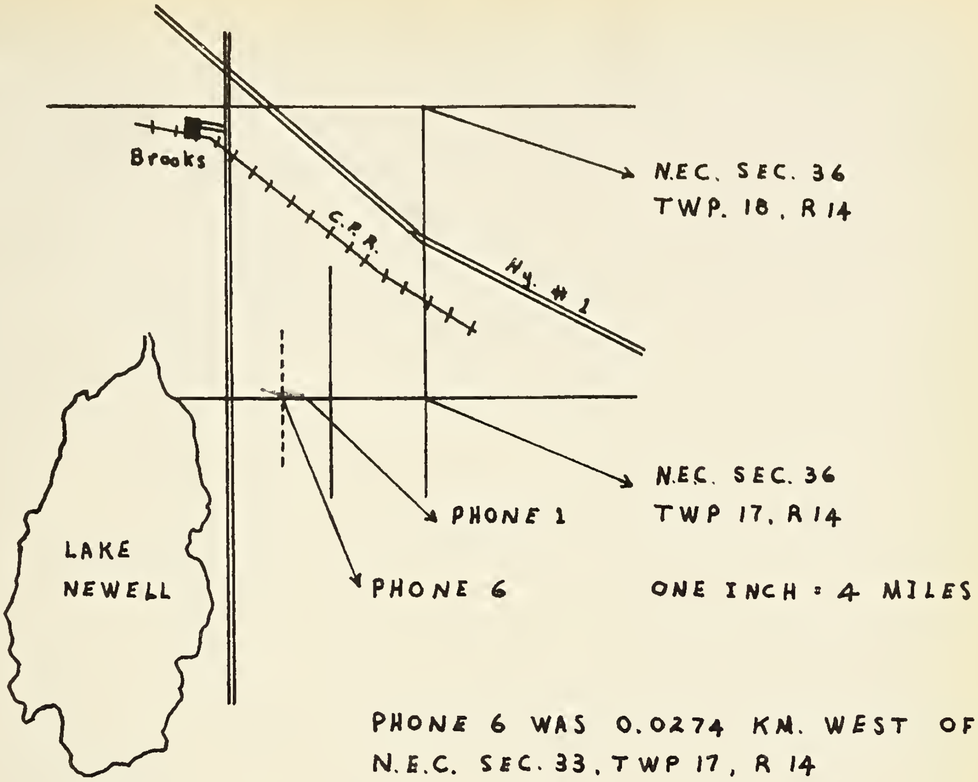

PHONE 6 WAS 0.0274 KM. WEST OF
N.E.C. SEC. 33, TWP 17, R 14

SHOT 14, TRUCK TWO

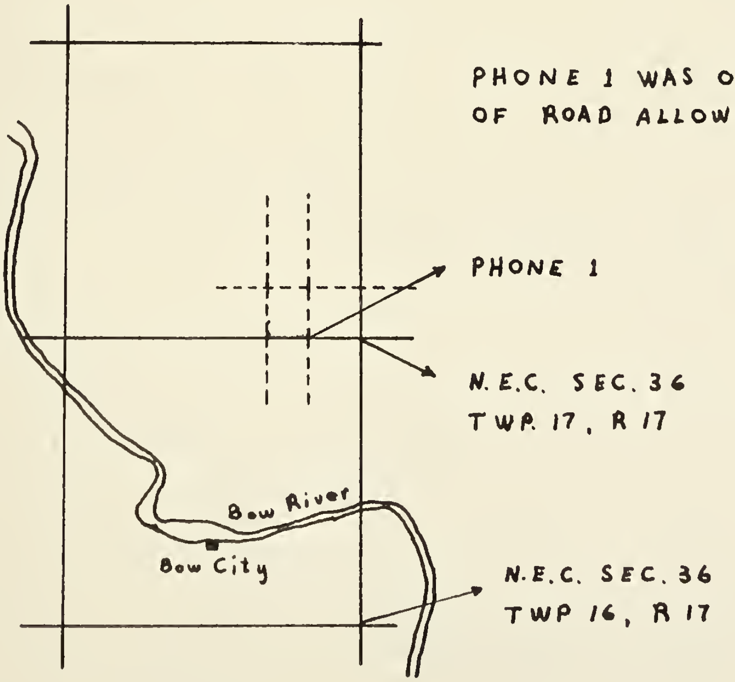

PHONE 1 WAS 0.097 KM. WEST
OF ROAD ALLOWANCE CENTRE

SHOT 15, TRUCK ONE

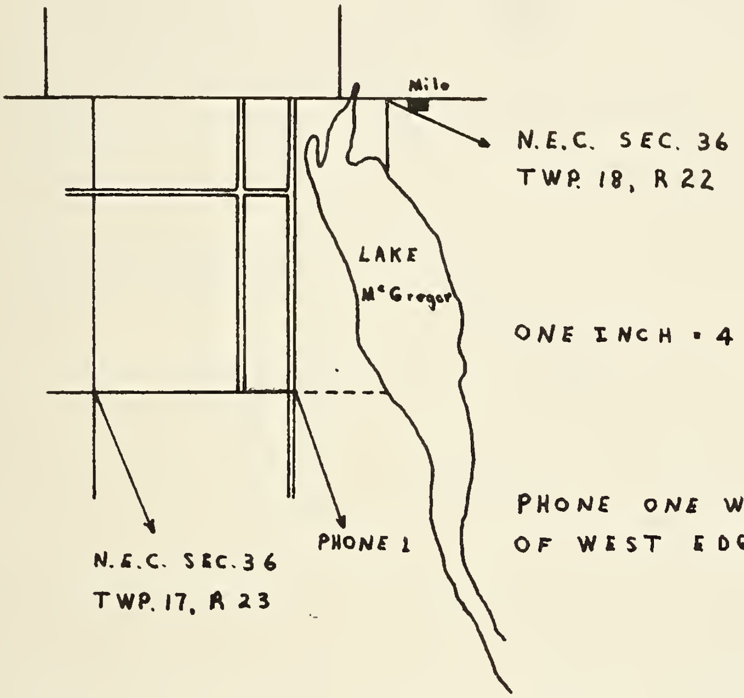

ONE INCH = 4 MILES

PHONE ONE WAS 0.09 KM. WEST OF WEST EDGE OF ROAD ALLOWANCE

SHOT 15, TRUCK TWO

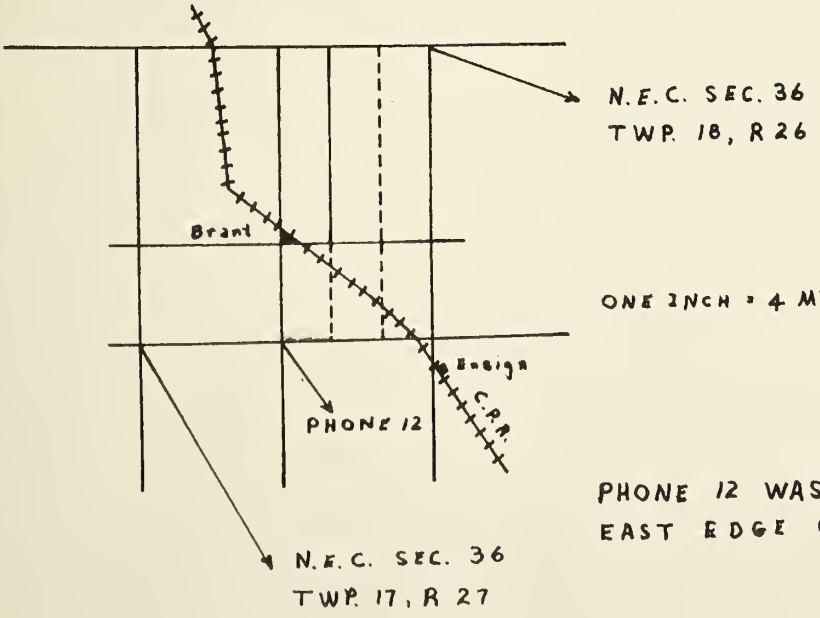

ONE INCH = 4 MILES

PHONE 12 WAS 0.118 KM. FROM EAST EDGE OF ROAD ALLOWANCE

SHOT 16, TRUCK ONE

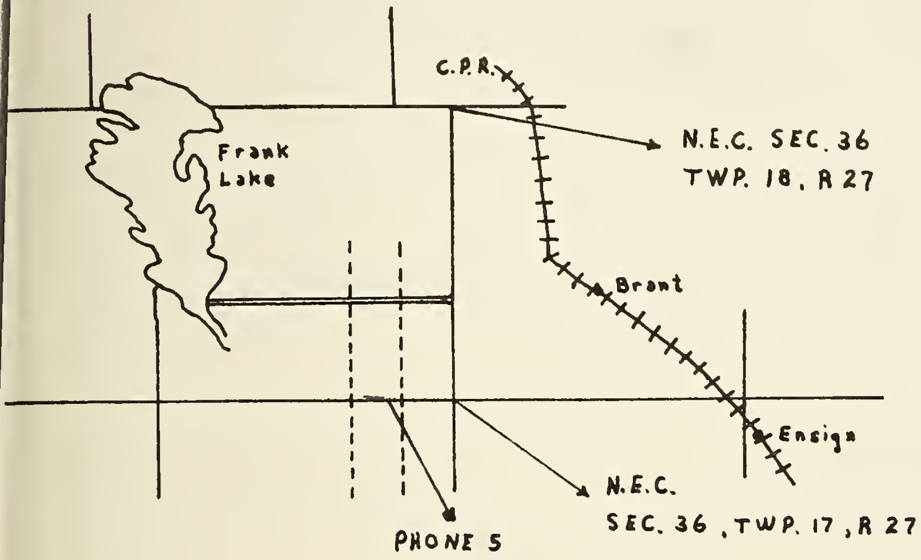

PHONES 1,2,3,4 OMITTED

ONE INCH = 4 MILES

PHONE 5 WAS 0.151 KM. WEST OF WEST EDGE OF ROAD ALLOWANCE

SHOT 16, TRUCK TWO

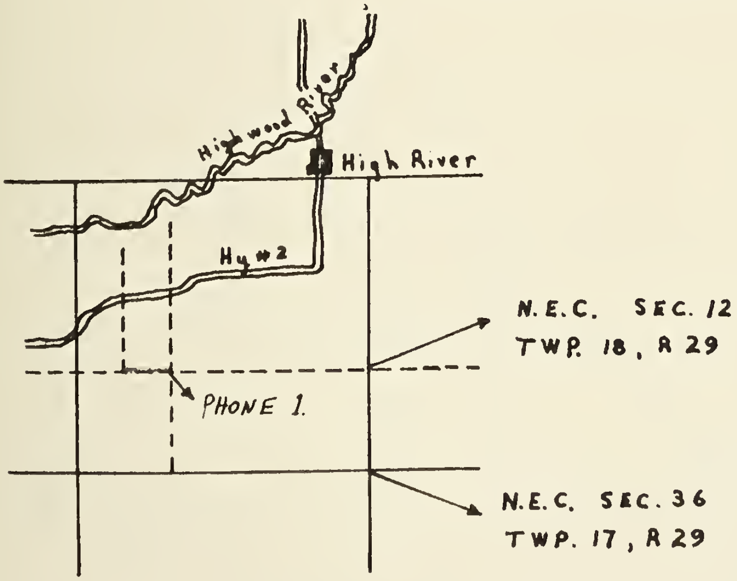

ONE INCH = 4 MILES

PHONE 12 WAS 0.020 KM. EAST OF CENTRE OF THE ROAD ALLOWANCE. WILLMORES WERE 0.024 KM. EAST OF SAME.

SHOTS NO. 11 AND 12

SHOT LOCATION :

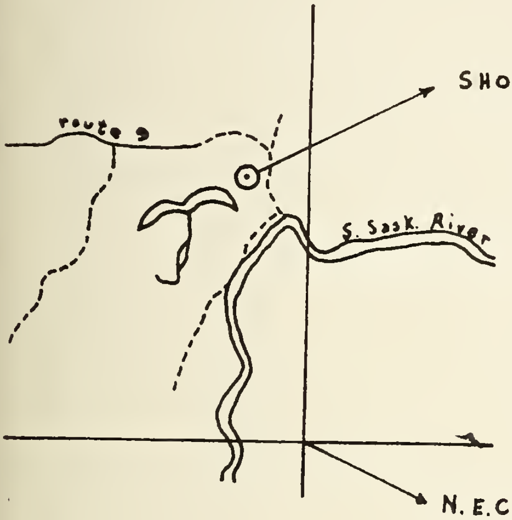

SHOT POINT

N.E.C. SEC. 36
TWP 16, R 5

ONE INCH = 4 MILES

MILITARY GRID REFERENCE:
SHOT # 11 : 29619117
SHOT # 12 : 29609118

SHOT # 13

SHOT LOCATION:

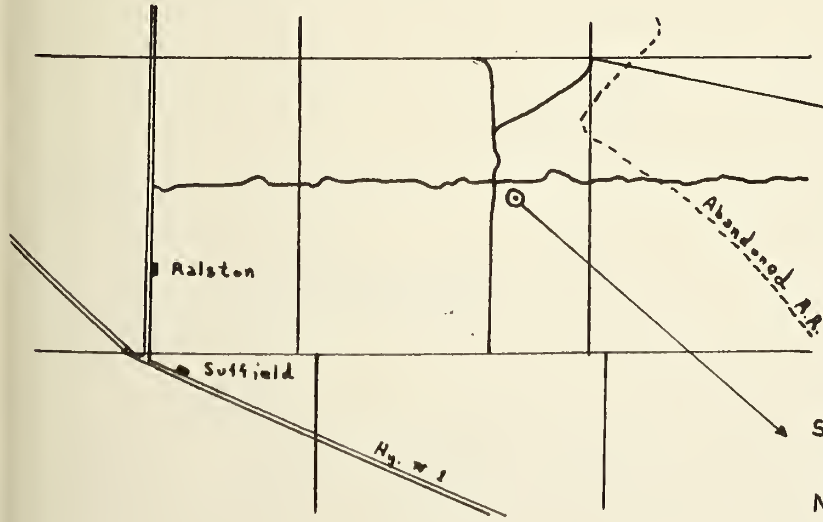

N.E.C. SEC. 36
TWP 15, R 8

SHOT POINT

MILITARY GRID REFERENCE:
SHOT #13 : E. 500 353.8
N. 556 8395.3

ONE INCH = 4 MILES

DR.

SHOTS NO. 5, 14, 15 AND 16

SHOT LOCATION:

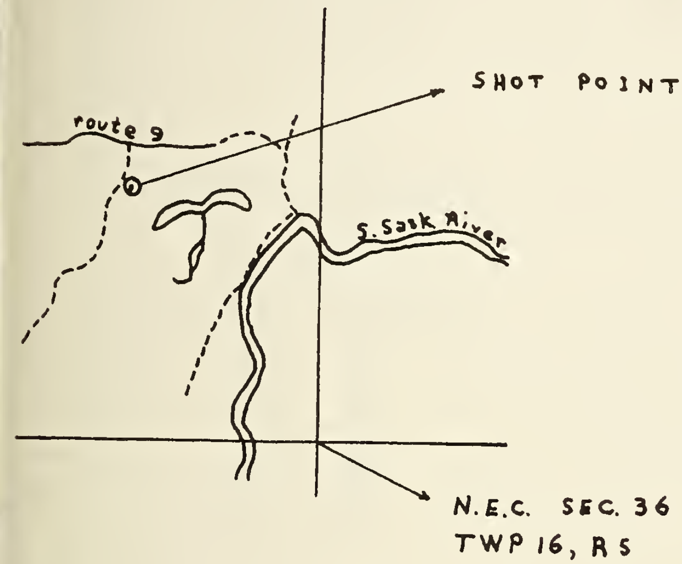

ONE INCH = 4 MILES

MILITARY GRID REFERENCE:

E. 253.2

N. 908.5

SHOTS NO. 4, 8, AND 10

SHOT LOCATION:

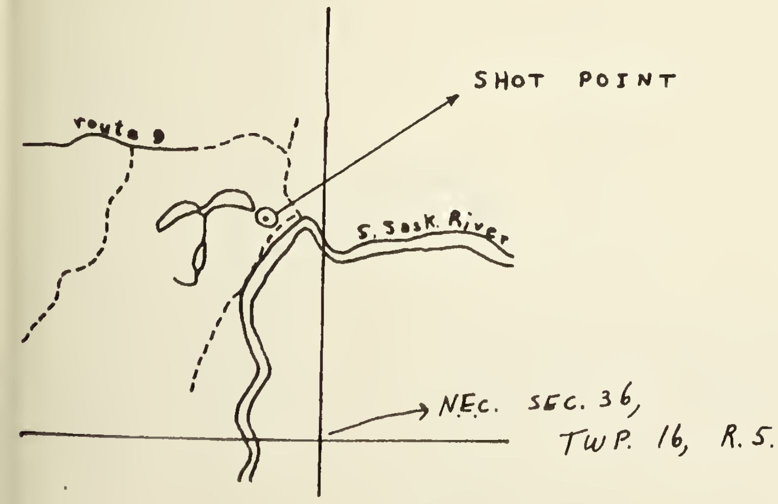

ONE INCH = 4 MILES

DR.

SHOT NO. 2, 3 AND 7

SHOT LOCATION:

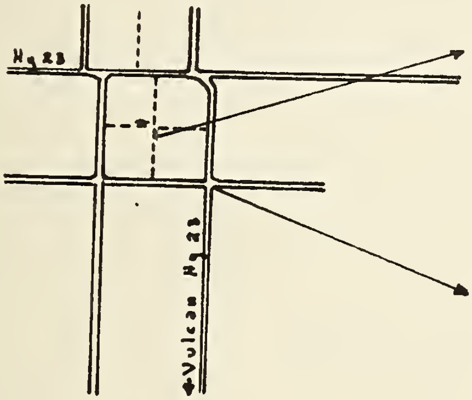

SHOT POINT, N.E.C. SEC. 30, TWP 18, R 24

N.E.C. SEC. 20, TWP. 18 R 24
GLEICHEN SHEET

ONE INCH = 4 MILES

SHOT NO. 2, TRUCKS 1 AND 2

DROWNING FORD RANGE

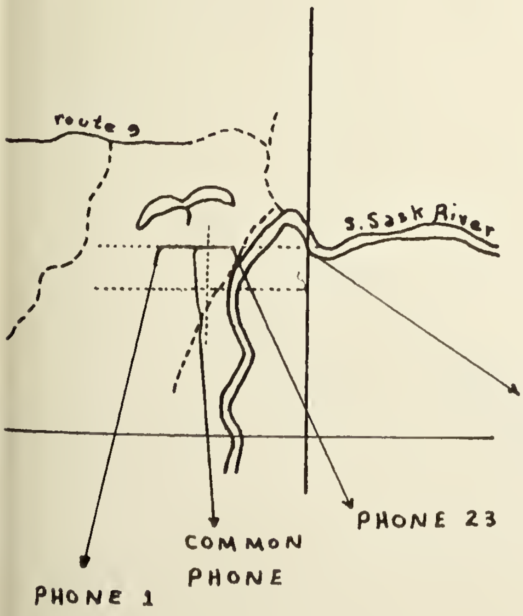

N.E.C. SEC. 24, TWP 17, R 5
MEDICINE HAT SHEET

ONE INCH = 4 MILES

DR.

SHOT NO. 2, ROMEO 2

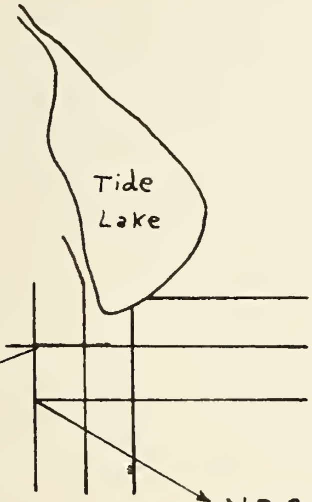

ONE INCH = 4 MILES

PHONE 1
ON EAST
EDGE OF
ROAD
ALLOWANCE

NE.C. SEC. 36 TWP 17, R 11
MEDICINE HAT SHEET

SHOT NO. 2, JUL. 2

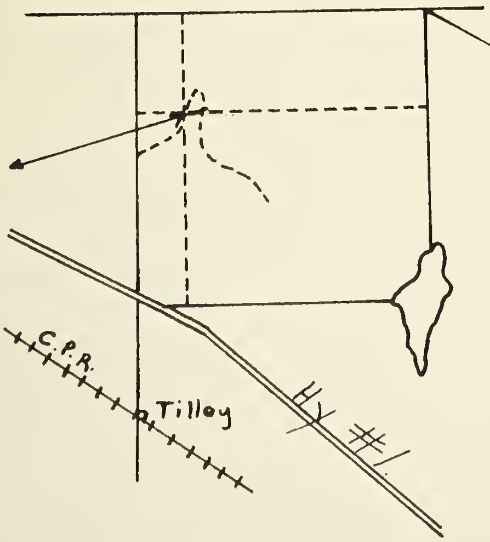

N. E. C. SEC. 36
TWP. 18, R 12

PHONE 1

PHONE ONE ON SEC. LINE

ONE INCH = 4 MILES

DR

SHOT NO. 3 ROMEO 3

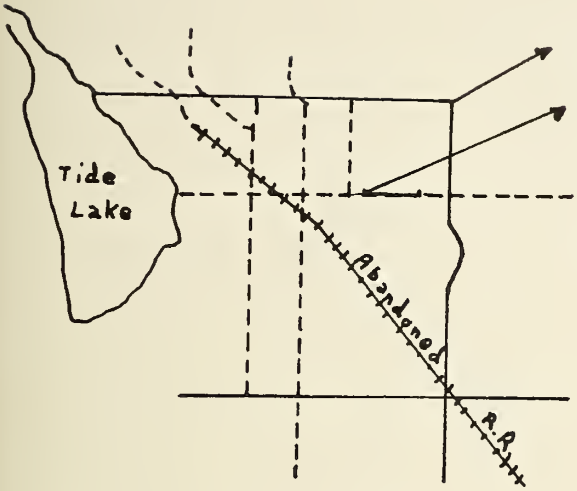

N.E.C. SEC. 33, TWP. 18, R 9

PHONE 1

ONE INCH = 4 MILES

PHONE 1 IS AT N.E.C. SEC. 19
TWP. 18, R 9

SHOT NO. 3 JUL. 3

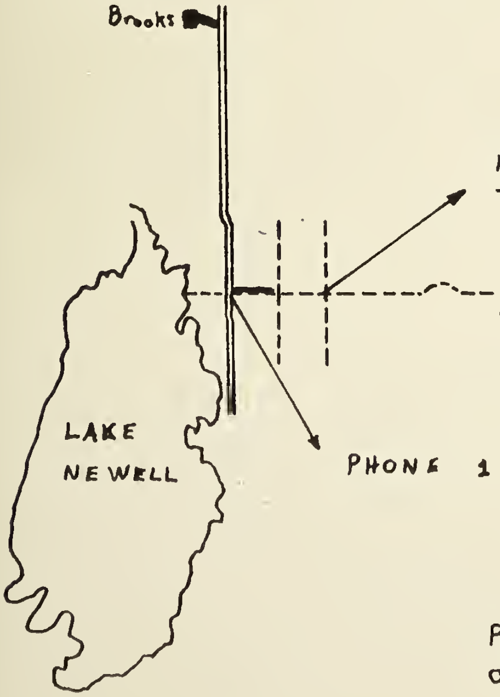

N.E.C. SEC. 34.
TWP 17, R 14

ONE INCH = 4 MILES

PHONE 1

PHONE 1 IS AT EAST EDGE
OF THE ROAD ALLOWANCE

SHOT NO. 7 U.S.C.G.S. GROUP NO. 1 (307) (BOW RIVER)

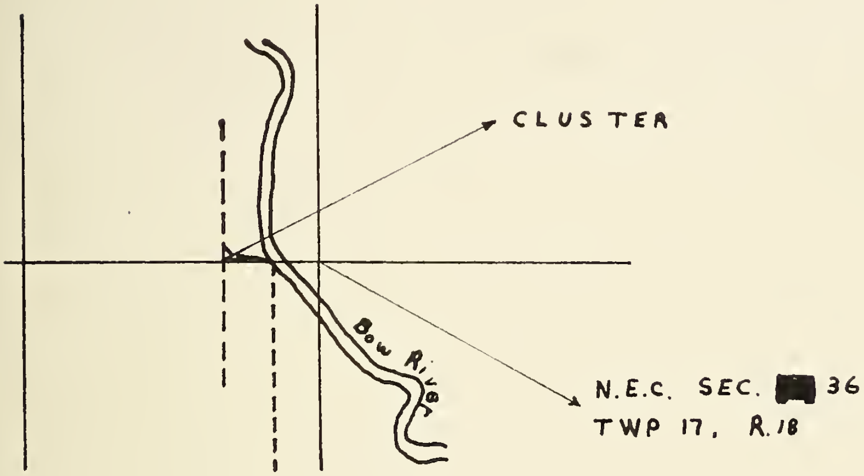

CLUSTER AT N.E.C. SEC. 34, TWP. 17, R 18

SHOT NO. 7 U.S.C.G.S. GROUP NO. 2 (305)

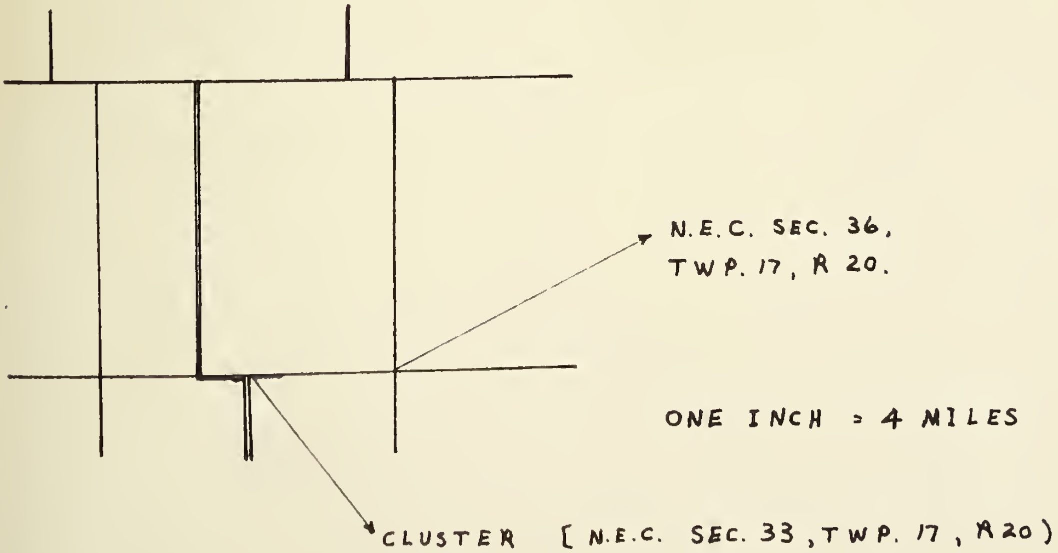

DR.

B29808